

# **DYNAMICS OF FRACTALS IN EUCLIDEAN AND MEASURE SPACES**

A Dissertation Submitted in Fulfillment of  
Requirement for the Degree of

**DOCTOR OF PHILOSOPHY (Ph.D)**  
**IN**  
**MATHEMATICS**

**Under the Supervision of**  
**Professor Dr. Md. Shahidul Islam**  
**Department of Mathematics**  
**University of Dhaka**

Submitted by  
**MD. JAHURUL ISLAM**  
Registration Number: 47  
Session: 2013-2014



**DEPARTMENT OF MATHEMATICS, NATURAL SCIENCE GROUP**  
**UNIVERSITY OF DHAKA, DHAKA-1000**  
**BANGLADESH**  
**December, 2017**

***Dedicated to my parents***

*who made me to realize what I am capable of...*

## **DECLARATION**

It is hereby declared that the thesis entitled “**Dynamics of Fractals in Euclidean and Measure Spaces**” is a record of research work carried out by me and all the sources that I have used or quoted have been indicated and acknowledged by means of complete references. Neither this thesis nor any part of it has been submitted elsewhere for the award of any degree, diploma or a higher study in any university.

Signature of the candidate

---

Md. Jahurul Islam

Certified that the thesis entitled “**Dynamics of Fractals in Euclidean and Measure Spaces**” submitted in fulfillment of the requirements for the degree of Doctor of Philosophy in Mathematics under University of Dhaka, has been completed under my supervision. I believe that this research work is an original one and it has not been submitted elsewhere for any degree.

---

**Dr. Md. Shahidul Islam**

Professor

Department of Mathematics

University of Dhaka, Dhaka, Bangladesh.



## **Acknowledgments**

It is my pleasure to acknowledge a deep gratitude to my guide **Professor Dr. Md. Shahidul Islam**, Department of Mathematics, University of Dhaka, Dhaka, Bangladesh for advising me to choose a contemporary and most recent topic for this dissertation. I would like to do so for his numerous and meticulous supervision at various segments of this work. His interest and enthusiastic responses encouraged me to continue with my drafts keep writing.

I shall remain ever grateful to **Dr. Md. Kamrujjaman**, Associate Professor, Department of Mathematics, University of Dhaka, Dhaka, Bangladesh for gracing his valuable time in helping me to understand and generate some basic graphs using MATHEMATICA and MATHLAB.

I am also very grateful to **Professor Dr. Md. Anwar Hossain**, Honorary Professor, Department of Mathematics, University of Dhaka, Dhaka, Bangladesh, **Professor Dr. Amal Krishna Halder, Chairman**, Department of Mathematics, University of Dhaka, Dhaka, Bangladesh and **Professor Dr. Amulay Chandra Mandal**, Department of Mathematics, University of Dhaka, Dhaka, Bangladesh for delivering their right directions to complete this research work properly.

I would like to express my gratitude to all honorable **Teachers** of the **Department of Mathematics**, University of Dhaka, Dhaka, Bangladesh for their kind cooperation and useful mathematical discussions.

And I should express my gratitude to some other personnel of the department of mathematics who helped me to use computer lab and office equipments.

## **Abstract**

In this thesis, we discuss the constructions of the generalized Cantor sets which are the prototypical fractals and also discuss the Markov operators defined on separable complete metric space. We show that these special types of sets are Borel set as well as Borel measurable whose Lebesgue measures are zero. We formulate Iterated Function System of the Generalized Cantor Sets (IFSGCS for short) using affine transformation method and fixed points method of Devaney [1]. We find the Hausdorff dimension of the invariant set for iterated function system of generalized Cantor sets. We also formulate Iterated Function System with probabilities of the Generalized Cantor Sets (IFSPGCS for short). We show their invariant measures using Markov operators and Barnsley-Hutchinson multifunction. We observe that these functions satisfy the sweeping properties of Markov operator. In addition, we show that these iterated function system with probabilities are non-expansive and asymptotically stable if the Markov operator has the corresponding property. Further we study two dimensional fractals such as the Koch snowflake, the Koch curve, the Sierpinski triangles, the Sierpinski carpet, the box fractal and also three dimensional fractals such as the Menger sponge and the Sierpinski tetrahedron. We show fractal and topological dimensions and Lebesgue measures of those fractals. We also formulate iterated function system of higher dimensional fractals such as the square fractals, the Menger sponge, the Sierpinski tetrahedron and the octahedron fractal. We find the Hausdorff dimension of the invariant set for iterated function system of those fractals.

**Keywords:** Cantor set, Borel measure, Lebesgue measure, Iterated function system, Hausdorff dimension, Topological dimension, Invariant measure and Markov operator.

## **Acknowledgments**

It is my pleasure to acknowledge a deep gratitude to my guide **Professor Dr. Md. Shahidul Islam**, Department of Mathematics, University of Dhaka, Dhaka, Bangladesh for advising me to choose a contemporary and most recent topic for this dissertation. I would like to do so for his numerous and meticulous supervision at various segments of this work. His interest and enthusiastic responses encouraged me to continue with my drafts keep writing.

I shall remain ever grateful to **Dr. Md. Kamrujjaman**, Associate Professor, Department of Mathematics, University of Dhaka, Dhaka, Bangladesh for gracing his valuable time in helping me to understand and generate some basic graphs using MATHEMATICA and MATHLAB.

I am also very grateful to **Professor Dr. Md. Anwar Hossain**, Honorary Professor, Department of Mathematics, University of Dhaka, Dhaka, Bangladesh, **Professor Dr. Amal Krishna Halder, Chairman**, Department of Mathematics, University of Dhaka, Dhaka, Bangladesh and **Professor Dr. Amulay Chandra Mandal**, Department of Mathematics, University of Dhaka, Dhaka, Bangladesh for delivering their right directions to complete this research work properly.

I would like to express my gratitude to all honorable **Teachers** of the **Department of Mathematics**, University of Dhaka, Dhaka, Bangladesh for their kind cooperation and useful mathematical discussions.

And I should express my gratitude to some other personnel of the department of mathematics who helped me to use computer lab and office equipments.

# CONTENTS

Chapter	Page No.
<b>Introduction</b>	<b>xi-xiii</b>
<b>Chapter 1. Fractal Geometry</b>	<b>(1-15)</b>
1.1. History of Fractal Geometry	1-2
1.2. What's Fractal?	2-3
1.3. Types of Fractals	3-15
1.3.1. Geometric Fractals	3-10
1.3.1.1. The Cantor Set	3-4
1.3.1.2 Two Dimensional Fractals	4-8
1.3.1.2.1. The Von Koch Snowflake	4
1.3.1.2.2. The Koch Curve	5
1.3.1.2.3. The Sierpinski Gaskets or Triangles	5-7
1.3.1.3. Three Dimensional Fractals	8-10
1.3.1.3.1. The Menger Sponge	8
1.3.1.3.2. The Sierpinski Tetrahedron	9
1.3.1.3.3. The Octahedron Fractal	9-10
1.3.2. Algebraic Fractals	10-15
1.3.2.1. The Julia Sets	10-11
1.3.2.2. The Mandelbrot Set	11-13
1.3.3. The Stochastic Fractals	13-15
<b>Chapter 2. The Cantor Set Prototypical Fractal</b>	<b>(16-26)</b>
2.1. The Cantor Set	16
2.1.1. Construction of the Cantor middle $\frac{1}{3}$ set	16-17
2.1.2. Properties of the Cantor middle $\frac{1}{3}$ set	17-18
2.1.3. Construction of the Cantor middle $\frac{1}{5}$ set	18-19
2.1.4. Properties of the Cantor middle $\frac{1}{5}$ set	19-20
2.1.5. Construction of the Cantor middle $\frac{1}{7}$ set	20-21
2.1.6. Properties of the Cantor middle $\frac{1}{7}$ set	21-22

2.1.7. Construction of the Cantor middle $\frac{1}{2m-1}, (2 \leq m < \infty)$ set	22-18
2.1.8. Properties of the Cantor middle $\frac{1}{2m-1}, (2 \leq m < \infty)$ set	23
2.2. Lemma	24-25
2.3 Proposition	25-26
<b>Chapter 3. Fractal and Topological Dimensions of Fractals</b>	<b>(27-36)</b>
3.1. Basic Definitions and Formulas	27-28
3.2. Fractal and Topological Dimensions of the Generalized Cantor Sets	28-30
3.2.1. Fractal and Topological Dimension of the Cantor middle $\frac{1}{3}$ set	28
3.2.2. Fractal and Topological Dimension of the Cantor middle $\frac{1}{5}$ set	28-29
3.1.3. Fractal and Topological Dimension of the Cantor middle $\frac{1}{7}$ set	29
3.1.4. Fractal and Topological Dimension of the Cantor middle $\frac{1}{2m-1}, (2 \leq m < \infty)$ set	29-30
3.3. Fractal and Topological Dimensions of Two Dimensional Fractals	30-34
3.3.1. Construction of the Koch Curve	30
3.3.2. Construction of the Sierpinski Gasket or Equilateral Triangle	31
3.3.3. Construction of the Sierpinski Carpet	31-32
3.3.4. Construction of the Box Fractal	32-33
3.3.5. Construction of the Square Fractals	33-34
3.4. Fractal and Topological Dimensions of Three Dimensional Fractals	34-36
3.4.1. Construction of the Menger Sponge	34-35
3.4.2. Construction of the Sierpinski Tetrahedron	35-36
3.4.3. Construction of the Octahedron Fractal	36
<b>Chapter 4. Fractals in Measure Space</b>	<b>(37-47)</b>
4.1. Basic Measure Theory	37-39
4.2. Lebegues Measures of the Generalized Cantor Sets	39-42
4.3. Lebegues Measures of the Two Dimensional Fractals	43-45
4.4. Lebegues Measures of the Three Dimensional Fractals	45-47
<b>Chapter 5. Iterated Function Systems of Fractals</b>	<b>(48-80)</b>
5.1 Iterated Function Systems of Fractals	48-51
5.2 Iterated Function Systems of the Generalized Cantor Sets	51-56

5.2.1. Iterated Function System of the Cantor middle $\frac{1}{3}$ set	51-52
5.2.2. Iterated Function System of the Cantor middle $\frac{1}{5}$ set	52-53
5.2.3. Iterated Function System of the Cantor middle $\frac{1}{7}$ set	53-54
5.2.4. Iterated Function System of the Cantor middle $\frac{1}{2m-1}, (2 \leq m < \infty)$ set	55
5.3. Iterated Function System of the Two Dimensional Fractals	56-62
5.3.1. Iterated Function System of the Koch Snowflake	56-58
5.3.2. Iterated Function System of the Koch curve	58-59
5.3.3. Iterated Function System of the Sierpinski Equilateral Triangle	59-61
5.3.4. Iterated Function System of the Sierpinski Isosceles Triangle	61-62
5.3.5. Iterated Function System of the Sierpinski Isosceles Right Triangle	62-63
5.3.6. Iterated Function System of the Sierpinski Scalene Triangle	64-65
5.3.7. Iterated Function System of the Sierpinski Carpet	65-66
5.3.8. Iterated Function System of the Box Fractal	66-68
5.3.9. Iterated Function System of the Square Fractals	68-71
5.4. Iterated Function System of Three Dimensional Fractals	71-80
5.4.1 Iterated Function System of the Menger Sponge	71-75
5.4.2 Iterated Function System of the Sierpinski Tetrahedron	75-77
5.4.3 Iterated Function System of the Octahedron Fractal	78-80
<b>Chapter 6. Markov Operators</b>	<b>(81-90)</b>
6.1. Markov Operators	81-86
6.1.1. Markov Operators on $L^1(X)$	81-83
6.1.2. Markov Operators on Measures	83-85
6.1.2.1. Properties of Markov Operators	85
6.2. Existence of Stationary Distribution	86
6.3. A Criterion of Asymptotic Stability	86-88
6.4. Sweeping Properties Associated to Iterated Function System of the Generalized Cantor Sets	88-90
<b>Chapter 7. Hausdorff Measures of Fractals</b>	<b>(91-110)</b>
7.1. Basic Measure Theory on Euclidean Space	91
7.2. Hausdorff Measure and Hausdorff Dimension	91-96
7.2.1. Hausdorff Measure	91-92
7.2.1.1. Definition of Hausdorff Measure	92
7.2.1.2. Some Properties of Hausdorff Measure	92-94

7.2.2. Housdorff Dimension (HD)	94-96
7.2.2.1. Some Properties of Housdorff Dimension	95-96
7.2.2.2. Housdorff Dimension of the Cantor middle $\frac{1}{3}$ set	96-100
7.3. Housdorff Dimensions (HD) of the Invariant Sets for IFS of Fractals	100-110
7.3.1. HD of the Invariant Set for IFS of the Cantor middle $\frac{1}{3}$ set	100-101
7.3.2. HD of the Invariant Set for IFS of the Cantor middle $\frac{1}{5}$ set	101
7.3.3. HD of the Invariant Set for IFS of the Cantor middle $\frac{1}{7}$ set	101
7.3.4. HD of the Invariant Set for IFS of the Cantor middle $\frac{1}{2m-1}$ set	102
7.4. Housdorff Dimensions (HD) of the Invariant Sets for IFS of 2D Fractals	103-107
7.4.1. HD of the Invariant Set for IFS of the Koch curve	103
7.4.2. HD of the Invariant Set for IFS of the Sierpinski isosceles triangles	103
7.4.3. HD of the Invariant Set for IFS of the Sierpinski Carpet	104
7.4.4. HD of the Invariant Set for IFS of the Box Fractal	105
7.4.5. HD of the Invariant Set for IFS of the Square Fractals	106-107
7.5. Housdorff Dimensions (HD) of the Invariant Sets for IFS of 3D Fractals	108-110
7.5.1. HD of the Invariant Set for IFS of the Menger Sponge	108-109
7.5.2. HD of the Invariant Set for IFS of the Sierpinski Tetrahedron	109-110
7.5.3. HD of the Invariant Set for IFS of the Octahedron Fractal	110
<b>Chapter 8. Invariant Measures for IFS of Fractals</b>	<b>(111-120)</b>
8.1. Iterated Function System with Probabilities	111-112
8.2. Invariant Measure (IM)	112
8.3. Iterated Function System with Probabilities of the Generalized Cantor Sets	112-116
8.3.1. IFS with Probabilities of the Cantor middle $\frac{1}{3}$ set	112-113
8.3.2. IFS with Probabilities of the Cantor middle $\frac{1}{5}$ set	113-114
8.3.3. IFS with Probabilities of the Cantor middle $\frac{1}{2m-1}$ set	115-116
8.4. Invariant Measures (IM) for IFS with Probabilities of the G. Cantor Set	117-119
8.4.1. IM for IFS with Probabilities of the Cantor middle $\frac{1}{3}$ set	117

8.4.2. IM for IFS with Probabilities of the Cantor middle $\frac{1}{5}$ set	118-119
8.4.3. IM for IFS with Probabilities of the Cantor middle $\frac{1}{2m-1}$ set	119
8.5. Proposition	119-120
<b>Chapter 9. Dynamics of the Prototypical Fractal</b>	<b>(121-131)</b>
9.1. Barnsley's and Hutchinson Approach to Fractal Geometry	121-122
9.2. IFS with Probabilities of the Generalized Cantor sets (GCS)	122-125
9.3. Non-expansiveness of IFS with probabilities of the GCS	125-128
9.4. Asymptotic stability of IFS with probabilities of the GCS	129-131
<b>Chapter 10. Scientific Approach of Fractals</b>	<b>(132-138)</b>
10.1. Fractals in Nature and Applications	132-134
10.1.1. Fractals in Astronomy	132
10.1.2. Fractals in Nature	132
10.1.3. Fractals in Computer Science	133
10.1.4. Fractals in Fluid Mechanics	133
10.1.5. Fractals in Surface Physics	133
10.1.6. Fractals in Physiology and Medicine	133
10.1.6.1. Fractals in Physiology	
10.1.6.2. Fractals in Biological Time Series	
10.1.7. Fractals in Telecommunications	134
10.2. Some Applications of Fractals by Renowned Mathematicians	115-118
10.2.1. Fractals and Cancer	134
10.2.2. Microbial Growth Patterns described by Fractal Geometry	134
10.2.3. Fractals in the Nucleus	134-135
10.2.4. Fractal Geometry of Airway Remodeling in Human Asthma	135
10.2.5. Image Compression: A study of the iterated transform method	135
10.2.6. Image Coding Based on a Fractal Theory of Iterated Contractive Image Transformations	135-136
10.2.7. Fractal Block Coding Method Based on Iterated Function Systems	136
10.2.8. Iterated Function Systems Controlled by a Semi-Markov Chain	137
10.2.9. Five Vertices and a Compression Factor of 2.5	138
<b>Appendix. Algorithms of Fractals</b>	<b>(139-148)</b>
<b>References</b>	<b>(149-151)</b>



# ABSTRACT

In this thesis, we discuss the constructions of the generalized Cantor sets which are the prototypical fractals and also discuss the Markov operators defined on separable complete metric space. We show that these special types of sets are Borel set as well as Borel measurable whose Lebesgue measures are zero. We formulate Iterated Function System of the Generalized Cantor Sets (IFSGCS) using affine transformation and fixed points method. We discuss the Hausdorff dimension of the invariant set for iterated function system of generalized Cantor sets. We also formulate Iterated Function System with probabilities of the Generalized Cantor Sets (IFSPGCS). We show their invariant measures using Markov operators and Barnsley-Hutchinson multifunction. We observe that these functions satisfy the sweeping properties of Markov operator. In addition, we show that these iterated function systems with probabilities are non-expansive and asymptotically stable if the Markov operator has the corresponding property. Further we study two dimensional fractals such as the Koch snowflake, the Koch curve, the Sierpiński triangles, the Sierpiński carpet, the box fractal and also three dimensional fractals such as the Menger sponge and the Sierpinski tetrahedron. We show fractal and topological dimensions and Lebesgue measures of those fractals. We formulate iterated function system of higher dimensional fractals such as the square fractals, the Menger sponge, the Sierpinski tetrahedron and the octahedron fractal. We also discuss the Hausdorff dimension of the invariant set for iterated function system of those fractals.

**Keywords:** Cantor set, Borel measure, Lebesgue measure, Iterated function system, Hausdorff dimension, Topological dimension, Invariant measure and Markov operator.

# INTRODUCTION

Dynamics is an iterative process of objects; fractals are the attractors of iterated function systems that are static images. In recent years, the most chaotic regions for dynamical systems are fractals. The study of the geometric structure of fractals has significant roles understanding chaotic behavior of dynamical systems.

A Fractal, as defined by B. Mandelbrot, “is a shape made of parts similar to the whole in some way” [1]. A Fractal is a geometric object with two important properties: (i) self-similarity; (ii) non-integer dimension.

A non-empty set  $\Gamma \subset \mathbf{R}$  is called a Cantor set if (a)  $\Gamma$  is closed and bounded, (b)  $\Gamma$  contains no intervals, (c) Every point in  $\Gamma$  is an accumulation point of  $\Gamma$ . The Cantor set is the prototypical fractal [2]. The Cantor sets were discovered by the German George Cantor in the late 19th to early 20th centuries (1845-1918). He introduced fractal which has come to be known as the Cantor set, or Cantor dust.

We study the Cantor set and find the generalized Cantor sets and show its dynamical behaviors and fractal dimensions [3]. The Cantor middle  $\frac{1}{3}, \frac{1}{5}, \frac{1}{7}, \frac{1}{9}, \frac{1}{11}, \dots$  sets, in

general, the Cantor middle  $\frac{1}{2m-1}$ , ( $2 \leq m < \infty$ ) is called the generalized Cantor sets and it

is denoted by  $C_{1/(2m-1)}$  which is defined by the algorithm and also defined by the shrinking process. We study the generalized Cantor sets in measure space and find that these special types of sets are Borel set as well as Borel measurable whose Lebesgue measure is zero [4]. Then we formulate iterated function system of the generalized Cantor sets using Barnsley-Hutchinson multifunction [5] and show the Hausdorff dimension of the invariant sets for the IFSGCS. We also show the sweeping properties of Markov operator for IFSGCS. We formulate iterated function system with probabilities of generalized Cantor sets and shown their invariant measures using Markov operator and Barnsley-Hutchison multifunction in [6].

Then we study asymptotic stability of Markov operators define on locally compact space, which show the utility of the lower bound function technique in proving the convergence of iterates (asymptotic stability) for this class of operators [7]. This criterion is applied to iterated function system of generalized Cantor sets. In particular it is shown that iterated function system of the generalized Cantor sets are non-expansiveness and asymptotically stable if the Markov operator  $P_w$  has the corresponding property.

Finally, we study two dimensional fractals such as the Sierpi ski triangles, the Koch snowflake, the Koch curve, the Sierpi ski carpet, the box fractal, the square fractals and also three dimensional fractals such as the Menger sponge, the Sierpinski tetrahedron. We

show fractal and topological dimensions and Lebesgue measures of those fractals. The main aim is to formulate the iterated function system of higher dimensional fractals and show the Hausdorff dimension of the invariant set for iterated function system of those fractals. To the best of my knowledge first time we formulate iterated function system of three dimensional fractals such as the Menger sponge, the Sierpinski tetrahedron and the octahedron fractal also we formulate iterated function system of two dimensional the square fractals using the Cantor middle  $\frac{1}{3}$  set and the Cantor middle  $\frac{1}{5}$  set respectively.

**In Chapter 1**, we introduce a number of fractals that are created by a specific set of rules. Such fractals are referred to as deterministic fractals because their fate is determined by successive applications of the rules. All rules divide an image into smaller pieces, similar to the original and congruent to each other and then remove some of those pieces.

**In Chapter 2**, we discuss the construction and the properties of the classical Cantor set. We study the Cantor set and find the generalized Cantor sets. The Cantor middle  $\frac{1}{3}, \frac{1}{5}, \frac{1}{7}, \frac{1}{9}, \frac{1}{11}, \dots$  sets, in general, the Cantor middle  $\frac{1}{2m-1}$ , ( $2 \leq m < \infty$ ) sets are called the generalized Cantor sets and it is denoted by  $C_{1/(2m-1)}$ .

**In Chapter 3**, we discuss the constructions of the two and three dimensional fractals. We show fractal dimensions and topological dimensions of the one, two and three dimensional fractals.

**In Chapter 4**, we show that the special type generalized Cantor sets are Borel set as well as Borel measurable and whose Lebesgue measure is zero. Also we show that the Lebesgue measures of the two and three dimensional fractals are zero.

**In Chapter 5**, we formulate iterated function system of the generalized Cantor sets, two dimensional fractals such as the box fractal and the square fractals and also three dimensional fractals such as the Menger sponge, the Sierpinski tetrahedron and the octahedron fractal.

**In Chapter 6**, we discuss the properties of Markov operator on measure space. We show its applications to iterated function system of the generalized Cantor sets.

**In Chapter 7**, we discuss basic measure theory, Hausdorff measure and Hausdorff dimension. We show the Hausdorff measures and Hausdorff dimensions of the invariant

sets for iterated function system of the Generalized Cantor sets and also we show the Hausdorff measures and Hausdorff dimensions of the invariant sets for iterated function system of the two and three dimensional fractals.

**In Chapter 8**, we discuss iterated function system with probabilities and invariant measures. We formulate iterated function system with probabilities of the generalized Cantor sets and show their invariant measures using Barnsley-Hutchinson multifunction and Markov operator.

**In Chapter 9**, we define the transition operator  $P_w$  for iterated function system with probabilities of the generalized Cantor sets and show that this operator is a Markov operator. We show that the Iterated Function System with Probabilities of the Generalized Cantor sets is non-expansive and asymptotically stable if the Markov operator  $P_w$  has the corresponding property with respect to the metric  $\{(\dots(x, y))\}$ .

**In Chapter 10**, we survey some applications of fractals by renowned mathematicians. This section is ended with a comment to peruse further research.

# CHAPTER ONE

## FRACTAL GEOMETRY

### OVERVIEW

In this chapter, we discuss historical background of fractal geometry. There are two major variations of fractals such as deterministic fractals and random fractals. Deterministic fractals are composed of several scaled and rotated copies of itself such as algebraic fractals and geometric fractals. Random fractals consist of those fractals which exhibit property of statistical self-similarity. We discuss all types of fractals.

### 1.1. History of Fractal Geometry

The mathematics behind fractals began to take shape in the 17th century when the mathematician and philosopher Gottfried Leibniz considered recursive self-similarity. It was not until 1872 that a function appeared whose graph would today be considered fractal, when Karl Weierstrass gave an example of a function with the non-intuitive property of being everywhere continuous but nowhere differentiable.

In 1883, Georg Cantor also gave examples of subsets of the real line with unusual properties- these Cantor sets are also now recognized as fractals, which was self-similar. It was discovered by Henry John Stephen Smith in 1874.

In 1904, Helge von Koch, dissatisfied with Weierstrass's abstract and analytic definition, gave a more geometric definition of a similar function, which is now called the Koch curve. Waclaw Sierpinski constructed his triangle in 1915 and, one year later, his carpet. Also Paul Pierre Lévy described a self-similar curves in his paper "*Plane or Space curves and surfaces consisting of parts similar to the whole*" in 1938. The Lévy C curve was a new fractal curve.

In the 1960s, Benoit Mandelbrot started investigating self-similarity that was on earlier work by Lewis Fry Richardson, in his paper "*How Long is the Coast of Britain? Statistical Self-similarity and Fractional Dimension*" in 1967.

Finally, in 1975 Mandelbrot coined the term 'fractal' to denote an object whose Hausdorff–Besicovitch dimension is greater than its topological dimension. He illustrated this mathematical definition with striking computer-constructed visualizations. These images captured the popular imagination; many of them were based on recursion, leading to the popular meaning of the term 'fractal'.

Iterated functions in the complex plane were investigated in the late 19<sup>th</sup> and early 20<sup>th</sup> centuries by Henri Poincaré, Felix Klein, Pierre Fatou and Gaston Julia. Without the aid of modern computer graphics, however, they lacked the means to visualize the beauty of many of the objects that they had discovered.

Iterated functions in the complex plane were investigated in the late 19<sup>th</sup> and early 20<sup>th</sup> centuries by Henri Poincaré, Felix Klein, Pierre Fatou and Gaston Julia. Without the aid of modern computer graphics, however, they lacked the means to visualize the beauty of many of the objects that they had discovered. The mathematical concept of a fractal was

discovered by French mathematician Gaston Julia. Julia was interested in the set of points defined by iteration of functions.

In 1975, Benoit Mandelbrot observed that geometric objects like the Cantor set and the Sierpinski triangle were not mathematical pathologies. Rather, these complicated sets provided a geometry that is in many ways more natural than classical Euclidean geometry for describing intricate objects in nature such as coastlines and snowflakes. Thus was born fractal geometry.

## 1.2. What's a Fractal?

The word 'fractal' is related to the Latin verb *frangere*, which means "to break". In the Raman mind, *frangere* may have evoked the action of breaking a stone; since the adjective derived it combines the two most obvious properties of broken stones, irregular and fragmentation. This adjective is *fractus*, which lead to fractal. The etymological kinship with "fraction" is also significant if ones interprets "fraction" as a number that lies between integers. Indeed, a fractal set can be considered as lying between the shapes of Euclid.

In his founding paper, "*Fractal: Form, Chance and Dimension*" Benoit Mandelbrot coined the term Fractal, and described it as follows:

*A fractal is a rough or fragmented geometric shape that can be subdivided in parts, each of which is (at least approximately) a reduced-size copy of the whole.*

The word 'fractal' is derived from the Latin word *fractus* meaning broken, and is a collective name for a diverse class of geometrical objects, or sets, holding most of, or all of the following properties [8].

1. The set has a fine structure; it has details on arbitrary scales.
2. The set is too irregular to be described with classical Euclidean geometry, both locally and globally.
3. The set has some form of self-similarity; this could be approximate or statistical self-similarity.
4. Usually, the 'fractal dimension' of the set is strictly greater than its Topological dimension.
5. In most cases of interest the set has a very simple definition, that is, it can be defined recursively.

Property (4) is Mandelbrot's original definition of a fractal; however, this property has been proven not to hold for all sets that should be considered fractal. In fact, each of the above properties has been proven not to hold for at least one fractal.

Several attempts to give a Pure Mathematical Definition of Fractals have been proposed, but all proven unsatisfactory.

### Mathematical Definition of Fractal:

*A fractal is a subset of  $R^n$  which is self-similar and whose fractal dimension exceeds its topological dimension.*

Fractals can be classified in numerous manners, of which one stands out rather distinctly: exact (regular) fractals versus statistical (random) fractals. An exact fractal is an “object which appears self-similar under varying degrees of magnification in effect, possessing symmetry across scale with each small part replicating the structure of the whole.” On the other hand, the object replicates itself in its statistical properties only; it is defined as a “statistical fractal.” Statistical fractals have been observed in many physical systems, ranging from material structures (polymers, aggregation, interfaces, etc.) to biology, medicine, electric circuits, computer interconnects, galactic clusters, and many other surprising areas, including stock market price fluctuations [9].

### 1.3. Types of Fractals

There are two major variations of Fractals [10]

1. Deterministic Fractal
2. Random Fractal

The first category consists of those fractals that are composed of several scaled and rotated copies of itself such as Koch curve, Sierpinski triangles and Sierpinski carpet. They are called Geometric fractals. Julia set also falls in same category. The whole set can be obtained by applying a non-linear iterated map to all arbitrary small section of it. Thus the structure of Julia set is already contained in any small fraction. They are called algebraic fractals. Thus both algebraic and geometric fractals are termed deterministic fractals. If the generation requires use of a particular mapping or rule which repeated recursively over and over again, they exhibit the property of strict self-similarity. The second category consists of those fractals which have an additional element of randomness allowing for simulation of natural phenomenon. So they exhibit property of statistical self-similarity.

#### 1.3.1. Geometric Fractals

The fractals of this class are visual. These fractals are created from repeating a process or pattern over and over again.

##### 1.3.1.1. The Cantor Set

The Cantor set is created by removing the middle third segment of a unit line segment. Begin with the closed interval  $\Gamma_0 = [0,1]$  shown in Figure 1.1. Remove the middle open third. This leaves a new set  $\Gamma_1$ . Each iteration through the algorithm removes the open middle third from each segment of the previous iteration. Thus the next set would be  $\Gamma_2$ . In general, after  $n$  times iterations, we obtain  $\Gamma_n$  for all  $n \in \mathbf{N}$ , which consists of  $2^n$  closed intervals all of which the same length  $\frac{1}{3^n}$ . The Cantor middle third set is the

“limiting set” of this process, that is,  $C = \bigcap_{n=1}^{\infty} \Gamma_n$  and call it the Cantor middle  $\frac{1}{3}$  set.

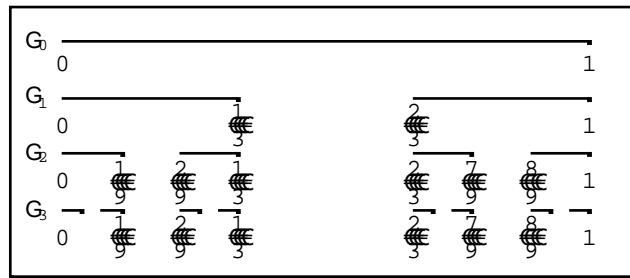


**Figure 1.1** Construction of the Cantor middle  $\frac{1}{3}$  set

**1.3.1.2. Two Dimensional Geometric Fractals**

Two classical examples of two dimensional geometric fractals are as follows:

1. The Von Koch Snowflake
2. The Seirpinski gasket or triangle

**1.3.1.2.1. [1] The Von Koch Snowflake**

The Koch snowflake is generated by an infinite succession of additions. Begin with the boundary of an equilateral triangle with sides of length 1. Remove the middle third of each side of the triangle just as we did in the construction of the Cantor set. This time, however, we replace each of these pieces with two pieces of equal length, giving star-shaped region depicted in Figure 1.2. This new figure has twelve sides, each of length  $\frac{1}{3}$ . Each iteration through the algorithm removes the middle third from each segment of the previous iteration and replace it with a triangular “bulge” made of two pieces of length  $\frac{1}{9}$ . The result is also shown in Figure 1.2.

We continue this process over and over. The ultimate result is a curve that is infinitely wiggly-there are no straight lines in it whatsoever. This object is called the Koch snowflake. Clearly, there are pieces of the Koch snowflake that are self-similar.

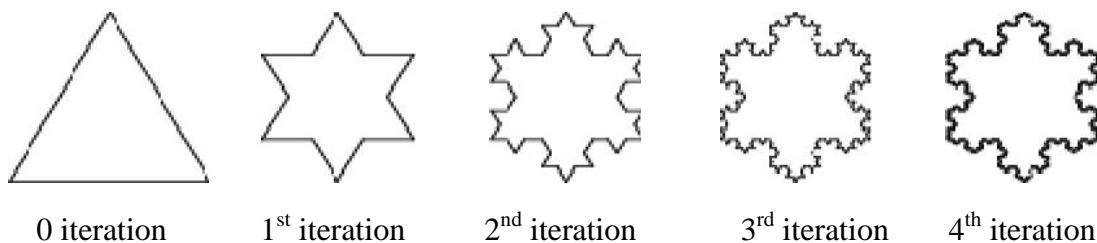


**Figure 1.2** Construction of the Koch snowflake



### 1.3.1.2.2. The Koch Curve

In two-dimensional case they are made of a broken line (or of a surface in three-dimensional case) so-called the generator. Each of the segments which form the broken line is replaced by broken line generator at corresponding scale for a step of algorithm. As a result of infinite repeating the steps geometrical fractal arises.

The process of construction begins from the segment of single length. It is zero generator of the Koch curve. Then each of section (one segment in zero generation) is replaced by formative element defined as Figure 1.3 as  $n=1$ . As a result of the substitution we get the next generation of the Koch curve. There are four rectilinear sections length  $\frac{1}{3}$  when the first generation is. Thus to produce the next generation all of the section of previous generation are replaced by diminished formative element. The curve of  $n$ -th generation is called prefractal when  $n$  is finite quantity. When  $n$  is infinite quantity the curve is considered a fractal object. [11]

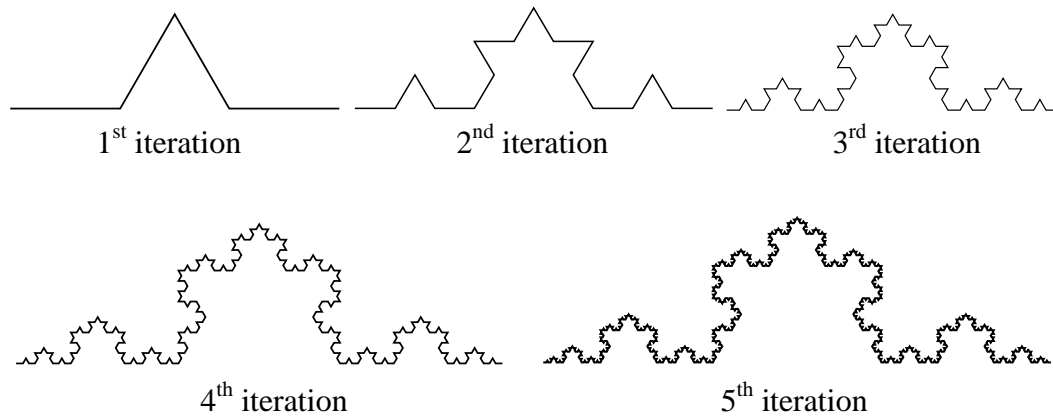


**Figure 1.3** Construction of the Koch curve

### 1.3.1.2.3. [1] The Sierpinski Gasket or Triangle

Like the Cantor middle-third set, this object may also be obtained by an infinite sequence of 'removals'. Begin with the equilateral triangle shown in Figure 1.4. Then remove from the middle a triangle whose dimensions are exactly half that of the original triangle. This leaves three smaller equilateral triangles, each of which has dimensions one-half the dimensions of the original triangle. Now continue this process. Remove the middle portions of each of the remaining triangles, leaving nine equilateral triangles. In general, after  $n$  times iterations, we remove  $3^n$  open triangles of size  $\frac{1}{2^n}$  from each to form the previous images. The resulting image after carrying this procedure to the limit and is called the Sierpinski triangle.

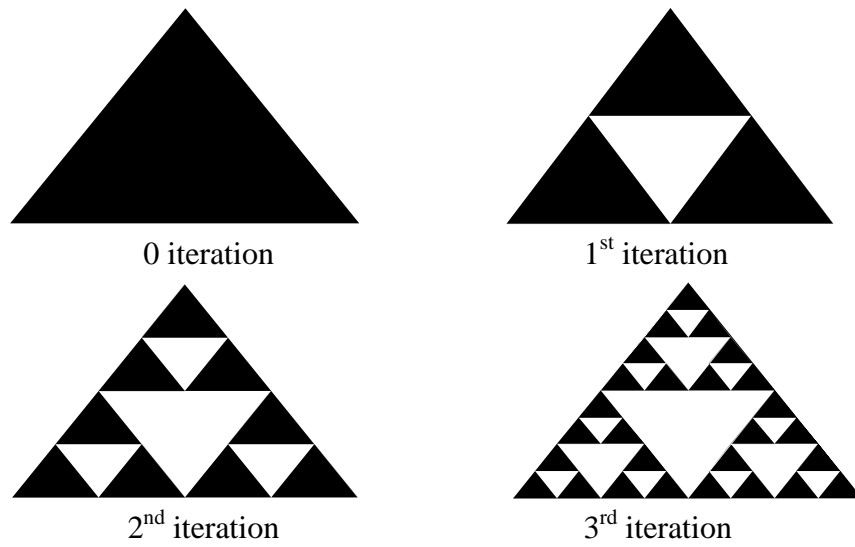


**Figure 1.4** Construction of the Sierpinski triangle

There are many fractals that may be constructed via variations on this theme of infinite removals. For example, we may construct a similar sets by beginning with a isocetes right triangle and a scalene triangle, as in Figure 1.5, Figure 1.6.

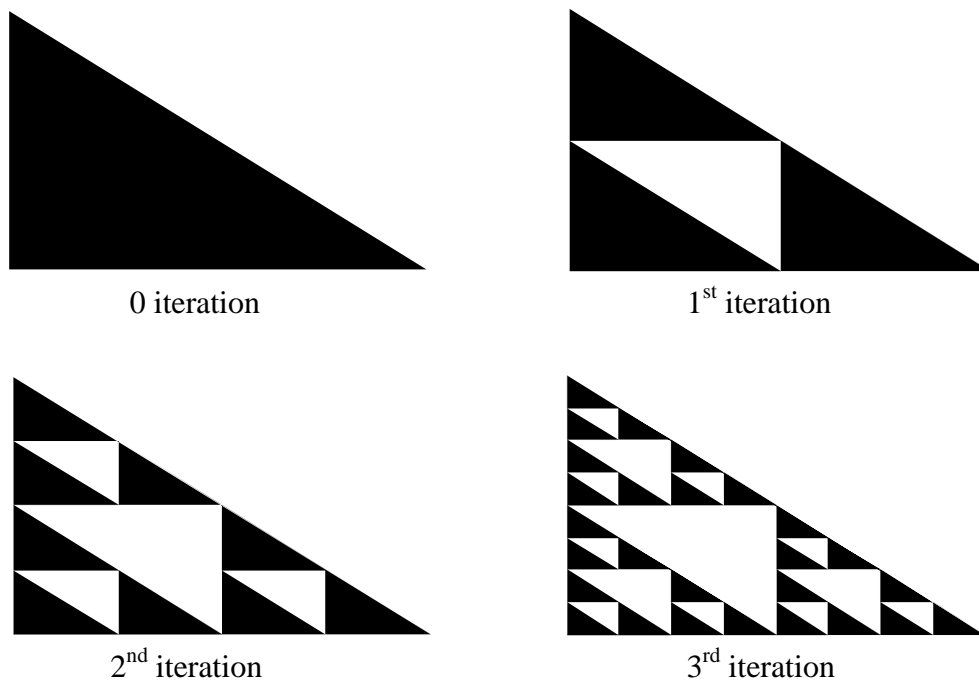


**Figure 1.5** Construction of the Sierpinski right isosceles triangle

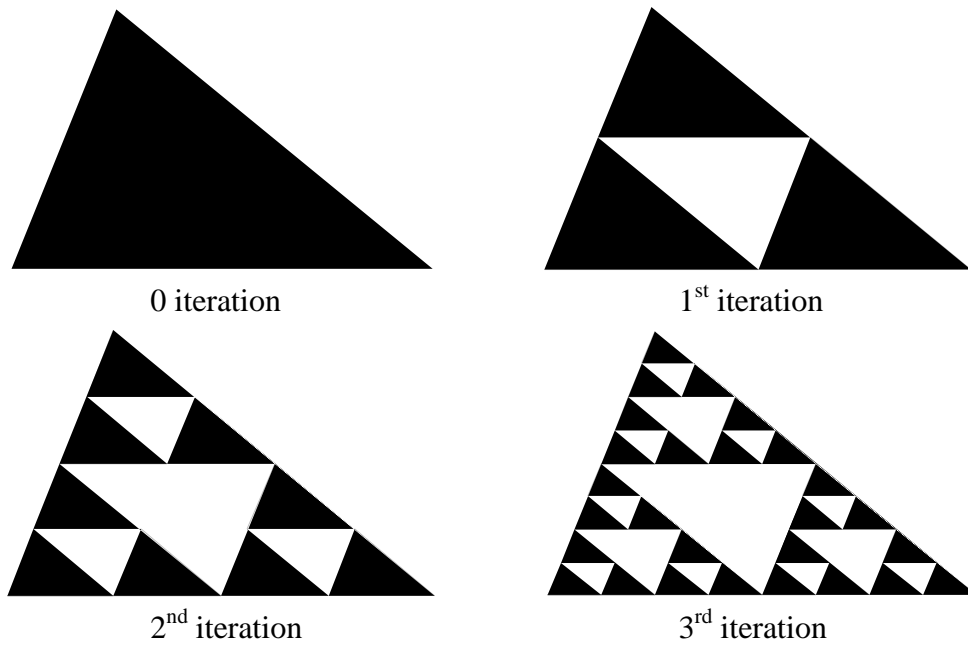


**Figure 1.6** Construction of the Sierpinski scalene triangle

Another fractals, the “Sierpinski carpet” fractal is obtained by successively removing middle square whose sides are one-third as long as their predecessor, as shown in Figure 1.7. The “box” fractal is obtained by successively removing squares whose sides are one-third as long as their predecessors, as shown in Figure 1.8.

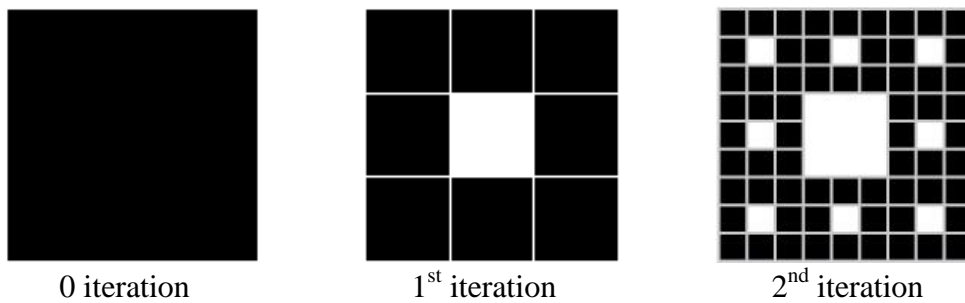


**Figure 1.7** Construction of the Sierpinski carpet

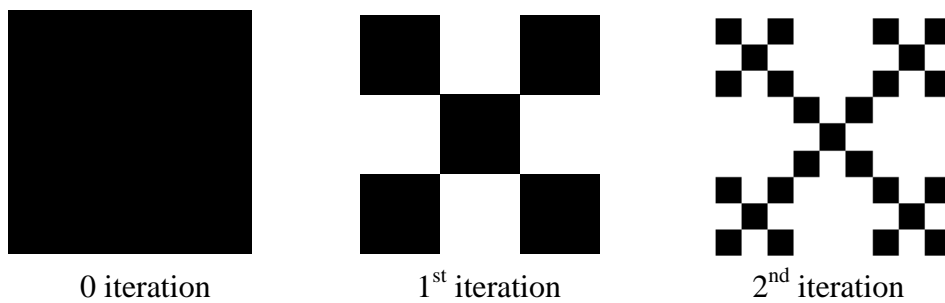


**Figure 1.8** Construction of the box fractal

Similarly, we construct the “square” (using the Cantor middle one-third set) fractal which is obtained by removing squares whose sides are one-third as long as their predecessor, as shown in Figure 1.9.

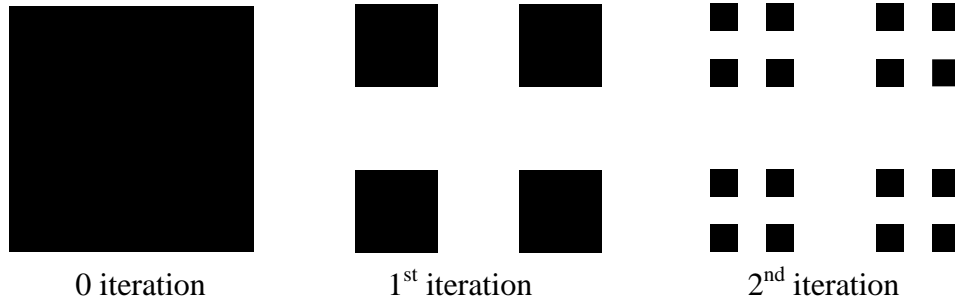


**Figure 1.9** Construction of the square fractal (using the Cantor middle third set)

**1.3.1.3. Three Dimensional Geometric Fractals**

Two classical examples of three dimensional geometric fractals are as follows:

1. The Menger sponge
2. The Sierpinski tetrahedron

**1.3.1.3.1. The Menger Sponge**

The Menger sponge is a fractal curve also known as the Menger universal curve. It is a three-dimensional generalization of the Cantor set and the Sierpinski carpet. Begin with a closed (filled) unit cube shown in Figure 1.10. Divide every face of the cube into 9 cubes, like a Rubik’s cube (Magic cube). This will sub-divide the cube into 27 smaller cubes. We remove the smaller cube in the middle of each face and remove the smaller cube in the very center of larger cube; totally we remove 7 open cubes of size  $\frac{1}{3}$  and leaving 20 smaller cubes. Now continue the process. Remove the smaller cube in the middle of each of the remaining cubes, we remove 7.20 open cubes of size  $\frac{1}{9}$  and leaving  $(20)^2$  smaller cubes. In general,  $n$  time’s iterations, we remove  $7.(20)^{n-1}$  open cubes of size  $\frac{1}{3^n}$ . The Menger sponge itself is the limit of this process after an infinite number of iterations.

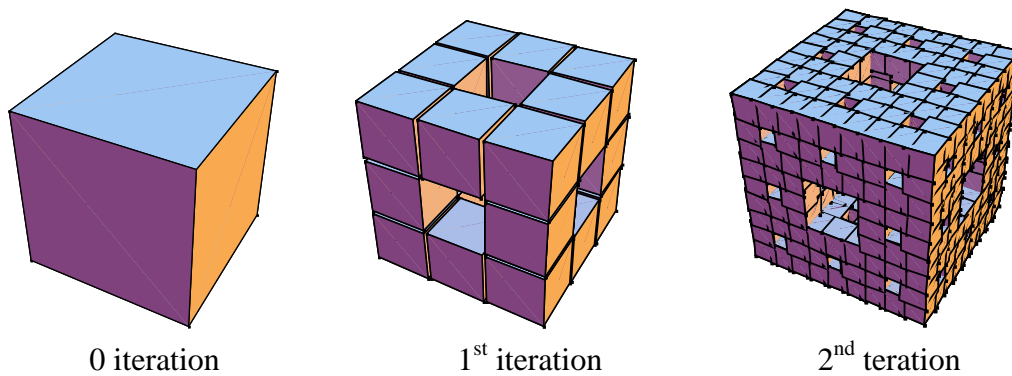


**Figure 1.10** Construction of the Menger sponge

### 1.3.1.3.2. The Sierpinski Tetrahedron

Like the Menger sponge, this object may also be obtained by an infinite number of iterations. Begin with a closed (filled) tetrahedron with unit edge shown in Figure 1.11. Divide every face of the tetrahedron into 3 triangles. This will sub-divide the tetrahedron into 8 smaller tetrahedrons. We remove the smaller tetrahedron in the middle of each face and remove the smaller tetrahedron in the very center of larger tetrahedron; totally we remove 4 open tetrahedrons of size  $\frac{1}{2}$  and leaving 4 smaller tetrahedron. Now continue this process. Remove the smaller cube in the middle of each of the remaining cubes, we remove 4.4 open tetrahedron of size  $\frac{1}{4}$  and leaving  $(4)^2$  smaller tetrahedrons. In general,  $n$  time's iterations, we remove  $4.4^{n-1}$  open cubes of size  $\frac{1}{2^n}$ . The Sierpinski tetrahedron itself is the limit of this process after an infinite number of iterations.

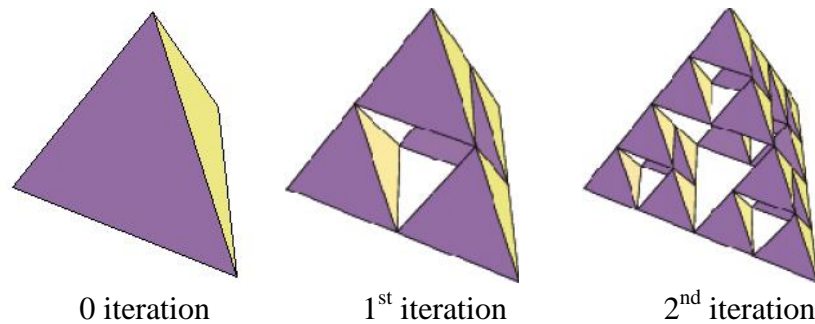


**Figure 1.11** Construction of the Sierpinski tetrahedron

Similarly, we construct another three dimensional fractal, the ‘octahedron’ fractal is obtained by the following algorithm:

### 1.3.1.3.3. The Octahedron Fractal

Begin with a closed (filled) octahedron with unit edge shown in Figure 1.12. Divide every face of the octahedron into 3 triangles. This will sub-divide the octahedron into 8 smaller octahedrons. We remove the octahedron in the middle of each face and remove the smaller octahedron in the very center of larger octahedron; totally we remove 2 open octahedrons of edge size  $\frac{1}{2}$ . and leaving 6 smaller octahedron. Now continue this process. Remove the smaller octahedron in the middle of each of the remaining octahedron, we remove 2.6 open octahedron of size  $\frac{1}{4}$  and leaving  $6^2$  smaller octahedrons. In general, after  $n$  time's iteration, we remove  $2.6^{n-1}$  open octahedrons of edge size  $\frac{1}{2^n}$ . The octahedron fractal itself is the limit of this process after an infinite number of iterations.

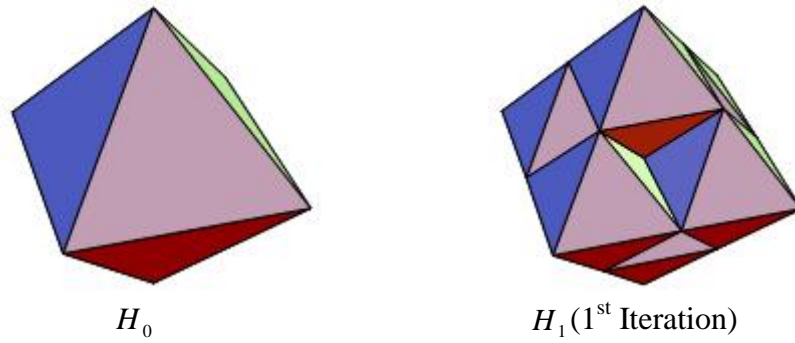


**Figure 1.12** Construction of the octahedron fractal

### 1.3.2. Algebraic Fractals

Algebraic fractal is the biggest class of fractals. These fractals are created by an equation over and over in  $n$ -dimensional spaces. Two classical examples of algebraic fractals are as follows:

1. The Julia set
2. The Mandelbrot set

#### 1.3.2.1. [8] The Julia Set

The Julia set is the place where all of the chaotic behavior of a complex function occurs. We consider the functions  $f : \mathbf{C} \rightarrow \mathbf{C}$  of the form  $f = z^2 + c$ , where both  $z$  and  $c$  are complex numbers. For the simplest case,  $c = 0$ , we have  $f(z) = z^2$  and  $|f(z)| = |z^2| = |z|^2$ .

- (i) If  $|z| < 1$  then  $f^n(z) \rightarrow 0$ .
- (ii) If  $|z| > 1$  then  $f^n(z) \rightarrow \infty$ .
- (iii) If  $|z| = 1$  then  $|f^n(z)| = 1$  for all  $n$ .

Thus the circle  $|z| = 1$  is the boundary between these two types of behavior, and is the Julia set for  $f(z) = z^2$ .

Now consider  $f = z^2 + c$ , where  $c$  is a small complex number. We get a closed curve  $J$ , such that if  $z$  is inside of  $J$ , then  $f^n(z) \rightarrow z_0$  for some  $z_0$  close to 0, and if  $z$  is outside of  $J$ , then  $|f^n(z)| \rightarrow \infty$ . For  $c \neq 0$  and small this curve  $J$  is a fractal curve.

**Definition 1.3.2.1.1. [8]** For  $f = z^2 + c$ , we define

$$F = \{z : |f^n(z)| \text{ does not tend to infinity}\} = \{z : f^n(z) \text{ is a bounded sequence}\}$$

to be the filled Julia set of  $J$ . We define the Julia set  $J$  of  $f$  to be boundary of the filled Julia set, that is,  $J = \overline{F} \setminus \text{int}(F)$ .

For example, if  $c = 0.27 + 0.53i$ , then the filled Julia sets shown in Figure 1.13.

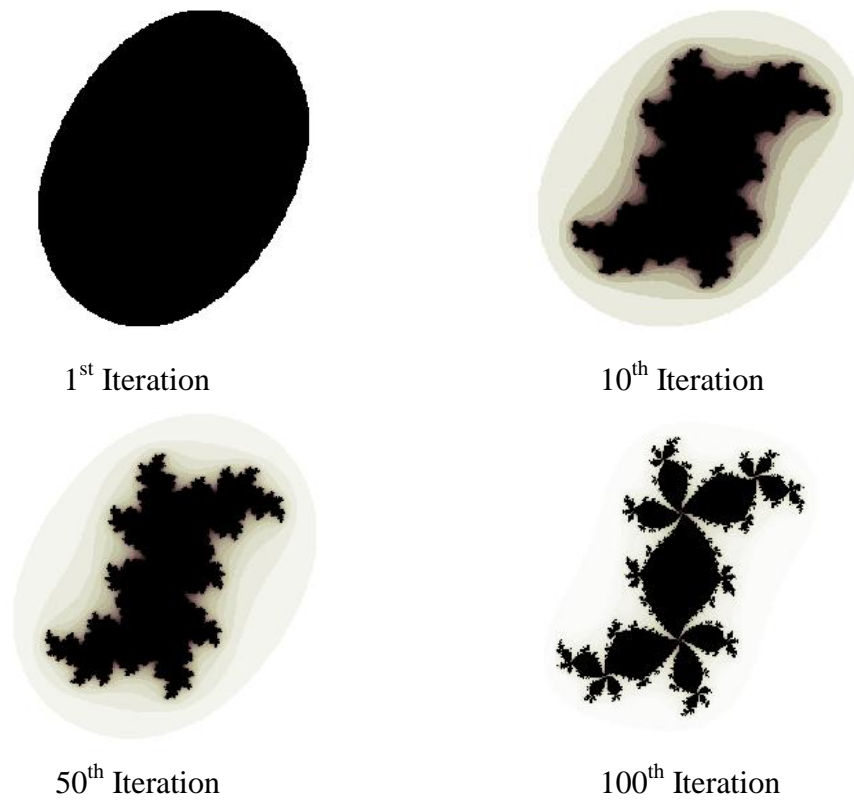


**Figure 1.13** Construction of the filled Julia sets

#### 1.3.2.1.2. [8] Some Properties of Julia Sets

1. Both forms of  $F$  are the same.
2.  $J$  is closed and bounded.
3.  $J$  is non-empty.
4.  $J$  has empty interior.
5.  $J$  contains no isolated points.
6.  $J$  is uncountable.

#### 1.3.2.2. The Mandelbrot Set

The Mandelbrot set is the famous example of Fractal. The Mandelbrot set is a particular mathematical set of points, whose boundary generates a distinctive and easily recognizable two-dimensional fractal shape.

The set is closely related to the Julia set (which generates similarly complex shapes), and is named after the mathematician Benoit Mandelbrot, who studied and popularized it. More technically, the Mandelbrot set is the set of values of  $c$  in the complex plane for which the orbit of 0 under iteration of the complex quadratic polynomial  $f(z) = z^2 + c$  remains bounded.

We define the Mandelbrot set

$$M := \{c \in \mathbf{C} : \text{the Julia set of } f(z) = z^2 + c \text{ is connected}\} [8].$$

For example, if  $c = 1$  and  $z = 0$ , then the function gives the sequence  $1, 2, 5, 26, \dots$ , which tends to infinity. As this sequence is unbounded,  $1$  is not an element of the Mandelbrot set.

On the other hand, if  $c = i$  and  $z = 0$  (where  $i$  is defined as  $i^2 = -1$ ), then the function gives the sequence  $i, (-1+i), -i, (-1+i), -i, \dots$ , which is bounded and so  $i$  belongs to the Mandelbrot set.

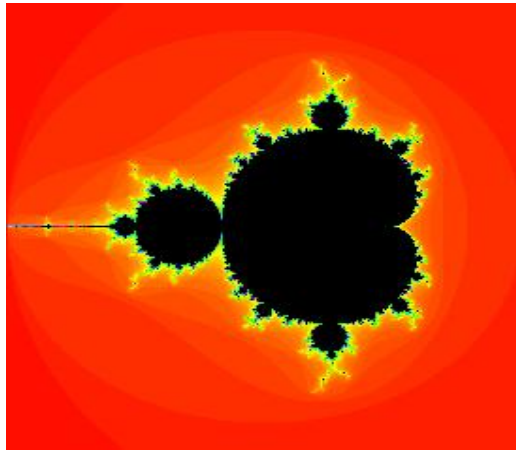


**Figure 1.14** Construction of the Mandelbrot set

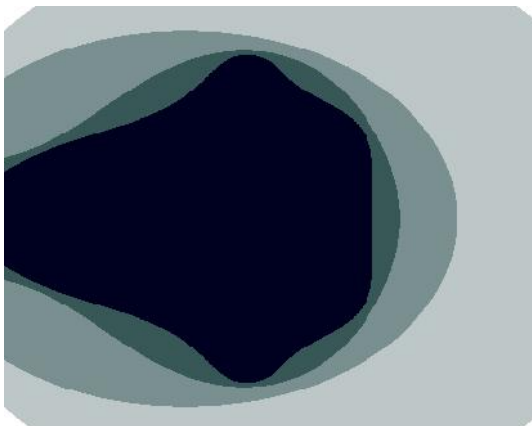
### Generating the Mandelbrot Set:

We consider the following functions to generate the Mandelbrot set:

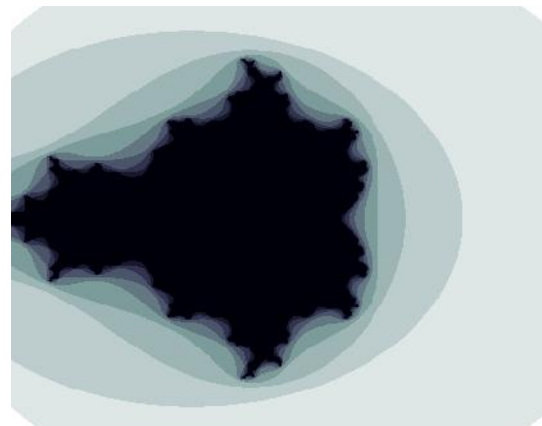
$$f_1(x, y) = x^2 - y^2 + a \quad \text{and} \quad f_2(x, y) = 2xy + b$$

Initial seed:  $x = 0, y = 0$  with the parameter values  $a = 0, b = 0$ .

Then the generating Mandelbrot set is shown in Figure 1.15.

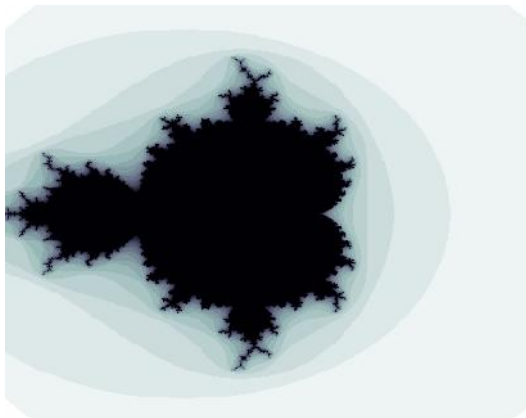
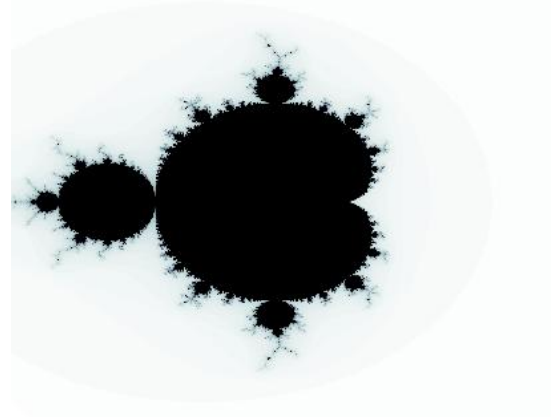


5<sup>th</sup> iteration



10<sup>th</sup> iteration



20<sup>th</sup> iteration100<sup>th</sup> iteration**Figure 1.15** Construction of the Mandelbrot Set**1.3.2.2.1. [8] Some Properties of the Mandelbrot Set**

1.  $M$  is bounded.
2.  $M$  has a proper interior.
3.  $M$  is closed, and so by (1) is compact.
4.  $M$  is connected.

**1.3.3. [12] Stochastic Fractals**

A stochastic fractal is a self-similar random process  $x(t)$ . The stochastic fractals are found in the case iterate process has accidental parameters. These fractals like natural can be created. Two-dimensional stochastic fractals are used for designing surface of sea or relief modeling.

**1.3.3.1. Example of Stochastic Fractal**

A fractal is a complex geometric figure that is made of identically repeated shapes. These shapes are symmetrical, show self-similarity, and repeat on all scales. This means that a single section of a fractal has the same shape as the whole. The natural fern in figure demonstrates this fractal quality as does the mathematically created fern. Each frond of the ferns resembles the entire fern and at each smaller scale the same fern shape is recreated.

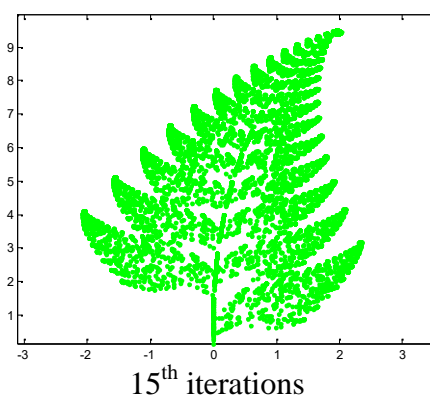
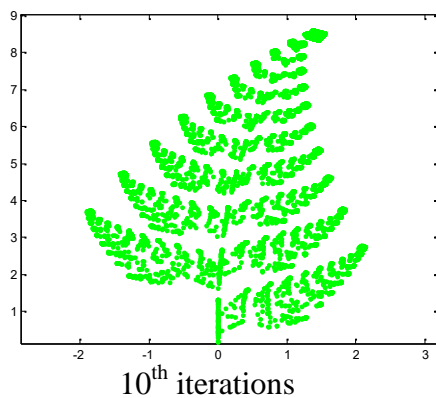
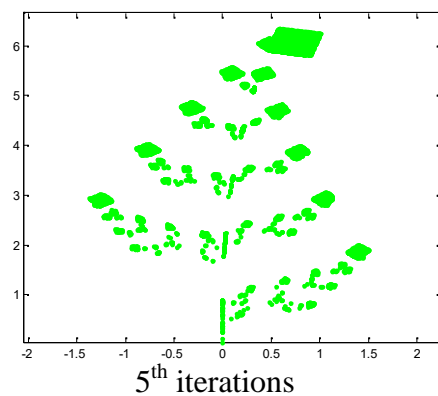
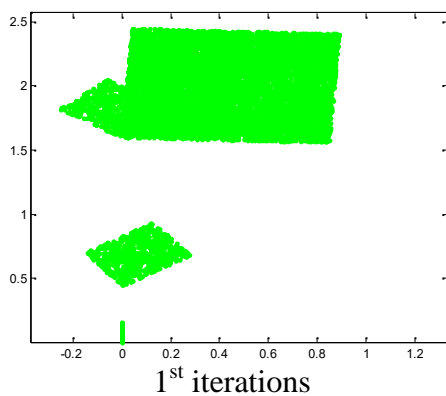


**Figure 1.16** The Natural Fern (captured from nature)

We consider the following functions to generate fractal fern:

$$f_1(x, y) = ax + by \text{ and } f_2(x, y) = cx + dy + e$$

Initial seed:  $x = 0$  and  $y = 0.16y$  with the parameter values  $a = 0.2, b = -0.26, c = 0.23, d = 0.22, e = 1.6$ . Then the generating fern is shown in Figure 1.16.



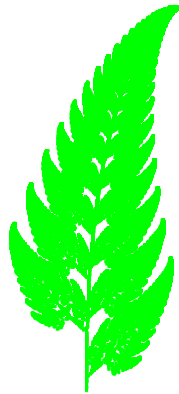


**Figure 1.17** Construction of the complete Fern (after 50000<sup>th</sup> iterations)

# CHAPTER TWO

## THE CANTOR SET PROTOTYPICAL FRACTAL

### OVERVIEW

In this chapter, we discuss the construction and properties of the classical Cantor set. We generalize the Cantor middle third set and also discuss the construction and properties of the generalized Cantor sets.

### 2.1. The Cantor Set

A non empty set  $\Gamma \subset \mathbf{R}$  is called a Cantor set if

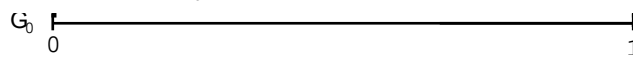
- (a)  $\Gamma$  is closed and bounded.
- (b)  $\Gamma$  contains no intervals.
- (c) Every point in  $\Gamma$  is an accumulation point of  $\Gamma$ .

The Cantor sets were discovered by the German Mathematician, George Cantor in the late 19th to early 20th centuries (1845-1918). He introduced fractal which has come to be known as the Cantor set, or Cantor dust. The Cantor set is the prototypical fractal [1].

The Mathematician George Cantor found the Cantor middle  $\frac{1}{3}$  set. We study the Cantor set and find the generalized Cantor sets and show its dynamical behaviors and fractal dimensions [3]. The Cantor middle  $\frac{1}{3}, \frac{1}{5}, \frac{1}{7}, \frac{1}{9}, \frac{1}{11}, \dots$  sets, in general, the Cantor middle  $\frac{1}{2m-1}$ , ( $2 \leq m < \infty$ ) set is called the generalized Cantor sets and it is denoted by  $C_{1/(2m-1)}$  which is defined by algorithm and also defined by the shrinking process.

#### 2.1.1. Construction of the Cantor middle $\frac{1}{3}$ set

We start with the closed interval  $\Gamma_0 = [0, 1]$ .



Remove the middle open third. This leaves a new set  $\Gamma_1 = [0, \frac{1}{3}] \cup [\frac{2}{3}, 1]$ .



Each iteration through the algorithm removes the open middle third from each segment of the previous iteration. Thus the next set would be

$$\Gamma_2 = [0, \frac{1}{9}] \cup [\frac{2}{9}, \frac{1}{3}] \cup [\frac{2}{3}, \frac{7}{9}] \cup [\frac{8}{9}, 1].$$

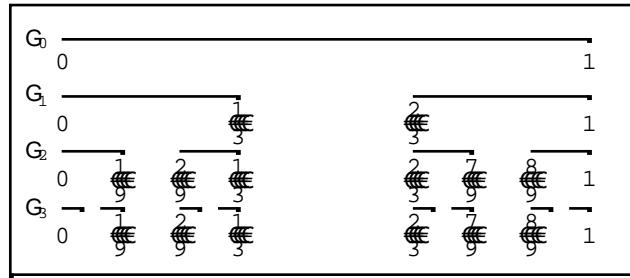


**Figure 2.1** Construction of the Cantor middle  $\frac{1}{3}$  set

In general, after  $n$  times iterations, we obtain  $\Gamma_n$  which as follows

$$\Gamma_n = [0, \frac{1}{3^n}] \cup [\frac{2}{3^n}, \frac{3}{3^n}] \cup \dots \cup [\frac{3^n - 3}{3^n}, \frac{3^n - 2}{3^n}] \cup [\frac{3^n - 1}{3^n}, 1], \text{ where } n \geq 1.$$

Therefore we construct a decreasing sequence  $(\Gamma_n)$  of closed sets, that is  $\Gamma_{n+1} \subseteq \Gamma_n$  for all  $n \in \mathbf{N}$ , so that every  $\Gamma_n$  consists of  $2^n$  closed intervals all of which the same length  $\frac{1}{3^n}$ .

The Cantor ternary set, which we denote  $C_{1/3}$ , is the “limiting set” of this process, that is,

$$C_{1/3} = \bigcap_{n=1}^{\infty} \Gamma_n \text{ and call it the Cantor middle } \frac{1}{3} \text{ set.}$$

Alternative process of constructing  $C_{1/3}$  is in physical terms as taking a length of string and repeatedly cutting it into shorter pieces. If we think first piece as the interval  $[0,1]$  and cut it at the points  $1/2$ , then it becomes two pieces of string each with two endpoints such as the intervals  $[0,1/2]$ , and  $[1/2,1]$ . In order to make all these pieces disjoint subsets of  $\mathbf{R}$  one can image the string as being stretched so tightly that each time it is cut, it pulls apart at the cut and shrinks to  $2/3$  of its length, so after the first cut,  $[0,1/2]$  shrinks to  $[0,1/3]$ ,  $[1/2,1]$  shrinks to  $[2/3,1]$ . Then at the next stage we cut  $[0,1/3]$  at the point  $1/6$ , and then two pieces are  $[0,1/6]$ ,  $[1/6,1/3]$ , shrink to  $[0,1/9]$  and  $[2/9,1/3]$ . similarly for the piece  $[2/3,1]$ , and so on.

### 2.1.2. [1] Properties of the Cantor middle $\frac{1}{3}$ set

#### 2.1.2.1. The set $C_{1/3}$ is disconnected

The set  $C_{1/3}$  is totally disconnected since it was constructed so as to contain no intervals other than points. Namely, if  $C_{1/3}$  contained an interval of positive length  $v$  then this interval would be contained in each  $\Gamma_n$ , but  $\Gamma_n$  contains no interval of length greater than  $\frac{1}{3^n}$  so if  $n$  is chosen to be large enough so that  $\frac{1}{3^n}$  is less than  $v$ , then there is no interval of length  $v$  in  $\Gamma_n$ .

**2.1.2.2. The set  $C_{1/3}$  contains no intervals**

We will show that the length of the complement of the set  $C_{1/3}$  is equal to 1, hence  $C_{1/3}$  contains no intervals. At the  $n^{th}$  stage, we are removing  $2^{n-1}$  intervals from the previous set of intervals, and each one has length of  $\frac{1}{3^n}$ .

The length of the removing intervals within  $[0,1]$  after an infinite number of removals is

$$\sum_{n=1}^{\infty} 2^{n-1} \left(\frac{1}{3^n}\right) = \frac{1}{3} \sum_{n=1}^{\infty} \left(\frac{2}{3}\right)^{n-1} = \frac{1}{3} \sum_{n=0}^{\infty} \left(\frac{2}{3}\right)^n = \frac{1/3}{1-2/3} = 1$$

Thus we are removing a length of 1 from the unit interval  $[0,1]$  which has a length of 1.

**Alternative method:**

Note that in the first iteration we removed  $1/3$ , in the second iteration we removed  $2/9$ , in the third iteration we removed  $4/27$ , and in the fourth iteration we removed  $8/81$ , and so forth.

This is a geometric series with first term  $a = \frac{1}{3}$  and common ratio  $r = \frac{2}{3}$ .

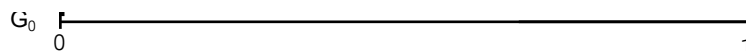
This converges, and the sum is  $S_{\infty} = \frac{1/3}{1-2/3} = 1$ .

Thus the length of the complement of the set  $C_{1/3}$  is equal to 1.

Therefore, the total length of  $C_{1/3}$  is 0, which means it has no intervals.

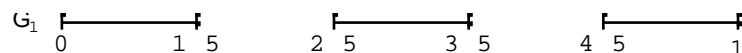
**2.1.3. [3] Construction of the Cantor middle  $\frac{1}{5}$  set**

We start with the closed interval  $\Gamma_0 = [0,1]$ .



Remove the middle open interval  $(1/5, 2/5)$  and  $(3/5, 4/5)$ . This leaves a new set

$$\Gamma_1 = [0, \frac{1}{5}] \cup [\frac{2}{5}, \frac{3}{5}] \cup [\frac{4}{5}, 1].$$



Each iteration through the algorithm removes the open 2nd and 4<sup>th</sup> interval from each segment of the previous iteration. Thus the next set would be

$$\Gamma_2 = [0, \frac{1}{25}] \cup [\frac{2}{25}, \frac{3}{25}] \cup [\frac{4}{25}, \frac{1}{5}] \cup [\frac{2}{5}, \frac{11}{25}] \cup [\frac{12}{25}, \frac{13}{25}] \cup [\frac{14}{25}, \frac{3}{5}] \cup [\frac{4}{5}, \frac{21}{25}] \cup [\frac{22}{25}, \frac{23}{25}] \cup [\frac{24}{25}, 1].$$

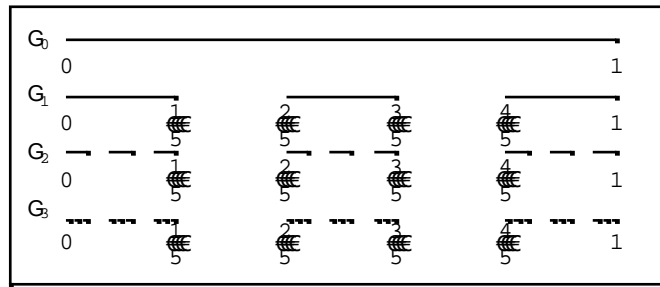


**Figure 2.2** Construction of the Cantor middle  $\frac{1}{5}$  set

In general, after  $n$  times iterations, we obtain  $\Gamma_n$  which as follows

$$\Gamma_n = [0, \frac{1}{5^n}] \cup [\frac{2}{5^n}, \frac{3}{5^n}] \cup \dots \cup [\frac{5^n - 3}{5^n}, \frac{5^n - 2}{5^n}] \cup [\frac{5^n - 1}{5^n}, 1], \text{ where } n \geq 1.$$

Therefore, we construct a decreasing sequence  $(\Gamma_n)$  of closed sets, that is,  $\Gamma_{n+1} \subseteq \Gamma_n$  for all  $n \in \mathbf{N}$ , so that every  $\Gamma_n$  consists of  $3^n$  closed intervals all of which the same length  $\frac{1}{5^n}$ .

We define  $C_{1/5} = \bigcap_{n=1}^{\infty} \Gamma_n$  and call it the Cantor middle  $\frac{1}{5}$  set.

Alternative process of constructing  $C_{1/5}$  is in physical terms as taking a length of string and repeatedly cutting it into shorter pieces. If we think first piece as the interval  $[0,1]$  and cut it at the points  $1/3$  and  $2/3$ , then it becomes three pieces of string each with two endpoints such as the intervals  $[0,1/3]$ ,  $[1/3,2/3]$ , and  $[2/3,1]$ . In order to make all these pieces disjoint subsets of  $\mathbf{R}$  one can image the string as being stretched so tightly that each time it is cut, it pulls apart at the cut and shrinks to  $3/5$  of its length, so after the first cut,  $[0,1/3]$  shrinks to  $[0,1/5]$ ,  $[1/3,2/3]$  shrinks to  $[2/5,3/5]$ , and  $[2/3,1]$  shrinks to  $[4/5,1]$ . Then at the next stage we cut  $[0,1/5]$  at the points  $1/15$  and  $2/15$  and the three pieces  $[0,1/15]$ ,  $[1/15,2/15]$ , and  $[2/15,1/5]$  shrink to  $[0,1/25]$ ,  $[2/25,3/25]$ , and  $[4/25,1/5]$ , similarly for the pieces  $[2/5,3/5]$ , and  $[4/5,1]$ , and so on.

### 2.1.4. [3] Properties of the Cantor middle $\frac{1}{5}$ set

#### 2.1.4.1. The set $C_{1/5}$ is disconnected

The set  $C_{1/5}$  is totally disconnected since it was constructed so as to contain no intervals other than points. Namely, if  $C_{1/5}$  contained an interval of positive length  $v$  then this interval would be contained in each  $\Gamma_n$ , but  $\Gamma_n$  contains no interval of length greater than  $\frac{1}{5^n}$  so if  $n$  is chosen to be large enough so that  $\frac{1}{5^n}$  is less than  $v$ , then there is no interval of length  $v$  in  $\Gamma_n$ .

**2.1.4.2 The set  $C_{1/5}$  contains no intervals**

We will show that the length of the complement of the set  $C_{1/5}$  is equal to 1, hence  $C_{1/5}$  contains no intervals. At the  $n^{th}$  stage, we are removing  $2 \cdot 3^{n-1}$  intervals from the previous set of intervals, and each one has length of  $\frac{1}{5^n}$ .

The length of the removing intervals within  $[0,1]$  after an infinite number of removals is

$$\sum_{n=1}^{\infty} 2 \cdot 3^{n-1} \left(\frac{1}{5^n}\right) = \frac{2}{5} \sum_{n=1}^{\infty} \left(\frac{3}{5}\right)^{n-1} = \frac{2}{5} \sum_{n=0}^{\infty} \left(\frac{3}{5}\right)^n = \frac{2/5}{1-3/5} = 1$$

Thus we are removing a length of 1 from the unit interval  $[0,1]$  which has a length of 1.

**Alternative method:**

Note that in the first iteration we removed  $2/5$ , in the second iteration we removed  $6/25$ , in the third iteration we removed  $18/125$ , and so forth.

This is a geometric series with first term  $a = \frac{2}{5}$  and common ratio  $r = \frac{3}{5}$ .

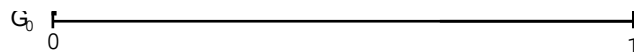
This converges, and the sum is  $S_{\infty} = \frac{2/5}{1-3/5} = 1$ .

Thus the length of the complement of the set  $C_{1/5}$  is equal to 1.

Therefore, the total length of  $C_{1/5}$  is 0, which means it has no intervals.

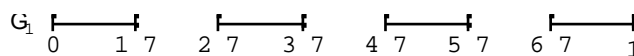
**2.1.5. [3] Construction of the Cantor middle  $\frac{1}{7}$  set**

We start with the closed interval  $\Gamma_0 = [0,1]$ .



Remove the middle open interval  $(1/7, 2/7)$ ,  $(3/7, 4/7)$ , and  $(5/7, 6/7)$ .

This leaves a new set  $\Gamma_1 = [0, \frac{1}{7}] \cup [\frac{2}{7}, \frac{3}{7}] \cup [\frac{4}{7}, \frac{5}{7}] \cup [\frac{6}{7}, 1]$ .



Each iteration through the algorithm removes the open 2<sup>nd</sup>, 4<sup>th</sup>, and 6<sup>th</sup> interval from each segment of the previous iteration. Thus the next set would be

$$\Gamma_2 = [0, \frac{1}{49}] \cup [\frac{2}{49}, \frac{3}{49}] \cup [\frac{4}{49}, \frac{5}{49}] \cup [\frac{6}{49}, \frac{7}{49}] \cup \dots \cup [\frac{46}{49}, \frac{47}{49}] \cup [\frac{48}{49}, 1].$$

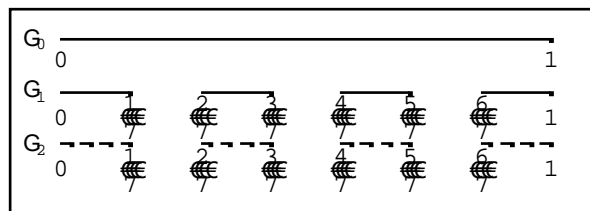


**Figure 2.3** Construction of the Cantor middle  $\frac{1}{7}$  set



In general, after  $n$  times iterations, we obtain  $\Gamma_n$  which as follows

$$\Gamma_n = [0, \frac{1}{7^n}] \cup [\frac{2}{7^n}, \frac{3}{7^n}] \cup \dots \cup [\frac{7^n - 3}{7^n}, \frac{7^n - 2}{7^n}] \cup [\frac{7^n - 1}{7^n}, 1], \text{ where } n \geq 1.$$

Therefore, we construct a decreasing sequence  $(\Gamma_n)$  of closed sets, that is,  $\Gamma_{n+1} \subseteq \Gamma_n$  for all  $n \in \mathbf{N}$ , so that every  $\Gamma_n$  consists of  $4^n$  closed intervals all of which the same length  $\frac{1}{7^n}$ .

We define  $C_{1/7} = \bigcap_{n=1}^{\infty} \Gamma_n$  and call it the Cantor middle  $\frac{1}{7}$  set.

### 2.1.6. [3] Properties of the Cantor middle $\frac{1}{7}$ set

#### 2.1.6.1. The set $C_{1/7}$ is disconnected

The set  $C_{1/7}$  is totally disconnected since it was constructed so as to contain no intervals other than points. Namely, if  $C_{1/7}$  contained an interval of positive length  $v$  then this interval would be contained in each  $\Gamma_n$ , but  $\Gamma_n$  contains no interval of length greater than  $\frac{1}{7^n}$  so if  $n$  is chosen to be large enough so that  $\frac{1}{7^n}$  is less than  $v$ , then there is no interval of length  $v$  in  $\Gamma_n$ .

#### 2.1.6.2. The set $C_{1/7}$ contains no intervals

We will show that the length of the complement of the set  $C_{1/7}$  is equal to 1, hence  $C_{1/7}$  contains no intervals. At the  $n^{\text{th}}$  stage, we are removing  $3 \cdot 4^{n-1}$  intervals from the previous set of intervals, and each one has length of  $\frac{1}{7^n}$ .

The length of the removing intervals within  $[0,1]$  after an infinite number of removals is

$$\sum_{n=1}^{\infty} 3 \cdot 4^{n-1} \left(\frac{1}{7^n}\right) = \frac{3}{7} \sum_{n=1}^{\infty} \left(\frac{4}{7}\right)^{n-1} = \frac{3}{7} \sum_{n=0}^{\infty} \left(\frac{4}{7}\right)^n = \frac{3/7}{1 - 4/7} = 1$$

Thus we are removing a length of 1 from the unit interval  $[0,1]$  which has a length of 1.

#### Alternative method:

Note that in the first iteration we removed  $3/7$ , in the second iteration we removed  $12/49$ , in the third iteration we removed  $48/343$ , and so forth.

This is a geometric series with first term  $a = \frac{3}{7}$  and common ratio  $r = \frac{4}{7}$ .

This converges, and the sum is  $S_{\infty} = \frac{3/7}{1 - 4/7} = 1$ .

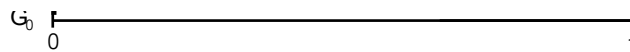
Thus the length of the complement of the set  $C_{1/7}$  is equal to 1.

Therefore, the total length of  $C_{1/7}$  is 0, which means it has no intervals.

Similarly, we can construct and show the properties of the Cantor middle  $\frac{1}{2m-1}, (2 \leq m < \infty)$  set which is denoted by  $C_{1/(2m-1)}$  and is called generalized Cantor set.

**2.1.7. [3] Construction of the Generalized Cantor Sets (The Cantor middle  $\frac{1}{2m-1}, (2 \leq m < \infty)$  sets)**

We start with the closed interval  $\Gamma_0 = [0, 1]$ .



Remove the middle open interval

$$\left(\frac{1}{2m-1}, \frac{2}{2m-1}\right), \left(\frac{3}{2m-1}, \frac{4}{2m-1}\right), \dots, \left(\frac{2m-3}{2m-1}, \frac{2m-2}{2m-1}\right), \text{ where } 2 \leq m < \infty.$$

This leaves a new set  $\Gamma_1$  which will depend on the value of  $m$ .

In general, after  $n$  times iterations, we obtain  $\Gamma_n$  which as follows:

$$\Gamma_n = [0, \frac{1}{(2m-1)^n}] \cup [\frac{2}{(2m-1)^n}, \frac{3}{(2m-1)^n}] \cup \dots \cup [\frac{(2m-1)^n - 3}{(2m-1)^n}, \frac{(2m-1)^n - 2}{(2m-1)^n}] \cup [\frac{(2m-1)^n - 1}{(2m-1)^n}, 1],$$

Therefore, we construct a decreasing sequence  $(\Gamma_n)$  of closed sets, that is  $\Gamma_{n+1} \subseteq \Gamma_n$  for all  $n \in \mathbf{N}$ , so that every  $\Gamma_n$  consists of  $m^n$  closed intervals all of which the same length  $\frac{1}{(2m-1)^n}$ . We define  $C_{1/(2m-1)} = \bigcap_{n=1}^{\infty} \Gamma_n$  and call it the Cantor middle  $\frac{1}{2m-1}, (2 \leq m < \infty)$  set or the generalized Cantor set.

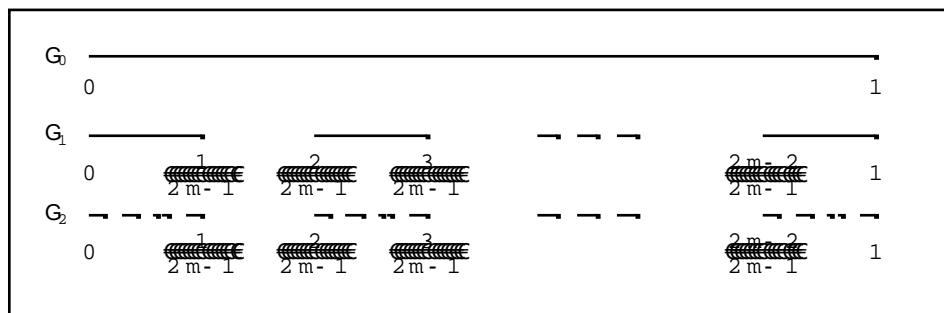


**Figure 2.4** Construction of the Cantor middle  $\frac{1}{2m-1}$  set

### 2.1.8. [3] Properties of the Generalized Cantor Sets

#### 2.1.8.1. The set $C_{1/(2m-1)}$ , $(2 \leq m < \infty)$ is disconnected

The set  $C_{1/(2m-1)}$  is totally disconnected since it was constructed so as to contain no intervals other than points. Namely, if  $C_{1/(2m-1)}$  contained an interval of positive length  $\nu$  then this interval would be contained in each  $\Gamma_n$ , but  $\Gamma_n$  contains no interval of length greater than  $\frac{1}{(2m-1)^n}$  so if  $n$  is chosen to be large enough so that  $\frac{1}{(2m-1)^n}$  is less than  $\nu$ , then there is no interval of length  $\nu$  in  $\Gamma_n$ .

#### 2.1.8.2. The set $C_{1/(2m-1)}$ , $(2 \leq m < \infty)$ contains no intervals

We will show that the length of the complement of the set  $C_{1/(2m-1)}$  is equal to 1, hence  $C_{1/(2m-1)}$  contains no intervals. At the  $n^{\text{th}}$  stage, we are removing  $(m-1).m^{n-1}$  intervals from the previous set of intervals, and each one has length of  $\frac{1}{(2m-1)^n}$ .

The length of the removing intervals within  $[0,1]$  after an infinite number of removals is

$$\sum_{n=1}^{\infty} (m-1).m^{n-1} \left( \frac{1}{(2m-1)^n} \right) = \frac{m-1}{(2m-1)} \sum_{n=1}^{\infty} \left( \frac{m}{2m-1} \right)^{n-1} = \frac{m-1}{(2m-1)} \sum_{n=0}^{\infty} \left( \frac{m}{2m-1} \right)^n = 1$$

Thus we are removing a length of 1 from the unit interval  $[0,1]$  which has a length of 1.

#### Alternative method:

Note that in the first iteration we removed  $(m-1)/(2m-1)$ , in the second iteration we removed  $m(m-1)/(2m-1)^2$ , in the third iteration we removed  $m^2(m-1)/(2m-1)^3$ , and so forth.

This is a geometric series with first term  $a = \frac{m-1}{2m-1}$  and common ratio  $r = \frac{m}{2m-1}$ .

This converges, and the sum is  $S_{\infty} = \frac{(m-1)/(2m-1)}{1 - m/(2m-1)} = 1$ .

Therefore, the total length of  $C_{1/(2m-1)}$  is 0, which means it has no intervals.

#### 2.1.8.3. The set $C_{1/(2m-1)}$ , $(2 \leq m < \infty)$ is nowhere dense

A set  $S$  is said to be nowhere dense if the interior of the closure of  $S$  is empty. The closure of the set is the union of the set with the set of limit points. Since every point in the set  $C_{1/(2m-1)}$  is a limit point of the set, the closure of the set is simply the set itself.

The interior of the set  $C_{1/(2m-1)}$  must be empty, since no two points in the set are adjacent to each other. Thus the set  $C_{1/(2m-1)}$  is nowhere dense.

**2.2. Lemma [3].** If  $\Gamma_n$  is defined in Cantor middle  $\frac{1}{2m-1}$  set, where  $2 \leq m < \infty$ , then

there are  $m^n$  closed intervals in  $\Gamma_n$  and the length of each closed interval is  $\left(\frac{1 - \frac{1}{2m-1}}{2m-2}\right)^n$ ,

where  $2 \leq m < \infty$ , Also the combined length of the intervals in  $\Gamma_n$  is  $\left(\frac{m}{2m-1}\right)^n$ , where  $2 \leq m < \infty$ , which is approaches to zero as  $n$  approaches to infinity.

**Proof:** We start with the interval  $[0, 1]$  whose length is 1. We proceed by mathematical induction. In the first step, we remove a gape of length  $\frac{1}{2m-1}$  and obtain  $m$  closed intervals whose combined length is  $\frac{m}{2m-1}$ .

So each interval has a length of  $\left(\frac{1 - \frac{1}{2m-1}}{2m-2}\right)$ , where  $2 \leq m < \infty$ .

In general, suppose that there are  $m^k$  intervals remain in  $\Gamma_k$ , each with a length of  $\left(\frac{1 - \frac{1}{2m-1}}{2m-2}\right)^k$ , where  $2 \leq m < \infty$ , for a combined length of  $\left(\frac{m}{2m-1}\right)^k$ , where  $2 \leq m < \infty$ .

We will show that there are  $m^{k+1}$  intervals remain in  $\Gamma_{k+1}$ , each with a length  $\left(\frac{1 - \frac{1}{2m-1}}{2m-2}\right)^{k+1}$ , where  $2 \leq m < \infty$ , for a combined length  $\left(\frac{m}{2m-1}\right)^{k+1}$ , where  $2 \leq m < \infty$ .

Note that each time we remove the middle  $\frac{1}{2m-1}$ , where  $2 \leq m < \infty$ , portion of a closed intervals, we split the interval into  $m$  closed intervals. So in passing from  $\Gamma_k$  to  $\Gamma_{k+1}$ , we multiple the number of intervals by  $m$ , and there are  $m(m^k) = m^{k+1}$ , where  $2 \leq m < \infty$ , intervals in  $\Gamma_{k+1}$ .

By assumption, each interval in  $\Gamma_k$  has a length of  $\left(\frac{1 - \frac{1}{2m-1}}{2m-2}\right)^k$ , where  $2 \leq m < \infty$ .

Since we remove the middle  $\frac{1}{2m-1}$ , where  $2 \leq m < \infty$ , portion of each interval in  $\Gamma_k$  to create  $\Gamma_{k+1}$ , the amount of each interval from  $\Gamma_k$  left in  $\Gamma_{k+1}$  is

$$\left(\frac{1 - \frac{1}{2m-1}}{2m-2}\right)^k - \frac{1}{2m-1} \left(\frac{1 - \frac{1}{2m-1}}{2m-2}\right)^k = \frac{\left(1 - \frac{1}{2m-1}\right)^{k+1}}{(2m-2)^k}, \text{ where } 2 \leq m < \infty.$$

As this length is left in  $2m-2$  intervals, the length of each remaining interval is

$$\frac{1}{2m-2} \times \frac{\left(1 - \frac{1}{2m-1}\right)^{k+1}}{(2m-2)^k} = \left(\frac{1 - \frac{1}{2m-1}}{2m-2}\right)^{k+1}, \text{ where } 2 \leq m < \infty.$$

Finally, there are  $m^{k+1}$  intervals in  $\Gamma_{k+1}$ , so the combined length of the intervals in  $\Gamma_{k+1}$  is

$$m^{k+1} \cdot \left(\frac{1 - \frac{1}{2m-1}}{2m-2}\right)^{k+1} = \left(\frac{m}{2m-1}\right)^{k+1}, \text{ where } 2 \leq m < \infty.$$

Since  $0 < \frac{1}{2m-1} < 1$ ,  $\left(\frac{m}{2m-1}\right)^n$  converges to 0 as  $n$  grows without bound and it follows that the combined length of the intervals in  $\Gamma_n$  approaches 0 as  $n$  goes to infinity.  $\square$

**2.3. Proposition [3].** The Cantor middle  $\frac{1}{2m-1}$  set is a Cantor set, where  $2 \leq m < \infty$ .

**Proof:** Let  $\Gamma$  be a Cantor middle  $\frac{1}{2m-1}$  set, where  $2 \leq m < \infty$ . Since 0 is in every  $\Gamma_n$ ,  $\Gamma$

is not empty. To complete the proof, we must show that (i)  $\Gamma$  is closed and bounded, (ii)  $\Gamma$  contains no intervals, and (iii) every point of  $\Gamma$  is an accumulation point of  $\Gamma$ .

(i) Since  $\Gamma$  is the intersection of closed intervals, it is closed. As  $\Gamma$  is contained in  $[0, 1]$ , it is also bounded.

(ii) If  $\Gamma$  contains an open interval  $(x, y)$  with length  $|y-x|$ , then at each stage in the construction of  $\Gamma$ ,  $(x, y)$  must be contained in one of the remaining closed intervals. However, Lemma 2.2 implies that after  $n$  steps the length of one of these intervals is

$$\left(\frac{1 - \frac{1}{2m-1}}{2m-2}\right)^n, \text{ where } 2 \leq m < \infty,$$

and we can find an  $n_0$  such that  $\left(\frac{1 - \frac{1}{2m-1}}{2m-2}\right)^{n_0} < |y - x|$ , where  $2 \leq m < \infty$ .

That is, the length of each of the closed intervals in  $\Gamma_{n_0}$  is less than the length of  $(x, y)$ . Hence, the entire interval  $(x, y)$  cannot be contained in  $\Gamma_{n_0}$  and  $\Gamma$  contains no intervals.

(iii) Suppose that  $x$  is a point in  $\Gamma$  and let  $N_\nu(x) = (x - \nu, x + \nu)$  be a neighborhood of  $x$ . We must show that there exists a point in  $\Gamma$  that is contained in  $N_\nu(x)$  and is not equal to  $x$ . Notice that if  $x_1$  is an endpoint of one of the intervals that is removed, then  $x_1$  is in  $\Gamma$ . Now at each stage in the construction of the Cantor set,  $x$  must be in one of the remaining closed intervals. That is, for each  $n$  there is an intervals in  $\Gamma_n$  that contains  $x$ .

Choose  $n$  large enough so that  $\left(\frac{1 - \frac{1}{2m-1}}{2m-2}\right)^n < \nu$ , where  $2 \leq m < \infty$ .

Then  $x$  is in one of the closed intervals that comprise  $\Gamma_n$ . Call this interval  $I_n$ .

By Lemma 2.2, the length of  $I_n$  is  $\left(\frac{1 - \frac{1}{2m-1}}{2m-2}\right)^n$ , where  $2 \leq m < \infty$ .

Since  $\left(\frac{1 - \frac{1}{2m-1}}{2m-2}\right)^n < \nu$ , where  $2 \leq m < \infty$  it must be the endpoints of  $I_n$  are in  $N_\nu(x)$ .

As there are two endpoints and  $x$  can be equal to at one of them, other endpoint is an accumulation point of  $\Gamma$ .  $\square$

# CHAPTER THREE

## FRACTAL AND TOPOLOGICAL DIMENSIONS OF FRACTALS

### OVERVIEW

In this chapter, we discuss fractal dimensions and topological dimensions of fractals and also discuss the construction of the two and three dimensional fractals. We find fractal dimensions and topological dimensions of the one, two and three dimensional fractals.

### 3.1. Basic Definitions and Formulas

**Definition 3.1.1. [1]** A set  $S$  is called *affine self-similar* if  $S$  can be subdivided into  $N$  congruent subsets, each of which may be magnified by a constant factor  $r$  to yield the whole set  $S$ .

For example, the line, the plane, the cube are affine self-similar. We may now use this fact to provide a different notion of dimension, for one way to realize that these objects have different dimensions is to do the following.

A line is a very self-similar object: It may be decomposed into  $n = n^1$  little “bite-size” pieces, each of which is exactly  $\frac{1}{n}$  the size of the original line and each of which, when magnified by a factor of  $n$ . On the other hand, if we decompose a square into pieces that are  $\frac{1}{n}$  the size of the original square, then we find we need  $n^2$  such pieces to reassemble the square. Similarly, a cube may be decomposed into  $n^3$  pieces, each  $\frac{1}{n}$  the size of the original. So the exponent in each of those cases distinguishes the dimension of the object in equation. This exponent is the fractal dimension.

**Definition 3.1.2. [1]** Suppose the affine self-similar set may be subdivided into  $N$  congruent pieces, each of which may be magnified by a factor of  $r$  to yield the whole set  $S$ . Then the fractal dimension  $D$  of  $S$  is

$$D = \frac{\log(\text{number of pieces})}{\log(\text{magnification factor})} = \frac{\log(N)}{\log(r)}.$$

One of the crudest measurements of dimension is the notion of topological dimension. This dimension agrees with our naïve expectation that a set should have an integer dimension. We define the topological dimension inductively.

**Definition 3.1.3. [1]** A set  $S$  has topological dimension 0 if every point has arbitrarily small neighborhoods whose boundaries do not intersect the set.

For example, a scatter of isolated points has topological dimension 0, since each point may be surrounded by arbitrarily small neighborhoods whose boundaries are disjoint from the set.

**Definition 3.1.4. [1]** A set  $S$  has topological dimension  $k$  if every point has arbitrarily small neighborhoods whose boundaries meet in a set of dimension  $k - 1$ , and  $k$  is the least nonnegative integer for which this holds.

For example, a curve or line segment in the plane has topological dimension 1 since small disks in the plane have boundaries that meet the line in one or two points.

Similarly, a planar region has topological dimension 2 because points in the set have arbitrarily small neighborhoods whose boundaries are one-dimensional.

## 3.2. Fractal and Topological Dimensions of the Generalized Cantor Sets

### 3.2.1. Fractal and Topological Dimension of the Cantor middle $\frac{1}{3}$ set

From Figure 2.1 of the chapter 2, we see that the set  $\Gamma$  is contained in  $\Gamma_n$  for each  $n$ . Just as  $\Gamma_1$  consists of 2 intervals of length  $\frac{1}{3}$ , and  $\Gamma_2$  consists of  $2^2$  intervals of length  $\frac{1}{3^2}$ , and  $\Gamma_3$  consists of  $2^3$  intervals of length  $\frac{1}{3^3}$ . In general,  $\Gamma_n$  consists of  $2^n$  intervals, each of length  $\frac{1}{3^n}$ . After  $n \rightarrow \infty$ , we are left with a self-similar set which is called the Cantor middle  $\frac{1}{3}$  set. Arbitrary small neighborhoods intersect the Cantor middle  $\frac{1}{3}$  set at a finite set of points, so it has topological dimension 1.

The Cantor middle  $\frac{1}{3}$  set consists of  $2^n$  intervals with magnification factor  $3^n$ .

Hence the fractal dimension of the Cantor middle  $\frac{1}{3}$  set [13] is  $D = \frac{\ln 2}{\ln 3} = 0.63$ .

### 3.2.2. [3] Fractal and Topological Dimension of the Cantor middle $\frac{1}{5}$ set

From Figure 3.2 of the chapter 2, we see that the set  $\Gamma$  is contained in  $\Gamma_n$  for each  $n$ . Just as  $\Gamma_1$  consists of 3 intervals of length  $\frac{1}{5}$ , and  $\Gamma_2$  consists of  $3^2$  intervals of length  $\frac{1}{5^2}$ , and  $\Gamma_3$  consists of  $3^3$  intervals of length  $\frac{1}{5^3}$ . In general,  $\Gamma_n$  consists of  $3^n$  intervals, each of length  $\frac{1}{5^n}$ . After  $n \rightarrow \infty$ , we are left with a self-similar set which is called the Cantor middle  $\frac{1}{5}$  set. Arbitrary small neighborhoods intersect the Cantor middle  $\frac{1}{5}$  set at a finite set of points, so it has topological dimension 1.

The Cantor middle  $\frac{1}{5}$  set consists of  $3^n$  intervals with magnification factor  $5^n$ .



Therefore, the fractal dimension of the Cantor middle  $\frac{1}{5}$  set is  $D = \frac{\ln 3}{\ln 5} = 0.68$ .

### 3.2.3. [3] Fractal and Topological Dimension of the Cantor middle $\frac{1}{7}$ set

From Figure 3.3 of the chapter 2, we see that the set  $\Gamma$  is contained in  $\Gamma_n$  for each  $n$ . Just as  $\Gamma_1$  consists of 4 intervals of length  $\frac{1}{7}$ , and  $\Gamma_2$  consists of  $4^2$  intervals of length  $\frac{1}{7^2}$ , and  $\Gamma_3$  consists of  $4^3$  intervals of length  $\frac{1}{7^3}$ . In general,  $\Gamma_n$  consists of  $4^n$  intervals, each of length  $\frac{1}{7^n}$ . After  $n \rightarrow \infty$ , we are left with a self-similar set which is called the Cantor middle  $\frac{1}{7}$  set. Arbitrary small neighborhoods intersect the Cantor middle  $\frac{1}{7}$  set at a finite set of points, so it has topological dimension 1.

The Cantor middle  $\frac{1}{7}$  set consists of  $4^n$  intervals with magnification factor  $7^n$ .

Hence the fractal dimension of the Cantor middle  $\frac{1}{7}$  set is  $D = \frac{\ln 4}{\ln 7} = 0.71$ .

Similarly, we can find the fractal and topological dimension of the Cantor middle  $\frac{1}{9}$ ,  $\frac{1}{11}, \dots, \frac{1}{2m-1}$  set, where  $2 \leq m < \infty$ .

### 3.2.4. [3] Fractal and Topological Dimension of the Cantor middle $\frac{1}{2m-1}$ set

From Figure 3.4 of the chapter 2, we see that the set  $\Gamma$  is contained in  $\Gamma_n$  for each  $n$ . Just as  $\Gamma_1$  consists of  $m$  intervals of length  $\frac{1}{2m-1}$ , and  $\Gamma_2$  consists of  $m^2$  intervals of length  $\frac{1}{(2m-1)^2}$ , and  $\Gamma_3$  consists of  $m^3$  intervals of length  $\frac{1}{(2m-1)^3}$ . In general,  $\Gamma_n$  consists of  $m^n$  intervals, each of length  $\frac{1}{(2m-1)^n}$ .

After  $n \rightarrow \infty$ , we are left with a self-similar set which is called the Cantor middle  $\frac{1}{2m-1}$  set.

Arbitrary small neighborhoods intersect the Cantor middle  $\frac{1}{2m-1}$  set at a finite set of points, so it has topological dimension 1.

The Cantor middle  $\frac{1}{2m-1}$  sets consist of  $m^n$  intervals with magnification factor  $(2m-1)^n$ .

Hence the fractal dimension of the Cantor middle  $\frac{1}{2m-1}$  set is

$$D = \frac{\ln m}{\ln(2m-1)}, \text{ where } 2 \leq m < \infty.$$

**Remark:** The fractal dimension of the Generalized Cantor sets is  $\frac{\ln m}{\ln(2m-1)}$ , where  $2 \leq m < \infty$ . If we increase the value of  $m$ , then the value of fractal dimension of the Generalized Cantor sets will be increase.

### 3.3. Fractal and Topological Dimensions of Two Dimensional Fractals

#### 3.3.1. [12] Construction of the Koch Curve

We start with a closed unit interval. At the first stage we remove the middle third of the interval and replace it with two line segments of length  $\frac{1}{3}$  to make a tent. The resulting set consists of 4 line segments of length  $\frac{1}{3}$ . At the second stage, we repeat this procedure on all of the existing line segments and remove 4 line segments of length  $\frac{1}{9}$ . The resulting set consists of 16 line segments of length  $\frac{1}{9}$ . Similarly, at the third stage, we remove 16 line segments of length  $\frac{1}{9}$ . At the nth stage, we remove  $4^n$  open triangles of size  $\frac{1}{3^n}$ .

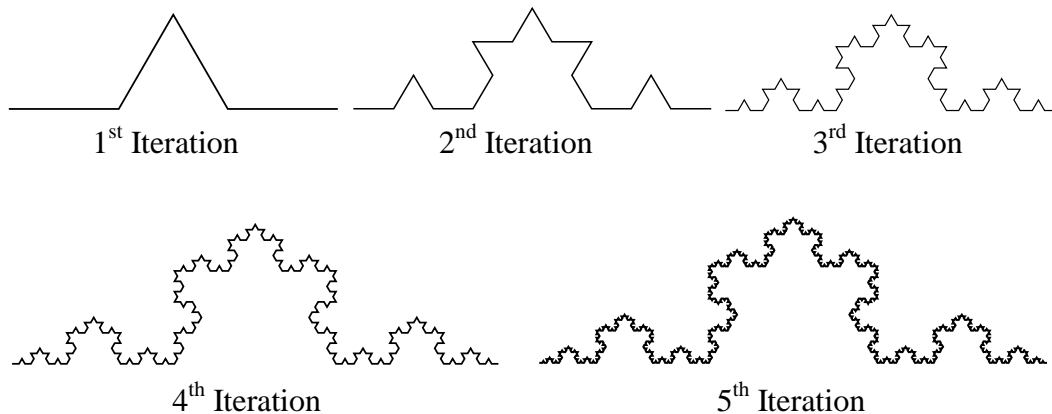


**Figure 3.1** The first five stages of the standard Koch curve.

After  $n \rightarrow \infty$ , we are left with a self-similar set which is called the Koch curve.

Arbitrary small neighborhoods intersect the Koch curve at a finite set of points, so it has topological dimension 1.

The Koch curve consists of  $4^n$  subsets with magnification factor  $3^n$ .

Hence the fractal dimension of the Koch curve [13] is  $D = \frac{\ln 4}{\ln 3} = 1.262$ .

**3.3.2. [1] Construction of the Sierpinski Gasket or Equilateral Triangle**

The Sierpinski triangle is a fractal described by Waclaw Sierpinski in 1915. It is a self-similar structure that occurs of different level of iterations or magnifications.

We start with a closed (filled) equilateral triangle. At the first stage we subdivide this into 4 smaller congruent equilateral triangles and remove the central one open triangle of size  $\frac{1}{2}$  to form a new image  $A_1$ . At the second stage, we subdivide each of the three remaining triangle into 4 congruent equilateral triangles and remove three open triangles of size  $\frac{1}{4}$  from each to form the image  $A_2$ . Similarly, at the third stage we remove nine open triangles of size  $\frac{1}{8}$  from each to form the image  $A_3$ . At the nth stage, we remove  $3^n$  open triangles of size  $\frac{1}{2^n}$  from each to form the image  $A_n$ .

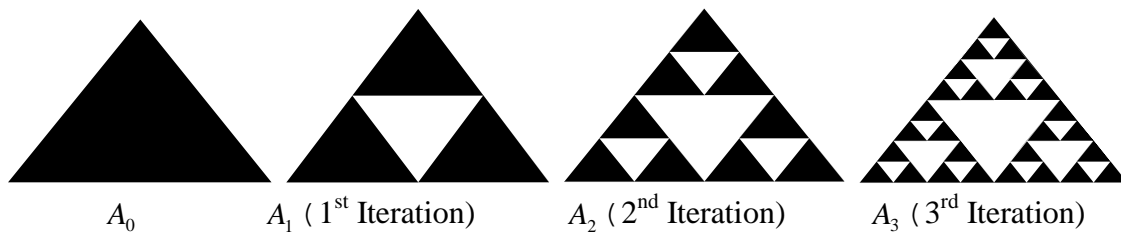


**Figure 3.2** The first four stages of the Sierpinski gasket or equilateral triangle

After  $n \rightarrow \infty$ , we are left with a self-similar set which is called the Sierpinski equilateral triangle. Arbitrary small neighborhoods intersect the Sierpinski equilateral triangle at a finite set of points, so it has topological dimension 1.

The Sierpinski equilateral triangle consists of  $3^n$  subsets with magnification factor  $2^n$ .

Hence the fractal dimension of the Sierpinski equilateral Triangle [14] is  $D = \frac{\ln 3}{\ln 2} = 1.585$ .

Similarly, we can construct the Sierpinski isosceles, isosceles right and scalene triangle and also we can find the fractal and topological dimension of those fractals, which is same to the Sierpinski equilateral triangle.

**3.3.3. [1] Construction of the Sierpinski Carpet**

The Sierpinski carpet is a plane fractal described by Waclaw Sierpinski in 1916. The carpet is one generalization of the Cantor set to two dimensions; another is the Cantor dust.

We start with a solid (filled) unit square. At the first stage we divide this into 9 smaller congruent squares. Remove the interior of the center open square of size  $\frac{1}{3}$  (that is, do not remove the boundary) to form a new image  $A_1$ . At the second stage, we subdivide each of the eight remaining solid squares into 9 congruent squares and remove 8 open squares of

size  $\frac{1}{3^2}$  from each to form the image  $A_2$ . Similarly, at the third stage we remove  $8^2$  open squares of size  $\frac{1}{3^3}$  from each to form the image  $A_3$ . At the  $n$ th stage, we remove  $8^{n-1}$  open squares of size  $\frac{1}{3^n}$  from each to form the image  $A_n$ .

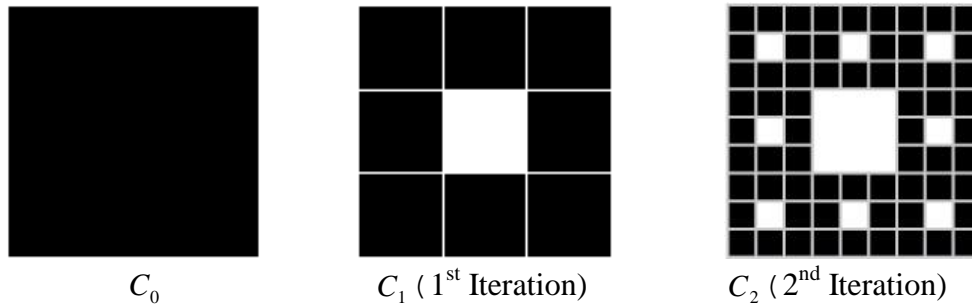


**Figure 3.3** The first three stages of the Sierpinski carpet

The Sierpinski carpet itself is the limit of this process after an infinite number of iterations. Arbitrary small neighborhoods intersect the Sierpinski equilateral triangle at a finite set of points, so it has topological dimension 1.

The Sierpinski carpet consists of  $8^n$  subsets with magnification factor  $3^n$ .

Thus the fractal dimension of the Sierpinski carpet [14] is  $D = \frac{\ln 8}{\ln 3} = 1.893$ .

**3.3.4. [15] Construction of the Box Fractal**

The Vicsek fractal is known as Vicsek snowflake or box fractal. It is a fractal arising from a construction similar to that of the Sierpinski carpet, proposed by Thomas Vicsek.

We start with a closed (filled) unit square. At 1<sup>st</sup> stage the square is decomposed into 9 smaller squares in the 3-by-3 grid. The four squares at the corners and the middle square are left, the other squares being removed. Thus we remove 4 open squares of size  $\frac{1}{3}$ . At 2<sup>nd</sup> stage, we remove 4.5 open squares of size  $\frac{1}{9}$ . At 3<sup>rd</sup> stage, we remove  $4.5^2$  open squares of size  $\frac{1}{27}$ .

At  $n$ th stage, we remove  $4.5^{n-1}$  open triangles of size  $\frac{1}{3^n}$ .

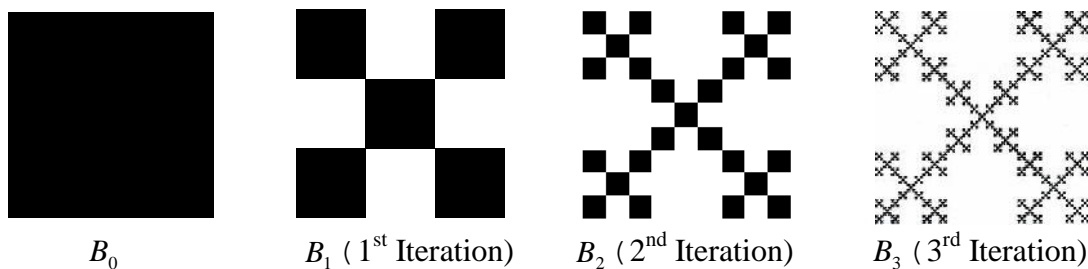


**Figure 3.4** The first four stages of the box fractal

The box fractal itself is the limit of this process after an infinite number of iterations. Arbitrary small neighborhoods intersect the box fractal at a finite set of points, so it has topological dimension is 1.

The box fractal consists of  $5^n$  subsets with magnification factor  $3^n$ .

Hence the fractal dimension of the box fractal [13] is  $D = \frac{\ln 5}{\ln 3} = 1.465$ .

### 3.3.5. Construction of the Square Fractal (using Cantor middle $\frac{1}{3}$ set)

We start with a closed (filled) unit square. At the first stage it is decomposed into 9 smaller squares in the 3-by-3 grid. The four squares at the corners are left, the other squares being removed. Thus we remove 5 open square of size  $\frac{1}{3}$ . At the second stage, we remove 5.4 open squares of size  $\frac{1}{9}$ . At the third stage, we remove  $5.4^2$  open squares of size  $\frac{1}{27}$ . At the nth stage, we remove  $5.4^{n-1}$  open squares of size  $\frac{1}{3^n}$ .

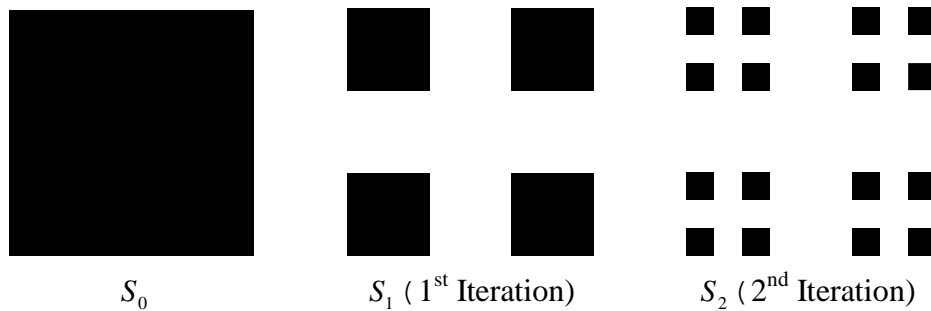


**Figure 3.5** The first three stages of the square fractal

After  $n \rightarrow \infty$ , we are left with a self-similar set which is called the square fractal.

Arbitrary small neighborhoods intersect the square fractal at a finite set of points, so it has topological dimension is 1.

The square fractal consists of  $4^n$  subsets with magnification factor  $3^n$ .

Therefore, the fractal dimension of the square fractal is  $D = \frac{\ln 4}{\ln 3} = 1.262$ .

### 3.3.6. Construction of the Square Fractal (using Cantor middle $\frac{1}{5}$ set)

We start with a closed (filled) unit square. At the first stage the basic square is decomposed into 25 smaller squares in the 5-by-5 grid. The nine squares are left, the other squares being removed. Thus we remove 16 open square of size  $\frac{1}{5}$ . At the second stage, we remove 16.9

open squares of size  $\frac{1}{25}$ . At the third stage, we remove  $16 \cdot 9^2$  open squares of size  $\frac{1}{125}$ . At the  $n$ th stage, we remove  $16 \cdot 9^{n-1}$  open squares of size  $\frac{1}{5^n}$ .

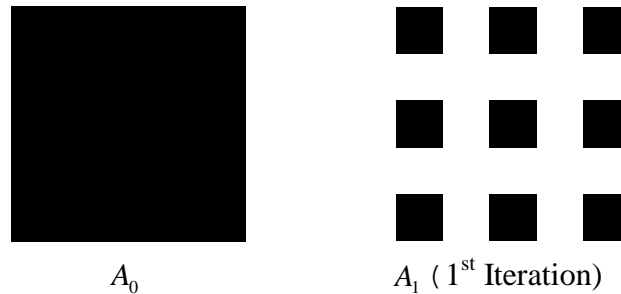


**Figure 3.6** The first two stages of the square fractal

After  $n \rightarrow \infty$ , we are left with a self-similar set which is called the square fractal. Arbitrary small neighborhoods intersect the square fractal at a finite set of points, so its topological dimension is 1.

The square fractal consists of  $9^n$  subsets with magnification factor  $5^n$ .

Hence the fractal dimension of the square fractal is  $D = \frac{\ln 9}{\ln 5} = 1.365$ .

### 3.4. Fractal and Topological Dimensions of Three Dimensional Fractals

#### 3.4.1. [15] Construction of the Menger Sponge

The Menger sponge is a fractal curve also known as the Menger universal curve. It is a three-dimensional generalization of the Cantor set and Sierpinski carpet, though it is slightly different from a Sierpinski sponge. It was first described by Karl Menger in 1926.

We start with a closed (filled) unit cube. Divide every face of the cube into 9 cubes, like a Rubik's cube (Magic cube). This will sub-divide the cube into 27 smaller cubes. We remove the smaller cube in the middle of each face and remove the smaller cube in the very center of larger cube; totally we remove 7 open cubes of size  $\frac{1}{3}$  and leaving 20 smaller cubes. This is a level-1 Menger sponge (resembling a Void cube). At the second stage we remove 7.20 open cubes of size  $\frac{1}{9}$  and leaving  $(20)^2$  smaller cubes. This is a level-2 Menger sponge.

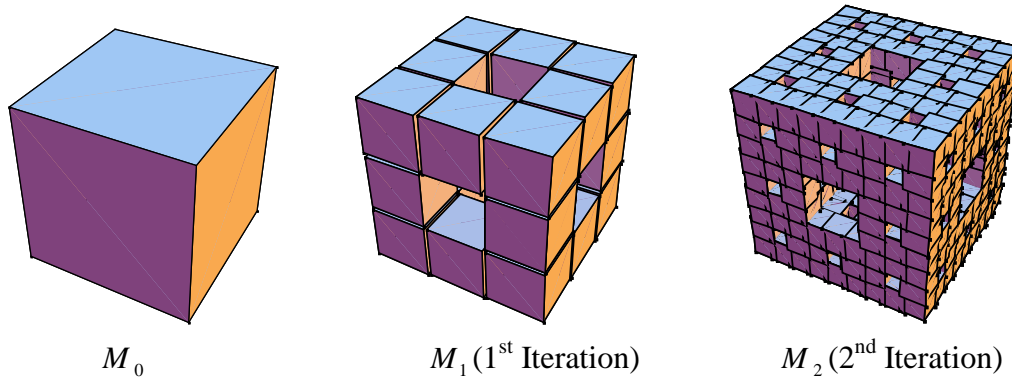


**Figure 3.7** The first three stages of the Menger sponge

6. At the  $n$ th stage, we remove  $7 \cdot (20)^{n-1}$  open cubes of size  $\frac{1}{3^n}$ .

The Menger sponge itself is the limit of this process after an infinite number of iterations. Arbitrary small neighborhoods intersect the Menger sponge at a finite set of points, so it has topological dimension 1.

The Menger sponge consists of  $(20)^n$  subsets with magnification factor  $3^n$ .

Therefore, the fractal dimension of the Menger sponge is  $D = \frac{\ln 20}{\ln 3} = 2.726$ .

### 3.4.2. Construction of the Sierpinski Tetrahedron

We start with a closed (filled) tetrahedron with unit edge. Divide every face of the tetrahedron into 3 triangles. This will sub-divide the tetrahedron into 8 smaller tetrahedrons. At the first stage, we remove 4 open tetrahedrons of size  $\frac{1}{2}$ . At the second stage, we remove 4.4 open tetrahedrons of size  $\frac{1}{4}$ . At the third stage, we remove  $4.4^2$  open tetrahedrons of size  $\frac{1}{8}$ . At the  $n$ th stage, we remove  $4.4^{n-1}$  open cubes of size  $\frac{1}{2^n}$ .

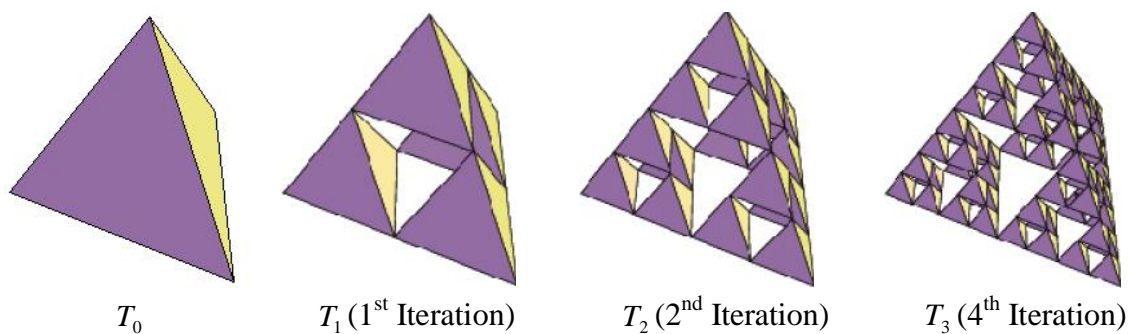


**Figure 3.8** The first four stages of the Sierpinski tetrahedron

After  $n \rightarrow \infty$ , we are left with a self-similar set which is called the Sierpinski tetrahedron. Arbitrary small neighborhoods intersect the Sierpinski tetrahedron at a finite set of points, so it has topological dimension 1.

The Sierpinski tetrahedron consists of  $4^n$  subsets with magnification factor  $2^n$ .

Hence the fractal dimension of the tetrahedron is  $D = \frac{\ln 4}{\ln 2} = 2$ .

### 3.4.3. Construction of the Octahedron Fractal

We start with a closed (filled) octahedron with unit edge. Divide every face of the Octahedron into 3 triangles. This will sub-divide the octahedron into 14 smaller octahedrons. At the first stage, we remove 2 open octahedrons of edge size  $\frac{1}{2}$ . At the second stage, we remove 2.6 open Octahedrons of edge size  $\frac{1}{4}$ . At the third stage, we remove  $2.6^2$  open Octahedrons of edge size  $\frac{1}{8}$ . At the  $n$ th stage, we remove  $2.6^{n-1}$  open octahedrons of edge size  $\frac{1}{2^n}$ .

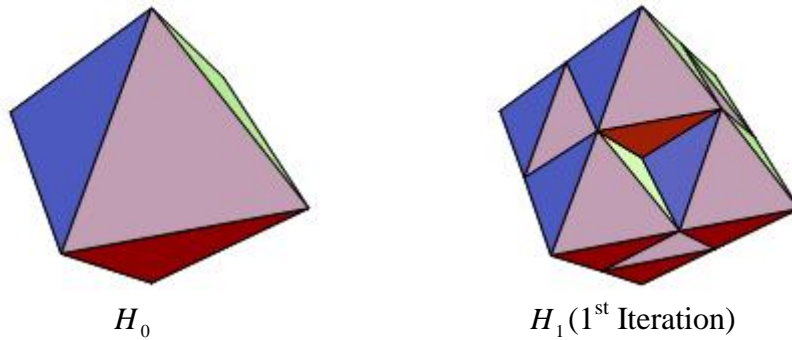


**Figure 3.9** The first two stages of the octahedron fractal

The octahedron fractal itself is the limit of this process after an infinite number of iterations. Arbitrary small neighborhoods intersect the octahedron fractal at a finite set of points, so it has topological dimension 1.

The octahedron fractal consists of  $6^n$  subsets with magnification factor  $2^n$ .

Therefore, the fractal dimension of the octahedron fractal is

$$D = \frac{\ln 6}{\ln 2} = 1 + \ln 3 = 2.5849.$$



# CHAPTER FOUR

## FRACTALS IN MEASURE SPACE

### OVERVIEW

In this chapter, we discuss basic measure theory. We show that the special type generalized Cantor sets are Borel set as well as Borel measurable whose Lebesgue measures are zero. Also we show that the Lebesgue measures of the two and three dimensional fractals are zero.

### 4.1. Basic Measure Theory

#### 4.1.1. [16] Outer Measure

Let  $A$  be a set of real numbers. Let  $\{I_n\}$  be a countable collections of open intervals that cover  $A$ , that is,  $A \subset \bigcup I_n$ , and for each such collection consider the sum of the length of the intervals in the collection. Then we define the outer measure  $\}^*(A) = \inf_{A \subset \bigcup I_n} \sum l(I_n)$ .

Example, the outer measure of any interval  $I$  on  $\mathbf{R}$  with endpoints  $a < b$  is  $b - a$  and is denoted as  $\}^*(I) = b - a$ .

**Definition 4.1.2. [16]** A set  $E \subset \mathbf{R}$  is said to be measurable if for each set  $A \subset \mathbf{R}$  we have  $\}^*(A) = \}^*(A \cap E) + \}^*(A \cap \bar{E})$ .

**Definition 4.1.3. [18]** The inner measure of any set  $A \subset E$ , denoted  $\}_*(A)$ , is defined as  $\}_*(A) = \}^*(E) - \}^*(E \setminus A)$ , where  $E \setminus A$  is the complement of  $A$  with respect to  $E$ .

**Definition 4.1.4. [16]** If  $A$  is a measurable set, we define the Lebesgue measure  $\}(A)$  to be the outer measure of  $A$ . Thus  $\}$  is the set function obtained by restricting the set function  $\}^*$  to the family  $M$  of measurable sets.

#### 4.1.4.1. [16] Some Properties of Lebesgue Measure

1. Let  $(A_i)$  be a sequence of measurable sets. Then

$$\}(\bigcup A_i) \leq \sum \}(A_i).$$

2. If the sets  $A_i$  are pairwise disjoint, then

$$\}(\bigcup A_i) = \sum \}(A_i).$$

3. Let be an infinite decreasing sequence of measurable sets, that is, a sequence with  $A_{n+1} \subset A_n$  for each  $n$ . Let  $\}(A_1)$  be finite. Then

$$\}(\bigcap_{i=1}^{\infty} A_i) = \lim_{n \rightarrow \infty} \}(A_n).$$

**Example 4.1.4.2. [8] Lebesgue Measure on  $\mathbf{R}$**

If  $A \subset \mathbf{R}$  and  $A = \bigcup [a_i, b_i]$  is a finite or countable union of disjoint intervals, then  $\lambda(A) = \sum (b_i - a_i)$ , that is, the sum of the length of the intervals. We define the Lebesgue measure  $\lambda^1(A)$  of an arbitrary set  $A$ ,

$$\lambda^1(A) = \inf \left\{ \sum_{i=1}^{\infty} (b_i - a_i) : A \subset \bigcup_{i=1}^{\infty} [a_i, b_i] \right\}.$$

**Example 4.1.4.3. [8] Lebesgue Measure on  $\mathbf{R}^n$**

If  $A = \{(x_1, x_2, \dots, x_n) \in \mathbf{R}^n : a_i \leq x_i \leq b_i\}$  is a coordinate parallelepiped in  $\mathbf{R}^n$ , and then  $n$ -dimensional volume of  $A$  is given by

$$\text{vol}^n(A) = (b_1 - a_1)(b_2 - a_2) \cdots (b_n - a_n).$$

If  $n = 1$ , a coordinate parallelepiped is just an interval with  $\text{vol}^1$  as length, as in Example 4.1.4.2. If  $n = 2$ , it is a rectangle with  $\text{vol}^2$  as area, and if  $n = 3$ , it is a cuboid with  $\text{vol}^3$  as the three-dimensional volume. Then we obtain  $n$ -dimensional Lebesgue measure  $\lambda^n(A)$  on  $\mathbf{R}^n$  by defining

$$\lambda^n(A) = \inf \left\{ \sum_{i=1}^{\infty} \text{vol}^n(A_i) : A \subset \bigcup_{i=1}^{\infty} A_i \right\},$$

where the infimum is taken over all coverings of  $A$  by coordinate parallelepipeds  $A_i$ .

**Definition 4.1.5. [17]** A collection  $\mathcal{B}$  of subsets of a set  $X$  is called a  $\sigma$ -algebra if  $\mathcal{B}$  satisfies the following axioms:

- A1:  $X \in \mathcal{B}$ ,
- A2: If  $A \in \mathcal{B}$ , then  $X \setminus A \in \mathcal{B}$ ,
- A3: If  $A = \bigcup_{n=1}^{\infty} A_n$  and if  $A_n \in \mathcal{B}$  for  $n = 1, 2, 3, \dots$ , then  $A \in \mathcal{B}$ .

**Definition 4.1.6. [18]** Let  $X = [a, b]$  be a closed set and let  $\mathcal{B}$  be a collection of subsets of  $X$ . A set function  $\lambda$  on  $\mathcal{B}$  (i.e.  $\lambda : \mathcal{B} \rightarrow [0, \infty]$ ) is called a measure if the following properties hold:

1. *Semi-Positive-Definite*:  $0 \leq \lambda(A) \leq b - a$  for all  $A \in \mathcal{B}$
2. *Trivial Case*:  $\lambda(\emptyset) = 0$
3. *Monotonicity*:  $\lambda(A) \leq \lambda(B)$  for all  $A, B \in \mathcal{B}$ ,  $A \subset B$
4. *Countable Additivity*: If  $A_1, A_2, A_3, \dots$  are in  $\mathcal{B}$ , with  $A_i \cap A_j = \emptyset$  for  $i \neq j$ , then

$$\lambda\left(\bigcup_{i=1}^{\infty} A_i\right) = \sum_{i=1}^{\infty} \lambda(A_i).$$

The pair  $(X, \mathcal{B})$  is called a measurable space and the triple  $(X, \mathcal{B}, \lambda)$  a measure space.

A measure  $\mu$  defined on a  $\sigma$ -algebra  $\mathcal{B}$  of subsets of a set  $X$  is called finite if  $\mu(X)$  is a finite real number (rather than  $\infty$ ). The measure  $\mu$  is called  $\sigma$ -finite if  $X$  is the countable union of measurable sets with finite measure. A set in a measure space is said to have  $\sigma$ -finite measure if it is a countable union of sets with finite measure.

**Definition 4.1.7. [19]** Let  $X$  be a non-empty set and  $\tau$  is a collection of subsets of  $X$ . Then  $\tau$  is a topology on  $X$  iff it satisfies the following axioms:

1. The empty set and  $X$  itself belong to  $\tau$ .
2. The union of any numbers of sets in  $\tau$  belongs to  $\tau$ .
3. The intersection of any finite number of sets in  $\tau$  belongs to  $\tau$ .

The members of  $\tau$  are then called  $\tau$ -open sets, or simply open sets and  $(X, \tau)$  is called a topological space.

**Definition 4.1.8. [20]** A Borel set is any set in topological space that can be formed from open sets (or, equivalently, from closed sets) through the operations of countable union, countable intersection and relative complement. Borel sets are named after Emile Borel.

**Definition 4.1.9. [20]** The Borel  $\sigma$ -algebra of a set  $X$  is the smallest  $\sigma$ -algebra of  $X$  that contains all of the open balls in  $X$ . Any element of a Borel  $\sigma$ -algebra is a Borel set.

#### 4.2. [4] Lebesgue Measures of the Generalized Cantor Sets

**Lemma 4.2.1.** Let  $X = [0, 1]$  be a closed set and  $\tau$  be a topology on  $X$ . Then  $(X, \tau)$  be a topological space. Let  $C_{1/(2^{m-1})} = \bigcap_{n \in \mathbf{N}} \Gamma_n$  be closed subsets in  $X$ . Then each  $C_{1/(2^{m-1})}, (2 \leq m < \infty)$  is Borel set and measurable set.

**Proof:** Since every intersection of closed sets is again closed set,  $\bigcap_{n \in \mathbf{N}} \Gamma_n$  is closed set.

By the definition of Borel set,  $C_{1/(2^{m-1})}$  is a Borel set.

Thus each  $C_{1/(2^{m-1})}, (2 \leq m < \infty)$  is a Borel set. Since every Borel set is a measurable set, then each  $C_{1/(2^{m-1})}, (2 \leq m < \infty)$  is a measurable set.  $\square$

**Theorem 4.2.2. [4]** Let  $X = [0, 1]$  be a closed set, and let  $\Sigma$  be a  $\sigma$ -algebra on  $X$  containing  $\Gamma_n, n$  in  $\mathbf{N}$ . Then  $(X, \Sigma)$  is a measurable space and each  $C_{1/(2^{m-1})} \in \Sigma$ , where  $2 \leq m < \infty$ .

**Proof:** We know  $C_{1/(2^{m-1})} = \bigcap_{n \in \mathbf{N}} \Gamma_n, (2 \leq m < \infty)$ .

For each  $n \in \mathbf{N}, \Gamma_n \in \Sigma$ . This implies that  $X \setminus \Gamma_n \in \Sigma$ . Axiom (2) for  $\sigma$ -algebra.

Then  $\bigcup_{n \in \mathbf{N}} (X \setminus \Gamma_n) \in \Sigma$ . Axiom (3) for  $\sigma$ -algebra.

This implies that  $X \setminus \left( \bigcup_{n \in \mathbb{N}} (X \setminus \Gamma_n) \right) \in \Sigma$ . Axiom (2) for  $\dagger$  – algebra.

Now using De Morgan’s laws, we have

$$\bigcup_{n \in \mathbb{N}} (X \setminus \Gamma_n) = X \setminus \bigcap_{n \in \mathbb{N}} \Gamma_n \in \Sigma \text{ and } X \setminus \left( \bigcup_{n \in \mathbb{N}} (X \setminus \Gamma_n) \right) = X \setminus \left( X \setminus \bigcap_{n \in \mathbb{N}} \Gamma_n \right) = \bigcap_{n \in \mathbb{N}} \Gamma_n \in \Sigma.$$

Thus each  $C_{1/(2m-1)} \in \Sigma$ , where  $2 \leq m < \infty$ . □

**Theorem 4.2.3. [4]** Let  $X = [0, 1]$  be a closed set and let  $(X, \dagger)$  be a topological space. Let  $B(\dagger)$  be the associated Borel  $\dagger$  – algebra. Let  $(\Gamma_n)_{n \in \mathbb{N}}$  be closed subset in  $X$ . Then each  $C_{1/(2m-1)}, (2 \leq m < \infty)$  is  $B(\dagger)$  – measurable.

**Proof:** We know  $C_{1/(2m-1)} = \bigcap_{n \in \mathbb{N}} \Gamma_n, (2 \leq m < \infty)$ . Since  $(\Gamma_n)_{n \in \mathbb{N}}$  is a closed set in  $X$ ,  $C_{1/(2m-1)}$  is a closed set in  $X$ . Then  $X \setminus C_{1/(2m-1)}$  is open set.

By the definition of Borel  $\dagger$  – algebra,  $X \setminus C_{1/(2m-1)} \in B(\dagger)$ .

This implies that  $X \setminus (X \setminus C_{1/(2m-1)}) = C_{1/(2m-1)} \in B(\dagger)$ . Axioms (2) for  $\dagger$  – algebra.

Thus each  $C_{1/(2m-1)}, (2 \leq m < \infty)$  is  $B(\dagger)$  – measurable. □

**Theorem 4.2.4. [4]** If  $\}$  is the Lebesgue measure and  $\}(C_{1/(2m-1)}) = \lim_{n \rightarrow \infty} \}(\Gamma_n) = 0$ , then each  $C_{1/(2m-1)}, (2 \leq m < \infty)$  has Lebesgue measure zero.

**Proof:** We know  $C_{1/(2m-1)} = \bigcap_{n \in \mathbb{N}} \Gamma_n$ , where  $2 \leq m < \infty$  and

$$\Gamma_n = [0, \frac{1}{(2m-1)^n}] \cup [\frac{2}{(2m-1)^n}, \frac{3}{(2m-1)^n}] \cup \dots \cup [\frac{(2m-1)^n - 1}{(2m-1)^n}, 1], (n \geq 1, 2 \leq m < \infty).$$

$$\}(C_{1/(2m-1)}) = \lim_{n \rightarrow \infty} \}(\Gamma_n)$$

$$\begin{aligned} &= \lim_{n \rightarrow \infty} \}([0, \frac{1}{(2m-1)^n}] \cup [\frac{2}{(2m-1)^n}, \frac{3}{(2m-1)^n}] \cup \dots \\ &\quad \cup [\frac{(2m-1)^n - 3}{(2m-1)^n}, \frac{(2m-1)^n - 2}{(2m-1)^n}] \cup [\frac{(2m-1)^n - 1}{(2m-1)^n}, 1]) \\ &= \lim_{n \rightarrow \infty} [\}([0, \frac{1}{(2m-1)^n}]) + \}([\frac{2}{(2m-1)^n}, \frac{3}{(2m-1)^n}]) + \dots \\ &\quad + \}([\frac{(2m-1)^n - 3}{(2m-1)^n}, \frac{(2m-1)^n - 2}{(2m-1)^n}]) + \}([\frac{(2m-1)^n - 1}{(2m-1)^n}, 1])] \\ &= \lim_{n \rightarrow \infty} [\frac{1}{(2m-1)^n} + \frac{3}{(2m-1)^n} - \frac{2}{(2m-1)^n} + \dots \\ &\quad + \frac{(2m-1)^n - 2}{(2m-1)^n} - \frac{(2m-1)^n - 3}{(2m-1)^n} + 1 - \frac{(2m-1)^n - 1}{(2m-1)^n}] = 0 \end{aligned}$$

Therefore,  $\lambda(C_{1/2m-1}) = 0$ .

Hence each  $C_{1/2m-1}$ , ( $2 \leq m < \infty$ ) has Lebesgue measure zero.  $\square$

**Alternative method:**

**Theorem 4.2.5. [4]** The generalized Cantor sets  $C_{1/(2m-1)}$ , ( $2 \leq m < \infty$ ) is measurable and has Lebesgue measure zero.

**Proof:** We know  $C_{1/(2m-1)} = \bigcap_{n \in \mathbb{N}} \Gamma_n$ , ( $2 \leq m < \infty$ ),

where  $\Gamma_n = [0, \frac{1}{(2m-1)^n}] \cup [\frac{2}{(2m-1)^n}, \frac{3}{(2m-1)^n}] \cup \dots \cup [\frac{(2m-1)^n - 1}{(2m-1)^n}, 1]$ .

By Lemma 4.1.1, each  $C_{1/(2m-1)}$  is Borel set and measurable.

From the construction of  $C_{1/(2m-1)}$ , ( $2 \leq m < \infty$ ), we remove  $(m-1)m^{n-1}$  disjoint intervals from each previous segments and each having length  $1/(2m-1)^n$ , where  $n \geq 1$ .

Thus we will remove a total length

$$\begin{aligned} \sum_{n=1}^{\infty} (m-1)m^{n-1} \cdot \frac{1}{(2m-1)^n} &= \frac{m-1}{2m-1} \sum_{n=1}^{\infty} (m/(2m-1))^{n-1} = \frac{m-1}{2m-1} \sum_{n=0}^{\infty} (m/(2m-1))^n \\ &= \frac{m-1}{2m-1} \left( \frac{1}{1-m/(2m-1)} \right) = 1. \end{aligned}$$

Therefore, each  $C_{1/(2m-1)}$  is obtained by removing a total length 1 from the unit interval  $[0,1]$ . Hence  $\lambda(I \setminus C_{1/(2m-1)}) = 1$ .

Since  $\lambda(I) = \lambda(C_{1/(2m-1)}) + \lambda(I \setminus C_{1/(2m-1)})$ , then

$$\lambda(C_{1/(2m-1)}) = \lambda(I) - \lambda(I \setminus C_{1/(2m-1)}) = 1 - 1 = 0.$$

Thus each  $C_{1/(2m-1)}$ , ( $2 \leq m < \infty$ ) has Lebesgue measure zero.

Hence each  $C_{1/(2m-1)}$ , ( $2 \leq m < \infty$ ) is measurable and has Lebesgue measure zero.  $\square$

**Proposition 4.2.6. [4]** Let  $(\Gamma_n)$  be an infinite decreasing sequence of each measurable sets  $C_{1/(2m-1)}$ , that is, a sequence with  $\Gamma_{n+1} \subset \Gamma_n$  for each  $n$ , let  $\lambda(\Gamma_1)$  be finite. Then

$$\lambda\left(\bigcap_{i=1}^{\infty} \Gamma_i\right) = \lim_{n \rightarrow \infty} \lambda(\Gamma_n) \text{ for each } C_{1/(2m-1)}, \text{ where } 2 \leq m < \infty.$$

**Proof:** Since  $(\Gamma_n)$  is an infinite decreasing sequence of each measurable set  $C_{1/(2m-1)}$ ,

$C_{1/(2m-1)} = \bigcap_{i=1}^{\infty} \Gamma_i$ , where  $2 \leq m < \infty$ . Let  $\Omega_i = \Gamma_i \setminus \Gamma_{i+1}$ . Then  $\Gamma_1 \setminus C_{1/(2m-1)} = \bigcup_{i=1}^{\infty} \Omega_i$  and the

sets  $\Omega_i$  are pair wise disjoint.

$$\therefore \lambda(\Gamma_1 \setminus C_{1/(2m-1)}) = \lambda\left(\bigcup_{i=1}^{\infty} \Omega_i\right) = \sum_{i=1}^{\infty} \lambda(\Omega_i) = \sum_{i=1}^{\infty} \lambda(\Gamma_i \setminus \Gamma_{i+1}) \tag{4.1}$$

But we know  $\lambda(\Gamma_1) = \lambda(C_{1/(2m-1)}) + \lambda(\Gamma_1 \setminus C_{1/(2m-1)})$ , since  $C_{1/(2m-1)} \subset \Gamma_1$

and  $\}(\Gamma_i) = \}(\Gamma_{i+1}) + \}(\Gamma_i \sim \Gamma_{i+1})$ , since  $\Gamma_{i+1} \subset \Gamma_i$ .

Since  $\}(\Gamma_i) \leq \}(\Gamma_1) < \infty$ , we have

$$\begin{aligned} \}(\Gamma_1 \sim C_{1/(2m-1)}) &= \}(\Gamma_1) - \}(C_{1/(2m-1)}) \\ \}(\Gamma_i \sim \Gamma_{i+1}) &= \}(\Gamma_i) - \}(\Gamma_{i+1}) \end{aligned}$$

From (4.1), we have

$$\begin{aligned} \}(\Gamma_1) - \}(C_{1/(2m-1)}) &= \sum_{i=1}^{\infty} (\}(\Gamma_i) - \}(\Gamma_{i+1})) = \lim_{n \rightarrow \infty} \sum_{i=1}^{n-1} (\}(\Gamma_i) - \}(\Gamma_{i+1})) \\ &= \}(\Gamma_1) - \lim_{n \rightarrow \infty} \}(\Gamma_n) \end{aligned}$$

Since  $\}(\Gamma_1) < \infty$ , we have  $\}(C_{1/(2m-1)}) = \lim_{n \rightarrow \infty} \}(\Gamma_n)$ .

Hence  $\}(C_{1/(2m-1)}) = \lim_{n \rightarrow \infty} \}(\Gamma_n)$  for each  $C_{1/(2m-1)}$ , where  $2 \leq m < \infty$ . □

**Alternative method:**

**Proposition 4.2.7. [4]** If  $X = [0,1]$  is a closed and  $B$  is a collection of subsets of  $X$ , then  $(X, B)$  is a measurable space. If  $\Gamma_i \in B$ ,  $\sim(\Gamma_1) < \infty$  and  $\Gamma_{i+1} \subset \Gamma_i$ , then

$$\sim\left(\bigcap_{i=1}^{\infty} \Gamma_i\right) = \lim_{n \rightarrow \infty} \sim(\Gamma_n) \text{ for each } C_{1/(2m-1)}, \text{ where } 2 \leq m < \infty.$$

**Proof:** Since  $C_{1/(2m-1)} = \bigcap_{i=1}^{\infty} \Gamma_i$ , then  $\Gamma_1 = C_{1/(2m-1)} \cup \bigcup_{i=1}^{\infty} (\Gamma_i \sim \Gamma_{i+1})$ , and this is a disjoint union.

$$\text{Hence } \sim(\Gamma_1) = \sim(C_{1/(2m-1)}) + \sum_{i=1}^{\infty} \sim(\Gamma_i \sim \Gamma_{i+1}) \tag{4.2}$$

Since  $\Gamma_i = \Gamma_{i+1} \cup (\Gamma_i \sim \Gamma_{i+1})$  is a disjoint union, we have  $\sim(\Gamma_i \sim \Gamma_{i+1}) = \sim(\Gamma_i) - \sim(\Gamma_{i+1})$ .

Now from (4.2) we have

$$\begin{aligned} \sim(\Gamma_1) &= \sim(C_{1/(2m-1)}) + \sum_{i=1}^{\infty} (\sim(\Gamma_i) - \sim(\Gamma_{i+1})) \\ \sim(\Gamma_1) &= \sim(C_{1/(2m-1)}) + \lim_{n \rightarrow \infty} \sum_{i=1}^{n-1} (\sim(\Gamma_i) - \sim(\Gamma_{i+1})) \\ &= \sim(C_{1/(2m-1)}) + \sim(\Gamma_1) - \lim_{n \rightarrow \infty} \sim(\Gamma_n) \end{aligned}$$

That is,  $\}(C_{1/(2m-1)}) = \lim_{n \rightarrow \infty} \}(\Gamma_n)$ .

Hence  $\}(C_{1/(2m-1)}) = \lim_{n \rightarrow \infty} \}(\Gamma_n)$  for each  $C_{1/(2m-1)}$ , where  $2 \leq m < \infty$ . □

### 4.3. Lebesgue Measures of the Two Dimensional Fractals

**Lemma 4.3.1.** Let  $X = [0,1] \times [0,1]$  be a closed set and  $\tau$  be a topology on  $X$ . Then  $(X, \tau)$  be a topological space. Let  $A = \bigcap_{n=0}^{\infty} A_n$  be closed subsets in  $X$ . Then  $A$  is Borel set and measurable set.

**Proof:** Since every intersection of closed sets is again closed set,  $\bigcap_{n \in \mathbb{N}} A_n$  is closed set. By the definition of Borel set,  $\bigcap_{n \in \mathbb{N}} A_n$  is a Borel set. Thus  $A$  is a Borel set.

Since every Borel set is measurable, then  $A$  is a measurable set. □

**Theorem 4.3.2.** The Sierpinski equilateral triangle is measurable and has Lebesgue measure zero.

**Proof:** We know that the Sierpinski equilateral triangle is  $A = \bigcap_{n=0}^{\infty} A_n$ .

By Lemma 4.3.1,  $A$  is Borel set and measurable.

From the construction of Sierpinski equilateral triangle, we remove  $3^{n-1}$  open triangles from each previous triangles and each having size  $\frac{1}{2^n}$ , where  $n \geq 1$ .

We remove a total area

$$\sum_{n=1}^{\infty} 3^{n-1} \cdot \frac{\sqrt{3}}{4} \left(\frac{1}{2^n}\right)^2 = \frac{\sqrt{3}}{16} \sum_{n=1}^{\infty} (3/4)^{n-1} = \frac{\sqrt{3}}{16} \sum_{n=0}^{\infty} (3/4)^n = \frac{\sqrt{3}}{16} \left(\frac{1}{1-3/4}\right) = \frac{\sqrt{3}}{4}$$

Therefore, the Sierpinski equilateral triangle is obtained by removing a total area  $\frac{\sqrt{3}}{4}$

from the equilateral triangle whose area is  $A_0 = \frac{\sqrt{3}}{4}$ . Hence  $\mu(A_0 \setminus A) = \frac{\sqrt{3}}{4}$

Since  $\mu(A_0) = \mu(A) + \mu(A_0 \setminus A)$ , then  $\mu(A) = \mu(A_0) - \mu(A_0 \setminus A) = \frac{\sqrt{3}}{4} - \frac{\sqrt{3}}{4} = 0$ .

Thus the Lebesgue measure of the Sierpinski equilateral triangle is zero. □

**Theorem 4.3.3.** The Sierpinski isosceles right triangle is measurable and has Lebesgue measure zero.

**Proof:** We know that the Sierpinski isosceles right triangle is  $A = \bigcap_{n=0}^{\infty} A_n$ .

By Lemma 4.3.1,  $A$  is Borel set and measurable.

From the construction of Sierpinski isosceles right triangle, we remove  $3^{n-1}$  open triangles from each previous triangles and each having size  $\frac{1}{2^n}$ , where  $n \geq 1$ .

Then we remove a total area

$$\sum_{n=1}^{\infty} 3^{n-1} \cdot \frac{1}{2} \left( \frac{1}{2^n} \right)^2 = \frac{1}{8} \sum_{n=1}^{\infty} (3/4)^{n-1} = \frac{1}{8} \sum_{n=0}^{\infty} (3/4)^n = \frac{1}{8} \left( \frac{1}{1-3/4} \right) = \frac{1}{2}$$

Therefore, the Sierpinski isosceles right triangle is obtained by removing a total area  $\frac{1}{2}$

from the isosceles right triangle whose area is  $A_0 = \frac{1}{2}$ . Thus  $\lambda(A_0 \setminus A) = \frac{1}{2}$ .

Since  $\lambda(A_0) = \lambda(A) + \lambda(A_0 \setminus A)$ , then  $\lambda(A) = \lambda(A_0) - \lambda(A_0 \setminus A) = \frac{1}{2} - \frac{1}{2} = 0$ .

Hence the Lebesgue measure of the Sierpinski isosceles right triangle is zero.  $\square$

Similarly, we can show that the Lebesgue measures of the Sierpinski isosceles triangle and scalene triangle are zero.

**Theorem 4.3.4.** The box fractal is measurable and has Lebesgue measure zero.

**Proof:** We know that the box fractal is  $B = \bigcap_{n=0}^{\infty} B_n$ . Since every intersection of closed sets

is again closed set,  $\bigcap_{n \in \mathbb{N}} B_n$  is closed set. By the definition of Borel set,  $\bigcap_{n \in \mathbb{N}} B_n$  is a Borel set.

Thus  $B$  is a Borel set. Since every Borel set is measurable, then  $B$  is measurable.

From the construction of the Box fractal, we remove  $4 \cdot 5^{n-1}$  open squares from each previous squares and each having size  $\frac{1}{3^n}$ , where  $n \geq 1$ .

Now we remove a total area

$$\sum_{n=1}^{\infty} 4 \cdot 5^{n-1} \cdot \left( \frac{1}{3^n} \right)^2 = \frac{4}{9} \sum_{n=1}^{\infty} (5/9)^{n-1} = \frac{4}{9} \sum_{n=0}^{\infty} (5/9)^n = \frac{4}{9} \left( \frac{1}{1-5/9} \right) = 1.$$

Therefore, the box fractal is obtained by removing a total area 1 from the unit box fractal.

Hence  $\lambda(B_0 \setminus B) = 1$ .

Since  $\lambda(B_0) = \lambda(B) + \lambda(B_0 \setminus B)$ , then  $\lambda(B) = \lambda(B_0) - \lambda(B_0 \setminus B) = 1 - 1 = 0$ ,

This shows that the Lebesgue measure of the box fractal is zero.  $\square$

**Theorem 4.3.5.** The Sierpinski carpet is measurable and has Lebesgue measure zero.

**Proof:** We know that the Sierpinski carpet is  $C = \bigcap_{n=0}^{\infty} C_n$ . Since every intersection of closed

sets is again closed set,  $\bigcap_{n \in \mathbb{N}} C_n$  is closed set. By the definition of Borel set,  $\bigcap_{n \in \mathbb{N}} C_n$  is a Borel

set. Thus  $C$  is a Borel set. Since every Borel set is measurable, then  $C$  is measurable.



From the construction of the Sierpinski carpet, we remove  $8^{n-1}$  open squares from each previous squares and each having size  $\frac{1}{3^n}$ , where  $n \geq 1$ .

We remove a total area

$$\sum_{n=1}^{\infty} 8^{n-1} \cdot \left(\frac{1}{3^n}\right)^2 = \frac{1}{9} \sum_{n=1}^{\infty} (8/9)^{n-1} = \frac{1}{9} \sum_{n=0}^{\infty} (8/9)^n = \frac{1}{9} \left(\frac{1}{1-8/9}\right) = 1.$$

Therefore, the Sierpinski carpet is produced by removing a total area 1 from the original carpet whose area is  $C_0 = 1$ . Hence  $\lambda(C_0 \setminus C) = 1$ .

Since  $\lambda(C_0) = \lambda(C) + \lambda(C_0 \setminus C)$ , then  $\lambda(C) = \lambda(C_0) - \lambda(C_0 \setminus C) = 1 - 1 = 0$ .

Hence the Lebesgue measure of the Sierpinski carpet is zero. □

**Theorem 4.3.6.** The square fractal is measurable and has Lebesgue measure zero.

**Proof:** We know that the square fractal is  $S = \bigcap_{n=0}^{\infty} S_n$ . Since every intersection of closed sets is again closed set,  $\bigcap_{n \in \mathbb{N}} S_n$  is closed set. By the definition of Borel set,  $\bigcap_{n \in \mathbb{N}} S_n$  is a Borel set.

Thus  $S$  is a Borel set. Since every Borel set is measurable,  $S$  is measurable.

From the construction of the square fractal, we remove  $9^{n-1}$  open squares from each previous squares and each having size  $\frac{1}{5^n}$ , where  $n \geq 1$ .

We remove a total area

$$\sum_{n=1}^{\infty} 16 \cdot 9^{n-1} \cdot \left(\frac{1}{5^n}\right)^2 = \frac{16}{25} \sum_{n=1}^{\infty} \left(\frac{9}{25}\right)^{n-1} = \frac{16}{25} \sum_{n=0}^{\infty} \left(\frac{9}{25}\right)^n = \frac{16}{25} \left(\frac{1}{1-9/25}\right) = 1.$$

Therefore, the square fractal is produced by removing a total area 1 from the original carpet whose area is  $S_0 = 1$ . Hence  $\lambda(S_0 \setminus S) = 1$ .

Since  $\lambda(S_0) = \lambda(S) + \lambda(S_0 \setminus S)$ , then  $\lambda(S) = \lambda(S_0) - \lambda(S_0 \setminus S) = 1 - 1 = 0$ .

Therefore, the Lebesgue measure of the square fractal is zero. □

#### 4.4. Lebesgue Measures of the Three Dimensional Fractals

**Lemma 4.4.1.** Let  $X = [0,1] \times [0,1] \times [0,1]$  be a closed set and  $\tau$  be a topology on  $X$ . Then  $(X, \tau)$  be a topological space. Let  $M = \bigcap_{n=0}^{\infty} M_n$  be closed subsets in  $X$ . Then  $M$  is Borel set and measurable set.

**Proof:** Since every intersection of closed sets is again closed set,  $\bigcap_{n \in \mathbb{N}} M_n$  is closed set.

By the definition of Borel set,  $\bigcap_{n \in \mathbb{N}} M_n$  is a Borel set. Thus  $M$  is a Borel set.

Since every Borel set is measurable,  $M$  is a measurable set. □

**Theorem 4.4.2.** The Menger sponge is measurable and has Lebesgue measure zero.

**Proof:** We know that the Menger sponge is  $M = \bigcap_{n=0}^{\infty} M_n$ .

By Lemma 4.4.1,  $M$  is Borel set and measurable.

From the construction of the Menger sponge, we remove  $7 \cdot (20)^{n-1}$  open cubes from each previous cube and each having edge length  $\frac{1}{3^n}$ , where  $n \geq 1$ .

Now we remove a total volume

$$\sum_{n=1}^{\infty} 7 \cdot (20)^{n-1} \cdot \left(\frac{1}{3^n}\right)^3 = \frac{7}{27} \sum_{n=1}^{\infty} (20/27)^{n-1} = \frac{7}{27} \sum_{n=0}^{\infty} (20/27)^n = \frac{7}{27} \left(\frac{1}{1-20/27}\right) = 1$$

Therefore, the Menger sponge is obtained by removing a total volume 1 from the unit cube. Hence  $\lambda(M_0 \setminus M) = 1$

Since  $\lambda(M_0) = \lambda(M) + \lambda(M_0 \setminus M)$ , then  $\lambda(M) = \lambda(M_0) - \lambda(M_0 \setminus M) = 1 - 1 = 0$ .

This shows that the Lebesgue measure of the Menger sponge is zero.  $\square$

**Theorem 4.4.3.** The Sierpinski tetrahedron is measurable and has Lebesgue measure zero.

**Proof:** We know that the Sierpinski tetrahedron is  $T = \bigcap_{n=0}^{\infty} T_n$ .

Since every intersection of closed sets is again closed set,  $\bigcap_{n \in \mathbb{N}} T_n$  is closed set.

By the definition of Borel set,  $T$  is a Borel set and hence  $T$  is a measurable set.

From the construction of the Sierpinski tetrahedron, we have edge length 1 and volume  $\frac{1}{6\sqrt{2}}$

that is  $\lambda(T_0) = \frac{1}{6\sqrt{2}}$ . We remove  $4 \cdot 4^{n-1}$  open tetrahedron from each previous tetrahedron and

each having edge size  $\frac{1}{2^n}$ , where  $n \geq 1$ .

Now we remove a total volume

$$\begin{aligned} \sum_{n=1}^{\infty} 4 \cdot 4^{n-1} \cdot \frac{1}{6\sqrt{2}} \left(\frac{1}{2^n}\right)^3 &= \frac{2}{3\sqrt{2}} \cdot \frac{1}{8} \sum_{n=1}^{\infty} (4/8)^{n-1} = \frac{1}{12\sqrt{2}} \sum_{n=0}^{\infty} (1/2)^n \\ &= \frac{1}{12\sqrt{2}} \left(\frac{1}{1-1/2}\right) = \frac{1}{6\sqrt{2}} \end{aligned}$$

Therefore, the Sierpinski tetrahedron is obtained by removing a total volume  $\frac{1}{6\sqrt{2}}$  from

the original tetrahedron. Hence  $\lambda(T_0 \setminus T) = \frac{1}{6\sqrt{2}}$ .

Since  $\lambda(T_0) = \lambda(T) + \lambda(T_0 \setminus T)$ , then  $\lambda(T) = \lambda(T_0) - \lambda(T_0 \setminus T) = \frac{1}{6\sqrt{2}} - \frac{1}{6\sqrt{2}} = 0$ .

We conclude that the Sierpinski tetrahedron has Lebesgue measure zero.  $\square$

**Theorem 4.4.4.** The octahedron fractal is measurable and has Lebesgue measure zero.

**Proof:** We know that the octahedron fractal is  $O = \bigcap_{n=0}^{\infty} O_n$ .

Since every intersection of closed sets is again closed set,  $\bigcap_{n \in \mathbb{N}} O_n$  is closed set.

By the definition of Borel set,  $O = \bigcap_{n \in \mathbb{N}} O_n$  is a Borel set.

Since every Borel set is measurable, then  $O = \bigcap_{n \in \mathbb{N}} O_n$  is a measurable set.

From the construction of the octahedron, we have edge length 1 and volume is  $\frac{\sqrt{2}}{3}$  that is

$\}(H_0) = \frac{\sqrt{2}}{3}$ . We remove  $2 \cdot 6^{n-1}$  open octahedron from each previous octahedron and each

having edge size  $\frac{1}{2^n}$ , where  $n \geq 1$ .

We remove a total volume

$$\sum_{n=1}^{\infty} 2 \cdot 6^{n-1} \cdot \frac{\sqrt{2}}{3} \left(\frac{1}{2^n}\right)^3 = \frac{2\sqrt{2}}{3} \cdot \frac{1}{8} \sum_{n=1}^{\infty} (6/8)^{n-1} = \frac{\sqrt{2}}{12} \sum_{n=0}^{\infty} (3/4)^n = \frac{\sqrt{2}}{12} \left(\frac{1}{1-3/4}\right) = \frac{\sqrt{2}}{3}.$$

Therefore, the octahedron is obtained by removing a total volume 1 from the original octahedron. Hence  $\}(H_0 \setminus H) = 1$

Since  $\}(H_0) = \}(H) + \}(H_0 \setminus H)$ , then  $\}(H) = \}(H_0) - \}(H_0 \setminus H) = \frac{\sqrt{2}}{3} - \frac{\sqrt{2}}{3} = 0$ .

Hence the octahedron fractal has Lebesgue measure zero. □

# CHAPTER FIVE

## ITERATED FUNCTION SYSTEMS OF FRACTALS

### OVERVIEW

In this chapter, we formulate Iterated Function Systems (IFS) of two dimensional square fractals and three dimensional fractals such as the Menger sponge, the Sierpinski tetrahedron and the octahedron fractal by affine transformation method and fixed points method of R. L. Devaney [1]. We observe that different fractals are generated by different iterated function system using Mathematica and MatLab programming. We show that these functions are asymptotically stable and the fixed points are sink.

### 5.1. Iterated Function Systems of Fractals

Any fractal has some infinitely repeating pattern. When creating such fractal, we would suspect that the easiest way is to repeat a certain series of steps which create that pattern. Instead of the word “repeat” we use a mathematical synonym “iterate” and the process is called *iteration*. Iterated Function System is another way of generating fractals. It is based on taking a point or a figure and substituting it with several other identical ones. Iterated function system represents an extremely versatile method for conveniently generating a wide variety of useful fractal structures [5]. The Iterated Function System is base on the application of a series of Affine Transformations. An Affine Transformation is a recursive transformation of the type [21]

$$\begin{pmatrix} x_{n+1} \\ y_{n+1} \end{pmatrix} = \begin{pmatrix} a & b \\ c & d \end{pmatrix} \begin{pmatrix} x_n \\ y_n \end{pmatrix} + \begin{pmatrix} e \\ f \end{pmatrix}$$

or equivalently

$$(x_{n+1}, y_{n+1}) = (ax_n + by_n + e, cx_n + dy_n + f)$$

where  $a, b, c, d, e$  and  $f$  are real numbers.

Thus an Affine Transformation is represented by six parameters such that  $a, b, c$  and  $d$  control rotation and scaling, while  $e$  and  $f$  control linear translation.

Each Affine Transformation will generally yield a new attractor (or fractal) in the final image. The form of the attractor is given through the choice of the coefficients  $a$  through  $f$ , which uniquely determines the Affine Transformation. To get a desire shape, the collage of several attractors may be used (i.e., several Affine Transformations). This method is referred to as an Iterated Function System (IFS).

Now suppose we consider  $w_1, w_2, \dots, w_N$  as a set of affine linear transformations, and let  $A$  be the initial geometry. Then a new geometry, produced by applying the set of transformations to the original geometry  $A$  and collecting the result from  $w_1(A), w_2(A), \dots, w_N(A)$  can be represented by

$$F(A) = \bigcup_{i=1}^N w_i(A) \tag{5.1}$$

where  $F$  is known as the Barnsley-Hutchinson operator [21, 22]. Fractal geometry can be obtained by repeated applying  $F$  to the previous geometry. For example, if the set  $A_0$  is the initial geometry, then we will have

$$A_1 = F(A_0), A_2 = F(A_1), \dots, A_{i+1} = F(A_i).$$

An iteration function system generates a sequence that converges to a final image  $A_\infty$ .

**Alternative method to formulate iterated function system:**

Let  $0 < S < 1$ . Let  $p_1, p_2, \dots, p_N$  be points in the plane. Let  $w_i(p) = S(p - p_i) + p_i$ , where  $p = \begin{pmatrix} x \\ y \end{pmatrix}$  and for each  $i = 1, 2, 3, \dots, N$ . The collection of functions  $\{w_1, w_2, \dots, w_N\}$  is called an iterated function system [1]. Iterated Function Systems are a method of constructing fractals; the resulting constructions are always self-similar.

**Definition 5.1.1. [23]** (Contraction) A map  $w: X \rightarrow X$ , where  $(X, d)$  is a metric space, is called a contraction if there exists  $L < 1$  such that

$$d(w(x), w(y)) \leq L \cdot d(x, y) \text{ for all } x, y \in X.$$

This condition is called Lipschitz condition, where  $L \geq 0$  is called Lipschitz constant. Contractions are thus Lipschitzian maps with a Lipschitz constant that is smaller than 1.

An iterated function system (IFS) is a finite collection  $\{w_1, w_2, \dots, w_N\}$  of contractions of a metric space  $X$ . A subset  $A \subseteq X$  is called an invariant set with respect to the IFS

$$\{w_i : i \in I\} \text{ if } A = \bigcup_{i=1}^N w_i(A).$$

If for every nonempty compact subset  $A$  of  $X$ , the sequence  $(F^n(A))$  converges in the Hausdorff distance to  $A_0$ , the set  $A_0$  is called an attractor (or fractal) corresponding to the IFS  $\{w_i : i \in I\}$  [24].

Assume that  $I$  is finite and for every  $i \in I$ , the function  $w_i$  is Lipschitzian with the Lipschitz constant. If  $L_i < 1$  for  $i \in I$ , then the IFS is  $\{w_i : i \in I\}$  asymptotically stable (on sets) [21, 25].

**5.1.2. [26] Fundamental Theorem of IFS:** Let  $\{S_1, S_2, \dots, S_m\}$  be an iterated function system on  $\mathbf{R}^n$ , and  $0 < c_i < 1$  such that

$$|S_i(x) - S_i(y)| \leq c_i |x - y| \text{ for each } x, y \in \mathbf{R}^n.$$

Then there exists a unique non-empty set  $F \subseteq \mathbf{R}^n$  such that  $F = \bigcup_{i=1}^m S_i(F)$ .

That is,  $F$  is an attractor of the iterated function systems.

Proof: The proof is omitted.

### 5.1.3. [26] Some Properties of an Iterated Function System

1. For any  $A \in S$ , the sequence  $S^k(F)$  converges to the attractor  $F$  in d. To see this,

$$d(S^k(A), F) = d(S^k(A), S^k(F)) \leq cd(S^{k-1}(A), S^{k-1}(F)) \leq \dots \leq c^k d(A, F),$$

where  $c = \max_{1 \leq i \leq m} c_i < 1$  and so  $c^k \rightarrow 0$ .

2. We have the attractor  $F = S(E) = S^2(E) = S^3(E)$ , that is,

$$F = S(F) = \bigcup_{i=1}^m S_i(F) = \bigcup_{j=1}^m \bigcup_{i=1}^m S_j(S_i(F)) = \bigcup_{k=1}^m \bigcup_{j=1}^m \bigcup_{i=1}^m S_k(S_j(S_i(F))) = \dots$$

$$\text{In general, } F = \bigcup_{1 \leq i_1, \dots, i_k \leq m} S_{i_1}(S_{i_2} \dots (S_{i_k}(F))) = \bigcup_{1 \leq i_1, \dots, i_k \leq m} S_{i_1} \circ S_{i_2} \circ \dots \circ (S_{i_k}(F))$$

3. Computing the attractor of an IFS:

(a) Use the property (1): Let  $A$  be any initial set. Plot  $S^k(A)$  for a suitable  $k$ .

That is,  $S^k(A) = \bigcup_{1 \leq i_1, \dots, i_k \leq m} S_{i_1} \circ S_{i_2} \circ \dots \circ (S_{i_k}(A))$ . Thus  $S^k(A)$  gives an approximation to  $F$ .

(b) Chaos game: Take any initial  $x \in \mathbf{R}^n$  and choose mappings from  $\{S_1, S_2, \dots, S_m\}$  at random (with equal probability). Plot the sequence given by  $x_0 = x, x_k = S_{i_k}(x_{k-1})$ , where  $S_{i_k}$  is the  $k$ th mapping chosen. Then the sequence  $x_k$  fills the attractor  $F$ .

**Theorem 5.1.4.** Let  $f$  be a (smooth) map on  $\mathbf{R}$  and assume that  $p$  is a fixed point of  $f$

1. If  $|f'(p)| < 1$ , then  $p$  is a sink.
2. If  $|f'(p)| > 1$ , then  $p$  is a source.

**Proof:** The proof of the theorem can be found in [27].

**Definition 5.1.5. [27]** Let  $f = (f_1, f_2, \dots, f_m)$  be a map on  $\mathbf{R}^n$ , and let  $p \in \mathbf{R}^n$ .

The Jacobian matrix of  $f$  at  $p$ , denoted  $\mathbf{D}f(p)$  is the matrix

$$\mathbf{D}f(p) = \begin{pmatrix} \frac{\partial f_1}{\partial x_1}(p) & \dots & \frac{\partial f_1}{\partial x_n}(p) \\ \vdots & & \vdots \\ \frac{\partial f_n}{\partial x_1}(p) & \dots & \frac{\partial f_n}{\partial x_n}(p) \end{pmatrix}$$

of partial derivatives evaluated at  $p$ .

**Theorem 5.1.6.** Let  $f$  be a map on  $\mathbf{R}^n$ , and assume  $f(p) = p$ .

1. If the magnitude of each eigenvalue of  $Df(p)$  is less than 1, then  $p$  is a sink.
2. If the magnitude of each eigenvalue of  $Df(p)$  is greater than 1, then  $p$  is a source.

**Proof:** The proof of the theorem can be found in [27].

**Definition 5.1.7.** [27] Let  $f$  be a map on  $\mathbf{R}^n$ . Assume that  $f(p) = p$ . Then the fixed point  $p$  is called hyperbolic if none of the eigenvalue of  $Df(p)$  has magnitude 1.

If  $p$  is hyperbolic and if at least one eigenvalue of  $Df(p)$  has magnitude greater than 1 and at least one eigenvalue has magnitude less than 1, then  $p$  is called a saddle.

## 5.2 Iterated Function Systems of the Generalized Cantor Sets

We may define the iterated function system of the generalized Cantor sets by choosing

different  $S$  values such as  $S = \frac{1}{2m-1}$ , where  $2 \leq m < \infty$ .

### 5.2.1. Iterated Function System of the Cantor middle $\frac{1}{3}$ set

The Cantor middle  $\frac{1}{3}$  set may be obtained by the following iterated function system

$$\begin{aligned} w_1(x) &= \frac{x}{3} \\ w_2(x) &= \frac{x}{3} + \frac{2}{3} \end{aligned} \tag{5.2}$$

The contraction factor is  $r = \frac{1}{3}$ , and the fixed points are located at 0 and 1 along the  $x$ -axis.

The Barnsley-Hutchinson operator is  $F(A) = \bigcup_{i=1}^2 w_i(A)$ .

Then the attractor of IFS (5.2) is  $A_{n+1} = F(A_n)$ ,  $A_0 \in [0,1]$ ,  $n = 0,1,2,\dots$  (5.3)

which is the well-know Cantor middle  $\frac{1}{3}$  set.

From (5.3) we obtain obviously,

$$\begin{aligned} A_1 &= F(A_0) = w_1(A_0) \cup w_2(A_0) = [0, \frac{1}{3}] \cup [\frac{2}{3}, 1]. \\ A_2 &= F(A_1) = w_1(A_1) \cup w_2(A_1) = [0, \frac{1}{3}] \cup [\frac{2}{9}, \frac{1}{3}] \cup [\frac{2}{3}, \frac{7}{9}] \cup [\frac{8}{9}, 1] \\ &\vdots \\ A_{n+1} &= [0, \frac{1}{3^n}] \cup [\frac{2}{3^n}, \frac{3}{3^n}] \cup \dots \cup [\frac{3^n-3}{3^n}, \frac{3^n-2}{3^n}] \cup [\frac{3^n-1}{3^n}, 1] \end{aligned}$$

Thus the Cantor middle  $\frac{1}{3}$  set is the set  $C_{\frac{1}{3}} = \bigcap_{n=0}^{\infty} A_n$ .

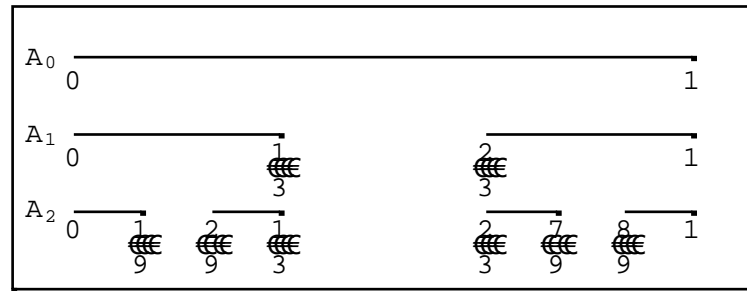


**Figure 5.1** Similar transform about Cantor middle  $\frac{1}{3}$  set  $w_1$  and  $w_2$

From Figure 5.1 we can see that if we iterate every one step, the scale is one third of the last image, so they form a self-similar structure [10].

### 5.2.2 Iterated Function System of the Cantor middle $\frac{1}{5}$ set

The constructed Cantor middle  $\frac{1}{5}$  set may be obtained as the attractor of an iterated function system by setting

$$\begin{aligned} w_1(x) &= \frac{x}{5} \\ w_2(x) &= \frac{x}{5} + \frac{2}{5} \\ w_3(x) &= \frac{x}{5} + \frac{4}{5} \end{aligned} \tag{5.4}$$

The contraction factor is  $r = \frac{1}{5}$ , and the fixed points are located at  $0, \frac{1}{5}$  and  $1$  along the

$x$ -axis. The Barnsley-Hutchinson operator is  $F(A) = \bigcup_{i=1}^3 w_i(A)$ .

Then the attractor of IFS (5.4) is  $A_{n+1} = F(A_n), A_0 \in [0, 1], n = 0, 1, 2, \dots$  (5.5)

which is the well-know Cantor middle  $\frac{1}{5}$  set.

From (5.5) we obtain obviously

$$A_1 = F(A_0) = w_1(A_0) \cup w_2(A_0) \cup w_3(A_0) = [0, \frac{1}{5}] \cup [\frac{2}{5}, \frac{3}{5}] \cup [\frac{4}{5}, 1]$$



$$\begin{aligned}
 A_2 &= F(A_1) = w_1(A_1) \cup w_2(A_1) \cup w_3(A_1) \\
 &= [0, \frac{1}{25}] \cup [\frac{2}{25}, \frac{3}{25}] \cup [\frac{4}{25}, \frac{1}{5}] \cup [\frac{2}{5}, \frac{11}{25}] \cup [\frac{12}{25}, \frac{13}{25}] \cup \\
 &\quad [\frac{14}{25}, \frac{3}{5}] \cup [\frac{4}{5}, \frac{21}{25}] \cup [\frac{22}{25}, \frac{23}{25}] \cup [\frac{24}{25}, 1] \\
 &\quad \vdots \\
 A_n &= [0, \frac{1}{5^n}] \cup [\frac{2}{5^n}, \frac{3}{5^n}] \cup \dots \cup [\frac{5^n - 3}{5^n}, \frac{5^n - 2}{5^n}] \cup [\frac{5^n - 1}{5^n}, 1]
 \end{aligned}$$

Thus the Cantor middle  $\frac{1}{5}$  set is the set  $C_{\frac{1}{5}} = \bigcap_{n=0}^{\infty} A_n$ .

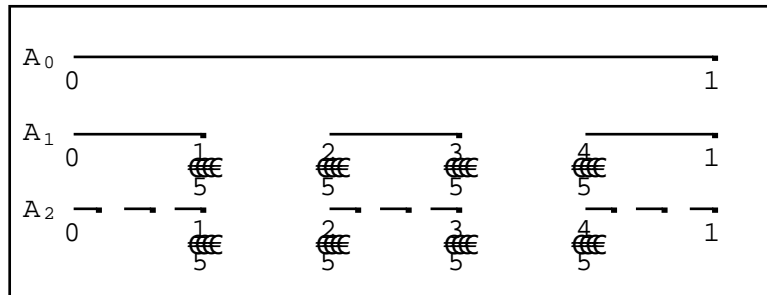


**Figure 5.2** Similar transform about Cantor middle  $\frac{1}{5}$  set  $w_1, w_2$  and  $w_3$

From Figure 5.2 we can see that if we iterate every one step, the scale is one five of the last image, so they form a self-similar structure.

### 5.2.3. Iterated Function System of the Cantor middle $\frac{1}{7}$ set

The constructed Cantor middle  $\frac{1}{7}$  set may be derived as the attractor from the following iterated function system

$$\begin{aligned}
 w_1(x) &= \frac{x}{7} \\
 w_2(x) &= \frac{x}{7} + \frac{2}{7} \\
 w_3(x) &= \frac{x}{7} + \frac{4}{7} \\
 w_4(x) &= \frac{x}{7} + \frac{6}{7}
 \end{aligned} \tag{5.6}$$

The contraction factor here is  $r = \frac{1}{7}$ , and the fixed points are located at  $0, \frac{1}{3}, \frac{2}{3}$  and  $1$

along the  $x$ -axis. The Barnsley-Hutchinson operator is  $F(A) = \bigcup_{i=1}^4 w_i(A)$ .

Then the attractor of IFS (5.6) is  $A_{n+1} = F(A_n)$ ,  $A_0 \in [0,1]$ ,  $n = 0,1,2,\dots$  (5.7)

which is the well-know Cantor middle  $\frac{1}{7}$  set.

From (5.7) we obtain obviously

$$A_1 = F(A_0) = w_1(A_0) \cup w_2(A_0) \cup w_3(A_0) \cup w_4(A_0) = [0, \frac{1}{7}] \cup [\frac{2}{7}, \frac{3}{7}] \cup [\frac{4}{7}, \frac{5}{7}] \cup [\frac{6}{7}, 1]$$

$$A_2 = F(A_1) = w_1(A_1) \cup w_2(A_1) \cup w_3(A_1) \cup w_4(A_1)$$

$$= [0, \frac{1}{49}] \cup [\frac{2}{49}, \frac{3}{49}] \cup [\frac{4}{49}, \frac{5}{49}] \cup [\frac{6}{49}, \frac{1}{7}] \cup \dots$$

$$\cup [\frac{6}{7}, \frac{43}{49}] \cup [\frac{44}{49}, \frac{45}{49}] \cup [\frac{46}{49}, \frac{47}{49}] \cup [\frac{48}{49}, 1]$$

⋮

$$A_n = [0, \frac{1}{7^n}] \cup [\frac{2}{7^n}, \frac{3}{7^n}] \cup \dots \cup [\frac{7^n - 3}{7^n}, \frac{7^n - 2}{7^n}] \cup [\frac{7^n - 1}{7^n}, 1]$$

Thus the Cantor middle  $\frac{1}{7}$  set is the set  $C_{\frac{1}{7}} = \bigcap_{n=0}^{\infty} A_n$ .

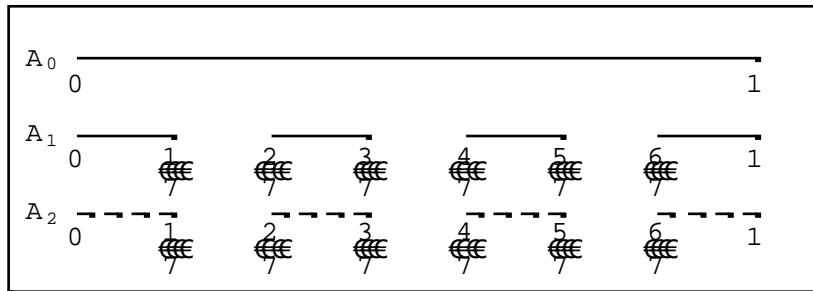


**Figure 5.3** Similar transform about Cantor middle  $\frac{1}{7}$  set  $w_1, w_2, w_3$  and  $w_4$

Figure 5.3 we can see that if we iterate every one step, the scale is one seven of the last image, so they form a self-similar structure.

**5.2.4. Iterated Function System of the Cantor middle  $\frac{1}{2m-1}$ ,  $(2 \leq m < \infty)$  set**

The constructed Generalized Cantor middle  $\frac{1}{2m-1}$ ,  $(2 \leq m < \infty)$  set may be obtained as the attractor of an iterated function system by setting

$$\begin{aligned}
 w_1(x) &= \frac{x}{2m-1} \\
 w_2(x) &= \frac{x}{2m-1} + \frac{2}{2m-1} \\
 w_3(x) &= \frac{x}{2m-1} + \frac{4}{2m-1} \\
 &\vdots \\
 w_k(x) &= \frac{x}{2m-1} + \frac{2(k-1)}{2m-1}, \quad (2 \leq m < \infty, 1 \leq k \leq m). \quad (5.8)
 \end{aligned}$$

The contraction factor is  $r = \frac{1}{2m-1}$ ,  $m \geq 2$  and the fixed points are located at  $\frac{k-1}{m-1}$  along

the  $x$ -axis. The Barnsley-Hutchinson operator is  $F(A) = \bigcup_{k=1}^m w_k(A)$ .

Then the attractor of IFS (5.8) is  $A_{n+1} = F(A_n)$ ,  $A_0 \in [0,1]$ ,  $n = 0,1,2,\dots$  (5.9)

which is well-know the Cantor middle  $\frac{1}{2m-1}$ ,  $(2 \leq m < \infty)$  set.

From (5.9) we obtain obviously

$$A_1 = F(A_0) = w_1(A_0) \cup w_2(A_0) \cup w_3(A_0) \cup \dots \cup w_m(A_0)$$

$$A_2 = F(A_1) = w_1(A_1) \cup w_2(A_1) \cup w_3(A_1) \cup \dots \cup w_m(A_1)$$

⋮

$$\begin{aligned}
 A_n = & [0, \frac{1}{(2m-1)^n}] \cup [\frac{2}{(2m-1)^n}, \frac{3}{(2m-1)^n}] \cup \dots \\
 & \cup [\frac{(2m-1)^n - 3}{(2m-1)^n}, \frac{(2m-1)^n - 2}{(2m-1)^n}] \cup [\frac{(2m-1)^n - 1}{(2m-1)^n}, 1]
 \end{aligned}$$

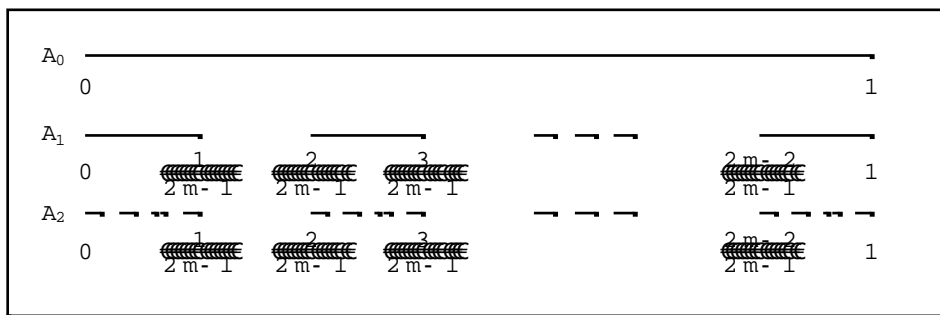


**Figure 5.4** Similar transform about Cantor middle  $\frac{1}{2m-1}$  set  $w_1, w_2, w_3, \dots, w_N$

From Figure 5.4 we can see that if we iterate every one step, the scale is one by  $\{(2m-1), 2 \leq m < \infty\}$  of the last image, so they form a self-similar structure.

We may summarize the above iterated function system in the following statement:

**Iterated Function System of the Generalized Cantor Sets:** Let  $X = [0,1]$ . Let  $(X, \dots)$  be a complete separable metric space. If  $w_k : X \rightarrow X$  is a function which is defined by

$$w_k(x) = \frac{x}{2m-1} + \frac{2(k-1)}{2m-1}, \quad (2 \leq m < \infty, 1 \leq k \leq m)$$

with contracting factor  $L_k = \frac{1}{2m-1}$ , and the fixed points are located at  $p = \frac{k-1}{m-1}$  along the  $x$ -axis, then the family  $\{w_k : k = 1, 2, \dots, m\}$  is called an *iterated function system of the generalized Cantor sets (IFSGCS for short)*.

**Dynamics of the Generalized Cantor Sets:**

Since  $L_k = \frac{1}{2m-1} < 1$  for  $2 \leq m < \infty, k = 1, 2, \dots, m$ , then iterated function system of the generalized Cantor sets  $\{w_k : k = 1, 2, \dots, m\}$  is asymptotically stable.

Since  $|w'_k(p)| = \frac{1}{2m-1} < 1$  for  $2 \leq m < \infty, k = 1, 2, \dots, m$ , then the fixed points of these functions are sink.

Thus IFS of the generalized Cantor sets is asymptotically stable and the fixed points are sink.

**5.3. Iterated Function Systems of the Two Dimensional Fractals**

**5.3.1. [28] Iterated Function System of the Koch Snowflake**

The Koch snowflake may be obtained as the attractor of an iterated function system by setting

$$\begin{aligned} w_1(x, y) &= \left(\frac{1}{2}x - \frac{\sqrt{3}}{6}y, \frac{\sqrt{3}}{6}x + \frac{1}{2}y\right), & w_2(x, y) &= \left(\frac{1}{3}x + \frac{1}{\sqrt{3}}, \frac{1}{3}y + \frac{1}{3}\right), \\ w_3(x, y) &= \left(\frac{1}{3}x, \frac{1}{3}y + \frac{2}{3}\right), & w_4(x, y) &= \left(\frac{1}{3}x - \frac{1}{\sqrt{3}}, \frac{1}{3}y + \frac{1}{3}\right), \\ w_5(x, y) &= \left(\frac{1}{3}x - \frac{1}{\sqrt{3}}, \frac{1}{3}y - \frac{1}{3}\right), & w_6(x, y) &= \left(\frac{1}{3}x, \frac{1}{3}y - \frac{2}{3}\right), \\ w_7(x, y) &= \left(\frac{1}{3}x + \frac{1}{\sqrt{3}}, \frac{1}{3}y - \frac{1}{3}\right) \end{aligned} \tag{5.10}$$

The contraction factor is  $r = \frac{1}{\sqrt{3}}$  and the fixed points of these functions are located at

$$(0,0), \left(\frac{\sqrt{3}}{2}, \frac{1}{2}\right), (0,1), \left(-\frac{\sqrt{3}}{2}, \frac{1}{2}\right), \left(-\frac{\sqrt{3}}{2}, -\frac{1}{2}\right), (0,-1), \text{ and } \left(\frac{\sqrt{3}}{2}, -\frac{1}{2}\right).$$

The Barnsley-Hutchinson operator is  $F(K) = \bigcup_{i=1}^7 w_i(K)$ .

Then the attractor of IFS (5.10) is  $K_{n+1} = F(K_n), n = 0,1,2,\dots$  (5.11)

where  $K_0 \in \{(0,0), \left(\frac{\sqrt{3}}{2}, \frac{1}{2}\right), (0,1), \left(-\frac{\sqrt{3}}{2}, \frac{1}{2}\right), \left(-\frac{\sqrt{3}}{2}, -\frac{1}{2}\right), (0,-1), \left(\frac{\sqrt{3}}{2}, -\frac{1}{2}\right)\}$

From (5.11) we obtain obviously

$$\begin{aligned} K_1 &= F(K_0) = w_1(K_0) \cup w_2(K_0) \cup \dots \cup w_7(K_0) \\ &= (0,0) \cup \left(\frac{1}{\sqrt{3}}, \frac{1}{3}\right) \cup \left(0, \frac{2}{3}\right) \cup \left(-\frac{1}{\sqrt{3}}, \frac{1}{3}\right) \cup \left(-\frac{1}{\sqrt{3}}, -\frac{1}{3}\right) \cup \dots \cup \left(\frac{1}{\sqrt{3}}, -\frac{1}{3}\right). \end{aligned}$$

$$\begin{aligned} K_2 &= F(K_1) = w_1(K_1) \cup w_2(K_1) \cup \dots \cup w_7(K_1) \\ &\vdots \end{aligned}$$

We obtain a sequence

$$K_0 \supset K_1 \supset K_2 \supset \dots$$

Thus the Koch snowflake is  $K = \bigcap_{n=0}^{\infty} K_n$ .

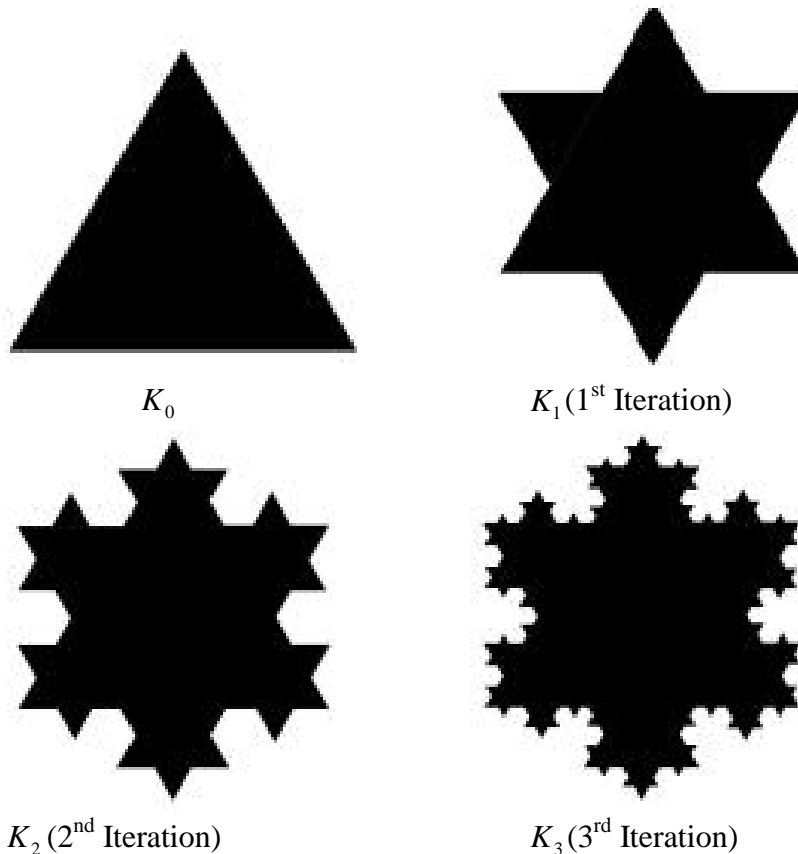


**Figure 5.5** The first four stages in the construction of the Koch snowflake as IFS  
Chapter Five

**Dynamics of the Koch Snowflake:**

Since  $L_k = \frac{1}{3} < 1$  for  $k = 1, 2, \dots, 7$ , then iterated function system of the Koch snowflake

$\{w_k : k = 1, 2, \dots, 7\}$  is asymptotically stable.

The Jacobian matrix of IFS of the Koch snowflake at the fixed points is

$$Dw(x, y) = \begin{pmatrix} \frac{1}{3} & 0 \\ 0 & \frac{1}{3} \end{pmatrix},$$

with eigenvalues equal to  $\frac{1}{3}$  and  $\frac{1}{3}$ . Thus the fixed points of these IFS  $(0, 0)$ ,  $(\frac{1}{\sqrt{3}}, \frac{1}{3})$ ,

$(0, \frac{2}{3})$ ,  $(-\frac{1}{\sqrt{3}}, \frac{1}{3})$ ,  $(-\frac{1}{\sqrt{3}}, -\frac{1}{3})$ ,  $(0, -\frac{2}{3})$  and  $(\frac{1}{\sqrt{3}}, -\frac{1}{3})$  are sink.

Therefore, IFS of the Koch snowflake is asymptotically stable and the fixed points are sink.

**5.3.2. [29] Iterated Function System of the Koch curve**

The Koch curve may be obtained by the following iterated function system

$$\begin{aligned} w_1(x, y) &= (\frac{1}{3}x + 0.y + 0, 0.x + \frac{1}{3}y + 0) = (\frac{1}{3}x, \frac{1}{3}y) \\ w_2(x, y) &= (\frac{1}{6}x - \frac{\sqrt{3}}{6}y + \frac{1}{3}, \frac{\sqrt{3}}{6}.x + \frac{1}{6}y + 0) = (\frac{1}{6}x - \frac{\sqrt{3}}{6}y + \frac{1}{3}, \frac{\sqrt{3}}{6}.x + \frac{1}{6}y) \\ w_3(x, y) &= (\frac{1}{6}x + \frac{\sqrt{3}}{6}y + \frac{1}{2}, -\frac{\sqrt{3}}{6}x + \frac{1}{6}y + \frac{\sqrt{3}}{6}) \\ w_4(x, y) &= (\frac{1}{3}x + 0.y + \frac{2}{3}, 0.x + \frac{1}{3}y + 0) = (\frac{1}{3}x + \frac{2}{3}, \frac{1}{3}y) \end{aligned} \tag{5.12}$$

The contraction factor is  $r = \frac{1}{3}$ , and the fixed points are located at

$(0, 0)$ ,  $(\frac{5}{11}, \frac{\sqrt{3}}{11})$ ,  $(\frac{18}{25}, \frac{\sqrt{3}}{5})$ ,  $(1, 0)$  along the  $x$ -axis.

The Barnsley-Hutchinson operator is  $F(A) = \bigcup_{i=1}^4 w_i(A)$

Then the attractor of IFS (5.12) is  $A_{n+1} = F(A_n)$ ,  $A_0 \in (0, 0)$ ,  $n = 0, 1, 2, \dots$  (5.13)

which is the well-know Koch curve.

From (5.13) we obtain obviously

$$\begin{aligned} A_1 &= F(A_0) = w_1(A_0) \cup w_2(A_0) \cup w_3(A_0) \cup w_4(A_0) \\ &= (0, 0) \cup (\frac{1}{3}, 0) \cup (\frac{1}{2}, \frac{\sqrt{3}}{6}) \cup (\frac{2}{3}, 0) \end{aligned}$$

$$\begin{aligned}
 A_2 &= F(A_1) = w_1(A_1) \cup w_2(A_1) \cup w_3(A_1) \cup w_4(A_1) \\
 &= (0,0) \cup \left(\frac{1}{3}, 0\right) \cup \left(\frac{1}{2}, \frac{\sqrt{3}}{6}\right) \cup \left(\frac{2}{3}, 0\right) \cup \left(\frac{1}{9}, 0\right) \cup \left(\frac{7}{18}, \frac{\sqrt{3}}{18}\right) \cup \left(\frac{2}{9}, 0\right) \cup \left(\frac{4}{9}, \frac{\sqrt{3}}{9}\right) \\
 &\quad \cup \left(\frac{11}{18}, \frac{\sqrt{3}}{18}\right) \cup \left(\frac{8}{9}, 0\right) \cup \left(\frac{1}{6}, \frac{\sqrt{3}}{18}\right) \cup \left(\frac{1}{3}, \frac{\sqrt{3}}{9}\right) \cup \left(\frac{2}{3}, \frac{\sqrt{3}}{9}\right) \cup \left(\frac{5}{6}, \frac{\sqrt{3}}{18}\right) \\
 &\quad \vdots
 \end{aligned}$$

We obtain a sequence

$$A_0 \supset A_1 \supset A_2 \supset \dots$$

Thus the Koch curve is  $A = \bigcap_{n=0}^{\infty} A_n$ .

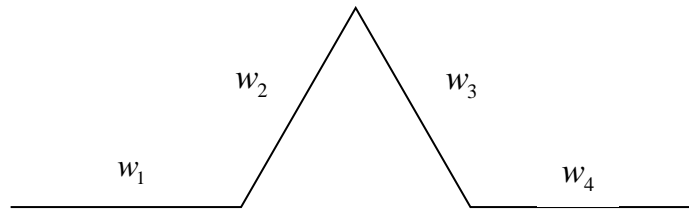


**Figure 5.6** The standard Koch curve as an iterated function system (IFS)

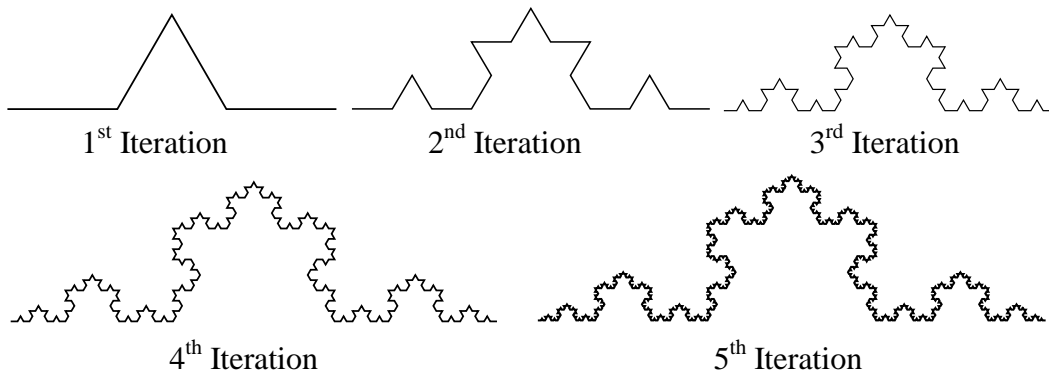


**Figure 5.7** The first five stages of the standard Koch curve as an IFS

### 5.3.3. [29] Iterated Function System of the Sierpinski Gasket or Equilateral Triangle

The Sierpinski gasket or equilateral triangle consists of three self-similar pieces that may be obtained by the following iterated function system

$$\begin{aligned}
 w_1(x, y) &= \left(\frac{1}{2}x, \frac{1}{2}y\right) \\
 w_2(x, y) &= \left(\frac{1}{2}x + \frac{1}{2}, \frac{1}{2}y\right) \\
 w_3(x, y) &= \left(\frac{1}{2}x + \frac{1}{4}, \frac{1}{2}y + \frac{\sqrt{3}}{4}\right)
 \end{aligned} \tag{5.14}$$

The contraction factor is  $r = \frac{1}{2}$ , and the fixed points are  $(0,0)$ ,  $(1,0)$  and  $(\frac{1}{2}, \frac{\sqrt{3}}{2})$ .

The Barnsley-Hutchinson operator is  $F(A) = \bigcup_{i=1}^3 w_i(A)$ .

Then the attractor of IFS (5.14) is

$$A_{n+1} = F(A_n), A_0 \in \{(0,0), (1,0), (\frac{1}{2}, \frac{\sqrt{3}}{2})\} \quad n = 0, 1, 2, \dots \tag{5.15}$$

which is the Sierpinski gasket or equilateral triangle.

From (5.15) we obtain obviously

$$A_1 = F(A_0) = w_1(A_0) \cup w_2(A_0) \cup w_3(A_0) = (0,0) \cup (\frac{1}{2}, 0) \cup (\frac{1}{4}, \frac{\sqrt{3}}{4}) \cup (\frac{1}{2}, 0) \cup (1,0) \cup (\frac{3}{4}, \frac{\sqrt{3}}{4}) \cup (\frac{1}{4}, \frac{\sqrt{3}}{4}) \cup (\frac{3}{4}, \frac{\sqrt{3}}{4}) \cup (\frac{1}{2}, \frac{\sqrt{3}}{2})$$

$$A_2 = F(A_1) = w_1(A_1) \cup w_2(A_1) \cup w_3(A_1) = (0,0) \cup (\frac{1}{2}, 0) \cup (\frac{1}{4}, \frac{\sqrt{3}}{4}) \cup (\frac{1}{4}, 0) \cup (\frac{3}{4}, 0) \cup (\frac{1}{2}, \frac{\sqrt{3}}{4}) \cup (\frac{1}{8}, \frac{\sqrt{3}}{8}) \cup (\frac{5}{8}, \frac{\sqrt{3}}{8}) \cup (\frac{3}{8}, \frac{3\sqrt{3}}{8}) \dots$$

⋮

In general,  $A_n$  is the union of  $3^{n+1}$  vertices, each of size of equilateral triangle is  $\frac{1}{3^n}$ .

We obtain a sequence

$$A_0 \supset A_1 \supset A_2 \supset \dots$$

Thus the Sierpinski gasket or equilateral triangle is  $A = \bigcap_{n=0}^{\infty} A_n$ .

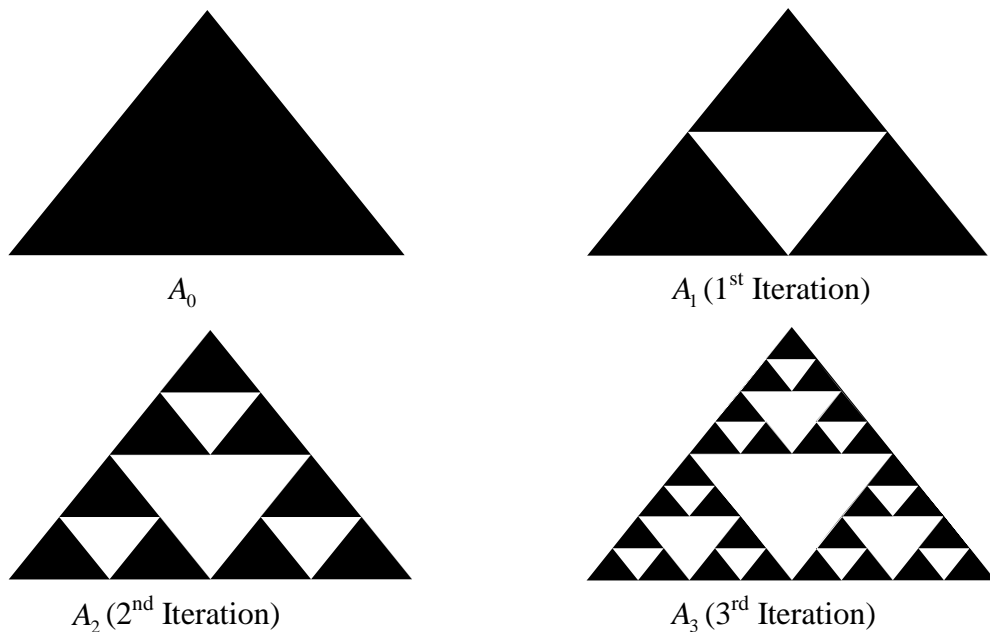


**Figure 5.8** The first four stages of the Sierpinski equilateral triangle as IFS



### Dynamics of the Sierpinski Equilateral Triangle:

Since  $L_k = \frac{1}{2} < 1$  for  $k = 1, 2, 3$ , then iterated function system of the Sierpinski equilateral triangle  $\{w_k : k = 1, 2, 3\}$  is asymptotically stable.

The Jacobian matrix of IFS of the Sierpinski equilateral triangle at the fixed points is

$$Dw(x, y) = \begin{pmatrix} \frac{1}{2} & 0 \\ 0 & \frac{1}{2} \end{pmatrix},$$

with eigenvalues equal to  $\frac{1}{2}$  and  $\frac{1}{2}$ . Thus the fixed points of these IFS  $(0, 0)$ ,  $(1, 0)$  and  $(\frac{1}{2}, \frac{\sqrt{3}}{2})$  are sink.

Therefore, IFS of the Sierpinski equilateral triangle is asymptotically stable and the fixed points are sink.

Similarly, we can show that IFS of the following Sierpinski triangles is asymptotically stable and the fixed points are sink.

#### 5.3.4. Iterated Function System of the Sierpinski Isosceles Triangle

The Sierpinski isosceles triangle consists of three self-similar pieces that may be obtained by the following iterated function system

$$\begin{aligned} w_1(x, y) &= \left(\frac{1}{2}x, \frac{1}{2}y\right) \\ w_2(x, y) &= \left(\frac{1}{2}x + \frac{1}{2}, \frac{1}{2}y\right) \\ w_3(x, y) &= \left(\frac{1}{2}x + \frac{1}{4}, \frac{1}{2}y + \frac{1}{2\sqrt{2}}\right) \end{aligned} \quad (5.16)$$

The contraction factor is  $\tau = \frac{1}{2}$ , and the fixed points are located at  $(0, 0)$ ,  $(1, 0)$  and  $(\frac{1}{2}, \frac{1}{\sqrt{2}})$ . The Barnsley-Hutchinson operator is  $F(A) = \bigcup_{i=1}^3 w_i(A)$ .

Then the attractor of IFS (5.16) is

$$A_{n+1} = F(A_n), A_0 \in \{(0, 0), (1, 0), (\frac{1}{2}, \frac{1}{\sqrt{2}})\} \quad n = 0, 1, 2, \dots \quad (5.17)$$

which is the Sierpinski isosceles triangle.

From (5.17) we obtain obviously

$$A_1 = F(A_0) = w_1(A_0) \cup w_2(A_0) \cup w_3(A_0) = (0, 0) \cup \left(\frac{1}{2}, 0\right) \cup \left(\frac{1}{4}, \frac{1}{2\sqrt{2}}\right)$$

$$\begin{aligned}
 A_2 &= F(A_1) = w_1(A_1) \cup w_2(A_1) \cup w_3(A_1) \\
 &= (0,0) \cup \left(\frac{1}{2}, 0\right) \cup \left(\frac{1}{4}, \frac{1}{2\sqrt{2}}\right) \cup \left(\frac{1}{4}, 0\right) \cup \left(\frac{5}{8}, 0\right) \cup \left(\frac{9}{16}, \frac{1}{2\sqrt{2}}\right) \dots \\
 &\quad \cup \left(\frac{1}{4}, \frac{1}{4\sqrt{2}}\right) \cup \left(\frac{5}{8}, \frac{1}{8\sqrt{2}}\right) \cup \left(\frac{9}{16}, \frac{9}{16\sqrt{2}}\right) \\
 &\quad \vdots
 \end{aligned}$$

In general,  $A_n$  is the union of  $3^{n+1}$  vertices, each of size of isosceles triangle is  $\frac{1}{3^n}$ .

We obtain a sequence

$$A_0 \supset A_1 \supset A_2 \supset \dots$$

Thus the Sierpinski isosceles triangle is  $A = \bigcap_{n=0}^{\infty} A_n$ .

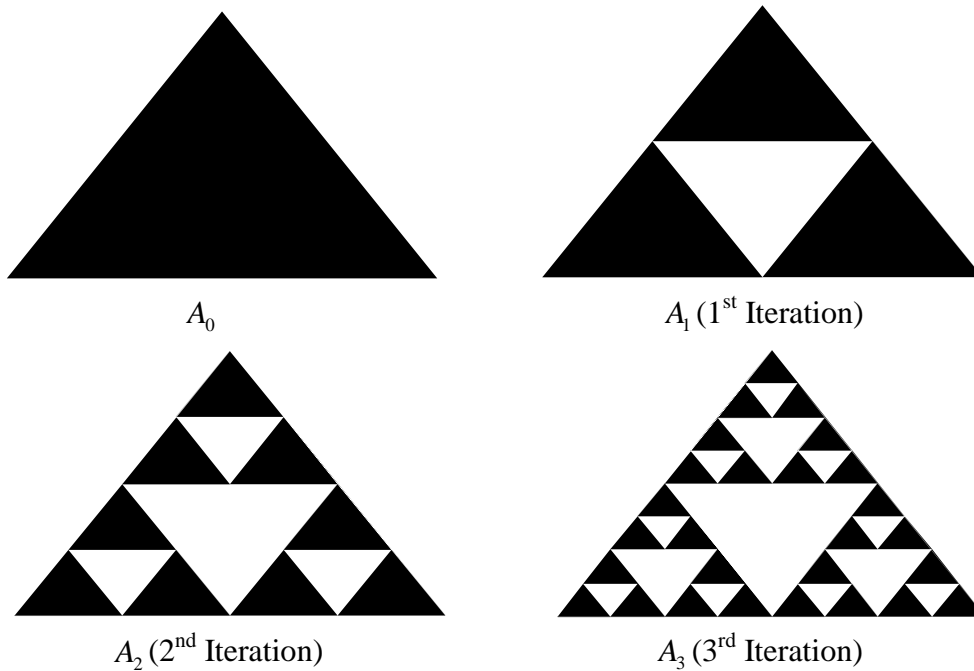


**Figure 5.9** The first four stages of the Sierpinski isosceles triangle as IFS

### 5.3.5. Iterated Function System of the Sierpinski Isosceles Right Triangle

The Sierpinski isosceles right triangle consists of three self-similar pieces that may be obtained as the attractor of an iterated function system by setting

$$\begin{aligned}
 w_1(x, y) &= \left(\frac{1}{2}x, \frac{1}{2}y\right) \\
 w_2(x, y) &= \left(\frac{1}{2}x + \frac{1}{2}, \frac{1}{2}y\right) \\
 w_3(x, y) &= \left(\frac{1}{2}x, \frac{1}{2}y + \frac{1}{2}\right)
 \end{aligned} \tag{5.18}$$

The contraction factor is  $r = \frac{1}{2}$ , and the fixed points are  $(0,0)$ ,  $(1,0)$  and  $(0,1)$ .

The Barnsley-Hutchinson operator is  $F(A) = \bigcup_{i=1}^3 w_i(A)$ .

Then the attractor of IFS (5.18) is

$$A_{n+1} = F(A_n), A_0 \in \{(0,0), (1,0), (0,1)\} \quad n = 0, 1, 2, \dots \tag{5.19}$$

which is the Sierpinski isosceles right triangle.

From (5.19) we obtain obviously

$$\begin{aligned} A_1 = F(A_0) &= w_1(A_0) \cup w_2(A_0) \cup w_3(A_0) = (0,0) \cup \left(\frac{1}{2}, 0\right) \cup \left(0, \frac{1}{2}\right) \\ &\cup \left(\frac{1}{2}, 0\right) \cup (1,0) \cup \left(\frac{1}{2}, \frac{1}{2}\right) \cup \left(0, \frac{1}{2}\right) \cup \left(\frac{1}{2}, \frac{1}{2}\right) \cup (0,1) \end{aligned}$$

$$\begin{aligned} A_2 = F(A_1) &= w_1(A_1) \cup w_2(A_1) \cup w_3(A_1) \\ &= (0,0) \cup \left(\frac{1}{2}, 0\right) \cup \left(0, \frac{1}{2}\right) \cup \left(\frac{1}{4}, 0\right) \cup \left(\frac{3}{4}, 0\right) \cup \left(\frac{1}{4}, \frac{1}{2}\right) \cup \left(0, \frac{1}{4}\right) \cup \left(\frac{1}{2}, \frac{1}{4}\right) \cup \left(0, \frac{3}{4}\right) \\ &\vdots \end{aligned}$$

In general,  $A_n$  is the union of  $3^{n+1}$  vertices, each of size of isosceles right triangle  $\frac{1}{3^n}$ .

We have a sequence

$$A_0 \supset A_1 \supset A_2 \supset \dots$$

Thus the Sierpinski gasket or right isosceles triangle is  $A = \bigcap_{n=0}^{\infty} A_n$ .

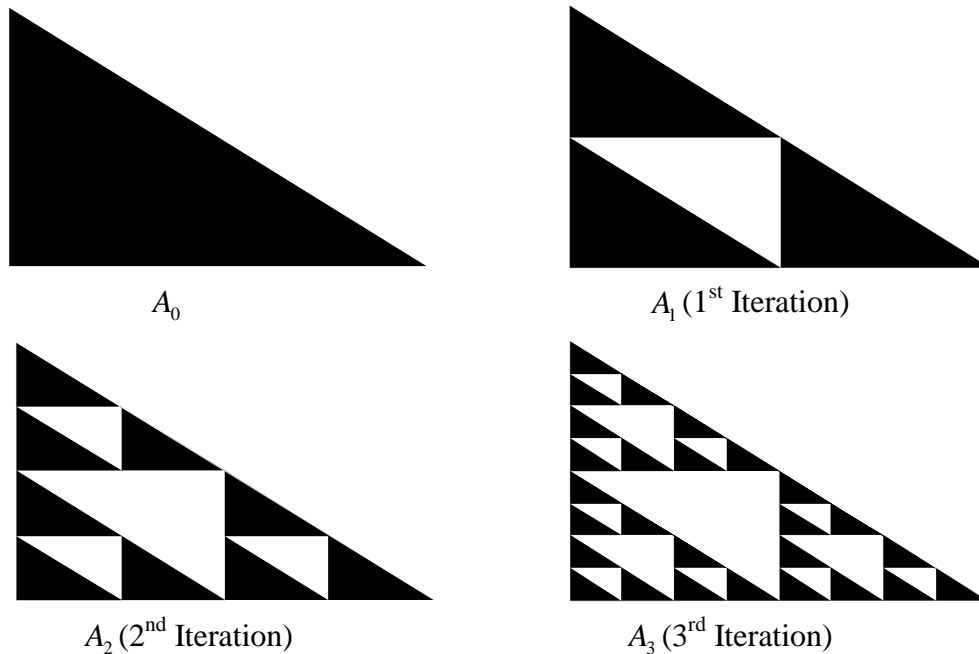


**Figure 5.10** The first four stages of the Sierpinski right isosceles triangle as IFS

### 5.3.6. Iterated Function System of the Sierpinski Scalene Triangle

The Sierpinski scalene triangle consists of three self-similar pieces that may be obtained as the attractor of an iterated function system by setting

$$\begin{aligned} w_1(x, y) &= \left(\frac{1}{2}x, \frac{1}{2}y\right) \\ w_2(x, y) &= \left(\frac{1}{2}x + \frac{1}{2}, \frac{1}{2}y\right) \\ w_3(x, y) &= \left(\frac{1}{2}x + \frac{1}{8}, \frac{1}{2}y + \frac{\sqrt{3}}{8}\right) \end{aligned} \tag{5.20}$$

The contraction factor is  $r = \frac{1}{2}$ , and the fixed points are  $(0, 0)$ ,  $(1, 0)$  and  $(\frac{1}{4}, \frac{\sqrt{3}}{4})$ .

The Barnsley-Hutchinson operator is  $F(A) = \bigcup_{i=1}^3 w_i(A)$ .

Then the attractor of IFS (5.20) is

$$A_{n+1} = F(A_n), A_0 \in \{(0, 0), (1, 0), (0, 1)\} \quad n = 0, 1, 2, \dots \tag{5.21}$$

which is the Sierpinski scalene triangle.

From (5.21) we obtain obviously

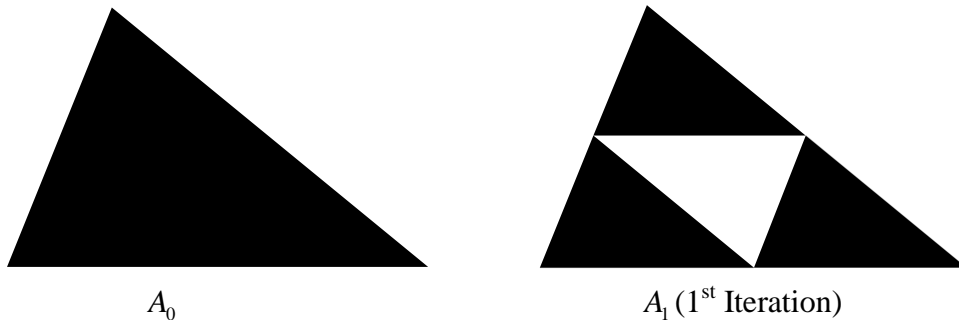
$$\begin{aligned} A_1 &= F(A_0) = w_1(A_0) \cup w_2(A_0) \cup w_3(A_0) = (0, 0) \cup \left(\frac{1}{2}, 0\right) \cup \left(\frac{3}{8}, \frac{\sqrt{3}}{8}\right) \\ A_2 &= F(A_1) = w_1(A_1) \cup w_2(A_1) \cup w_3(A_1) \\ &= (0, 0) \cup \left(\frac{1}{2}, 0\right) \cup \left(\frac{3}{8}, \frac{\sqrt{3}}{8}\right) \cup \\ &\quad \vdots \end{aligned}$$

In general,  $A_n$  is the union of  $3^{n+1}$  vertices, each of size of scalene triangle is  $\frac{1}{3^n}$ .

We obtain a sequence

$$A_0 \supset A_1 \supset A_2 \supset \dots$$

Thus the Sierpinski scalene triangle is  $A = \bigcap_{n=0}^{\infty} A_n$ .



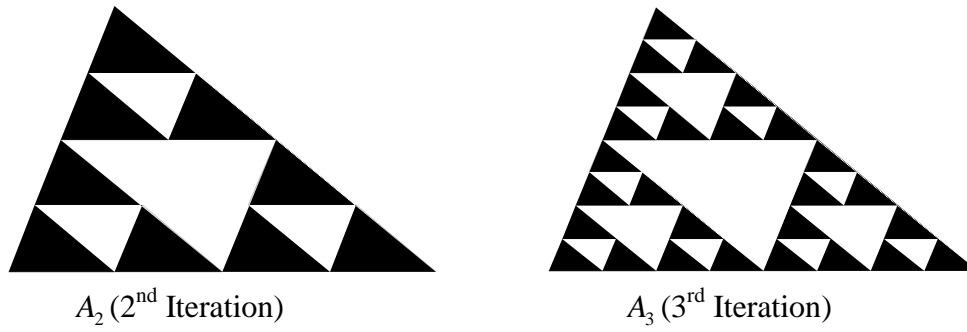


**Figure 5.11** The first four stages of the Sierpinski scalene triangle as IFS

**5.3.7. [30] Iterated Function System of the Sierpinski Carpet**

The Sierpinski carpet consists of eight self-similar pieces that may be obtained as the attractor of an iterated function system by setting

$$\begin{aligned}
 w_1(x, y) &= \left(\frac{1}{3}x, \frac{1}{3}y\right), & w_2(x, y) &= \left(\frac{1}{3}x + \frac{1}{3}, \frac{1}{3}y\right), \\
 w_3(x, y) &= \left(\frac{1}{3}x + \frac{2}{3}, \frac{1}{3}y\right), & w_4(x, y) &= \left(\frac{1}{3}x, \frac{1}{3}y + \frac{1}{3}\right), \\
 w_5(x, y) &= \left(\frac{1}{3}x + \frac{2}{3}, \frac{1}{3}y + \frac{1}{3}\right), & w_6(x, y) &= \left(\frac{1}{3}x, \frac{1}{3}y + \frac{2}{3}\right) \\
 w_7(x, y) &= \left(\frac{1}{3}x + \frac{1}{3}, \frac{1}{3}y + \frac{2}{3}\right), & w_8(x, y) &= \left(\frac{1}{3}x + \frac{2}{3}, \frac{1}{3}y + \frac{2}{3}\right)
 \end{aligned} \tag{5.22}$$

The contraction factor  $r = \frac{1}{3}$ , and the fixed points are located at  $(0,0)$ ,  $(\frac{1}{2}, 0)$ ,  $(1,0)$ ,  $(0, \frac{1}{2})$ ,  $(\frac{1}{2}, \frac{1}{2})$ ,  $(0,1)$ ,  $(\frac{1}{2}, 1)$ , and  $(1,1)$ .

The Barnsley-Hutchinson operator is  $F(C) = \bigcup_{i=1}^8 w_i(C)$ . Then the attractor of IFS (5.22) is

$$C_{n+1} = F(C_n), \text{ where } C_0 \in \{(0,0), (1,0), (0,1), (1,1)\}, \quad n = 0, 1, 2, \dots \tag{5.23}$$

From (5.23) we obtain obviously

$$\begin{aligned}
 C_1 &= F(C_0) = w_1(C_0) \cup w_2(C_0) \cup \dots \cup w_8(C_0) = (0,0) \cup \left(\frac{1}{3}, 0\right) \cup \dots \cup (1,1), \\
 C_2 &= F(C_1) = w_1(C_1) \cup w_2(C_1) \cup \dots \cup w_8(C_1) \\
 &= (0,0) \cup \left(\frac{1}{3}, 0\right) \cup \dots \cup (1,1) \\
 &\vdots
 \end{aligned}$$

In general,  $C_n$  is the union of  $4^{n+1}$  vertices, each of size of Sierpinski carpet is  $\frac{1}{3^n}$ .

We obtain a sequence

$$C_0 \supset C_1 \supset C_2 \dots$$

We conclude that the Sierpinski carpet is  $C = \bigcap_{n=0}^{\infty} C_n$ .

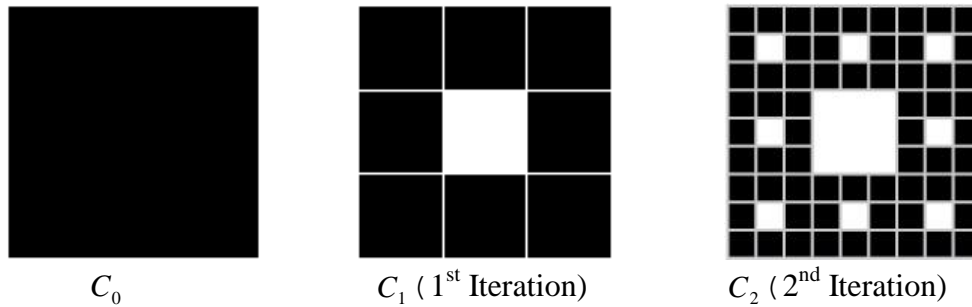


**Figure 5.12** The first three stages of the Sierpinski carpet as IFS

**Dynamics of the Sierpinski Carpet:**

Since  $L_k = \frac{1}{3} < 1$  for  $k = 1, 2, \dots, 8$ , then iterated function system of the Sierpinski carpet  $\{w_k : k = 1, 2, \dots, 8\}$  is asymptotically stable.

The Jacobian matrix of IFS of the Sierpinski carpet at the fixed points is

$$Dw(x, y) = \begin{pmatrix} \frac{1}{3} & 0 \\ 0 & \frac{1}{3} \end{pmatrix},$$

with eigenvalues equal to  $\frac{1}{3}$  and  $\frac{1}{3}$ . Thus the fixed points of these IFS  $(0, 0)$ ,

$(\frac{1}{2}, 0)$ ,  $(1, 0)$ ,  $(0, \frac{1}{2})$ ,  $(1, \frac{1}{2})$ ,  $(0, 1)$ ,  $(\frac{1}{2}, 1)$ , and  $(1, 1)$  are sink.

Therefore, IFS of the Sierpinski carpet is asymptotically stable and the fixed points are sink.

**5.3.8. [13] Iterated Function System of the Box Fractal**

The box fractal consists of five self-similar pieces that may be obtained as the attractor of an iterated function system by setting

$$\begin{aligned} w_1(x, y) &= \left(\frac{1}{3}x, \frac{1}{3}y\right) \\ w_2(x, y) &= \left(\frac{1}{3}x + \frac{2}{3}, \frac{1}{3}y\right) \\ w_3(x, y) &= \left(\frac{1}{3}x, \frac{1}{3}y + \frac{2}{3}\right) \\ w_4(x, y) &= \left(\frac{1}{3}x + \frac{2}{3}, \frac{1}{3}y + \frac{2}{3}\right) \\ w_5(x, y) &= \left(\frac{1}{3}x + \frac{1}{3}, \frac{1}{3}y + \frac{1}{3}\right) \end{aligned} \tag{5.24}$$

The contraction factor is  $r = \frac{1}{3}$ , and the fixed points are located at  $(0,0)$ ,  $(1,0)$ ,  $(0,1)$ ,

$(\frac{1}{2}, \frac{1}{2})$ , and  $(1,1)$ . The Barnsley-Hutchinson operator is  $F(B) = \bigcup_{i=1}^3 w_i(B)$ .

Then the attractor of IFS (5.24) is  $B_{n+1} = F(B_n)$ ,  $n = 0, 1, 2, \dots$  (5.25)

where  $B_0 \in \{(0,0), (1,0), (0,1), (1,1)\}$ , which is the box fractal.

From (5.25) we obtain obviously

$$B_1 = F(B_0) = w_1(B_0) \cup w_2(B_0) \cup \dots \cup w_5(B_0) = (0,0) \cup (\frac{1}{3}, 0) \cup (\frac{1}{3}, \frac{1}{3}) \cup (0, \frac{1}{3}) \\ \cup (\frac{2}{3}, 0) \cup (1,0) \cup (1, \frac{1}{3}) \cup (\frac{2}{3}, \frac{1}{3}) \cup (\frac{1}{3}, \frac{2}{3}) \cup (\frac{2}{3}, \frac{2}{3}) \cup (\frac{2}{3}, 1)$$

$$B_2 = F(B_1) = w_1(B_1) \cup w_2(B_1) \cup \dots \cup w_5(B_1) = (0,0) \cup (\frac{1}{2}, 0) \cup (\frac{3}{8}, \frac{\sqrt{3}}{8}) \cup \dots \cup (\frac{8}{9}, 1) \\ \vdots$$

In general,  $B_n$  is the union of  $4^{n+1}$  vertices, each of size of the box fractal is  $\frac{1}{3^n}$ .

We have a sequence

$$B_0 \supset B_1 \supset B_2 \supset \dots$$

Thus the box fractal is  $B = \bigcap_{n=0}^{\infty} B_n$ .

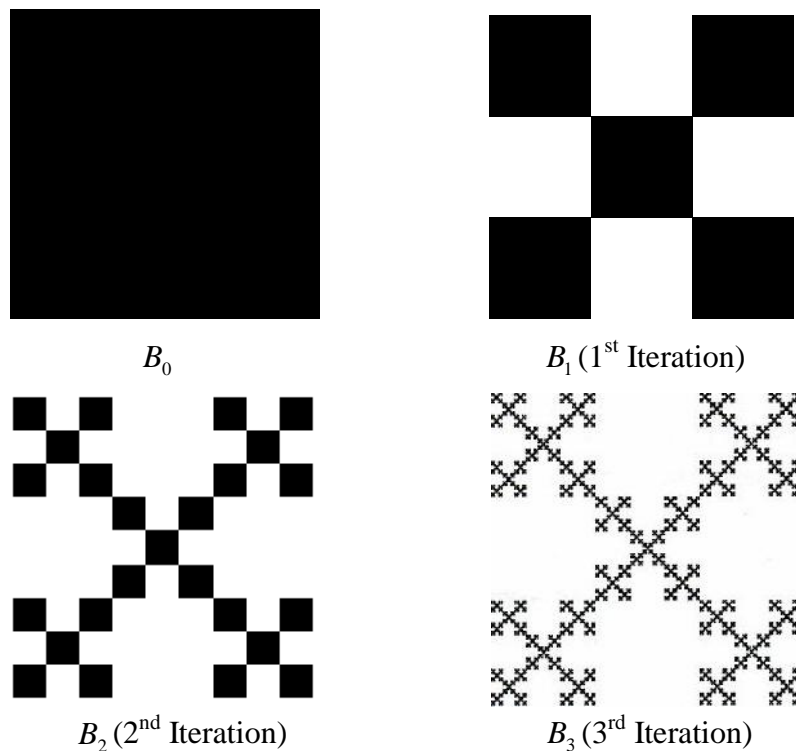


**Figure 5.13** The first four stages in the construction of the box fractal as IFS

**Dynamics of the Box Fractal:**

Since  $L_k = \frac{1}{3} < 1$  for  $k = 1, 2, \dots, 5$ , then iterated function system of the box fractal  $\{w_k : k = 1, 2, \dots, 5\}$  is asymptotically stable.

The Jacobian matrix of IFS of the box fractal at the fixed points is

$$Dw(x, y) = \begin{pmatrix} \frac{1}{3} & 0 \\ 0 & \frac{1}{3} \end{pmatrix},$$

with eigenvalues equal to  $\frac{1}{3}$  and  $\frac{1}{3}$ .

Thus the fixed points of these IFS  $(0, 0)$ ,  $(1, 0)$ ,  $(0, 1)$ ,  $(\frac{1}{2}, \frac{1}{2})$ , and  $(1, 1)$  are sink.

Therefore, IFS of the box fractal is asymptotically stable and the fixed points are sink.

**5.3.9 Iterated Function System of the Square Fractal (using the Cantor middle  $\frac{1}{3}$  set)**

The constructed square fractal (using the Cantor middle  $\frac{1}{3}$  set) consists of four self-similar pieces that may be obtained as the attractor of an iterated function system by setting

$$\begin{aligned} w_1(x, y) &= (\frac{1}{3}x, \frac{1}{3}y), & w_2(x, y) &= (\frac{1}{3}x + \frac{2}{3}, \frac{1}{3}y) \\ w_3(x, y) &= (\frac{1}{3}x, \frac{1}{3}y + \frac{2}{3}), & w_4(x, y) &= (\frac{1}{3}x + \frac{2}{3}, \frac{1}{3}y + \frac{2}{3}) \end{aligned} \tag{5.26}$$

The contraction factor is  $r = \frac{1}{3}$ , and the fixed points are located at  $(0, 0)$ ,  $(1, 0)$ ,  $(0, 1)$

and  $(1, 1)$ . The Barnsley-Hutchinson operator is  $F(S) = \bigcup_{i=1}^4 w_i(S)$ .

Then the attractor of IFS (5.26) is

$$S_{n+1} = F(S_n), \quad n = 0, 1, 2, \dots, \text{ where } S_0 \in \{(0, 0), (1, 0), (0, 1), (1, 1)\}, \tag{5.27}$$

From (5.27) we have obviously

$$\begin{aligned} S_1 &= F(S_0) = w_1(S_0) \cup w_2(S_0) \cup w_3(S_0) \cup w_4(S_0) \\ &= (0, 0) \cup (\frac{2}{3}, 0) \cup (0, \frac{2}{3}) \cup (\frac{2}{3}, \frac{2}{3}) \cup (\frac{1}{3}, 0) \cup (1, 0) \cup (\frac{1}{3}, \frac{2}{3}) \cup (1, \frac{2}{3}) \cup (0, \frac{1}{3}) \\ &\quad \cup (\frac{2}{3}, \frac{1}{3}) \cup (0, 1) \cup (\frac{2}{3}, 1) \cup (\frac{1}{3}, \frac{1}{3}) \cup (1, \frac{1}{3}) \cup (\frac{1}{3}, 1) \cup (1, 1), \end{aligned}$$

$$S_2 = F(S_1) = w_1(S_1) \cup S_2(A_1) \cup S_3(A_1) \cup S_4(A_1)$$

$\vdots$



In general,  $S_n$  is the union of  $4^{n+1}$  vertices, each of size of the square fractal is  $\frac{1}{3^n}$ .

We get a sequence

$$S_0 \supset S_1 \supset S_2 \cdots$$

Hence the square fractal is  $S = \bigcap_{n=0}^{\infty} S_n$ .

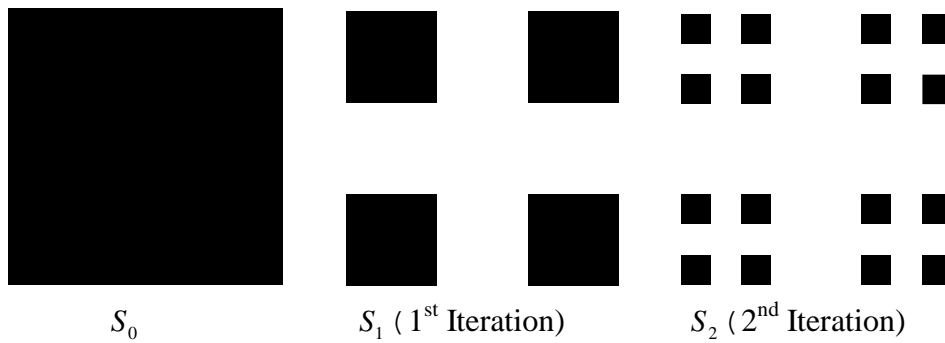


**Figure 5.14** The first three stages in the construction of the square fractal as IFS

**Dynamics of the Square Fractal:**

Since  $L_k = \frac{1}{3} < 1$  for  $k = 1, 2, 3, 4$ , then iterated function system of the square fractal  $\{w_k : k = 1, 2, 3, 4, \}$  is asymptotically stable.

The Jacobian matrix of IFS of the box fractal at the fixed points is

$$Dw(x, y) = \begin{pmatrix} \frac{1}{3} & 0 \\ 0 & \frac{1}{3} \end{pmatrix},$$

with eigenvalues equal to  $\frac{1}{3}$  and  $\frac{1}{3}$ .

Thus the fixed points of these IFS  $(0, 0)$ ,  $(1, 0)$ ,  $(0, 1)$  and  $(1, 1)$  are sink.

Therefore, IFS of the square fractal is asymptotically stable and the fixed points are sink.

**5.3.10. Iterated Function System of the Square Fractal (using the Cantor middle  $\frac{1}{5}$  set)**

The constructed square fractal (using the Cantor middle  $\frac{1}{5}$  set) consists of nine self-similar pieces that may be derived as the attractor from the following iterated function system

$$\begin{aligned} w_1(x, y) &= \left(\frac{1}{5}x, \frac{1}{5}y\right), & w_2(x, y) &= \left(\frac{1}{5}x + \frac{2}{5}, \frac{1}{5}y\right), \\ w_3(x, y) &= \left(\frac{1}{5}x, \frac{1}{5}y + \frac{2}{5}\right), & w_4(x, y) &= \left(\frac{1}{5}x + \frac{4}{5}, \frac{1}{5}y\right), \\ w_5(x, y) &= \left(\frac{1}{5}x, \frac{1}{5}y + \frac{4}{5}\right), & w_6(x, y) &= \left(\frac{1}{5}x + \frac{2}{5}, \frac{1}{5}y + \frac{2}{5}\right), \end{aligned}$$

$$\begin{aligned}
 w_7(x, y) &= \left(\frac{1}{5}x + \frac{2}{5}, \frac{1}{5}y + \frac{4}{5}\right), & w_8(x, y) &= \left(\frac{1}{5}x + \frac{4}{5}, \frac{1}{5}y + \frac{2}{5}\right), \\
 w_9(x, y) &= \left(\frac{1}{5}x + \frac{4}{5}, \frac{1}{5}y + \frac{4}{5}\right)
 \end{aligned}
 \tag{5.28}$$

The contraction factor is  $r = \frac{1}{5}$ , and the fixed points are located at  $(0,0)$ ,  $(1/2,0)$ ,  $(1,0)$ ,  $(0,1/2)$ ,  $(1/2,1/2)$ ,  $(1,1/2)$ ,  $(0,1)$ ,  $(1/2,1)$  and  $(1,1)$ .

The Barnsley-Hutchinson operator is  $F(S) = \bigcup_{i=1}^9 w_i(S)$ .

Then the attractor of IFS (5.28) is  $S_{n+1} = F(S_n)$ ,  $n = 0, 1, 2, \dots$  (5.29)

where  $S_0 \in \{(0,0), (1/2,0), (1,0), (0,1/2), (1/2,1/2), (1,1/2), (0,1), (1/2,1), (1,1)\}$ ,

From (5.29) we obtain obviously

$$S_1 = F(S_0) = w_1(S_0) \cup \dots \cup w_9(S_0) = (0,0) \cup \left(\frac{2}{5}, 0\right) \cup \left(0, \frac{2}{5}\right) \cup \dots \cup (1,1),$$

$$S_2 = F(S_1) = w_1(S_1) \cup \dots \cup w_9(S_1)$$

⋮

In general,  $S_n$  is the union of  $4^{n+1}$  vertices, each of size of the square fractal is  $\frac{1}{5^n}$ .

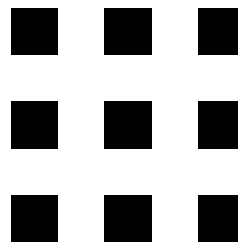
We have a sequence

$$S_0 \supset S_1 \supset S_2 \dots$$

Therefore, the square fractal (using the Cantor middle  $\frac{1}{5}$  set) is  $S = \bigcap_{n=0}^{\infty} S_n$ .



$S_0$



$S_1$  (1<sup>st</sup> Iteration)

**Figure 5.15** The first two stages of the square fractal (using the Cantor middle  $\frac{1}{5}$  set) as IFS

**Dynamics of the Square Fractal (using the Cantor middle  $\frac{1}{5}$  set):**

Since  $L_k = \frac{1}{5} < 1$  for  $k = 1, 2, \dots, 9$ , then iterated function system of the square fractal  $\{w_k : k = 1, 2, \dots, 9, \}$  is asymptotically stable.

The Jacobian matrix of IFS of the square fractal at the fixed points is

$$Dw(x, y) = \begin{pmatrix} \frac{1}{5} & 0 \\ 0 & \frac{1}{5} \end{pmatrix},$$

with eigenvalues equal to  $\frac{1}{5}$  and  $\frac{1}{5}$ .

Thus the fixed points of these IFS  $(0, 0)$ ,  $(1/2, 0)$ ,  $(1, 0)$ ,  $(0, 1/2)$ ,  $(1/2, 1/2)$ ,  $(1, 1/2)$ ,  $(0, 1)$ ,  $(1/2, 1)$  and  $(1, 1)$  are sink.

Therefore, IFS of the square fractal is asymptotically stable and the fixed points are sink.

## 5.4. Iterated Function Systems of the Three Dimensional Fractals

### 5.4.1. Iterated Function System of the Menger Sponge

The Menger sponge consists of twenty self-similar pieces that may be derived as the attractor from the following iterated function system

$$w_1 \begin{pmatrix} x \\ y \\ z \end{pmatrix} = \begin{pmatrix} \frac{1}{3} & 0 & 0 \\ 0 & \frac{1}{3} & 0 \\ 0 & 0 & \frac{1}{3} \end{pmatrix} \begin{pmatrix} x \\ y \\ z \end{pmatrix} + \begin{pmatrix} 0 \\ 0 \\ 0 \end{pmatrix} = \left( \frac{1}{3}x, \frac{1}{3}y, \frac{1}{3}z \right)$$

$$w_2 \begin{pmatrix} x \\ y \\ z \end{pmatrix} = \begin{pmatrix} \frac{1}{3} & 0 & 0 \\ 0 & \frac{1}{3} & 0 \\ 0 & 0 & \frac{1}{3} \end{pmatrix} \begin{pmatrix} x \\ y \\ z \end{pmatrix} + \begin{pmatrix} \frac{1}{3} \\ 0 \\ 0 \end{pmatrix} = \left( \frac{1}{3}(x+1), \frac{1}{3}y, \frac{1}{3}z \right)$$

$$w_3 \begin{pmatrix} x \\ y \\ z \end{pmatrix} = \begin{pmatrix} \frac{1}{3} & 0 & 0 \\ 0 & \frac{1}{3} & 0 \\ 0 & 0 & \frac{1}{3} \end{pmatrix} \begin{pmatrix} x \\ y \\ z \end{pmatrix} + \begin{pmatrix} 0 \\ \frac{1}{3} \\ 0 \end{pmatrix} = \left( \frac{1}{3}x, \frac{1}{3}(y+1), \frac{1}{3}z \right)$$

$$w_4 \begin{pmatrix} x \\ y \\ z \end{pmatrix} = \begin{pmatrix} \frac{1}{3} & 0 & 0 \\ 0 & \frac{1}{3} & 0 \\ 0 & 0 & \frac{1}{3} \end{pmatrix} \begin{pmatrix} x \\ y \\ z \end{pmatrix} + \begin{pmatrix} 0 \\ 0 \\ \frac{1}{3} \end{pmatrix} = \left( \frac{1}{3}(x+1), \frac{1}{3}y, \frac{1}{3}(z+1) \right)$$

$$w_5 \begin{pmatrix} x \\ y \\ z \end{pmatrix} = \begin{pmatrix} \frac{1}{3} & 0 & 0 \\ 0 & \frac{1}{3} & 0 \\ 0 & 0 & \frac{1}{3} \end{pmatrix} \begin{pmatrix} x \\ y \\ z \end{pmatrix} + \begin{pmatrix} \frac{2}{3} \\ 0 \\ 0 \end{pmatrix} = \left( \frac{1}{3}(x+2), \frac{1}{3}y, \frac{1}{3}z \right)$$

$$w_6 \begin{pmatrix} x \\ y \\ z \end{pmatrix} = \begin{pmatrix} \frac{1}{3} & 0 & 0 \\ 0 & \frac{1}{3} & 0 \\ 0 & 0 & \frac{1}{3} \end{pmatrix} \begin{pmatrix} x \\ y \\ z \end{pmatrix} + \begin{pmatrix} 0 \\ \frac{2}{3} \\ 0 \end{pmatrix} = \left( \frac{1}{3}x, \frac{1}{3}(y+2), \frac{1}{3}z \right)$$

$$w_7 \begin{pmatrix} x \\ y \\ z \end{pmatrix} = \begin{pmatrix} 1/3 & 0 & 0 \\ 0 & 1/3 & 0 \\ 0 & 0 & 1/3 \end{pmatrix} \begin{pmatrix} x \\ y \\ z \end{pmatrix} + \begin{pmatrix} 0 \\ 0 \\ \frac{2}{3} \end{pmatrix} = \left( \frac{1}{3}x, \frac{1}{3}y, \frac{1}{3}(z+2) \right)$$

$$w_8 \begin{pmatrix} x \\ y \\ z \end{pmatrix} = \begin{pmatrix} \frac{1}{3} & 0 & 0 \\ 0 & \frac{1}{3} & 0 \\ 0 & 0 & \frac{1}{3} \end{pmatrix} \begin{pmatrix} x \\ y \\ z \end{pmatrix} + \begin{pmatrix} \frac{1}{3} \\ \frac{2}{3} \\ 0 \end{pmatrix} = \left( \frac{1}{3}(x+1), \frac{1}{3}(y+2), \frac{1}{3}z \right)$$

$$w_9 \begin{pmatrix} x \\ y \\ z \end{pmatrix} = \begin{pmatrix} \frac{1}{3} & 0 & 0 \\ 0 & \frac{1}{3} & 0 \\ 0 & 0 & \frac{1}{3} \end{pmatrix} \begin{pmatrix} x \\ y \\ z \end{pmatrix} + \begin{pmatrix} \frac{1}{3} \\ 0 \\ \frac{2}{3} \end{pmatrix} = \left( \frac{1}{3}(x+1), \frac{1}{3}y, \frac{1}{3}(z+2) \right)$$

$$w_{10} \begin{pmatrix} x \\ y \\ z \end{pmatrix} = \begin{pmatrix} \frac{1}{3} & 0 & 0 \\ 0 & \frac{1}{3} & 0 \\ 0 & 0 & \frac{1}{3} \end{pmatrix} \begin{pmatrix} x \\ y \\ z \end{pmatrix} + \begin{pmatrix} 0 \\ \frac{1}{3} \\ \frac{2}{3} \end{pmatrix} = \left( \frac{1}{3}x, \frac{1}{3}(y+1), \frac{1}{3}(z+2) \right)$$

$$w_{11} \begin{pmatrix} x \\ y \\ z \end{pmatrix} = \begin{pmatrix} \frac{1}{3} & 0 & 0 \\ 0 & \frac{1}{3} & 0 \\ 0 & 0 & \frac{1}{3} \end{pmatrix} \begin{pmatrix} x \\ y \\ z \end{pmatrix} + \begin{pmatrix} \frac{2}{3} \\ \frac{1}{3} \\ 0 \end{pmatrix} = \left( \frac{1}{3}(x+2), \frac{1}{3}(y+1), \frac{1}{3}z \right)$$

$$w_{12} \begin{pmatrix} x \\ y \\ z \end{pmatrix} = \begin{pmatrix} \frac{1}{3} & 0 & 0 \\ 0 & \frac{1}{3} & 0 \\ 0 & 0 & \frac{1}{3} \end{pmatrix} \begin{pmatrix} x \\ y \\ z \end{pmatrix} + \begin{pmatrix} \frac{2}{3} \\ 0 \\ \frac{1}{3} \end{pmatrix} = \left( \frac{1}{3}(x+2), \frac{1}{3}y, \frac{1}{3}(z+1) \right)$$

$$w_{13} \begin{pmatrix} x \\ y \\ z \end{pmatrix} = \begin{pmatrix} \frac{1}{3} & 0 & 0 \\ 0 & \frac{1}{3} & 0 \\ 0 & 0 & \frac{1}{3} \end{pmatrix} \begin{pmatrix} x \\ y \\ z \end{pmatrix} + \begin{pmatrix} 0 \\ \frac{2}{3} \\ \frac{1}{3} \end{pmatrix} = \left( \frac{1}{3}x, \frac{1}{3}(y+2), \frac{1}{3}(z+1) \right)$$

$$w_{14} \begin{pmatrix} x \\ y \\ z \end{pmatrix} = \begin{pmatrix} \frac{1}{3} & 0 & 0 \\ 0 & \frac{1}{3} & 0 \\ 0 & 0 & \frac{1}{3} \end{pmatrix} \begin{pmatrix} x \\ y \\ z \end{pmatrix} + \begin{pmatrix} \frac{2}{3} \\ \frac{2}{3} \\ 0 \end{pmatrix} = \left( \frac{1}{3}(x+2), \frac{1}{3}(y+2), \frac{1}{3}z \right)$$

$$w_{15} \begin{pmatrix} x \\ y \\ z \end{pmatrix} = \begin{pmatrix} \frac{1}{3} & 0 & 0 \\ 0 & \frac{1}{3} & 0 \\ 0 & 0 & \frac{1}{3} \end{pmatrix} \begin{pmatrix} x \\ y \\ z \end{pmatrix} + \begin{pmatrix} \frac{2}{3} \\ 0 \\ \frac{2}{3} \end{pmatrix} = \left( \frac{1}{3}(x+2), \frac{1}{3}y, \frac{1}{3}(z+2) \right)$$

$$w_{16} \begin{pmatrix} x \\ y \\ z \end{pmatrix} = \begin{pmatrix} \frac{1}{3} & 0 & 0 \\ 0 & \frac{1}{3} & 0 \\ 0 & 0 & \frac{1}{3} \end{pmatrix} \begin{pmatrix} x \\ y \\ z \end{pmatrix} + \begin{pmatrix} 0 \\ \frac{2}{3} \\ \frac{2}{3} \end{pmatrix} = \left( \frac{1}{3}x, \frac{1}{3}(y+2), \frac{1}{3}(z+2) \right)$$

$$w_{17} \begin{pmatrix} x \\ y \\ z \end{pmatrix} = \begin{pmatrix} \frac{1}{3} & 0 & 0 \\ 0 & \frac{1}{3} & 0 \\ 0 & 0 & \frac{1}{3} \end{pmatrix} \begin{pmatrix} x \\ y \\ z \end{pmatrix} + \begin{pmatrix} \frac{2}{3} \\ \frac{2}{3} \\ \frac{1}{3} \end{pmatrix} = \left( \frac{1}{3}(x+2), \frac{1}{3}(y+2), \frac{1}{3}(z+1) \right)$$

$$w_{18} \begin{pmatrix} x \\ y \\ z \end{pmatrix} = \begin{pmatrix} \frac{1}{3} & 0 & 0 \\ 0 & \frac{1}{3} & 0 \\ 0 & 0 & \frac{1}{3} \end{pmatrix} \begin{pmatrix} x \\ y \\ z \end{pmatrix} + \begin{pmatrix} \frac{2}{3} \\ \frac{1}{3} \\ \frac{2}{3} \end{pmatrix} = \left( \frac{1}{3}(x+2), \frac{1}{3}(y+1), \frac{1}{3}(z+2) \right)$$

$$\begin{aligned}
 w_{19} \begin{pmatrix} x \\ y \\ z \end{pmatrix} &= \begin{pmatrix} \frac{1}{3} & 0 & 0 \\ 0 & \frac{1}{3} & 0 \\ 0 & 0 & \frac{1}{3} \end{pmatrix} \begin{pmatrix} x \\ y \\ z \end{pmatrix} + \begin{pmatrix} \frac{1}{3} \\ \frac{2}{3} \\ \frac{2}{3} \end{pmatrix} = \left( \frac{1}{3}(x+1), \frac{1}{3}(y+2), \frac{1}{3}(z+2) \right) \\
 w_{20} \begin{pmatrix} x \\ y \\ z \end{pmatrix} &= \begin{pmatrix} \frac{1}{3} & 0 & 0 \\ 0 & \frac{1}{3} & 0 \\ 0 & 0 & \frac{1}{3} \end{pmatrix} \begin{pmatrix} x \\ y \\ z \end{pmatrix} + \begin{pmatrix} \frac{2}{3} \\ \frac{2}{3} \\ \frac{2}{3} \end{pmatrix} = \left( \frac{1}{3}(x+2), \frac{1}{3}(y+2), \frac{1}{3}(z+2) \right) \tag{5.30}
 \end{aligned}$$

The contraction factor is  $r = \frac{1}{3}$ , and the fixed points are located at  $(0, 0, 0), (\frac{1}{2}, 0, 0), (0, \frac{1}{2}, 0), (0, 0, \frac{1}{2}), (1, 0, 0), (0, 1, 0), (0, 0, 1), (1, 0, \frac{1}{2}), (1, \frac{1}{2}, 0), (0, 1, \frac{1}{2}), (\frac{1}{2}, 1, 0), (\frac{1}{2}, 0, 1), (0, \frac{1}{2}, 1), (1, 1, 0), (1, 0, 1), (0, 1, 1), (1, 1, \frac{1}{2}), (\frac{1}{2}, 1, 1), (1, \frac{1}{2}, 1), (1, 1, 1)$ .

The Barnsley-Hutchinson operator is  $F(M) = \bigcup_{i=1}^{20} w_i(M)$ .

Then the attractor of IFS (5.30) is  $M_{n+1} = F(M_n), n = 0, 1, 2, \dots$  (5.31)

where  $M_0 \in \{(0, 0, 0), (1, 0, 0), (0, 1, 0), (0, 0, 1), (1, 1, 0), (1, 0, 1), (0, 1, 1), (1, 1, 1)\}$ .

From (5.31) we obtain obviously

$$\begin{aligned}
 M_1 &= F(M_0) = \bigcup_{i=1}^{20} w_i(M_0) \\
 &= (0, 0, 0) \cup (\frac{1}{3}, 0, 0) \cup (0, \frac{1}{3}, 0) \cup (0, 0, \frac{1}{3}) \cup (\frac{2}{3}, 0, 0) \cup (0, \frac{2}{3}, 0) \cup (0, 0, \frac{2}{3}) \\
 &\quad \dots \cup (\frac{2}{3}, 1, 1) \cup (1, \frac{2}{3}, 1) \cup (1, 1, \frac{2}{3}) \cup (1, 1, 1).
 \end{aligned}$$

$$M_2 = F(M_1) = \bigcup_{i=1}^{20} w_i(M_1), \dots$$

In general,  $M_n$  is the union of  $8 \cdot (20)^{n-1}$  vertices, each of size of the Menger sponge is  $\frac{1}{3^n}$ .

We obtain a sequence

$$M_0 \supset M_1 \supset M_2 \dots$$

Hence the Menger sponge is  $M = \bigcap_{n=0}^{\infty} M_n$ .

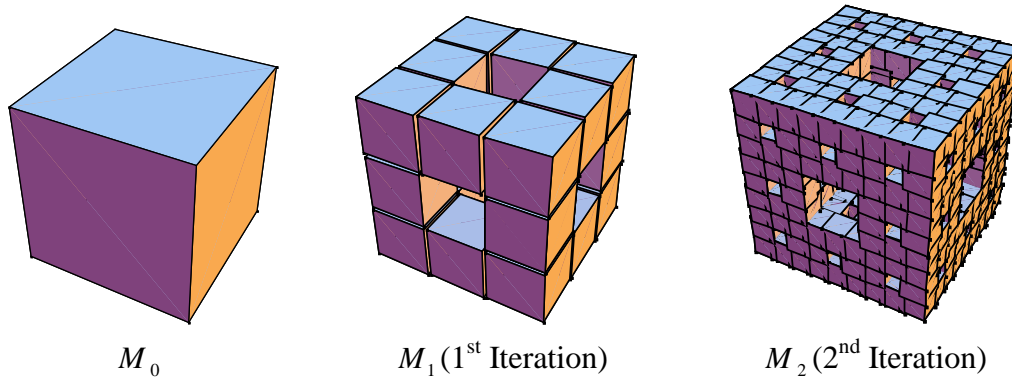


**Figure 6.16** The first three stages in the construction of the Menger sponge as IFS

**Dynamics of the Menger Sponge:**

Since  $L_k = \frac{1}{3} < 1$  for  $k = 1, 2, \dots, 20$ , then iterated function system of the square fractal  $\{w_k : k = 1, 2, \dots, 20\}$  is asymptotically stable.

The Jacobian matrix of IFS of the Menger sponge at the fixed points is

$$Dw(x, y) = \begin{pmatrix} \frac{1}{3} & 0 & 0 \\ 0 & \frac{1}{3} & 0 \\ 0 & 0 & \frac{1}{3} \end{pmatrix},$$

with eigenvalues equal to  $\frac{1}{3}, \frac{1}{3}$  and  $\frac{1}{3}$ .

Thus the fixed points of these IFS  $(0, 0, 0), (\frac{1}{2}, 0, 0), (0, \frac{1}{2}, 0), (0, 0, \frac{1}{2}), (1, 0, 0), (0, 1, 0), (0, 0, 1), (1, 0, \frac{1}{2}), (1, \frac{1}{2}, 0), (0, 1, \frac{1}{2}), (\frac{1}{2}, 1, 0), (\frac{1}{2}, 0, 1), (0, \frac{1}{2}, 1), (1, 1, 0), (1, 0, 1), (0, 1, 1), (1, 1, \frac{1}{2}), (\frac{1}{2}, 1, 1), (1, \frac{1}{2}, 1),$  and  $(1, 1, 1)$  are sink.

Therefore, IFS of the Menger sponge is asymptotically stable and the fixed points are sink.

**6.4.2. Iterated Function System of the Sierpinski Tetrahedron**

The Sierpinski tetrahedron consists of four self-similar pieces that may be obtained as the attractor of an iterated function system by setting

$$w_1 \begin{pmatrix} x \\ y \\ z \end{pmatrix} = \begin{pmatrix} \frac{1}{2} & 0 & 0 \\ 0 & \frac{1}{2} & 0 \\ 0 & 0 & \frac{1}{2} \end{pmatrix} \begin{pmatrix} x \\ y \\ z \end{pmatrix} + \begin{pmatrix} 0 \\ 0 \\ \frac{\sqrt{3}}{2} \end{pmatrix} = \begin{pmatrix} \frac{x}{2}, \frac{y}{2}, \frac{(z + \sqrt{3})}{2} \end{pmatrix},$$

$$\begin{aligned}
 w_2 \begin{pmatrix} x \\ y \\ z \end{pmatrix} &= \begin{pmatrix} \frac{1}{2} & 0 & 0 \\ 0 & \frac{1}{2} & 0 \\ 0 & 0 & \frac{1}{2} \end{pmatrix} \begin{pmatrix} x \\ y \\ z \end{pmatrix} + \begin{pmatrix} 0 \\ \frac{\sqrt{2}}{\sqrt{3}} \\ \frac{-1}{2\sqrt{3}} \end{pmatrix} = \left( \frac{x}{2}, \frac{y}{2} + \frac{\sqrt{2}}{\sqrt{3}}, \frac{z}{2} - \frac{1}{2\sqrt{3}} \right), \\
 w_3 \begin{pmatrix} x \\ y \\ z \end{pmatrix} &= \begin{pmatrix} \frac{1}{2} & 0 & 0 \\ 0 & \frac{1}{2} & 0 \\ 0 & 0 & \frac{1}{2} \end{pmatrix} \begin{pmatrix} x \\ y \\ z \end{pmatrix} + \begin{pmatrix} \frac{-1}{\sqrt{2}} \\ \frac{\sqrt{2}}{\sqrt{6}} \\ \frac{-1}{2\sqrt{3}} \end{pmatrix} = \left( \frac{x}{2} - \frac{1}{\sqrt{2}}, \frac{y}{2} - \frac{1}{\sqrt{6}}, \frac{z}{2} - \frac{1}{2\sqrt{3}} \right), \\
 w_4 \begin{pmatrix} x \\ y \\ z \end{pmatrix} &= \begin{pmatrix} \frac{1}{2} & 0 & 0 \\ 0 & \frac{1}{2} & 0 \\ 0 & 0 & \frac{1}{2} \end{pmatrix} \begin{pmatrix} x \\ y \\ z \end{pmatrix} + \begin{pmatrix} \frac{1}{\sqrt{2}} \\ \frac{-1}{\sqrt{6}} \\ \frac{-1}{2\sqrt{3}} \end{pmatrix} = \left( \frac{x}{2} + \frac{1}{\sqrt{2}}, \frac{y}{2} - \frac{1}{\sqrt{6}}, \frac{z}{2} - \frac{1}{2\sqrt{3}} \right) \tag{5.32}
 \end{aligned}$$

The contraction factor is  $\tau = \frac{1}{2}$ , and the fixed points are located at  $(0,0,\sqrt{3})$ ,  $(0, 2\sqrt{2/3}, -1/\sqrt{3})$ ,  $(-\sqrt{2}, -\sqrt{2/3}, -\sqrt{1/3})$  and  $(\sqrt{2}, -\sqrt{2/3}, -\sqrt{1/3})$ .

The Barnsley-Hutchinson operator is  $F(T) = \bigcup_{i=1}^4 w_i(T)$ .

Then the attractor of IFS (5.32) is  $T_{n+1} = F(T_n)$ , where  $n = 0, 1, 2, \dots$ , (5.33)

$T_0 \in \{(0, 0, \sqrt{3}), (0, 2\sqrt{2/3}, -1/\sqrt{3}), (-\sqrt{2}, -\sqrt{2/3}, -\sqrt{1/3}), (\sqrt{2}, -\sqrt{2/3}, -\sqrt{1/3})\}$ ,

which is the Sierpinski tetrahedron.

From (5.33) we obtain obviously

$$\begin{aligned}
 T_1 &= F(T_0) = w_1(T_0) \cup w_2(T_0) \cup w_3(T_0) \cup w_4(T_0) \\
 &= (0, 0, \sqrt{3}) \cup (0, \sqrt{2/3}, \frac{1}{\sqrt{3}}) \cup (-\frac{1}{\sqrt{2}}, -\frac{1}{\sqrt{6}}, \frac{1}{\sqrt{3}}) \cup \dots \cup (\frac{1}{\sqrt{2}}, -\frac{1}{\sqrt{6}}, \frac{1}{\sqrt{3}}).
 \end{aligned}$$

$$T_2 = F(T_1) = \bigcup_{i=1}^4 w_i(T_1), \dots$$

In general,  $T_n$  is the union of  $4 \cdot 4^{n-1}$  vertices, each of size of the Tetrahedron is  $\frac{1}{2^n}$ .

We obtain a sequence

$$T_0 \supset T_1 \supset T_2 \supset \dots$$

Thus the Sierpinski tetrahedron is  $T = \bigcap_{n=0}^{\infty} T_n$ .



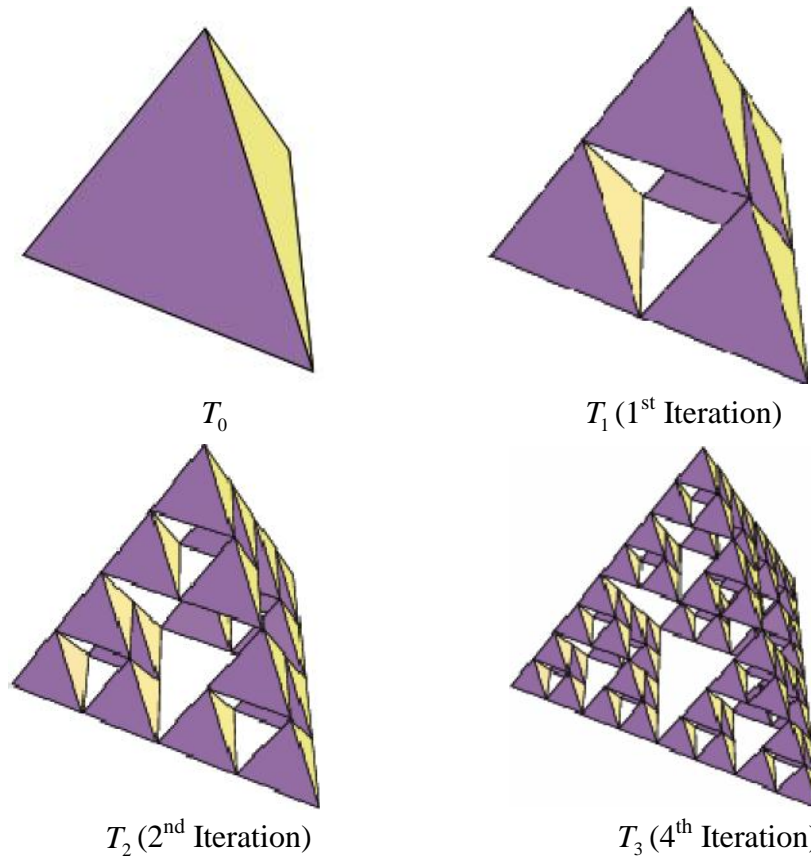


**Figure 5.17** The first four stages in the construction of the Sierpinski tetrahedron as IFS

**Dynamics of the Sierpinski Tetrahedron:**

Since  $L_k = \frac{1}{2} < 1$  for  $k = 1, 2, 3, 4$ , then iterated function system of the square fractal  $\{w_k : k = 1, 2, 3, 4, \}$  is asymptotically stable.

The Jacobian matrix of IFS of the Sierpinski tetrahedron at the fixed points is

$$Dw(x, y) = \begin{pmatrix} \frac{1}{2} & 0 & 0 \\ 0 & \frac{1}{2} & 0 \\ 0 & 0 & \frac{1}{2} \end{pmatrix},$$

with eigenvalues equal to  $\frac{1}{2}, \frac{1}{2}$  and  $\frac{1}{2}$ . Thus the fixed points of these IFS  $(0, 0, \sqrt{3}), (0, 2\sqrt{2/3}, -1/\sqrt{3}), (-\sqrt{2}, -\sqrt{2/3}, -\sqrt{1/3})$  and  $(\sqrt{2}, -\sqrt{2/3}, -\sqrt{1/3})$  are sink. Hence IFS of the Sierpinski tetrahedron is asymptotically stable and the fixed points are sink.

### 5.4.3. Iterated Function System of the Octahedron Fractal

The constructed octahedron fractal consists of six self-similar pieces that may be derived as the attractor form the following iterated function system

$$\begin{aligned}
 w_1 \begin{pmatrix} x \\ y \\ z \end{pmatrix} &= \begin{pmatrix} \frac{1}{2} & 0 & 0 \\ 0 & \frac{1}{2} & 0 \\ 0 & 0 & \frac{1}{2} \end{pmatrix} \begin{pmatrix} x \\ y \\ z \end{pmatrix} + \begin{pmatrix} 0 \\ 0 \\ \frac{1}{\sqrt{2}} \end{pmatrix} = \left( \frac{x}{2}, \frac{y}{2}, \frac{z}{2} + \frac{1}{\sqrt{2}} \right), \\
 w_2 \begin{pmatrix} x \\ y \\ z \end{pmatrix} &= \begin{pmatrix} \frac{1}{2} & 0 & 0 \\ 0 & \frac{1}{2} & 0 \\ 0 & 0 & \frac{1}{2} \end{pmatrix} \begin{pmatrix} x \\ y \\ z \end{pmatrix} + \begin{pmatrix} \frac{1}{\sqrt{2}} \\ 0 \\ 0 \end{pmatrix} = \left( \frac{x}{2} + \frac{1}{\sqrt{2}}, \frac{y}{2}, \frac{z}{2} \right), \\
 w_3 \begin{pmatrix} x \\ y \\ z \end{pmatrix} &= \begin{pmatrix} \frac{1}{2} & 0 & 0 \\ 0 & \frac{1}{2} & 0 \\ 0 & 0 & \frac{1}{2} \end{pmatrix} \begin{pmatrix} x \\ y \\ z \end{pmatrix} + \begin{pmatrix} 0 \\ \frac{1}{\sqrt{2}} \\ 0 \end{pmatrix} = \left( \frac{x}{2}, \frac{y}{2} + \frac{1}{\sqrt{2}}, \frac{z}{2} \right), \\
 w_4 \begin{pmatrix} x \\ y \\ z \end{pmatrix} &= \begin{pmatrix} \frac{1}{2} & 0 & 0 \\ 0 & \frac{1}{2} & 0 \\ 0 & 0 & \frac{1}{2} \end{pmatrix} \begin{pmatrix} x \\ y \\ z \end{pmatrix} + \begin{pmatrix} 0 \\ 0 \\ -\frac{1}{\sqrt{2}} \end{pmatrix} = \left( \frac{x}{2}, \frac{y}{2}, \frac{z}{2} - \frac{1}{\sqrt{2}} \right), \\
 w_5 \begin{pmatrix} x \\ y \\ z \end{pmatrix} &= \begin{pmatrix} \frac{1}{2} & 0 & 0 \\ 0 & \frac{1}{2} & 0 \\ 0 & 0 & \frac{1}{2} \end{pmatrix} \begin{pmatrix} x \\ y \\ z \end{pmatrix} + \begin{pmatrix} -\frac{1}{\sqrt{2}} \\ 0 \\ 0 \end{pmatrix} = \left( \frac{x}{2} - \frac{1}{\sqrt{2}}, \frac{y}{2}, \frac{z}{2} \right), \\
 w_6 \begin{pmatrix} x \\ y \\ z \end{pmatrix} &= \begin{pmatrix} \frac{1}{2} & 0 & 0 \\ 0 & \frac{1}{2} & 0 \\ 0 & 0 & \frac{1}{2} \end{pmatrix} \begin{pmatrix} x \\ y \\ z \end{pmatrix} + \begin{pmatrix} 0 \\ -\frac{1}{\sqrt{2}} \\ 0 \end{pmatrix} = \left( \frac{x}{2}, \frac{y}{2} - \frac{1}{\sqrt{2}}, \frac{z}{2} \right)
 \end{aligned} \tag{5.34}$$

The contraction factor is  $r = \frac{1}{2}$ , and the fixed points are located at  $(0, 0, \sqrt{2})$ ,

$(\sqrt{2}, 0, 0)$ ,  $(0, \sqrt{2}, 0)$ ,  $(0, 0, -\sqrt{2})$ ,  $(-\sqrt{2}, 0, 0)$  and  $(0, -\sqrt{2}, 0)$ .

The Barnsley-Hutchinson operator is  $F(O) = \bigcup_{i=1}^6 w_i(O)$ .

Then the attractor of IFS (5.34) is  $O_{n+1} = F(O_n)$ , where  $n = 0, 1, 2, \dots$ , (5.35)

and  $O_0 \in \{(0, 0, \sqrt{2}), (\sqrt{2}, 0, 0), (0, \sqrt{2}, 0), (0, 0, -\sqrt{2}), (-\sqrt{2}, 0, 0), (0, -\sqrt{2}, 0)\}$ , which is the octahedron fractal. From (5.35) we obtain obviously

$$O_1 = F(O_0) = \bigcup_{i=1}^6 w_i(O_0) \\ = (0, 0, \sqrt{3}) \cup (0, \sqrt{2/3}, \frac{1}{\sqrt{3}}) \cup (-\frac{1}{\sqrt{2}}, -\frac{1}{\sqrt{6}}, \frac{1}{\sqrt{3}}) \cup \dots \cup (\frac{1}{\sqrt{2}}, -\frac{1}{\sqrt{6}}, \frac{1}{\sqrt{3}}).$$

$$O_2 = F(O_1) = \bigcup_{i=1}^6 w_i(O_1), \dots$$

In general,  $O_n$  is the union of  $6 \cdot 6^{n-1}$  vertices, each of size of the octahedron fractal is  $\frac{1}{2^n}$ .

We obtain a sequence  $O_0 \supset O_1 \supset O_2 \supset \dots$

Therefore, the octahedron fractal is  $O = \bigcap_{n=0}^{\infty} O_n$ .

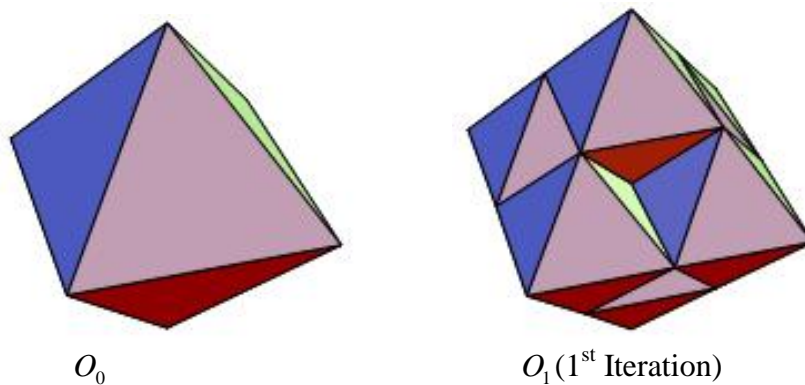


**Figure 5.18** The first two stages in the construction of the octahedron fractal as IFS

**Dynamics of the Octahedron fractal:**

Since  $L_k = \frac{1}{2} < 1$  for  $k = 1, 2, \dots, 6$ , then iterated function system of the octahedron fractal  $\{w_k : k = 1, 2, \dots, 6\}$  is asymptotically stable.

The Jacobian matrix of IFS of the octahedron fractal at the fixed points is

$$Dw(x, y) = \begin{pmatrix} \frac{1}{2} & 0 & 0 \\ 0 & \frac{1}{2} & 0 \\ 0 & 0 & \frac{1}{2} \end{pmatrix},$$

with eigenvalues equal to  $\frac{1}{2}, \frac{1}{2}$  and  $\frac{1}{2}$ .

Thus the fixed points of these IFS  $(0,0,\sqrt{2})$ ,  $(\sqrt{2},0,0)$ ,  $(0,\sqrt{2},0)$ ,  $(0,0,-\sqrt{2})$ ,  $(-\sqrt{2},0,0)$  and  $(0,-\sqrt{2},0)$  are sink.

Therefore, IFS of the octahedron fractal is asymptotically stable and the fixed points are sink.

# CHAPTER SIX

## MARKOV OPERATORS

### OVERVIEW

In this chapter, we discuss the properties of Markov operators on  $L^1(X)$  space and Borel measure. We observe that Markov operator is non-expansive and asymptotically stable. Also we show the sweeping properties of Markov operator associated to iterated function system of the generalized Cantor sets.

### 6.1. Markov Operators

Markov operators which occur in diverse branches of pure and applied Mathematics [31]. Processes described by these operators arise in mathematical theory of learning [32, 33, 34], population dynamics [35], theory of stochastic differential equations [36, 37] and many others. Recently such processes have been extensively studied because of the close connection to fractals and their generalization, semifractals [38, 39, 40, 41]. These operators are also used in computer graphics. If  $(Z_n)_{n \geq 1}$  is a homogeneous Markov chain taking values in some metric space  $X$  and  $f$  is its transition kernel, i.e.,

$$\text{prob}\{Z_{n+1} \in A \mid Z_n = x_n, \dots, Z_0 = x_0\} = f(x_n, A)$$

for  $n \in \mathbf{N}$  and all Borel sets  $A$ , the corresponding Markov operator is given by

$$P_{\sim}(A) = \int_X f(x, A) \sim(dx).$$

#### 6.1.1. [42] Markov Operators on $L^1(X)$

Let the triple  $(X, \Sigma, \sim)$  be a  $\dagger$ -finite measure space, that is,  $\Sigma$  is a  $\dagger$ -algebra of subsets of a set  $X$  and  $\sim$  is a  $\dagger$ -finite positive measure defined on  $\Sigma$ . Let  $L^1 \equiv L^1(X, \Sigma, \sim)$  be the Banach space of all  $\sim$ -integrable real functions defined on  $X$  with the  $L^1$ -norm  $\|f\| = \int |f| d\sim$ , and let  $L^\infty \equiv L^\infty(X, \Sigma, \sim)$  be the Banach space of all bounded almost everywhere real  $\Sigma$ -measurable functions on  $X$  with the  $L^\infty$ -norm  $\|g\|_\infty = \text{ess sup } |g|$ . It is well known that  $L^\infty$  is the dual space of  $L^1$ . A linear operator  $P: L^1 \rightarrow L^1$  is called a *Markov operator* if  $Pf$  is nonnegative with the same integral for any nonnegative function  $f \in L^1$ . Denote  $D = \{f \in L^1 : f \geq 0, \|f\| = 1\}$ . Then the Markov operator  $P$  can be characterized as a linear operator  $P$  such that  $P(D) \subset D$ .

Each  $f \in D$  is referred to as a density function (with respect to the chosen measure  $\sim$ ), and is also the density (the Radon-Nikodym derivative) of the probability measure

$$\sim_f(f) = \int_A f d\sim, \text{ for each } A \in \Sigma$$

with respect to  $\sim$ . The measure  $\sim_f$  is said to be absolutely continuous with respect  $\sim$ .

Thus a Markov operator is a linear operator that maps densities to densities.

Some basic properties of Markov operators  $P$  are as follows [37A]:

- (i)  $\|Pf\| \leq \|f\|, \forall f \in L^1$ .
- (ii)  $P|f| \leq |f|, \forall f \in L^1$ , that is,  $P|f(x)| \leq |f(x)|$ , for  $\sim$ -almost all  $x$ .
- (iii) If  $Pf = f$ , then  $Pf^+ = f^+$  and  $Pf^- = f^-$ . Here  $f^+(x) = \max\{f(x), 0\}$  and  $f^-(x) = \max\{-f(x), 0\}$ .

**Definition 6.1.1.1 [43]** A family  $\{P(t)\}_{t \geq 0}$  of Markov operators which satisfies conditions

- (a)  $P(0) = \text{Id}$
- (b)  $P(s+t) = P(s)P(t)$  for  $s, t \geq 0$
- (c) for each  $f \in L^1$  the function  $t \mapsto P(t)f$  is continuous

is called a *Markov semi-group*.

**Markov operators:** Types of Markov operators such as Frobenius-Perron operator, Iterated Function System and Integral operator.

1. *Frobenius-Perron operator:* This operator describes statistical properties of simple point to point transformations [44]. Let  $S : X \rightarrow X$  be a non-singular transformation, that is,  $S$  is a measurable and  $\sim(S^{-1}(A)) = 0$  for all  $A \in \Sigma$  such that  $\sim(A) = 0$ . For a given  $f \in L^1$  define

$$\sim_f(f) = \int_{S^{-1}(A)} f d\sim, A \in \Sigma.$$

Since  $S$  is a non-singular,  $\sim(A) = 0$  implies that then  $\sim_f(A) = 0$ . Thus the Radon-Nikodym Theorem implies that there exists a unique  $\hat{f} \in L^1$ , denoted as  $Pf$ , such that

$$\sim_f(f) = \int_{S^{-1}(A)} \hat{f} d\sim, A \in \Sigma.$$

Define  $\hat{f} = Pf$ . Then the operator  $P \equiv P_S : L^1 \rightarrow L^1$  defined by

$$\int_A Pf d\sim = \int_{S^{-1}(A)} f d\sim \text{ for all } A \in \Sigma$$

is called the Frobenius-Perron operator is also a Markov operator [42].

2. *Markov Operator for Iterated function systems:* [43] Let  $S_1, S_2, \dots, S_N$  be non-singular transformations of the space  $X = [0,1]$ . Let  $P_1, P_2, \dots, P_N$  be the Frobenius-Perron operators corresponding to the transformations  $S_1, S_2, \dots, S_N$ . Let  $p_1, p_2, \dots, p_N$  be non-negative measurable functions defined on  $X$  such that  $\sum_{i=1}^N p_i(x) = 1$  for all  $x \in X$ .

We consider the following process. Take a point  $x$ . We choose a transformation  $S_i$  with probability  $p_i(x)$  and  $S_i(x)$  describes the position of  $x$  after the action of the system. The evolution of densities of the distribution is described by the Markov operator

$$Pf = \sum_{i=1}^N P_i(p_i f).$$

That is,

$$Pf(x) = \sum_{i=1}^N P_i(p_i f)(x) = \sum_{i=1}^N p_i \frac{d\sim \circ S_i^{-1}}{d\sim}(x) f(S_i^{-1}(x)), \text{ where } f \in L^1(x), x \in X. \quad (6.1)$$

3. *Integral operator*: [43] If  $k : X \times X \rightarrow [0, \infty)$  is a measurable function such that

$$\int_X k(x, y) \sim(dx) = 1 \text{ for each } y \in X,$$

then

$$Pf(x) = \int_X k(x, y) f(y) \sim(dy)$$

is a *Markov operator*.

### 6.1.1.2. [45] Sweeping Property of Markov Operators

Let a family  $M \in \Sigma$  be given. A Markov operator  $P$  is called  $\nu$ -sweeping ( $\nu > 0$ ) with respect to  $M$  if

$$\limsup_{n \rightarrow \infty} \int_A P^n f d\sim \leq 1 - \nu \text{ for } A \in M \text{ and } f \in D.$$

A 1-sweeping operator is shortly called *sweeping*, and inequality (6.1) may be replaced by

$$\lim_{n \rightarrow \infty} \int_A P^n f d\sim = 0 \text{ for } A \in M \text{ and } f \in D.$$

A Markov operator  $P$  is called *Cesaro-sweeping* with respect to  $M$  if

$$\lim_{n \rightarrow \infty} \frac{1}{n} \sum_{k=0}^{n-1} \int_A P^k f d\sim = 0 \text{ for } A \in M \text{ and } f \in D.$$

### 6.1.2. [46] Markov Operators on Measures

Let  $(X, \dots)$  be a separable complete metric space. We assume that every closed ball in  $X$

$$B(r, x) = \{y \in X : \dots(x, y) \leq r\}$$

is a compact set. We denote by  $\mathbf{B}(X)$  the  $\dagger$ -algebra of Borel subsets of  $X$ . By  $\mathbf{B}_b(X)$  we denote the families of all bounded Borel subsets of  $X$ . By  $\mathbf{M}$  we denote the family of Borel measures (nonnegative,  $\dagger$ -additive) on  $X$  such that  $\sim(B) < \infty$  for every ball  $B$ . By  $\mathbf{M}_{fin}$  and  $\mathbf{M}_1$  we denote the subsets of  $\mathbf{M}$  such that  $\sim(X) < \infty$  for  $\sim \in \mathbf{M}_{fin}$  and  $\sim(X) = 1$  for  $\sim \in \mathbf{M}_1$ . The elements of  $\mathbf{M}_1$  will be distributions. Further by  $C(X)$  we denote the space of bounded continuous functions  $F : X \rightarrow \mathbf{R}$  with the supremum norm. As usual we denote by  $C_0(X)$  the subspace  $C(X)$  of which contains functions with compact supports. The indicator function of a set  $A \subset X$  will be denoted by  $1_A$ .

A linear functional  $\{ : C_0 \rightarrow \mathbf{R}$  is called positive if  $\{ (f) \geq 0$  for  $f \geq 0$ . According to the Riesz theorem for every linear positive functional  $\{ : C_0 \rightarrow \mathbf{R}$  there is a unique measure  $\sim \in M$  such that

$$\{ (f) = \int_X f d\sim =: \langle f, \sim \rangle \text{ for } f \in C_0.$$

An operator  $P : M_{fin} \rightarrow M_{fin}$  will be called a *Markov operator* if it satisfies the following two conditions.

- (i) Positive linearity:  $P(\{_1 \sim_1 + \{_2 \sim_2) = \{_1 P\sim_1 + \{_2 P\sim_2$  for  $\{_1, \{_2 \geq 0; \sim_1, \sim_2 \in M_{fin}$
- (ii) Preservation of the norm:  $P\sim(X) = \sim(X)$  for  $\sim \in M_{fin}$ .

A Markov operator  $P$  is called a *Feller operator* if there is a linear operator  $U : C_0(X) \rightarrow C(X)$  (dual to  $P$ ) such that

$$\langle Uf, \sim \rangle = \langle f, P\sim \rangle \text{ for } f \in C_0, \sim \in M_{fin}. \tag{6.2}$$

Observe that the range of the operator  $U$  is contained in  $C(X)$  but not necessarily in  $C_0(X)$ . We may extend  $U$  to all bounded measurable (or nonnegative measurable) function by setting

$$Uf(x) = \langle Uf, u_x \rangle = \langle f, P u_x \rangle \tag{6.3}$$

where  $u_x \in M_1$  is a point (Dirac) measure supported at  $x$ . For  $f \geq 0$  the function  $Uf$  is nonnegative but may be unbounded or even admit infinite values for unbounded  $f$ .

Every Markov operator  $P$  can be easily extended to the space of signed measures

$$M_{sig} = \{ \sim_1 - \sim_2 : \sim_1, \sim_2 \in M_{fin} \}.$$

We say that  $\sim \in M_{fin}$  is concentrated on  $A \in \mathbf{B}(X)$  if  $\sim(X \setminus A) = 0$ . By  $M_1^A$  we denote the set of all distributions concentrated on  $A \in \mathbf{B}(X)$ .

Namely for every  $\epsilon \in M_{sig}$  we define

$$P\epsilon = P\sim_1 - P\sim_2 \text{ where } \epsilon = \sim_1 - \sim_2 : \sim_1, \sim_2 \in M_{fin}.$$

It is easy to verify that this definition of  $P$  does not depend on the choice of  $\sim_1, \sim_2$ .

In the space  $M_{sig}$  we define the *Fortet–Mourier* norm

$$\|\epsilon\| = \sup_F \{ |\langle f, \epsilon \rangle| : f \in F \}, \tag{6.4}$$

where  $\langle f, \sim \rangle = \int_X f(x) \sim(dx)$  and  $F = \{ f \in C(X) \}$  is the set of all  $f$  such that  $\|f\|_c \leq 1$  and  $|f(x) - f(y)| \leq \dots(x, y)$  for  $x, y \in X$ . It is easy to verify that the value (6.4) will not change if  $F$  is replaced by  $F_0 = F \cap C_0$ . For  $\sim \in M_{fin}$ , we have  $\|\sim\| = \sim(X)$ . The space  $M_1$  with the distance  $\|\sim_1 - \sim_2\|$  is a complete metric space and the convergence

$$\lim_{n \rightarrow \infty} \|\sim_n - \sim\| = 0 \text{ for } \sim_n, \sim \in M_1$$

is equivalent to the condition



$$\lim_{n \rightarrow \infty} \langle f, \tilde{\sim}_n \rangle = \langle f, \tilde{\sim} \rangle \tag{6.5}$$

for all  $f \in C(X)$ , or equivalently for all  $f \in C_0(X)$ .

A family  $\{P^t\}_{t \geq 0}$  of Markov operators is called a semi-group if  $P^{t+s} = P^t P^s$  for all  $t, s \in \mathbf{R}_+$  and  $P^0$  is the identity operator on  $M_{fin}$ .

**6.1.2.1. [31] Properties of Markov Operators**

A Markov operator  $P$  is called *non-expansive* if

$$\|P\tilde{\sim}_1 - P\tilde{\sim}_2\| = \|\tilde{\sim}_1 - \tilde{\sim}_2\| \text{ for } \tilde{\sim}_1, \tilde{\sim}_2 \in M_1. \tag{6.6}$$

Let  $P$  be a Markov operator. A measure  $\tilde{\sim} \in M_{fin}$  is called *stationary or invariant* if  $P\tilde{\sim} = \tilde{\sim}$ , and A Markov operator  $P$  is called *asymptotically stable* if there exists a stationary distribution  $\tilde{\sim}_*$  such that

$$\lim_{n \rightarrow \infty} \|P^n \tilde{\sim} - \tilde{\sim}_*\| = 0 \text{ for } \tilde{\sim} \in M_1. \tag{6.7}$$

Clearly the distribution  $\tilde{\sim}_*$  satisfying (6.7) is unique.

Let  $\{P^t\}_{t \geq 0}$  be a Markov semigroup. The Markov semigroup  $\{P^t\}_{t \geq 0}$  is called *non-expansive* if every Markov operator  $P^t, t \geq 0$  is non-expansive. A measure  $\tilde{\sim} \in M_{fin}$  is called *stationary or invariant* for the Markov semigroup  $\{P^t\}_{t \geq 0}$  if  $P^t \tilde{\sim} = \tilde{\sim}$  for all  $t \geq 0$ .

The Markov semigroup  $\{P^t\}_{t \geq 0}$  is called *asymptotically stable* if there exists a stationary distribution  $\tilde{\sim}_*$  such that

$$\lim_{n \rightarrow \infty} \|P^n \tilde{\sim} - \tilde{\sim}_*\| = 0 \text{ for } \tilde{\sim} \in M_1. \tag{6.8}$$

An Operator  $P$  is called *globally concentrating* if for every  $\nu > 0$  and every  $A \in \mathbf{B}_b(X)$  there exist  $B \in \mathbf{B}_b(X)$  and  $n_0 \in \mathbf{N}$  such that

$$P^n \tilde{\sim}(B) \geq 1 - \nu \text{ for } n \geq n_0, \tilde{\sim} \in M_1^A. \tag{6.9}$$

An Operator  $P$  is called *locally concentrating* if for every  $\nu > 0$  there is  $\tau > 0$  such that for every  $A \in \mathbf{B}_b(X)$  there exist  $C \in \mathbf{B}_b(X)$  with  $\text{diam } C \leq \nu$  and  $n_0 \in \mathbf{N}$  satisfying

$$P^{n_0} \tilde{\sim}(C) > \tau \text{ for } \tilde{\sim} \in M_1^A. \tag{6.10}$$

An Operator  $P$  is called *concentrating* if for every  $\nu > 0$  there exist  $C \in \mathbf{B}_b(X)$  with  $\text{diam } C \leq \nu$  and  $\tau > 0$  such that

$$\liminf_{n \rightarrow \infty} P^n \tilde{\sim}(C) > \tau \text{ for } \tilde{\sim} \in M_1. \tag{6.11}$$

**6.2. Existence of Stationary Distributions**

The proof of existence of a stationary density usually goes as follows: Let  $X$  be a compact space. We construct an invariant operator  $U$  on  $C(X)$  and then using the Riesz representation theorem we define an invariant measure. In our case the proof is more difficult, since a positive functional may not correspond to a measure. Thus we start with the following.

**Lemma 6.2.1. [46]** Let  $P$  be a Feller operator. Assume that there exists a linear positive functional  $\{ :C(X) \rightarrow \mathbf{R}$  such that  $\{ (1_X) = 1_X$  and

$$\{ (U(h)) = \{ (h) \text{ for } h \in C_0(X) \tag{6.11}$$

where  $U$  is dual to  $P$ . Further let  $\sim_* \in M$  be the unique (Riesz theorem) measure satisfying  $\{ (h) = \langle h, \sim_* \rangle$  for  $h \in C_0(X)$ . Then  $\sim_* \in M$  and  $P\sim_* = \sim_*$ .

**Proof:** From the inequality

$$\{ (h) = \langle h, \sim_* \rangle \text{ for } 0 \leq h \leq 1$$

immediately follows that  $\{ (X) \leq 1$ . Thus  $\sim_* \in M$  and we may define a new functional  $\{_*$  on  $C(X)$  setting

$$\langle h, \sim_* \rangle = \{ (h) \leq \{ (1_X) = 1 \text{ for } h \in C(X).$$

We claim the  $\{_*(h) = \{ (h)$  for  $h \geq 0$ . In fact let  $h \in C(X)$ ,  $h \geq 0$  be fixed. Using the Tietze extension theorem we may construct an increasing sequence of nonnegative functions  $h_n \in C_0$  such that  $h_n(x) \rightarrow h(x)$  for  $x \in X$ . Since  $\{$  is positive we have

$$\{_*(h_n) = \{ (h_n) \leq \{ (h) \text{ or } \langle h_n, \sim_* \rangle \leq \{ (h).$$

By the Lebesgue monotone convergence theorem this yields  $\langle h, \sim_* \rangle \leq \{ (h)$  and completes the proof of the claim. Now according to (6.11) we have

$$\{_*(U(h)) \leq \{ (U(h)) = \{ (h) = \{_*(h) \text{ for } h \in C_0, h \geq 0$$

which in turn implies

$$\langle h, P\sim_* \rangle = \langle Uh, \sim_* \rangle = \{_*(U(h)) \leq \{_*(h) = \langle h, \sim_* \rangle$$

Consequently,

$$P\sim_* \leq \sim_*.$$

Since  $P$  preserves the measure the last inequality is equivalent to  $P\sim_* = \sim_*$ .

This completes the proof. □

### 6.3. A Criterion of Asymptotic Stability

**Lemma 6.3.1. [46]** A non-expansive Markov operator is a Feller operator.

**Proof:** We know

$$Uf(x) = \langle Uf, u_x \rangle = \langle f, Pu_x \rangle \text{ for } f \in C_0,$$

where  $u_x \in M_1$  is a point (Dirac) measure supported at  $x$ .

Now

$$|Uf(x)| = |\langle f, Pu_x \rangle| \leq \sup |f|.$$

Clearly,  $Uf$  is bounded.

Further if  $f \in C_0$  is Lipschitzian with Lipschitz constant  $k_f$  then

$$|Uf(x) - Uf(y)| = |\langle f, Pu_x - Pu_y \rangle| \leq e_f \|Pu_x - Pu_y\| \leq e_f \|u_x - u_y\| \leq e_f \dots(x, y).$$

where  $e_f = \max(k_f, \sup |f|)$ . Thus for Lipschitzian the function is continuous. For an arbitrary  $f \in C_0$  we choose a sequence of Lipschitzian functions  $f_n \in C_0$  which

converges uniformly to  $f$ . (Using the Stone Weierstrass theorem it is easy to verify that the Lipschitz functions are dense in  $C_0$ ). From the inequality

$$|Uf(x) - Uf_n(x)| = |\langle f - f_n, P u_x \rangle| \leq \sup |f_n - f|$$

it follows that  $Uf$  is continuous as the uniform limit of the sequence of continuous function  $Uf_n$ . Thus we have verified that  $Uf \in C(X)$ . According to the definition of  $U$  we have

$$\langle Uf, \sim \rangle = \langle f, P \sim \rangle$$

for  $f \in C_0$  and  $\sim = u_x$ . Since linear combinations of point measures are dense in  $M_{fin}$  (with the Fortet Mourier norm). The above equation holds for every  $\sim \in M_{fin}$ .

This completes the proof.  $\square$

**Theorem 6.3.2. [46]** Let  $P$  be a non-expansive Markov operator. Assume that for every  $v > 0$  there is a Borel set  $A$  with  $diam A \leq v$ , a real number  $r > 0$  and an integer  $n$  such that

$$\liminf_{n \rightarrow \infty} P^n \sim(A) \geq r \text{ for } \sim \in M_1. \tag{6.12}$$

Then  $P$  is asymptotically stable.

**Proof:** Since a non-expansive Markov operator is a Feller operator,  $P$  is a Feller operator. Then  $P$  has an invariant distribution  $\sim_*$ . To complete the proof of asymptotic stability it remains to verify condition

$$\lim_{n \rightarrow \infty} \langle f, \sim_n \rangle = \langle f, \sim \rangle \text{ for all } f \in C(X).$$

When an invariant distribution exists the above condition is equivalent to a more symmetric relation

$$\lim_{n \rightarrow \infty} \|P^n(\sim_1 - \sim_2)\| = 0 \text{ for } \sim_1, \sim_2 \in M_1. \tag{6.13}$$

Let  $\sim_1, \sim_2 \in M_1$  and  $v > 0$ . Choose  $A \subset X$  and  $r, 0 < r < 1$  according to (6.12) and fix a number  $\dagger \in (0, r)$ . We will define by an induction argument a sequences of integers  $(n_k)$  and four sequences of distributions  $(\sim_i^k), (\epsilon_i^k), k = 0, 1, 2, \dots, i = 1, 2$ . If  $k = 0$  we define  $n_0 = 0$  and  $\epsilon_i^0 = \sim_i^0 = \sim_i$ . If  $k \geq 1$  is fixed and  $n_{k-1}, \sim_i^{k-1}, \epsilon_i^{k-1}$  are given we choose according (6.12) a number  $n_k$  such that

$$P^{n_k} \sim_i^{k-1}(A) \geq \dagger \text{ for } i = 1, 2.$$

and we define

$$\begin{aligned} \epsilon_i^k(B) &= \frac{P^{n_k} \sim_i^{k-1}(B \cap A)}{P^{n_k} \sim_i^{k-1}(A)} \\ \sim_i^k(B) &= \frac{1}{1-r} \{P^{n_k} \sim_i^{k-1}(B) - r \epsilon_i^{k-1}(B)\}. \end{aligned} \tag{6.14}$$

Since  $P^{n_k} \sim_i^{k-1}(A) \geq \dagger$ , we have

$$P^{nk} \sim_i^{k-1}(B) = P^{nk} \sim_i^{k-1}(B \cap A) = P^{nk} \sim_i^{k-1}(A) \epsilon_i^k(B) \geq r \epsilon_i^k(B).$$

Observe that  $\epsilon_i^k(X \setminus A) = 0$  and consequently

$$\|\epsilon_1^k - \epsilon_2^k\| = \sup_{f \in F} \left| \int_X f d\epsilon_1^k - \int_X f d\epsilon_2^k \right| = \sup_{f \in F} \left| \int_A f d\epsilon_1^k - \int_A f d\epsilon_2^k \right| \leq \text{diam } A \leq v. \tag{6.15}$$

Using equation (6.14) it is easy to verify by an induction argument that

$$P^{n_1+\dots+n_k} \sim_i = \dagger P^{n_1+\dots+n_k} \epsilon_i^1 + \dagger(1-\dagger) P^{n_1+\dots+n_k} \epsilon_i^2 + \dots + \dagger(1-\dagger)^{k-1} \epsilon_i^k + (1-\dagger)^k \sim_i^k, k \geq 1.$$

Since  $P$  is non-expansive this implies

$$\begin{aligned} \|P^{n_1+\dots+n_k}(\sim_1 - \sim_2)\| &\leq \dagger \|\epsilon_1^1 - \epsilon_2^1\| + \dagger(1-\dagger) \|\epsilon_1^2 - \epsilon_2^2\| \\ &\quad + \dots + \dagger(1-\dagger)^{k-1} \|\epsilon_1^k - \epsilon_2^k\| + (1-\dagger)^k \|\sim_1^k - \sim_2^k\|. \end{aligned}$$

From this, condition (6.15) and the obvious inequality  $\|\sim_1^k - \sim_2^k\| \leq 2$  it follows

$$\|P^{n_1+\dots+n_k}(\sim_1 - \sim_2)\| \leq v + 2(1-\dagger)^k$$

Again, using the non-expansiveness of  $P^n$  we obtain

$$\|P^n(\sim_1 - \sim_2)\| \leq v + 2(1-\dagger)^n \text{ for } n \geq n_1 + \dots + n_k.$$

Since  $v > 0$  and  $k > 0$  are arbitrary, this implies (6.13).

This completes the proof. □

### 6.4. Sweeping Properties Associated to Iterated Function System of the Generalized Cantor Sets (IFSGCS)

**6.4.1.** By equation (6.1) we may define the operator  $P$  associated to IFS of the Cantor middle  $\frac{1}{3}$  set as follows:

$$Pf(x) = \begin{cases} \frac{3}{2}f(3x), & \text{for } 0 \leq x \leq 1/3 \\ 0, & \text{for } 1/3 \leq x \leq 2/3 \\ \frac{3}{2}f(3x-2), & \text{for } 2/3 \leq x \leq 1 \end{cases}$$

It is easy to verify that

$$P^n f(x) = 0 \text{ for } v_n \leq x \leq 1 - v_n \text{ and } \int_0^{v_n} P^n f(x) dx = \int_0^{v_n} \frac{3^{2n}}{2^{n-1}} x dx = \frac{1}{2^n},$$

$$\int_{1-v_n}^1 P^n f(x) dx = \int_0^{v_n} \frac{3^{2n}}{2^{n-1}} x - \frac{3^{2n} - 3^n}{2^{n-1}} dx = \frac{1}{2^n}, \text{ where } v_n = 3^{-n}.$$

$$\therefore \lim_{n \rightarrow \infty} \int_X P^n f(x) dx = \lim_{n \rightarrow \infty} \left( \frac{1}{2^n} + \frac{1}{2^n} \right) = 0.$$

Thus  $P$  is sweeping as an operator on  $L_1(0,1)$  and  $\frac{1}{2^n}$ -sweeping on  $L_1[0,1)$ .

However,  $P$  is neither sweeping nor Cesaro-sweeping on  $L_1[0,1)$ .

**6.4.2.** By equation (6.1), we may define the operator  $P$  associated to IFS of the Cantor middle  $\frac{1}{5}$  set as follows:

$$Pf(x) = \begin{cases} \frac{5}{3}f(5x), & \text{for } 0 \leq x \leq 1/5 \\ 0, & \text{for } 1/5 \leq x \leq 2/5 \\ \frac{5}{3}f(5x-2), & \text{for } 2/5 \leq x \leq 3/5 \\ 0, & \text{for } 3/5 \leq x \leq 4/5 \\ \frac{5}{3}f(5x-4), & \text{for } 4/5 \leq x \leq 1 \end{cases}$$

It is easy to verify that,  $P^n f(x) = 0$  for  $v_n \leq x \leq 1-3v_n, 1-2v_n \leq x \leq 1-v_n$

and

$$\int_0^{v_n} P^n f(x) dx = \int_0^{v_n} \frac{2 \cdot 5^{2n}}{3^{n-1}} x dx = \frac{1}{3^n}, \quad \int_{1-3v_n}^{1-2v_n} P^n f(x) dx = \int_{1-3v_n}^{1-2v_n} \left( \frac{2 \cdot 5^{2n}}{3^n} x - \frac{(5^{2n} - 5^n)}{3^n} \right) dx = \frac{1}{3^n},$$

$$\int_{1-v_n}^1 P^n f(x) dx = \int_{1-v_n}^1 \left( \frac{2 \cdot 5^{2n}}{3^n} x - \frac{2 * (5^{2n} - 5^n)}{3^n} \right) dx = \frac{1}{3^n}, \text{ where } v_n = 5^{-n}.$$

$$\therefore \lim_{n \rightarrow \infty} \int_X P^n f(x) dx = \lim_{n \rightarrow \infty} \left( \frac{1}{3^n} + \frac{1}{3^n} + \frac{1}{3^n} \right) = 0.$$

Thus  $P$  is sweeping as an operator on  $L_1(0,1)$  and  $\frac{1}{3^n}$ -sweeping on  $L_1[0,1)$ .

However,  $P$  is neither sweeping nor Cesaro-sweeping on  $L_1[0,1)$ .

**6.4.3.** By equation (6.1), we may define the operator  $P$  associated to IFS of the Cantor middle  $\frac{1}{2m-1}$ , ( $2 \leq m < \infty$ ) set as follows:

$$Pf(x) = \begin{cases} \frac{2m-1}{m} f((2m-1)x), & \text{for } 0 \leq x \leq 1/(2m-1) \\ 0, & \text{for } 1/(2m-1) \leq x \leq 2/(2m-1) \\ \frac{2m-1}{m} f((2m-1)x-2), & \text{for } 2/(2m-1) \leq x \leq 3/(2m-1) \\ 0, & \text{for } 3/(2m-1) \leq x \leq 4/(2m-1) \\ \frac{2m-1}{m} f((2m-1)x-4), & \text{for } 4/(2m-1) \leq x \leq 5/(2m-1) \\ 0, & \text{for } 5/(2m-1) \leq x \leq 6/(2m-1) \\ \vdots \\ \frac{2m-1}{m} f((2m-1)x-(2m-2)), & \text{for } (2m-2)/(2m-1) \leq x \leq 1 \end{cases}$$

It is easy to verify that

$$P^n f(x) = 0 \text{ for } v_n \leq x \leq 1 - ((2m-1) - 2)v_n,$$

$$1 - ((2m-1) - 3)v_n \leq x \leq 1 - ((2m-1) - 4)v_n, \dots, 1 - 2v_n \leq x \leq 1 - v_n$$

$$\text{and } \int_0^{v_n} P^n f(x) dx = \int_{1 - ((2m-1) - 2)v_n}^{1 - ((2m-1) - 3)v_n} P^n f(x) dx = \dots = \int_{1 - v_n}^1 P^n f(x) dx = \frac{1}{m^n}, \text{ where } v_n = m^{-n}$$

$$\therefore \lim_{n \rightarrow \infty} \int_X P^n f(x) dx = \lim_{n \rightarrow \infty} \left( \frac{1}{m^n} + \frac{1}{m^n} + \dots + \frac{1}{m^n} \right) = 0.$$

Thus  $P$  is sweeping as an operator on  $L_1(0,1)$  and  $\frac{1}{m^n}$ -sweeping on  $L_1[0,1)$ .

However,  $P$  is neither sweeping nor Cesaro-sweeping on  $L_1[0,1)$ .

# CHAPTER SEVEN

## HAUSDORFF MEASURES OF FRACTALS

### OVERVIEW

In this chapter, we discuss basic measure theory, Hausdorff measure and Hausdorff dimension. We show the Hausdorff measures and dimensions of the invariant set for iterated function system of the Generalized Cantor sets and also we show the Hausdorff measures and dimensions of the invariant set for iterated function system of the two and three dimensional fractals.

### 7.1. [47] Basic Measure Theory on Euclidean Space

We say  $\sim$  is a measure on elements in the  $\dagger$ -algebra of subsets of  $X$  if satisfies the following three properties:

- (1)  $\sim(W) = 0$ ;
- (2)  $\sim(A) \leq \sim(B)$  if  $A \subseteq B$  and  $A, B \in \dagger$ -algebra;
- (3) If  $A_1, A_2, \dots$  is a countable sequence of sets, then

$$\sim\left(\bigcup_{i=1}^{\infty} A_i\right) \leq \sum_{i=1}^{\infty} \sim(A_i)$$

and

$$\sim\left(\bigcup_{i=1}^{\infty} A_i\right) = \sum_{i=1}^{\infty} \sim(A_i)$$

if  $A_i$  are disjoint Borel sets.

Furthermore, we say  $\sim$  is a probability measure if  $\sim(X) = 1$ . For the purpose of this chapter, we will always consider  $X \subseteq \mathbf{R}^n$ .

### 7.2. [47] Hausdorff Measure and Hausdorff Dimension

#### 7.2.1. Hausdorff Measure

If  $U$  is any non-empty subset of  $n$ -dimensional Euclidean space  $\mathbf{R}^n$ , the diameter of  $U$  is defined as  $|U| := \sup\{|x - y| : x, y \in U\}$ . Here we will use the Euclidean metric:  $|x - y| := ((x_1 - y_1)^2 + (x_2 - y_2)^2 + \dots + (x_n - y_n)^2)^{1/2}$ . However, as will be shown shortly, we may use any  $L_p$  metric. If  $E \subseteq \mathbf{R}^n$ , and a collection  $\{U_i\}_{i \in I}$  satisfies the following conditions:

- (1)  $|U_i| \leq u$  for each  $i \in I$ ;
- (2)  $E \subseteq \bigcup_{i \in I} U_i$ ,

then we say the collection is a  $u$ -cover of  $E$ . We may assume the collection is always countable.

**Definition 7.2.1.1. [26]** Let  $E \in \mathbf{R}^n$  be a borel set with  $\{U_i\}_{i \in I}$  a  $u$ -cover for it. Given any  $s > 0$ , we define the  $u$ -approximating  $s$ -dimensional Hausdorff measure  $H_u^s : \mathbf{R}^n \rightarrow \mathbf{R}$  by the following

$$H_u^s(E) = \inf \left\{ \sum_{i=1}^{\infty} |U_i|^s : \{U_i\}_{i \in I} \text{ forms a } u\text{-cover for } E \right\}$$

If  $u \rightarrow 0$ , then we have a more succinct formula

$$H^s(E) = \lim_{u \rightarrow 0} (H_u^s(E))$$

giving the  $s$ -dimensional Hausdorff measure of  $E$ .

This takes, for any  $s \in \mathbf{R}$ , a unique value between zero and infinity inclusive. It also forms a measure on  $\mathbf{R}^n$ . This measure is a rough analogue of Lebesgue measure for non-negative, real values of dimension:

$$H^0(E) = \text{cardinality of } E.$$

$$H^1(E) = \text{length of } E \text{ if } E \text{ is a curve.}$$

$$H^2(E) = \frac{4}{f} \cdot \text{area of } E \text{ if } E \text{ is a surface.}$$

$$H^3(E) = \frac{6}{f} \cdot \text{volume of } E \text{ if } E \text{ is a 3-space.}$$

It should be noted that Hausdorff measure can measure sets of non-integer dimension, and that the  $n$ -dimensional measure on a set of  $m$ -dimensions (assuming  $m \neq n$ ) will not give the meaningful result.

### 7.2.1.2. Some Properties of Hausdorff Measure

**Theorem 7.2.1.2.1. [48]** (Outer Measure) The following are true for any metric space

- (i) (Null Empty set)  $H^s(W) = 0$ .
- (ii) (Monotonicity) If  $E \subseteq F$ , then  $H^s(E) \leq H^s(F)$ .
- (iii) (Countable Subadditivity)  $H^s\left(\bigcup_{i=1}^{\infty} E_i\right) \leq \sum_{i=1}^{\infty} H^s(E_i)$ .

**Proof:** (i) and (ii) follow directly from the definition.

(iii) Assume that  $H^s(E_i)$  is finite for all  $i \in I$ ; otherwise, it is trivial. Then it follows that  $H_u^s(E_i)$  is also finite for all  $i \in I$  and any  $u > 0$ . It suffices to show that  $H_u^s\left(\bigcup_{i=1}^{\infty} E_i\right) \leq \sum_{i=1}^{\infty} H_u^s(E_i)$  for all  $u > 0$ . Let  $v > 0$ . Then, for any  $i$ , there exists a countable  $u$ -cover  $\{U_{i,j}\}_{j=1}^{\infty}$  of  $E_i$  such that

$$\sum_{j=1}^{\infty} |U_{i,j}|^s < H_u^s(E_i) + \frac{v}{2^i}.$$

Since  $\{U_{i,j}\}_{j=1}^{\infty} \bigcup_{i=1}^{\infty}$  is countable  $u$ -cover of  $\bigcup_{i=1}^{\infty} E_i$ , we have



$$H_u^s(\bigcup_{i=1}^{\infty} E_i) \leq \sum_{i=1}^{\infty} \sum_{j=1}^{\infty} |U_{i,j}|^s < \sum_{i=1}^{\infty} (H_u^s(E_i) + \frac{v}{2^i}) = \sum_{i=1}^{\infty} (H_u^s(E_i) + v).$$

By taking  $u \rightarrow 0$ , the result follows. □

**Theorem 7.2.1.2.2. [48]** (Countable Additivity) Let  $\{E_i\}_{i=1}^{\infty}$  be a countable collection of disjoint  $H^s$ -measurable subsets of  $X$ . Then we have

$$H^s(\bigcup_{i=1}^{\infty} E_i) = \sum_{i=1}^{\infty} H^s(E_i).$$

**Proof:** If  $E_1$  and  $E_2$  are disjoint  $H^s$ -measurable set, then it follows by definition that

$$H^s(E_1 \cup E_2) = H^s((E_1 \cup E_2) \cap E_1) + H^s((E_1 \cup E_2) \cap E_1^c) = H^s(E_1) + H^s(E_2).$$

By induction based on this idea, we see that  $H^s(\bigcup_{i=1}^k E_i) = \sum_{i=1}^k H^s(E_i)$  for all  $k \in I$ . Since, for

any  $k \in I$ , we have  $\bigcup_{i=1}^k E_i \subseteq \bigcup_{i=1}^{\infty} E_i$ , we obtain the inequality

$$H^s(\bigcup_{i=1}^{\infty} E_i) \geq H^s(\bigcup_{i=1}^k E_i) = \sum_{i=1}^k H^s(E_i).$$

Letting  $k \rightarrow \infty$ , we have

$$H^s(\bigcup_{i=1}^{\infty} E_i) \geq \sum_{i=1}^{\infty} H^s(E_i).$$

Moreover, the converge of this inequality follows directly from the countable subadditivity property.

Hence the equality holds, as required. □

**Theorem 7.2.1.2.3. [48]** (Hausdorff and Lebesgue Measure) Let be a Borel subset of  $\mathbf{R}^n$ . Then

$$H^s(E) = \frac{1}{\tilde{S}_n} \cdot |E|,$$

where  $\tilde{S}_n$  is the volume of an  $n$ -dimensional ball of diameter 1, and where  $|E|$  denotes the Lebesgue measure of  $E$ .

**Proof:** It is easy to show that any Lebesgue null set of  $\mathbf{R}^n$  has  $n$ -dimensional Hausdorff measure zero, since it may be covered by balls of arbitrary small total content. Then  $n$ -dimensional Hausdorff measure is absolutely continuous with respect to Lebesgue measure, so  $\frac{d}{d|\cdot|}(H^n) = c$  for some locally integrable function  $c$ . As Hausdorff measure

and Lebesgue measure are translation-invariant,  $c$  must also be translation-invariant and thus constant. Therefore,  $H^n(E) = c|E|$  for some  $c \geq 0$ . To calculate the constant  $c$ , we

compute the Hausdorff measure and Lebesgue measure of an  $n$ -dimensional ball of diameter 1, and this gives  $c = \frac{1}{S_n}$ , as required.  $\square$

**Theorem 7.2.1.2.4. [26]** (Scaling Property). Let  $S : \mathbf{R}^n \rightarrow \mathbf{R}^n$  be a similarity mapping, and any  $\lambda > 0$  such that  $|S(x) - S(y)| \leq \lambda |x - y|$  for any  $x, y \in \mathbf{R}^n$ , where  $\lambda$  is the scaling factor. If  $E \in \mathbf{R}^n$ , then  $H^s(S(E)) = \lambda^s H^s(E)$  is a scaling length, area etc.

**Proof:** Let  $\{U_i\}_{i=1}^\infty$  be a  $u$ -cover of  $E$ . Then  $\{S(U_i)\}_{i=1}^\infty$  is a  $\lambda u$ -cover of  $S(E)$ . Thus we see that, given  $s > 0$ :

$$H_{\lambda u}^s(S(E)) = \inf \left\{ \sum_{i=1}^\infty |S(U_i)|^s : \{U_i\}_{i=1}^\infty \text{ forms a } u\text{-cover} \right\}$$

Here 
$$\sum_{i=1}^\infty |S(U_i)|^s \leq \sum_{i=1}^\infty |\lambda U_i|^s = \lambda^s \sum_{i=1}^\infty |U_i|^s$$

We obtain

$$H_{\lambda u}^s(S(E)) \leq \lambda^s H_u^s(E).$$

So, letting  $u \rightarrow 0$  gives that

$$H^s(S(E)) \leq \lambda^s H^s(E).$$

Replacing  $\lambda$  by  $\frac{1}{\lambda}$  and  $E$  by  $S(E)$  gives the opposite inequality, as required.  $\square$

### 7.2.2. [26] Hausdorff Dimension

Let  $E$  be a given set. Note that  $H_u^s(E)$  decreases as  $s$  increases. This means that  $H^s(E)$  also decreases with  $s$  increasing. If  $t > s$  and  $\{U_i\}$  is a  $u$ -cover of  $E$ , then each  $|U_i|^{t-s} \leq u^{t-s}$  since  $|U_i| \leq u$ , so

$$\sum_{i=1}^\infty |U_i|^t = \sum_{i=1}^\infty (|U_i|^{t-s} |U_i|^s) \leq \sum_{i=1}^\infty (u^{t-s} |U_i|^s) \leq u^{t-s} \sum_{i=1}^\infty |U_i|^s.$$

After taking the infima over all  $u$ -covers, we can easily see that

$$H_u^t(E) \leq u^{t-s} H_u^s(E) \tag{7.1}$$

Let  $u \rightarrow 0$ . Then  $H_u^t(E) \rightarrow 0$  if  $H^s(E)$  is finite. Also if  $H_u^t$  is bounded and finite then  $H_u^s(E) \rightarrow \infty$ .

**Two applications of equation (7.1) should be noted:**

**1. If  $H^s(E) < \infty$  and  $t > s$ , then  $H^t(E) = 0$ .**

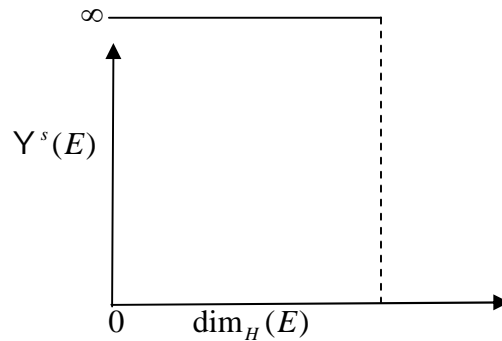
**Proof:** Equation (7.1) shows that  $H_u^t(E) \leq u^{t-s} H_u^s(E)$  for any positive  $u$ . The result follows after taking limits, since  $H^s(E) < \infty$ .  $\square$

**2. If  $H^s(E) > 0$  and  $t < s$ , then  $H^t(E) = \infty$ .**

**Proof:** Equation (7.1) shows that  $\frac{1}{u^{t-s}} H_u^t(E) \leq H_u^s(E)$  for any positive  $u$ . After taking limits, we see that  $H^t(E) = \infty$ , since  $\lim_{u \rightarrow 0} \frac{1}{u^{t-s}} = \infty$  and  $\lim_{u \rightarrow 0} H_u^s(E) = H^s(E) > 0$ .  $\square$

One immediate consequence of these observation is that  $H^s(E) = 0$  or  $\infty$  everywhere except at a unique value  $s$ , where this value may be finite. As a function of  $s$ ,  $H^s(E)$  is decreasing function. Therefore, the graph of  $H^s(E)$  will have a unique value where it jumps from infinity to zero. Thus, if we define the Hausdorff dimension of a set  $E$  as  $\dim_H(E) = \sup\{s : H^s(E) = \infty\} = \inf\{s : H^s(E) = 0\}$ , the graph of  $H^s(E)$  looks like

$$H^s(E) = \begin{cases} \infty & \text{if } s < \dim_H(E) \\ 0 & \text{if } s > \dim_H(E) \\ \text{finite, nonzero number} & \text{if } s = \dim_H(E) \end{cases}$$



We can see by the graph above, that for any set  $E$  and some non-negative real  $s$ , if  $s < \dim_H(E)$  then  $H^s(E) = \infty$ , and if  $s > \dim_H(E)$  then  $H^s(E) = 0$ .

As an example, we can see that the length of a square is infinite, it has a finite area and it has no volume, that is,  $H^3(E) = 0$  (volume),  $H^1(E) = \infty$  (length),  $H^2(E) = \frac{4}{f}$  · area of disc (positive and finite)

### 7.2.2.1. Some Properties of Hausdorff Dimension

**Theorem 7.2.2.1.1. [48]** The Hausdorff dimension for sets in  $\mathbf{R}^n$  satisfies the following properties:

- (i) If  $E \subseteq F$ , then  $\dim_H E \leq \dim_H F$ .
- (ii)  $\dim_H E \leq n$ .
- (iii) If  $|E| > 0$ , then  $\dim_H E = n$ .
- (iv) If  $E$  is countable, then  $\dim_H E = 0$ .
- (v) If  $\dim_H E < n$ , then  $|E| = 0$ ,

(vi) If  $E$  is open in  $\mathbf{R}^n$ , then  $\dim_H E = n$ .

(vii)  $\dim_H \left(\bigcup_{i=1}^{\infty} E_i\right) = \sup\{\dim_H E_i : i \in I\}$

Note that  $|E|$  is the Lebesgue measure of  $E$ .

**Proof:** (i) If  $E \subseteq F$ , then  $H^s(E) \leq H^s(F)$  for  $s \geq 0$ , which implies  $\dim_H E \leq \dim_H F$ .

(ii), (iii), (iv) and (v) can be deduced from the relationship between Hausdorff measure and Lebesgue measure in Theorem 7.2.1.1.3.

(vi) If  $E$  is open, then it contains a ball of positive  $n$ -dimensional volume.

(vii) By the monotonicity property,  $\dim_H \left(\bigcup_{i=1}^{\infty} E_i\right) \geq \dim_H E_i$  for each  $i$ . On the other hand,

if  $s > \dim_H E_i$  for all  $i$ , then  $H^s(E_i) = 0$ , and therefore  $H^s \left(\bigcup_{i=1}^{\infty} E_i\right) = 0$ , giving the opposite inequality. □

**Theorem 7.2.2.1.2. [26]** Let  $E \subseteq \mathbf{R}^n$  and  $f : E \rightarrow \mathbf{R}^n$  be Lipschitz, that is,  $|f(x) - f(y)| \leq c|x - y|$ , then  $H^s(f(E)) \leq c^s H^s(E)$ .

**Proof:** Let  $\{U_i\}$  be a  $u$ -cover of  $E$ , so  $\{E \cap U_i\}$  is a  $u$ -cover of  $E$ . Then

$$|f(E \cap U_i)| \leq c|E \cap U_i| \leq c|U_i| \leq cu$$

Thus  $\{f(E \cap U_i)\}$  is a  $cu$ -cover of  $f(E)$  with  $\sum_{i=1}^{\infty} |f(E \cap U_i)|^s \leq c^s \sum_{i=1}^{\infty} |U_i|^s$ .

Taking infima we have

$$H_{cu}^s(f(E)) \leq c^s H_u^s(E).$$

So, letting  $u \rightarrow 0$  then

$$H^s(f(E)) \leq c^s H^s(E). \quad \square$$

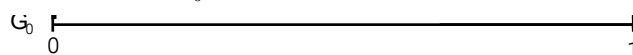
**Theorem 7.2.2.1.3.** Let (Hausdorff Dimension Theorem). For any real  $r \geq 0$  and integer  $n \geq r$ , there is a continuum fractals with Hausdorff dimension  $r$  in  $\mathbf{R}^n$ .

**Proof:** The proof can be found in [49].

### 7.2.2.2. Hausdorff Dimension of the Cantor middle $\frac{1}{3}$ set

The construction of the Cantor middle third set is as follows:

We start with the closed interval  $\Gamma_0 = [0, 1]$ .



Remove the middle open third. This leaves a new set  $\Gamma_1 = [0, \frac{1}{3}] \cup [\frac{2}{3}, 1]$ .



Each iteration through the algorithm removes the open middle third from each segment of the previous iteration. Thus the next set would be

$$\Gamma_2 = [0, \frac{1}{9}] \cup [\frac{2}{9}, \frac{1}{3}] \cup [\frac{2}{3}, \frac{7}{9}] \cup [\frac{8}{9}, 1].$$

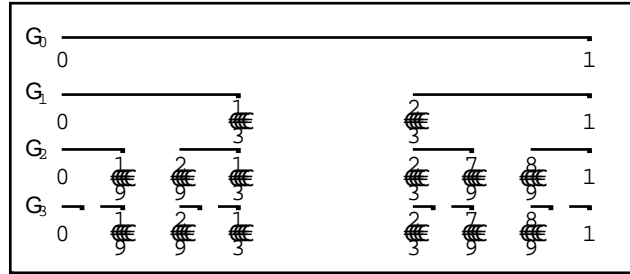


**Figure 7.1** Construction of the Cantor middle  $\frac{1}{3}$  set

In general, after  $n$  times iterations, we obtain  $\Gamma_n$  which as follows

$$\Gamma_n = [0, \frac{1}{3^n}] \cup [\frac{2}{3^n}, \frac{3}{3^n}] \cup \dots \cup [\frac{3^n - 3}{3^n}, \frac{3^n - 2}{3^n}] \cup [\frac{3^n - 1}{3^n}, 1], \text{ where } n \geq 1.$$

Therefore, we construct a decreasing sequence  $(\Gamma_n)$  of closed sets, that is  $\Gamma_{n+1} \subseteq \Gamma_n$  for all  $n \in \mathbf{N}$ , so that every  $\Gamma_n$  consists of  $2^n$  closed intervals all of which the same length  $\frac{1}{3^n}$ .

The Cantor ternary set, which we denote  $C_{1/3}$ , is the “limiting set” of this process, that is,

$$C_{1/3} = \bigcap_{n=1}^{\infty} \Gamma_n \text{ and call it the Cantor middle } \frac{1}{3} \text{ set.}$$

Following David C seal [47]. Since  $\Gamma_{n+1} \subset \Gamma_n$  for each  $n \in \mathbf{N}$ , and since each  $\Gamma_n$  is compact, we know that  $C_{1/(2^{m-1})}$  is non-empty. For example, a little observation will reveal that the set  $\{0, \frac{1}{3}, \frac{1}{9}, \frac{1}{27}, \dots\} \subset C_{1/3}$ . In fact, without proof we can say:  $|C_{1/3}| = |\mathbf{R}|$ . Take

$\{E_i\}$  to be a closed cover, where  $\bigcup_{i=1}^{2^n} E_i = \Gamma_n$  and  $|E_i| = 3^{-n}$  is the  $i^{\text{th}}$  interval of  $\Gamma_n$ .

It follows that

$$\sum_{i=1}^{2^n} |E_i|^s = \sum_{i=1}^{2^n} (3^{-n})^s = 2^n 3^{-ns}.$$

When  $s = \log_3 2$  the above equation becomes

$$2^n 3^{-ns} = 2^n 3^{-n \log_3 2} = 2^n 3^{\log_3 2^{-n}} = 2^n 2^{-n} = 1.$$

We can conclude that  $\dim_H(C_{1/3}) \leq \log_3(2)$ , since for every  $u > 0$ , this cover can become arbitrarily small. That is,  $H_u^s(C_{1/3}) \leq 1$  for each  $u > 0$ . To show that  $\log_3(2)$  is indeed the Hausdorff Dimension of  $C_{1/3}$ , we will need the following Lemma.

**Lemma 7.2.2.1. (Frostman's Lemma).** Suppose  $F$  is a measurable subset of and suppose  $\mu$  a probability measure on  $F$  such that

$$\lim_{r \rightarrow 0} \sup_{x \in F} \frac{\mu(B_r(x))}{r^s} \leq a.$$

Then,  $H^s(F) \geq \frac{1}{a \cdot 2^n}$ . (In particular,  $\dim_H(F) \geq s$ .)

**Proof:** The proof can be found in [47]

To show that  $\dim_H(C_{1/3}) = \log_3(2)$  it suffices to prove that  $\dim_H(C_{1/3}) \geq \log_3(2)$ . If we take the base-3 expansions for all real numbers  $x \in [0,1]$ , we can write  $x = \sum_{i=1}^{\infty} 3^{-i} x_i$  where each  $x_i \in \{0,1,2\}$ . If we consider

$$C^*_{1/3} := \left\{ \sum_{i=1}^{\infty} 3^{-i} x_i : x_i \in \{0,2\} \right\},$$

then we obtain a subset of  $C_{1/3}$ , and the set difference  $C_{1/3} \setminus C^*_{1/3} = \{x \in C_{1/3} : x \notin C^*_{1/3}\}$  is a countable set. Consider a sequence of independent identically distributed random variables  $\{X_i\}_{i=1}^{\infty}$ , where  $P\{X_1 = 2\} = P\{X_1 = 0\} = \frac{1}{2}$ .

For a fixed  $n$ , and by independence, we have

$$P\{X_1 = x_1, X_2 = x_2, \dots, X_n = x_n\} = P\{X_1 = x_1\} P\{X_2 = x_2\} \cdots P\{X_n = x_n\} = 2^{-n} \quad \text{if}$$

$x_i \in \{0,2\}$ . If we set  $X = \sum_{i=1}^{\infty} 3^{-i} X_i$ , we can define a probability measure  $\mu$  on  $C^*_{1/3}$  by

$$\mu(A) = P\{X \in A\} \text{ for measurable subsets } A \subseteq [0,1].$$

For a fixed  $x \in C^*_{1/3}$ , if  $y \in B_{3^{-n}}(x)$  then  $y_1 = x_1, \dots, y_n = x_n$  this implies that  $\mu(B_{3^{-n}}(x)) \leq 2^{-n} = 3^{-ns}$ , where  $s = \log_3 2$ . To finish the estimate, let  $1 > \nu > 0$ . There exists an  $n \in \mathbf{N}$ ,  $3^{-(n+1)} \leq \nu \leq 3^{-n}$ .

In particular,  $3^{-n} 3^{-1} \leq \nu$  this implies that  $3^{-n} \leq 3\nu$ .

also  $\mu(B_{\nu}(x)) \leq \mu(B_{3^{-n}}(x))$ , since  $B_{\nu}(x) \subseteq B_{3^{-n}}(x)$ .

Now

$$\mu(B_{\nu}(x)) \leq \mu(B_{3^{-n}}(x)) \leq 3^{-ns} \leq 3^s \nu^s = 2\nu^s.$$

Then this probability measure immediately satisfies

$$\sup_{x \in F} \mu(B_{\nu}(x)) \leq 2\nu^s$$

Appealing to Frostman's Lemma, we have  $\dim_H(C_{1/3}) \geq \log_3(2)$ . Another interesting variation of the Cantor middle set allows for a different size to be removed in each step of the construction of  $C_{1/3}$ . □

**Alternative Method:****7.2.2.2.2. Heuristic Method for Finding Hausdorff Dimensions of the Generalized Cantor Sets**

Let  $C_{1/3}$  be the Cantor middle  $\frac{1}{3}$  set. Let  $C_{1/3} = (C_{1/3})_L \cup (C_{1/3})_R$  with the union disjoint

$(C_{1/3})_L = C_{1/3} \cap [0, \frac{1}{3}]$  and  $(C_{1/3})_R = C_{1/3} \cap [\frac{2}{3}, 1]$ . Then

$H^s(C_{1/3}) = H^s((C_{1/3})_L) + H^s((C_{1/3})_R)$  (assuming  $0 < H^s(C_{1/3}) < \infty$  when  $s = \dim_H F$ )

$$= \left(\frac{1}{3}\right)^s H^s(C_{1/3}) + \left(\frac{1}{3}\right)^s H^s(C_{1/3})$$

Now cancelling  $H^s(C_{1/3})$  form both sides, we have

$$1 = \left(\frac{1}{3}\right)^s + \left(\frac{1}{3}\right)^s$$

This implies that,  $1 = 2 \times 3^{-s}$ . Taking log on both sides, we have

$$0 = \log 2 - s \log 3, \text{ that is, } s = \frac{\log 2}{\log 3} = 0.631$$

Thus the Hausdorff dimension of the Cantor middle  $\frac{1}{3}$  set is  $s = \frac{\log 2}{\log 3}$ , that is,

$$\dim_H C_{1/3} = \frac{\log 2}{\log 3} = 0.631.$$

Since the Cantor middle  $\frac{1}{3}$  set is in  $\mathbf{R}^1$ ,  $\dim_H C_{1/3} = 0.631 < 1$ .

Hence the Hausdorff measure of the Cantor middle  $\frac{1}{3}$  set is zero, that is,  $H^s(C_{1/3}) = 0$ .

Similarly,

we can show that the Hausdorff dimension of the Cantor middle  $\frac{1}{5}$  set is  $s = \frac{\log 3}{\log 5}$ , that is,

$$\dim_H C_{1/5} = \frac{\log 3}{\log 5} = 0.682. \text{ Since } \dim_H C_{1/5} = 0.682 < 1, \text{ the Hausdorff measure of the}$$

Cantor middle  $\frac{1}{5}$  set is zero, that is,  $H^s(C_{1/5}) = 0$ .

In general, we can show that the Hausdorff dimension of the Cantor middle  $\frac{1}{2m-1}$

$$(2 \leq m < \infty), \text{ set is } s = \frac{\log m}{\log(2m-1)}, \text{ that is, } \dim_H C_{1/(2m-1)} = \frac{\log m}{\log(2m-1)}, (2 \leq m < \infty).$$

Since  $\dim_H C_{1/(2m-1)} = \frac{\log m}{\log(2m-1)} < 1$  for  $2 \leq m < \infty$ , the Hausdorff measure of the Cantor

middle  $\frac{1}{2m-1}$  ( $2 \leq m < \infty$ ), set is zero, that is,  $H^s(C_{1/(2m-1)}) = 0$ .

Hence the Hausdorff measure of the generalized Cantor sets is zero, that is,  $H^s(C_{1/(2m-1)}) = 0$  for  $2 \leq m < \infty$ .

### 7.3. Hausdorff Dimensions of the Invariant Sets for Contractions or IFS of Fractals

Let  $S_1, S_2, \dots, S_N$  be contractions. A subset  $F$  of  $X$  is called invariant for the transformation  $S_i$  if

$$F = \bigcup_{i=1}^N S_i(F)$$

In the case where  $S_i : X \rightarrow X$  are similarities with Lipschitz constants  $L_i$  for  $i = 1, 2, \dots, N$  respectively, a theorem proved by M. Hata (Theorem 10.3 of [50] and Proposition 9.7 of [40]) allows us to calculate the Hausdorff dimension of the invariant set for  $S_1, S_2, \dots, S_N$ . Namely, if we assume that  $F$  is an invariant set for the similarities  $S_1, S_2, \dots, S_N$  and  $S_i(F) \cap S_j(F) = \emptyset$  for  $i \neq j$ , then  $\dim_H F = s$ , where  $s$  is given by

$$\sum_{i=1}^N L_i^s = 1. \tag{7.2}$$

#### 7.3.1. Hausdorff dimension of the invariant set for IFS of the Cantor middle $\frac{1}{3}$ set

Let  $F$  be an invariant set for IFS of the Cantor middle  $\frac{1}{3}$  set which is

$$w_1(x) = \frac{x}{3}, \quad w_2(x) = \frac{x}{3} + \frac{2}{3}.$$

with contracting factor  $L_i = \frac{1}{3}$  for each  $i = 1, 2$ .

If  $F \subseteq X$ , then  $w_1(F) \cap w_2(F) = \emptyset$  and  $L_1 = \frac{1}{3}, L_2 = \frac{1}{3}$ .

Now from (7.2), we have

$$\left(\frac{1}{3}\right)^s + \left(\frac{1}{3}\right)^s = 1 \Rightarrow 3^s = 2 \Rightarrow s \log 3 = \log 2 \therefore s = \frac{\log 2}{\log 3} = 0.631.$$

Thus the Hausdorff dimension of the invariant set for IFS of the Cantor middle  $\frac{1}{3}$  set is

$$s = \frac{\log 2}{\log 3} = 0.631, \text{ that is, } \dim_H F = 0.631.$$



### 7.3.2. Hausdorff dimension of the invariant set for IFS of the Cantor middle $\frac{1}{5}$ set

Let  $F$  be an invariant set for IFS of the Cantor middle  $\frac{1}{5}$  set which is

$$w_1(x) = \frac{x}{5}, \quad w_2(x) = \frac{x}{5} + \frac{2}{5}, \quad w_3(x) = \frac{x}{5} + \frac{4}{5}.$$

with contracting factor  $L_i = \frac{1}{5}$  for each  $i = 1, 2, 3$ .

If  $F \subseteq X$ , then  $w_1(F) \cap w_2(F) \cap w_3(F) = \emptyset$  and  $L_1 = \frac{1}{5}, L_2 = \frac{1}{5}, L_3 = \frac{1}{5}$ .

Now from (7.2), we have

$$\left(\frac{1}{5}\right)^s + \left(\frac{1}{5}\right)^s + \left(\frac{1}{5}\right)^s = 1 \Rightarrow 3 \left(\frac{1}{5}\right)^s = 1 \Rightarrow 5^s = 3 \Rightarrow s \log 5 = \log 3 \therefore s = \frac{\log 3}{\log 5} = 0.682.$$

Thus the Hausdorff dimension of the invariant set for IFS of the Cantor middle  $\frac{1}{5}$  set is

$$s = \frac{\log 3}{\log 5} = 0.682, \text{ that is, } \dim_H F = 0.682.$$

### 7.3.3. Hausdorff dimension of the invariant set for IFS of the Cantor middle $\frac{1}{7}$ set

Let  $F$  be an invariant set for IFS of the Cantor middle  $\frac{1}{7}$  set which is

$$w_1(x) = \frac{x}{7}, \quad w_2(x) = \frac{x}{7} + \frac{2}{7}, \quad w_3(x) = \frac{x}{7} + \frac{4}{7}, \quad w_4(x) = \frac{x}{7} + \frac{6}{7}$$

with contracting factor  $L_i = \frac{1}{7}$  for each  $i = 1, 2, 3, 4$ .

If  $F \subseteq X$ , then  $w_i(F) \cap w_j(F) = \emptyset$  for  $i \neq j$ , and  $L_i = \frac{1}{7}$  for  $i = 1, \dots, 4$ .

Now from (7.2), we have

$$4 \cdot \left(\frac{1}{7}\right)^s = 1 \Rightarrow 7^s = 4 \Rightarrow s \log 7 = \log 4 \therefore s = \frac{\log 4}{\log 7} = 0.712.$$

Thus the Hausdorff dimension of the invariant set for IFS of Cantor middle  $\frac{1}{7}$  set is

$$s = \frac{\log 4}{\log 7} = 0.712, \text{ that is, } \dim_H F = 0.712.$$

**7.3.4. Hausdorff dimension of the invariant set for IFSGCS (the Cantor middle  $\frac{1}{2m-1}$ ,  $(2 \leq m < \infty)$  sets)**

*Iterated Function System of the Generalized Cantor Sets:* Let  $X = [0,1]$ . Let  $(X, \dots)$  be a complete separable metric space. If  $w_k : X \rightarrow X$  is a function which is defined by

$$w_k(x) = \frac{x}{2m-1} + \frac{2(k-1)}{2m-1}, m \geq 2$$

with contracting factor  $L = \frac{1}{2m-1}$ ,  $(2 \leq m < \infty)$  for  $k = 1, 2, \dots, m$  respectively, then the family  $\{w_k : k = 1, 2, \dots, m\}$  is called an *iterated function system of the generalized Cantor sets (IFSGCS)*. Now we have

$$\dots(w_i(x), w_i(y)) = \dots\left(w_i(0), w_i\left(\frac{1}{2m-1}\right)\right) = \dots\left(0, \frac{1}{(2m-1)^2}\right) = \frac{1}{(2m-1)^2}$$

$$L \cdot \dots(w_i(x), w_i(y)) = L \cdot \dots\left(0, \frac{1}{(2m-1)}\right) = \frac{1}{(2m-1)} \cdot \frac{1}{(2m-1)} = \frac{1}{(2m-1)^2} \text{ for } 2 \leq m < \infty.$$

Since  $\dots(w_i(x), w_i(y)) \leq L \cdot \dots(x, y)$  for all  $x, y \in X$ , and  $0 < L < 1$ , the mapping  $w_i : X \rightarrow X$  of iterated function system of the generalized Cantor sets is called a contraction or similarity with contracting factor or Lipschitz constant  $L$ .

Let  $F$  be an invariant set for IFS of the Cantor middle  $\frac{1}{2m-1}$  set which is

$$w_i(x) = \frac{x}{2m-1} + \frac{2i-2}{2m-1}, m \geq 2$$

with contracting factor  $L_i = \frac{1}{2m-1}$ ,  $(2 \leq m < \infty)$  for each  $i = 1, 2, \dots, m$ .

If  $F \subseteq X$ , then  $w_i(F) \cap w_j(F) = \emptyset$  for  $i \neq j$ , and  $L_i = \frac{1}{2m-1}$  for  $i = 1, 2, \dots, m$ .

Now from (7.2), we have

$$m \cdot \left(\frac{1}{2m-1}\right)^s = 1 \Rightarrow (2m-1)^s = m \Rightarrow s \log(2m-1) = \log m$$

$$\therefore s = \frac{\log m}{\log(2m-1)}, (2 \leq m < \infty).$$

Thus the Hausdorff dimension of the invariant set for IFS of the Cantor middle  $\frac{1}{2m-1}$  set is

$$s = \frac{\log m}{\log(2m-1)}, (2 \leq m < \infty), \text{ that is, } \dim_H F = \frac{\log m}{\log(2m-1)}, (2 \leq m < \infty).$$

Hence the Hausdorff dimension of the invariant set for IFS of the generalized Cantor sets is

$$\dim_H F = \frac{\log m}{\log(2m-1)}, (2 \leq m < \infty).$$

## 7.4. Hausdorff Dimensions of the Invariant Sets for IFS of Two Dimensional Fractals

### 7.4.1. Hausdorff dimension of the invariant set for IFS of the Koch curve

Let  $F$  be an invariant set for IFS of the Koch curve which is

$$\begin{aligned}w_1(x, y) &= \left(\frac{1}{3}x, \frac{1}{3}y\right), \\w_2(x, y) &= \left(\frac{1}{6}x + \frac{\sqrt{3}}{6}y + \frac{1}{3}, \frac{\sqrt{3}}{6}x + \frac{1}{6}y\right), \\w_3(x, y) &= \left(\frac{1}{6}x + \frac{\sqrt{3}}{6}y + \frac{1}{2}, \frac{\sqrt{3}}{6}x + \frac{1}{6}y + \frac{\sqrt{3}}{6}\right), \\w_4(x, y) &= \left(\frac{1}{3}x + \frac{2}{3}, \frac{1}{3}y\right)\end{aligned}$$

Now we have

$$\begin{aligned}\dots(w_3(x, y), w_3(x', y')) &= \sqrt{\frac{1}{36}(x-x')^2 + \frac{3}{36}(y-y')^2 + \frac{3}{36}(x-x')^2 + \frac{1}{36}(y-y')^2} \\&= \frac{1}{3}\sqrt{(x-x')^2 + (y-y')^2} \\&= \frac{1}{3}\dots((x, y), (x', y'))\end{aligned}$$

It follows that  $w_3$  is a contraction on  $\mathbf{R}^2$  with contraction factor  $L = \frac{1}{3}$ .

Similarly, we can show that  $w_1$ ,  $w_2$  and  $w_4$  are contraction on  $\mathbf{R}^2$  with  $L = \frac{1}{3}$ .

If  $F \subseteq X$ , then  $\bigcap_{i=1}^4 w_i(F) = F$  and  $L_i = \frac{1}{3}$  for each  $i = 1, 2, 3, 4$ .

Now from (7.2), we have

$$\left(\frac{1}{3}\right)^s + \left(\frac{1}{3}\right)^s + \left(\frac{1}{3}\right)^s + \left(\frac{1}{3}\right)^s = 1 \Rightarrow 3^s = 4 \Rightarrow s \log 3 = \log 4 \therefore s = \frac{\log 4}{\log 3} = 1.26.$$

Thus the Hausdorff dimension of the invariant set for IFS of the Koch curve is

$$s = \frac{\log 4}{\log 3} = 1.26, \text{ that is, } \dim_H F = 1.26.$$

Since the Koch curve is in  $\mathbf{R}^2$ , and  $\dim_H F = 1.26 < 2$ , the Hausdorff measure of the invariant set for IFS of the Koch curve is zero, that is,  $H^s(F) = 0$ .

### 7.4.2. Hausdorff dimension of the invariant set for IFS of the Sierpinski isosceles triangle

Let  $F$  be an invariant set for IFS of the Sierpinski isosceles triangle which is

$$w_1(x, y) = \left(\frac{1}{2}x, \frac{1}{2}y\right), \quad w_2(x, y) = \left(\frac{1}{2}x + \frac{1}{2}, \frac{1}{2}y\right), \quad w_3(x, y) = \left(\frac{1}{2}x + \frac{1}{4}, \frac{1}{2}y + \frac{1}{2\sqrt{2}}\right)$$

Now we have

$$\begin{aligned} \dots(w_1(x, y), w_1(x', y')) &= \sqrt{\frac{1}{4}(x-x')^2 + \frac{1}{4}(y-y')^2} = \frac{1}{2}\sqrt{(x-x')^2 + (y-y')^2} \\ &= \frac{1}{2} \dots((x, y), (x', y')) \end{aligned}$$

It follows that  $w_1$  is a contraction on  $\mathbf{R}^2$  with contraction factor  $L = \frac{1}{2}$ .

Similarly, we can show that  $w_2$  and  $w_3$  are contraction on  $\mathbf{R}^2$  with  $L = \frac{1}{2}$ .

If  $F \subseteq X$ , then  $w_1(F) \cap w_2(F) \cap w_3(F) = w$  and  $L_1 = \frac{1}{2}, L_2 = \frac{1}{2}, L_3 = \frac{1}{2}$ .

Now from (7.2), we have

$$\left(\frac{1}{2}\right)^s + \left(\frac{1}{2}\right)^s + \left(\frac{1}{2}\right)^s = 1 \Rightarrow 2^s = 3 \Rightarrow s \log 2 = \log 3 \therefore s = \frac{\log 3}{\log 2} = 1.58.$$

Thus Hausdorff dimension of the invariant set for IFS of the Sierpinski isosceles triangle is

$$s = \frac{\log 3}{\log 2} = 1.58, \text{ that is, } \dim_H F = 1.58.$$

Since the Sierpinski isosceles triangle is in  $\mathbf{R}^2$ , and  $\dim_H F = 1.58 < 2$ , the Hausdorff measure of the invariant set for IFS of the Sierpinski isosceles triangle is zero, that is,  $H^s(F) = 0$ .

Similarly, we can find the Hausdorff dimension and Hausdorff measure of the invariant set for IFS of the Sierpinski equilateral triangle, isosceles right triangle and scalene triangle.

### 7.4.3. Hausdorff dimension of the invariant set for IFS of the Sierpinski carpet

Let  $F$  be an invariant set for IFS of the Sierpinski carpet which is

$$\begin{aligned} w_1(x, y) &= \left(\frac{1}{3}x, \frac{1}{3}y\right), & w_2(x, y) &= \left(\frac{1}{3}x + \frac{1}{3}, \frac{1}{3}y\right), \\ w_3(x, y) &= \left(\frac{1}{3}x + \frac{2}{3}, \frac{1}{3}y\right), & w_4(x, y) &= \left(\frac{1}{3}x, \frac{1}{3}y + \frac{1}{3}\right), \\ w_5(x, y) &= \left(\frac{1}{3}x + \frac{2}{3}, \frac{1}{3}y + \frac{1}{3}\right), & w_6(x, y) &= \left(\frac{1}{3}x, \frac{1}{3}y + \frac{2}{3}\right), \\ w_7(x, y) &= \left(\frac{1}{3}x + \frac{1}{3}, \frac{1}{3}y + \frac{2}{3}\right), & w_8(x, y) &= \left(\frac{1}{3}x + \frac{2}{3}, \frac{1}{3}y + \frac{2}{3}\right) \end{aligned}$$

Now we have

$$\begin{aligned} \dots(w_1(x, y), w_1(x', y')) &= \sqrt{\frac{1}{9}(x-x')^2 + \frac{1}{9}(y-y')^2} = \frac{1}{3}\sqrt{(x-x')^2 + (y-y')^2} \\ &= \frac{1}{3} \dots((x, y), (x', y')) \end{aligned}$$

It follows that  $w_1$  is a contraction on  $\mathbf{R}^2$  with contraction factor  $L = \frac{1}{3}$ .

Similarly, we can show that  $w_2, w_3, w_4, w_5, w_6, w_7$  and  $w_8$  are contraction on  $\mathbf{R}^2$  with  $L = \frac{1}{3}$ .

If  $F \subseteq X$ , then  $\bigcap_{i=1}^8 w_i(F) = F$  and  $L_i = \frac{1}{3}$  for each  $i = 1, 2, \dots, 8$ .

Now from (7.2), we have

$$8 \cdot \left(\frac{1}{3}\right)^s = 1 \Rightarrow 3^s = 8 \Rightarrow s \log 3 = \log 8 \therefore s = \frac{\log 8}{\log 3} = 1.89.$$

The Hausdorff dimension of the invariant set for IFS of the Sierpinski carpet is

$$s = \frac{\log 8}{\log 3} = 1.89. \text{ That is } \dim_H F = 1.89.$$

Since the Sierpinski carpet is in  $\mathbf{R}^2$ , and  $\dim_H F = 1.89 < 2$ , the Hausdorff measure of the invariant set for IFS of the Sierpinski carpet is zero, that is,  $H^s(F) = 0$ .

#### 7.4.4. Hausdorff dimension of the invariant set for IFS of the box fractal

Let  $B$  be an invariant set for IFS of the box fractal which is

$$\begin{aligned} w_1(x, y) &= \left(\frac{1}{3}x, \frac{1}{3}y\right), & w_2(x, y) &= \left(\frac{1}{3}x + \frac{2}{3}, \frac{1}{3}y\right), \\ w_3(x, y) &= \left(\frac{1}{3}x, \frac{1}{3}y + \frac{2}{3}\right), & w_4(x, y) &= \left(\frac{1}{3}x + \frac{2}{3}, \frac{1}{3}y + \frac{2}{3}\right) \\ w_5(x, y) &= \left(\frac{1}{3}x + \frac{1}{3}, \frac{1}{3}y + \frac{1}{3}\right) \end{aligned}$$

Now we have

$$\begin{aligned} \dots(w_1(x, y), w_1(x', y')) &= \sqrt{\frac{1}{9}(x-x')^2 + \frac{1}{9}(y-y')^2} = \frac{1}{3}\sqrt{(x-x')^2 + (y-y')^2} \\ &= \frac{1}{3} \dots((x, y), (x', y')) \end{aligned}$$

It follows that  $w_1$  is a contraction on  $\mathbf{R}^2$  with contraction factor  $L = \frac{1}{3}$ .

Similarly, we can show that  $w_2, w_3, w_4$  and  $w_5$  are contraction on  $\mathbf{R}^2$  with  $L = \frac{1}{3}$ .

If  $B \subseteq X$ , then  $\bigcap_{i=1}^5 w_i(B) = B$  and  $L_i = \frac{1}{3}$  for each  $i = 1, 2, 3, 4, 5$ .

Now from (7.2), we have

$$\left(\frac{1}{3}\right)^s + \left(\frac{1}{3}\right)^s + \left(\frac{1}{3}\right)^s + \left(\frac{1}{3}\right)^s + \left(\frac{1}{3}\right)^s = 1 \Rightarrow 3^s = 5 \Rightarrow s \log 3 = \log 5 \therefore s = \frac{\log 5}{\log 3} = 1.46.$$

Thus the Hausdorff dimension of the invariant set for IFS of the box fractal is

$$s = \frac{\log 5}{\log 3} = 1.46. \text{ That is } \dim_H B = 1.46.$$

Since the box fractal is in  $\mathbf{R}^2$ , and  $\dim_H B = 1.46 < 2$ , the Hausdorff measure of the invariant set for IFS of the box fractal is zero, that is,  $H^s(B) = 0$ .

**7.4.5. Hausdorff dimension of the invariant set for IFS of the square fractal (using the Cantor middle  $\frac{1}{3}$  set)**

Let  $S$  be an invariant set for IFS of the square fractal which is

$$\begin{aligned} w_1(x, y) &= \left(\frac{1}{3}x, \frac{1}{3}y\right), & w_2(x, y) &= \left(\frac{1}{3}x + \frac{2}{3}, \frac{1}{3}y\right) \\ w_3(x, y) &= \left(\frac{1}{3}x, \frac{1}{3}y + \frac{2}{3}\right), & w_4(x, y) &= \left(\frac{1}{3}x + \frac{2}{3}, \frac{1}{3}y + \frac{2}{3}\right) \end{aligned}$$

Now we have

$$\begin{aligned} \dots(w_1(x, y), w_1(x', y')) &= \sqrt{\frac{1}{9}(x-x')^2 + \frac{1}{9}(y-y')^2} = \frac{1}{3}\sqrt{(x-x')^2 + (y-y')^2} \\ &= \frac{1}{3} \dots((x, y), (x', y')) \end{aligned}$$

It follows that  $w_1$  is a contraction on  $\mathbf{R}^2$  with contraction factor  $L = \frac{1}{3}$ .

Similarly, we can show that  $w_2, w_3$  and  $w_4$  are contraction on  $\mathbf{R}^2$  with  $L = \frac{1}{3}$ .

If  $S \subseteq X$ , then  $\bigcap_{i=1}^4 w_i(S) = S$  and  $L_i = \frac{1}{3}$  for each  $i = 1, 2, 3, 4$ .

Now from (7.2), we have

$$\left(\frac{1}{3}\right)^s + \left(\frac{1}{3}\right)^s + \left(\frac{1}{3}\right)^s + \left(\frac{1}{3}\right)^s = 1 \Rightarrow 3^s = 4 \Rightarrow s \log 3 = \log 4 \therefore s = \frac{\log 4}{\log 3} = 1.26.$$

Thus the Hausdorff dimension of the invariant set for IFS of the square fractal is

$$s = \frac{\log 4}{\log 3} = 1.26. \text{ That is } \dim_H S = 1.26.$$

Since the square fractal is in  $\mathbf{R}^2$ , and  $\dim_H S = 1.26 < 2$ , the Hausdorff measure of the invariant set for IFS of the square fractal is zero, that is,  $H^s(S) = 0$ .

#### 7.4.6. Hausdorff dimension of the invariant set for IFS of the square fractal (using the Cantor middle $\frac{1}{5}$ set)

Let  $F$  be an invariant set for IFS of the square fractal which is

$$\begin{aligned} w_1(x, y) &= \left(\frac{1}{5}x, \frac{1}{5}y\right), & w_2(x, y) &= \left(\frac{1}{5}x + \frac{2}{5}, \frac{1}{5}y\right), \\ w_3(x, y) &= \left(\frac{1}{5}x, \frac{1}{5}y + \frac{2}{5}\right), & w_4(x, y) &= \left(\frac{1}{5}x + \frac{4}{5}, \frac{1}{5}y\right), \\ w_5(x, y) &= \left(\frac{1}{5}x, \frac{1}{5}y + \frac{4}{5}\right), & w_6(x, y) &= \left(\frac{1}{5}x + \frac{2}{5}, \frac{1}{5}y + \frac{2}{5}\right), \\ w_7(x, y) &= \left(\frac{1}{5}x + \frac{2}{5}, \frac{1}{5}y + \frac{4}{5}\right), & w_8(x, y) &= \left(\frac{1}{5}x + \frac{4}{5}, \frac{1}{5}y + \frac{2}{5}\right), \\ w_9(x, y) &= \left(\frac{1}{5}x + \frac{4}{5}, \frac{1}{5}y + \frac{4}{5}\right) \end{aligned}$$

Now we have

$$\begin{aligned} \dots(w_1(x, y), w_1(x', y')) &= \sqrt{\frac{1}{25}(x-x')^2 + \frac{1}{25}(y-y')^2} = \frac{1}{5}\sqrt{(x-x')^2 + (y-y')^2} \\ &= \frac{1}{5}\dots((x, y), (x', y')) \end{aligned}$$

It follows that  $w_1$  is a contraction on  $\mathbf{R}^2$  with contraction factor  $L = \frac{1}{5}$ .

Similarly, we can show that  $w_2, w_3, \dots, w_8$  and  $w_9$  are contraction on  $\mathbf{R}^2$  with  $L = \frac{1}{5}$ .

If  $F \subseteq X$ , then  $\bigcap_{i=1}^9 w_i(F) = F$  and  $L_i = \frac{1}{5}$  for each  $i = 1, 2, 3, \dots, 9$ .

Now from (7.2), we have

$$9 \cdot \left(\frac{1}{5}\right)^s = 1 \Rightarrow 5^s = 9 \Rightarrow s \log 5 = \log 9 \therefore s = \frac{\log 9}{\log 5} = 1.36.$$

Thus the Hausdorff dimension of the invariant set for IFS of the square fractal is

$$s = \frac{\log 9}{\log 5} = 1.36. \text{ That is } \dim_H F = 1.36.$$

Since the square fractal is in  $\mathbf{R}^2$ , and  $\dim_H F = 1.36 < 2$ , the Hausdorff measure of the invariant set for IFS of the square fractal is zero, that is,  $H^s(F) = 0$ .

**7.5. Hausdorff Dimensions of the Invariant Sets for IFS of Three Dimensional Fractals**

**7.5.1. Hausdorff dimension of the invariant set for IFS of the Menger sponge**

Let  $M$  be an invariant set for IFS of the Menger sponge which is

$$\begin{aligned}
 w_1(x, y, z) &= \left(\frac{1}{3}x, \frac{1}{3}y, \frac{1}{3}z\right), & w_2(x, y, z) &= \left(\frac{1}{3}(x+1), \frac{1}{3}y, \frac{1}{3}z\right), \\
 w_3(x, y, z) &= \left(\frac{1}{3}x, \frac{1}{3}(y+1), \frac{1}{3}z\right), & w_4(x, y, z) &= \left(\frac{1}{3}(x+1), \frac{1}{3}y, \frac{1}{3}(z+1)\right), \\
 w_5(x, y, z) &= \left(\frac{1}{3}(x+2), \frac{1}{3}y, \frac{1}{3}z\right), & w_6(x, y, z) &= \left(\frac{1}{3}x, \frac{1}{3}(y+2), \frac{1}{3}z\right), \\
 w_7(x, y, z) &= \left(\frac{1}{3}x, \frac{1}{3}y, \frac{1}{3}(z+2)\right), & w_8(x, y, z) &= \left(\frac{1}{3}(x+1), \frac{1}{3}(y+2), \frac{1}{3}z\right), \\
 w_9(x, y, z) &= \left(\frac{1}{3}(x+1), \frac{1}{3}y, \frac{1}{3}(z+2)\right), & w_{10}(x, y, z) &= \left(\frac{1}{3}x, \frac{1}{3}(y+1), \frac{1}{3}(z+2)\right), \\
 w_{11}(x, y, z) &= \left(\frac{1}{3}(x+2), \frac{1}{3}(y+1), \frac{1}{3}z\right), & w_{12}(x, y, z) &= \left(\frac{1}{3}(x+2), \frac{1}{3}y, \frac{1}{3}(z+1)\right), \\
 w_{13}(x, y, z) &= \left(\frac{1}{3}x, \frac{1}{3}(y+2), \frac{1}{3}(z+1)\right), & w_{14}(x, y, z) &= \left(\frac{1}{3}(x+2), \frac{1}{3}(y+2), \frac{1}{3}z\right), \\
 w_{15}(x, y, z) &= \left(\frac{1}{3}(x+2), \frac{1}{3}y, \frac{1}{3}(z+2)\right), & w_{16}(x, y, z) &= \left(\frac{1}{3}x, \frac{1}{3}(y+2), \frac{1}{3}(z+2)\right), \\
 w_{17}(x, y, z) &= \left(\frac{1}{3}(x+2), \frac{1}{3}(y+2), \frac{1}{3}(z+1)\right), & w_{18}(x, y, z) &= \left(\frac{1}{3}(x+2), \frac{1}{3}(y+1), \frac{1}{3}(z+2)\right), \\
 w_{19}(x, y, z) &= \left(\frac{1}{3}(x+1), \frac{1}{3}(y+2), \frac{1}{3}(z+2)\right), & w_{20}(x, y, z) &= \left(\frac{1}{3}(x+2), \frac{1}{3}(y+2), \frac{1}{3}(z+2)\right)
 \end{aligned}$$

Now we have

$$\begin{aligned}
 \dots(w_1(x, y, z), w_1(x', y', z')) &= \sqrt{\frac{1}{9}(x-x')^2 + \frac{1}{9}(y-y')^2 + \frac{1}{9}(z-z')^2} \\
 &= \frac{1}{3}\sqrt{(x-x')^2 + (y-y')^2 + (z-z')^2} \\
 &= \frac{1}{3}\dots((x, y, z), (x', y', z'))
 \end{aligned}$$

It follows that  $w_1$  is a contraction on  $\mathbf{R}^3$  with contraction factor  $L = \frac{1}{3}$ .

Similarly, we can show that  $w_2, \dots, w_{19}$  and  $w_{20}$  are contraction on  $\mathbf{R}^3$  with  $L = \frac{1}{3}$ .

If  $M \subseteq X$ , then  $\bigcap_{i=1}^{20} w_i(M) = w$  and  $L_i = \frac{1}{3}$  for each  $i = 1, 2, \dots, 20$ .



Now from (7.2), we have

$$20 \cdot \left(\frac{1}{3}\right)^s = 1 \Rightarrow 3^s = 20 \Rightarrow s \log 3 = \log 20 \therefore s = \frac{\log 20}{\log 3} = 2.726.$$

$$20 \cdot \left(\frac{1}{3}\right)^s = 1 \Rightarrow 3^s = 20 \Rightarrow s \log 3 = \log 20 \therefore s = \frac{\log 20}{\log 3} = 2.726.$$

Thus the Hausdorff dimension of the invariant set for IFS of the Menger sponge is

$$s = \frac{\log 20}{\log 3} = 2.726, \text{ that is, } \dim_H M = 2.726.$$

Since the Menger sponge is in  $\mathbf{R}^3$ , and  $\dim_H M = 2.726 < 2$ , the Hausdorff measure of the invariant set for IFS of the Menger sponge is zero, that is,  $H^s(M) = 0$ .

### 7.5.2. Hausdorff dimension of the invariant set for IFS of the Sierpinski tetrahedron

Let  $T$  be an invariant set for IFS of the Sierpinski tetrahedron which is

$$\begin{aligned} w_1(x, y, z) &= \left(\frac{x}{2}, \frac{y}{2}, \frac{(z-\sqrt{3})}{2}\right), \\ w_2(x, y, z) &= \left(\frac{x}{2}, \frac{y}{2} + \sqrt{\frac{2}{3}}, \frac{z}{2} - \frac{1}{2\sqrt{3}}\right), \\ w_3(x, y, z) &= \left(\frac{x}{2} - \frac{1}{\sqrt{2}}, \frac{y}{2} - \frac{1}{\sqrt{6}}, \frac{z}{2} - \frac{1}{2\sqrt{3}}\right), \\ w_4(x, y, z) &= \left(\frac{x}{2} + \frac{1}{\sqrt{2}}, \frac{y}{2} - \frac{1}{\sqrt{6}}, \frac{z}{2} - \frac{1}{2\sqrt{3}}\right) \end{aligned}$$

Now we have

$$\begin{aligned} \dots(w_1(x, y, z), w_1(x', y', z')) &= \sqrt{\frac{1}{4}(x-x')^2 + \frac{1}{4}(y-y')^2 + \frac{1}{4}(z-z')^2} \\ &= \frac{1}{2} \sqrt{(x-x')^2 + (y-y')^2 + (z-z')^2} \\ &= \frac{1}{2} \dots((x, y, z), (x', y', z')) \end{aligned}$$

It follows that  $w_1$  is a contraction on  $\mathbf{R}^3$  with contraction factor  $L = \frac{1}{2}$ .

Similarly, we can show that  $w_2, w_3$  and  $w_4$  are contraction on  $\mathbf{R}^3$  with  $L = \frac{1}{2}$ .

If  $T \subseteq X$ , then  $\bigcap_{i=1}^4 w_i(T) = T$  and  $L_i = \frac{1}{2}$  for each  $i = 1, 2, 3, 4$ .

Now from (7.2), we have

$$4 \cdot \left(\frac{1}{2}\right)^s = 1 \Rightarrow 2^s = 4 \Rightarrow s \log 2 = \log 4 \therefore s = \frac{\log 4}{\log 2} = 2.$$

Hence the Hausdorff dimension of the invariant set for IFS of the Sierpinski tetrahedron is

$$s = \frac{\log 4}{\log 2} = 2. \text{ That is, } \dim_H T = 2.$$

Since the Sierpinski tetrahedron is in  $\mathbf{R}^3$ , and  $\dim_H T = 2 < 3$ , the Hausdorff measure of the invariant set for IFS of the Sierpinski tetrahedron is zero, that is,  $H^s(T) = 0$ .

### 7.5.3. Hausdorff dimension of the invariant set for IFS of the octahedron fractal

Let  $F$  be an invariant set for IFS of the octahedron fractal which is

$$\begin{aligned} w_1(x, y, z) &= \left(\frac{x}{2}, \frac{y}{2}, \frac{z}{2} + \frac{1}{\sqrt{2}}\right), & w_2(x, y, z) &= \left(\frac{x}{2} + \frac{1}{\sqrt{2}}, \frac{y}{2}, \frac{z}{2}\right), \\ w_3(x, y, z) &= \left(\frac{x}{2}, \frac{y}{2} + \frac{1}{\sqrt{2}}, \frac{z}{2}\right), & w_4(x, y, z) &= \left(\frac{x}{2}, \frac{y}{2}, \frac{z}{2} - \frac{1}{\sqrt{2}}\right), \\ w_5(x, y, z) &= \left(\frac{x}{2} - \frac{1}{\sqrt{2}}, \frac{y}{2}, \frac{z}{2}\right), & w_6(x, y, z) &= \left(\frac{x}{2}, \frac{y}{2} - \frac{1}{\sqrt{2}}, \frac{z}{2}\right) \end{aligned}$$

Now we have

$$\begin{aligned} \dots(w_1(x, y, z), w_1(x', y', z')) &= \sqrt{\frac{1}{4}(x-x')^2 + \frac{1}{4}(y-y')^2 + \frac{1}{4}(z-z')^2} \\ &= \frac{1}{2} \sqrt{(x-x')^2 + (y-y')^2 + (z-z')^2} \\ &= \frac{1}{2} \dots((x, y, z), (x', y', z')) \end{aligned}$$

It follows that  $w_1$  is a contraction on  $\mathbf{R}^3$  with contraction factor  $L = \frac{1}{2}$ .

Similarly, we can show that  $w_2, \dots, w_5$  and  $w_6$  are contraction on  $\mathbf{R}^3$  with  $L = \frac{1}{2}$ .

If  $F \subseteq X$ , then  $\bigcap_{i=1}^6 w_i(F) = F$  and  $L_i = \frac{1}{2}$  for each  $i = 1, \dots, 6$ .

Now from (7.2), we have

$$6 \cdot \left(\frac{1}{2}\right)^s = 1 \Rightarrow 2^s = 6 \Rightarrow s \log 2 = \log 6 \therefore s = \frac{\log 6}{\log 2} = 2.585.$$

Thus the Hausdorff dimension of the invariant set for IFS of the octahedron fractal is

$$s = \frac{\log 6}{\log 2} = 2.585. \text{ That is, } \dim_H F = 2.585.$$

Since the octahedron fractal is in  $\mathbf{R}^3$ , and  $\dim_H F = 2.585 < 3$ , the Hausdorff measure of the invariant set for IFS of the octahedron fractal is zero, that is,  $H^s(F) = 0$ .

# CHAPTER EIGHT

## INVARIANT MEASURES FOR IFS OF FRACTALS

### OVERVIEW

In this chapter, we discuss Iterated Function System with Probabilities and invariant measures. We formulate Iterated Function System with Probabilities of the Generalized Cantor Sets and show their invariant measures using the Barnsley-Hutchinson multifunction and Markov operator.

### 8.1. [24] Iterated Function System with Probabilities

Let  $(X, \dots)$  be a complete separable metric space. An iterated function system (IFS) is given by a family of contracting transformations

$$w_i : X \rightarrow X, i \in I \text{ where the index set } I \text{ is finite.}$$

If, in addition, there is given a family of continuous functions

$$p_i : X \rightarrow [0,1], i \in I$$

satisfying  $\sum_{i=1}^N p_i(x) = 1$  for every  $x \in X$ , then the family  $\{(w_i, p_i) : i \in I\}$  is called an iterated function system with probabilities.

If  $\{w_1, w_2, \dots, w_N\}$  is a finite family of strict contractions, we may define the Barnsley-Hutchinson multifunction given by the formula

$$F(A) = \bigcup_{i=1}^N w_i(A). \quad (8.1)$$

The attractor of iterated function system  $\{w_1, w_2, \dots, w_N\}$  is

$$A_{n+1} = F(A_n), A_0 \in X, n = 0, 1, 2, \dots \quad (8.2)$$

which is the well known fractal.

Fractals are strongly related to Markov operator acting on the space of all Borel measures [24]. If the functions  $w_1, w_2, \dots, w_N$  are given and  $\{p_1, p_2, \dots, p_N\}$  is a probability vector (i.e.,  $p_i \geq 0, \sum p_i = 1$ ), then we may define the Markov operator

$$p_{\sim}(A) = \sum_{i=1}^N p_i(\sim \circ w_i^{-1})(A) = \sum_{i=1}^N \int_{w_i^{-1}(A)} p_i \sim(dx) \text{ for } \sim \in M. \quad (8.3)$$

where  $M$  denotes the family of all Borel measure on  $X$ .

Let  $w_1, w_2, \dots, w_N$  be non-singular transformations of the space  $X = [0, 1]$ . Let  $P_1, P_2, \dots, P_N$  be the Frobenious-Perron operators corresponding to the transformations  $w_1, w_2, \dots, w_N$ . Let  $p_1, p_2, \dots, p_N$  be non-negative measurable functions defined on  $X$

such that  $\sum_{i=1}^N p_i(x) = 1$  for all  $x \in X$ .

The evolution of densities of the distribution is described by the Markov operator [43]

$$Pf = \sum_{i=1}^N P_i(p_i f).$$

$$\text{That is, } Pf(x) = \sum_{i=1}^N P_i(p_i f)(x) = \sum_{i=1}^N p_i \frac{d_{\sim} \circ w_i^{-1}}{d_{\sim}}(x) f(w_i^{-1}(x)), \quad (8.4)$$

where  $f \in L^1(x)$ ,  $x \in X$ .

### 8.2. [51] Invariant Measure

If  $w_1, w_2, \dots, w_N$  are strictly contractive, then the support of the unique probability measure  $\sim$  invariant with respect to  $P$  is equal to the fixed point of the Barnsley-Hutchinson multifunction  $F$  defined by (8.1). Also invariant measure can be defined by the following two methods.

A probability measure  $\sim$  is called *invariant* under Barnsley-Hutchinson multifunction  $F$  if and only if

$$\sim(A) = \sim(F^{-1}(\bigcup_{i=1}^N w_i(A))) = \sim(F^{-1}(A)) \quad (8.5)$$

A measure  $\sim \in M$  is called *invariant* with respect to Markov operator  $P$  defined by (8.3) if

$$P\sim = \sim.$$

### 8.3. Iterated Function System with Probabilities of the Generalized Cantor Sets

#### 8.3.1. [6] Iterated function system with probabilities of the Cantor middle $\frac{1}{3}$ set

The iterated function system with probabilities of the Cantor middle  $\frac{1}{3}$  set is as follows:

$$\begin{aligned} w_1(x) &= \frac{x}{3}, & p_1 &= \frac{1}{2}, \\ w_2(x) &= \frac{x}{3} + \frac{2}{3}, & p_2 &= \frac{1}{2}, \end{aligned} \quad (8.6)$$

where  $p_1$  and  $p_2$  are probabilities which control the evolution distribution of  $w_1(x)$  and  $w_2(x)$ . According to the theory of density evolution [25], the density for  $f(x)$  mapping satisfying the density evolution equation

$$f_{n+1}(x) = Pf_n(x), n = 0, 1, 2, \dots$$

with  $Pf(x) = \sum_{i=1}^n P_i(p_i f)$  which is called Markov operator [43].

By equation (8.4), we get

$$Pf(x) = p_1 \frac{d_{\sim} \circ w_1^{-1}}{d_{\sim}}(x) f(w_1^{-1}(x)) + p_2 \frac{d_{\sim} \circ w_2^{-1}}{d_{\sim}}(x) f(w_2^{-1}(x)).$$

$$\text{Thus } Pf(x) = \frac{3}{2} f(w_1^{-1}(x)) + \frac{3}{2} f(w_2^{-1}(x)).$$

Now follow [52] we assume the probability density over the initial interval  $[0, 1]$  is

$$f_0(x) = \begin{cases} 1, & x \in [0, 1], \\ 0, & \text{otherwise,} \end{cases}$$

then what will happen for  $f_0(x)$  under the Markov operator?

According to Barnsley-Hutchinson operator (8.1), the attractor of the equation (8.6) is the unit interval. That is,  $A_\infty = [0, 1]$ .

Now for a subset  $A \subset [0, \frac{1}{3}]$ , we have  $w_1^{-1}(A) \subset [0, 1]$ ,  $w_2^{-1}(A) \subset [-2, -1]$ , then

$f(w_2^{-1}(A)) = 0$ . In the same way, for a subset  $A \subset [\frac{2}{3}, 1]$ , there is  $w_1^{-1}(A) \subset [2, 3]$ ,

$w_2^{-1}(A) \subset [0, 1]$  and  $f(w_1^{-1}(A)) = 0$ . Thus after the first step  $f_0(x)$  becomes

$$f_1(x) = \begin{cases} \frac{3}{2}, & x \in [0, \frac{1}{3}] \\ \frac{3}{2}, & x \in [\frac{2}{3}, 1] \\ 0, & \text{otherwise} \end{cases}$$

under the Markov operator.

Similarly, Markov operator acting on  $f_1(x)$ , and so on. This is shown in Figure 8.1.

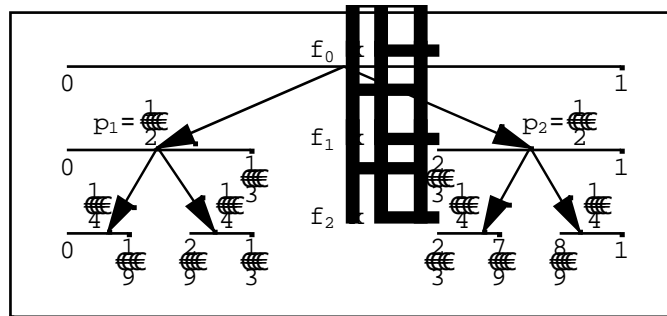


**Figure 8.1** Transform from  $p_1$  and  $p_2$  over unit interval.

Thus iterated function system with probabilities of the Cantor middle  $\frac{1}{3}$  set is

$$\{(w_k, p_k) : k = 1, 2\}.$$

### 8.3.2. [6] Iterated function system with probabilities of the Cantor middle $\frac{1}{5}$ set

The following constructed iterated function system with probabilities of the Cantor middle  $\frac{1}{5}$  set is as follows:

$$\begin{aligned} w_1(x) &= \frac{x}{5}, & p_1 &= \frac{1}{3}, \\ w_2(x) &= \frac{x}{5} + \frac{2}{5}, & p_2 &= \frac{1}{3}, \\ w_3(x) &= \frac{x}{5} + \frac{4}{5}, & p_3 &= \frac{1}{3}, \end{aligned} \tag{8.7}$$

where  $p_1$ ,  $p_2$  and  $p_3$  are probabilities which control the evolution distribution of  $w_1(x)$ ,  $w_2(x)$  and  $w_3(x)$ .

Now we assume the probability density over the initial interval  $[0, 1]$  is

$$f_0(x) = \begin{cases} 1, & x \in [0, 1], \\ 0, & \text{otherwise,} \end{cases}$$

then what will happen for  $f_0(x)$  under the Markov operator?

According to Barnsley-Hutchinson operator (8.1), the attractor of equation (8.7) is the unit interval. That is,  $A_\infty = [0, 1]$ .

Now for a subset  $A \subset [0, \frac{1}{5}]$ , we have  $w_1^{-1}(A) \subset [0, 1]$ ,  $w_2^{-1}(A) \subset [-2, -1]$ ,  $w_3^{-1}(A) \subset [-4, -3]$ , then  $f(w_2^{-1}(A)) = 0$  and  $f(w_3^{-1}(A)) = 0$ . In the same way, for a subset  $A \subset [\frac{2}{5}, \frac{3}{5}]$ , we have  $w_1^{-1}(A) \subset [2, 3]$ ,  $w_2^{-1}(A) \subset [0, 1]$ ,  $w_3^{-1}(A) \subset [-2, -1]$ , then  $f(w_1^{-1}(A)) = 0$  and  $f(w_3^{-1}(A)) = 0$ . For a subset  $A \subset [\frac{4}{5}, 1]$ , we have  $w_1^{-1}(A) \subset [4, 5]$ ,  $w_2^{-1}(A) \subset [2, 3]$  and  $w_3^{-1}(A) \subset [0, 1]$ , then  $f(w_1^{-1}(A)) = 0$  and  $f(w_2^{-1}(A)) = 0$ . Thus after the first step,  $f_0(x)$  becomes

$$f_1(x) = \begin{cases} \frac{5}{3}, & x \in [0, \frac{1}{5}] \\ \frac{5}{3}, & x \in [\frac{2}{5}, \frac{3}{5}] \\ \frac{5}{3}, & x \in [\frac{4}{5}, 1] \\ 0, & \text{otherwise} \end{cases}$$

under the Markov operator.

Similarly, Markov operator acting on  $f_1(x)$ , and so on. This is shown in Figure 8.2.

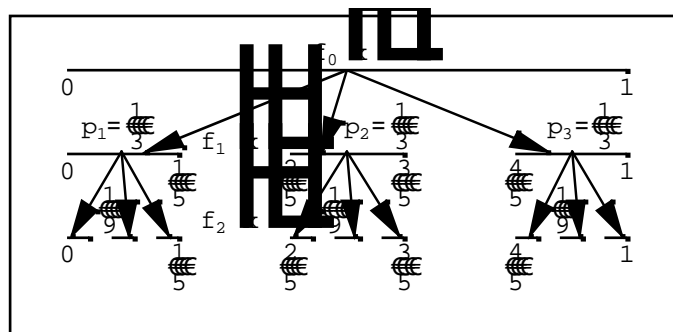


**Figure 8.2** Transform from  $p_1$ ,  $p_2$  and  $p_3$  over unit interval.

Thus iterated function system with probabilities of the Cantor middle  $\frac{1}{5}$  set is

$$\{(w_k, p_k) : k = 1, 2, 3\}.$$

**8.3.3. Iterated function system with probabilities of the Cantor middle  $\frac{1}{2m-1}$  set**

We have constructed iterated function system with probabilities of the Cantor middle  $\frac{1}{2m-1}$ ,  $(2 \leq m < \infty)$  set as follows:

$$\begin{aligned} w_1(x) &= \frac{x}{2m-1}, & p_1 &= \frac{1}{m} \\ w_2(x) &= \frac{x}{2m-1} + \frac{2}{2m-1}, & p_2 &= \frac{1}{m} \\ w_3(x) &= \frac{x}{2m-1} + \frac{4}{2m-1}, & p_3 &= \frac{1}{m} \\ & \vdots \\ w_k(x) &= \frac{x}{2m-1} + \frac{2(k-1)}{2m-1}, & p_k &= \frac{1}{m}, \end{aligned} \quad (2 \leq m < \infty, 1 \leq k \leq m). \quad (8.8)$$

where  $p_1, p_2, \dots, p_m$  are probabilities which control the evolution distribution of  $w_1(x), w_2(x), \dots, w_m(x)$ .  $\frac{1}{2m-1}, (2 \leq m < \infty)$

Now we assume the probability density over the initial interval  $[0, 1]$  is

$$f_0(x) = \begin{cases} 1, & x \in [0, 1], \\ 0, & \text{otherwise,} \end{cases}$$

then what will happen for  $f_0(x)$  under the Markov operator?

According to Barnsley-Hutchinson operator (8.1), the attractor of the equation (8.8) is the unit interval. That is,  $A_\infty = [0, 1]$ .

Now, for a subset  $A \subset \left[0, \frac{1}{2m-1}\right]$ , we have  $w_1^{-1}(A) \subset [0, 1]$ ,  $w_2^{-1}(A) \subset [-2, -1]$ ,  $w_3^{-1}(A) \subset [-4, -3]$ , ...,  $w_m^{-1}(A) \subset [-(2m-2), -(2m-3)]$ , then  $f(w_2^{-1}(A)) = 0$ ,  $f(w_3^{-1}(A)) = 0$ , ...,  $f(w_m^{-1}(A)) = 0$ . In the same way, for a subset  $A \subset \left[\frac{2}{2m-1}, \frac{3}{2m-1}\right]$ , we have  $w_1^{-1}(A) \subset [2, 3]$ ,  $w_2^{-1}(A) \subset [0, 1]$ ,  $w_3^{-1}(A) \subset [-2, -1]$ , ...,  $w_m^{-1}(A) \subset [-(2m-4), -(2m-5)]$ , then  $f(w_1^{-1}(A)) = 0$ ,  $f(w_3^{-1}(A)) = 0$ , ...,  $f(w_m^{-1}(A)) = 0$ . For a subset  $A \subset \left[\frac{2m-2}{2m-1}, 1\right]$ , we have  $w_1^{-1}(A) \subset [(2m-2), (2m-1)]$ ,  $w_2^{-1}(A) \subset [(2m-4), (2m-3)]$ , ...,  $w_{m-1}^{-1}(A) \subset [2, 3]$ , and  $w_m^{-1}(A) \subset [0, 1]$ , then  $f(w_1^{-1}(A)) = 0$ ,  $f(w_2^{-1}(A)) = 0$ , ...,  $f(w_{m-1}^{-1}(A)) = 0$ .

Thus after the first step,  $f_0(x)$  becomes

$$f_1(x) = \begin{cases} \frac{2m-1}{m}, & x \in [0, \frac{1}{2m-1}] \\ \frac{2m-1}{m}, & x \in [\frac{2}{2m-1}, \frac{3}{2m-1}] \\ \vdots \\ \frac{2m-1}{m}, & x \in [\frac{2(m-1)}{2m-1}, 1] \\ 0, & \text{otherwise} \end{cases}$$

under the Markov operator.

Similarly, Markov operator acting on  $f_1(x)$ , and so on. This is shown in Figure 8.3.

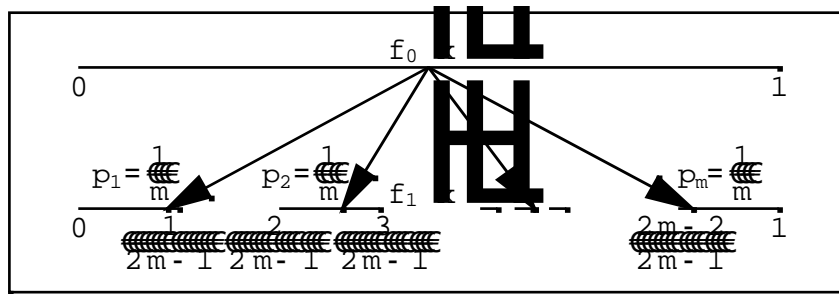


**Figure 8.3** Similar transform from  $p_1, p_2, \dots, p_m$  over unit interval.

Thus iterated function system with probabilities of the Cantor middle  $\frac{1}{2m-1}, (2 \leq m < \infty)$  sets is

$$\{(w_k, p_k) : k = 1, 2, \dots, m\}.$$

We may summarize iterated function system with probabilities of the Cantor middle  $\frac{1}{3}, \frac{1}{5}, \frac{1}{7}, \frac{1}{9}, \frac{1}{11}, \dots$  sets, in general, the Cantor middle  $\frac{1}{2m-1}, (2 \leq m < \infty)$  sets in the following statement:

**Iterated Function System with Probabilities of the Generalized Cantor Sets:**

Let  $X = [0, 1]$ . Let  $(X, \dots)$  be a complete separable metric space. If  $w_k : X \rightarrow X$  is defined by

$$w_k(x) = \frac{x}{2m-1} + \frac{2(k-1)}{2m-1}, p_k = \frac{1}{m},$$

where  $p_k(x)$  are probabilities such that  $\sum_{k=1}^m p_k(x) = 1$  for every  $x \in X$ , which control the

evolution distribution of  $w_k(x)$  with contracting factor or Lipschitz constant  $L_k = \frac{1}{2m-1}$  for  $(2 \leq m < \infty)$  and  $1 \leq k \leq m$ , then the family  $\{(w_k, p_k) : k = 1, 2, \dots, m\}$  is called *iterated function system with probabilities of the generalized Cantor sets*.



**8.4. [6] Invariant Measures for Iterated Function System with Probabilities of the Generalized Cantor Sets**

**8.4.1. Invariant measure for IFS with Probabilities of the Cantor middle  $\frac{1}{3}$  set:**

Let  $A_1 = [0, \frac{1}{3}] \cup [\frac{2}{3}, 1]$ . By equation (8.3) we have

$$\begin{aligned} P_{\sim}(A_1) &= \sum_{k=1}^2 \int_{w_k^{-1}(A_1)} p_k(x) \sim(dx) \\ &= \int_{w_1^{-1}(A_1)} p_1(x) f(x) dx + \int_{w_2^{-1}(A_1)} p_2(x) f(x) dx = \int_0^{\frac{1}{3}} \frac{1}{2} dx + \int_{\frac{2}{3}}^1 \frac{1}{2} dx = 1 \end{aligned}$$

and

$$\sim(A_1) = \sim([0, \frac{1}{3}]) + \sim([\frac{2}{3}, 1]) = \int_0^{\frac{1}{3}} \frac{3}{2} d\sim + \int_{\frac{2}{3}}^1 \frac{3}{2} d\sim = \frac{3}{2} \left( \frac{1}{3} + \frac{1}{3} \right) = 1$$

That is,  $P_{\sim} = \sim$ .

Thus  $\sim$  is an invariant measure for IFS of the Cantor middle  $\frac{1}{3}$  set with respect  $P$ .

**Alternative method 1:**

By equation (8.4) we have

$$\|Pf(x)\| = \int_0^{\frac{1}{3}} \frac{1}{2} \cdot 3 \cdot f(3x) d\sim + \int_{\frac{2}{3}}^1 \frac{1}{2} \cdot 3 \cdot f(3x-2) d\sim = \frac{3}{2} \left[ \int_0^{\frac{1}{3}} d\sim + \int_{\frac{2}{3}}^1 d\sim \right] = \frac{3}{2} \cdot \frac{2}{3} = 1$$

That is,  $\|Pf\| = \|f\|$ .

Thus  $f$  is an invariant for IFS of the Cantor middle  $\frac{1}{3}$  set with respect to  $P$ .

**Alternative method 2:**

Let  $\Delta = [0, \frac{1}{9}] \cup [\frac{2}{3}, \frac{7}{9}]$ . By equation (8.5) we have

$$\sim(\Delta) = \sim([0, \frac{1}{9}]) + \sim([\frac{2}{3}, \frac{7}{9}]) = \int_0^{\frac{1}{9}} \frac{9}{4} d\sim + \int_{\frac{2}{3}}^{\frac{7}{9}} \frac{9}{4} d\sim = \frac{9}{4} \left( \frac{1}{9} + \frac{1}{9} \right) = \frac{1}{2}$$

and

$$\sim(F^{-1}(\Delta)) = \sim(w_1^{-1}(x)) \cup \sim(w_2^{-1}(x)) = \sim([0, \frac{1}{3}]) = \int_0^{\frac{1}{3}} \frac{3}{2} d\sim = \frac{1}{2}$$

That is,  $\sim(\Delta) = \sim(F^{-1}(\Delta))$ .

Thus  $\sim$  is an invariant measure for IFS of the Cantor middle  $\frac{1}{3}$  set with respect to  $F$ .

**8.4.2. Invariant measure for IFS with Probabilities of the Cantor middle  $\frac{1}{5}$  set:**

Let  $A_1 = [0, \frac{1}{5}] \cup [\frac{2}{5}, \frac{3}{5}] \cup [\frac{4}{5}, 1]$ . By equation (8.3) we have

$$\begin{aligned} P_{\sim}(A_1) &= \sum_{k=1}^3 \int_{w_k^{-1}(A_1)} p_k(x) \sim(dx) \\ &= \int_{w_1^{-1}(A_1)} p_1(x) f(x) dx + \int_{w_2^{-1}(A_1)} p_2(x) f(x) dx + \int_{w_3^{-1}(A_1)} p_3(x) f(x) dx \\ &= \int_0^{\frac{1}{5}} \frac{1}{3} dx + \int_{\frac{2}{5}}^{\frac{3}{5}} \frac{1}{3} dx + \int_{\frac{4}{5}}^1 \frac{1}{3} dx = 1 \end{aligned}$$

and  $\sim(A_1) = \sim([0, \frac{1}{5}]) + \sim([\frac{2}{5}, \frac{3}{5}]) + \sim([\frac{4}{5}, 1])$

$$= \int_0^{1/5} \frac{5}{3} d\sim + \int_{2/5}^{3/5} \frac{5}{3} d\sim + \int_{4/5}^1 \frac{5}{3} d\sim = 1$$

That is,  $P_{\sim} = \sim$ .

Thus  $\sim$  is an invariant measure for IFS of the Cantor middle  $\frac{1}{5}$  set with respect  $P$ .

**Alternative method 1:**

By equation (8.4) we have

$$\begin{aligned} \|Pf(x)\| &= \int_0^{1/5} \frac{1}{3} \cdot 5 \cdot f(5x) d\sim + \int_{2/5}^{3/5} \frac{1}{3} \cdot 5 \cdot f(5x-2) d\sim + \int_{4/5}^1 \frac{1}{3} \cdot 5 \cdot f(5x-4) d\sim \\ &= \frac{5}{3} \left[ \int_0^{1/5} d\sim + \int_{2/5}^{3/5} d\sim + \int_{4/5}^1 d\sim \right] = \frac{5}{3} \cdot \frac{3}{5} = 1, \end{aligned}$$

That is,  $\|Pf\| = \|f\|$

Thus  $f$  is an invariant for IFS of the Cantor middle  $\frac{1}{5}$  set with respect to  $P$ .

**Alternative method 2:**

Let  $\Delta = [0, \frac{1}{25}] \cup [\frac{2}{5}, \frac{11}{25}] \cup [\frac{4}{5}, \frac{21}{25}]$ . By equation (8.5) we have

$$\begin{aligned} \sim(\Delta) &= \sim([0, \frac{1}{25}]) + \sim([\frac{2}{5}, \frac{11}{25}]) + \sim([\frac{4}{5}, \frac{21}{25}]) \\ &= \int_0^{1/25} \frac{25}{9} d\sim + \int_{2/5}^{11/25} \frac{25}{9} d\sim + \int_{4/5}^{21/25} \frac{25}{9} d\sim = \frac{1}{3}, \end{aligned}$$

and  $\sim(F^{-1}(\Delta)) = \sim(w_1^{-1}(x)) \cup \sim(w_2^{-1}(x)) \cup \sim(w_3^{-1}(x)) = \sim([0, \frac{1}{5}]) = \int_0^{1/5} \frac{5}{3} d\sim = \frac{1}{3}$

That is,  $\sim(\Delta) = \sim(F^{-1}(\Delta))$ .

Hence  $\sim$  is an invariant measure for IFS of the Cantor middle  $\frac{1}{5}$  set with respect to  $F$ .

**8.4.3. Invariant measure for IFS with Probabilities of the Cantor Middle  $\frac{1}{2m-1}$  sets**

By equation (8.4) we have

$$\begin{aligned} \|Pf(x)\| &= \int_0^{1/(2m-1)} \frac{1}{N} \cdot (2m-1) \cdot f((2m-1)x) d\sim + \int_{2/(2m-1)}^{3/(2m-1)} \frac{1}{N} \cdot (2m-1) \cdot f((2m-1)x-2) d\sim \\ &\quad + \dots + \int_{(2m-2)/(2m-1)}^1 \frac{1}{N} \cdot (2m-1) \cdot f((2m-1)x-2(N-1)) d\sim \\ &= \frac{2m-1}{N} \left[ \int_0^{1/(2m-1)} f((2m-1)x) d\sim + \dots + \int_{(2m-2)/(2m-1)}^1 f((2m-1)x-2(N-1)) d\sim \right] \\ &= \frac{2m-1}{N} \left[ \frac{1}{2m-1} + \frac{1}{2m-1} + \dots + \frac{1}{2m-1} \right] = \frac{2m-1}{N} \cdot \frac{N}{2m-1} = 1 \end{aligned}$$

That is,  $\|Pf\| = \|f\|$ .

Thus  $f$  is an invariant for IFS of the Cantor middle  $\frac{1}{2m-1}$ ,  $(2 \leq m < \infty)$  sets with respect to  $P$ .

**Alternative method 1:**

Similarly, by equation (8.3) we can prove that  $P\sim = \sim$ . Thus  $\sim$  is an invariant measure for IFS of the Cantor middle  $\frac{1}{2m-1}$ ,  $(2 \leq m < \infty)$  set with respect to  $P$ .

**Alternative method 2:**

Let  $\Delta = [0, \frac{1}{(2m-1)^2}] \cup [\frac{2}{(2m-1)^2}, \frac{3}{(2m-1)^2}] \cup \dots \cup [\frac{(2m-1)^2-1}{(2m-1)^2}, 1]$ .

By equation (8.5) we have

$$\begin{aligned} \sim(\Delta) &= \sim([0, \frac{1}{(2m-1)^2}]) + \sim([\frac{2}{(2m-1)^2}, \frac{3}{(2m-1)^2}]) + \dots + \sim([\frac{(2m-1)^2-1}{(2m-1)^2}, 1]) \\ &= \frac{1}{N^2} + \frac{1}{N^2} + \dots + \frac{1}{N^2} = \frac{N}{N^2} = \frac{1}{N} \end{aligned}$$

and  $\sim(F^{-1}(\Delta)) = \sim(w_1^{-1}(x)) \cup \sim(w_2^{-1}(x)) \cup \dots \cup \sim(w_k^{-1}(x))$

$$= \sim([0, \frac{1}{2m-1}]) = \int_0^{1/(2m-1)} \frac{2m-1}{N} = \frac{1}{N} \text{ i.e., } \sim(\Delta) = \sim(F^{-1}(\Delta)).$$

Thus  $\sim$  is an invariant measure for IFS of the Cantor middle  $\frac{1}{2m-1}$ ,  $(2 \leq m < \infty)$  set with respect to  $F$ .

**8.5. Proposition: [6]** Let  $w_k(x) = \frac{x}{2m-1} + \frac{2(k-1)}{2m-1}$ ,  $p_k = \frac{1}{m}$  be non-singular

transformations of the space  $X = [0,1]$ , where  $p_k(x)$  are probabilities such that

$\sum_{k=1}^N p_k(x) = 1$  for every  $x \in X$  and let  $P_k$  be the Frobenius-Perron operators

corresponding to the transformations  $w_k$  for  $(2 \leq m < \infty)$  and  $1 \leq k \leq m$ . Then the Markov

operator  $Pf = \sum_{k=1}^N P_k(p_k f)$  satisfy the following conditions:

(a)  $Pf \geq 0$  for all  $f$  in  $L^1(X)$  with  $f \geq 0$ .

(b)  $\|Pf\|_1 \leq \|f\|_1$  for all  $f$  in  $L^1(X)$  and  $\|Pf\|_1 = \|f\|_1$  if  $f \geq 0$ .

**Proof:** (a) Let  $f$  be a function in  $L^1(X)$ . Then

$$\begin{aligned} Pf(x) &= \sum_{k=1}^N p_k \frac{d \circ w_k^{-1}}{d}(x) f(w_k^{-1}(x)) \\ &= p_1 \frac{d \circ w_1^{-1}}{d}(x) f(w_1^{-1}(x)) + p_2 \frac{d \circ w_2^{-1}}{d}(x) f(w_2^{-1}(x)) + \\ &\quad \dots + p_N \frac{d \circ w_N^{-1}}{d}(x) f(w_N^{-1}(x)) \\ &= \frac{2m-1}{N} f((2m-1)x) + \frac{2m-1}{N} f((2m-1)x-2) + \dots + \frac{2m-1}{N} f((2m-1)x-2(N-1)) \end{aligned}$$

That is,  $Pf(x) = 2m-1$  for  $2 \leq m < \infty$ .

Thus  $Pf \geq 0$  for all  $f$  in  $L^1(X)$  with  $f \geq 0$ .

(b) Let  $f$  be a function in  $L^1(X)$ . Then it follows that

$$\begin{aligned} \|Pf\|_1 &= \int_X \left| \sum_{k=1}^N p_k \frac{d \circ w_k^{-1}}{d}(x) f(w_k^{-1}(x)) \right| d\sim \leq \sum_{k=1}^N \int_X \left| p_k \frac{d \circ w_k^{-1}}{d}(x) f(w_k^{-1}(x)) \right| d\sim \\ &= \sum_{k=1}^N \int_{X_k} \left| p_k \frac{d \circ w_k^{-1}}{d}(w_k(y)) f(y) \right| d(\sim \circ w_k) \\ &= \sum_{k=1}^N \int_{X_k} \left| p_k \frac{d \circ w_k^{-1}}{d}(w_k(y)) f(y) \right| \frac{d(\sim \circ w_k)}{d}(y) d\sim \\ &= \sum_{k=1}^N \int_{X_k} \left| p_k \frac{d \circ w_k^{-1}}{d}(w_k(y)) \frac{d(\sim \circ w_k)}{d}(y) f(y) \right| d\sim \\ &= \sum_{k=1}^N \int_{X_k} p_k |f(y)| d\sim = \sum_{k=1}^N \int_{X_k} |f(y)| d\sim = \|f\|_1 \end{aligned}$$

Thus  $\|Pf\|_1 \leq \|f\|_1$  for all  $f$  in  $L^1(X)$ .

Hence  $\|Pf\|_1 = \|f\|_1$  if  $f \geq 0$ . □

# CHAPTER NINE

## DYNAMICS OF THE PROTOTYPICAL FRACTAL

### OVERVIEW

In this chapter, we define the Transition Operator  $P_w$  for the Iterated Function System with Probabilities of the Generalized Cantor sets (IFSPGCS) and show that this operator is a Markov operator. We also show that the Iterated Function System with Probabilities of the Generalized Cantor sets is non-expansive and asymptotically stable if the Markov operator  $P_w$  has the corresponding property with respect to the metric  $\{(\dots(x, y))\}$ .

### 9.1. [24] Barnsley's and Hutchinson Approach to Fractal Theory

Let  $(X, \dots)$  be a complete separable metric space. We assume that every closed ball in  $X$

$$B(r, x) = \{y \in X : \dots(x, y) \leq r\}$$

is a compact set. We denote by  $\mathbf{B}$  the  $\dagger$ -algebra of Borel subsets of  $X$ . By  $\mathbf{M}$  we denote the family of Borel measure (nonnegative,  $\dagger$ -additive) on  $X$  such that  $\sim(B) < \infty$  for every ball  $B$ . By  $\mathbf{M}_1$  we denote the subsets of  $\mathbf{M}$  such that  $\sim(X) = 1$  for  $\sim \in \mathbf{M}_1$ . The elements of  $\mathbf{M}_1$  will be distributions. An iterated function system is given by a family of contracting transformations

$$w_i : X \rightarrow X, i \in I \text{ where the index set } I \text{ is finite.}$$

If, in addition, there is given a family of continuous functions

$$p_i : X \rightarrow [0, 1], i \in I$$

satisfying  $\sum_{i=1}^N p_i(x) = 1$  for every  $x \in X$ , then the family  $\{(w_i, p_i) : i \in I\}$  is called an iterated function system (IFS) with probabilities.

Having an IFS  $\{w_i : i \in I\}$ , we define the corresponding Barnsley-Hutchinson multiplication [21, 22] by the formula

$$F(A) = \bigcup_{i=1}^N w_i(A) \text{ for } A \in \mathbf{B}.$$

and having an IFS with probabilities we define the Markov operator acting on measures by

$$P\sim(A) = \sum_{k=1}^N \int_{w_k^{-1}(A)} p_k(x) \sim(dx) \text{ for } \sim \in \mathbf{M}, A \in \mathbf{B}. \quad (9.1)$$

It is easy to verify that  $P$  is a Markov-Feller operator and its dual  $U$  is given by

$$Uf(x) = \sum_{i \in I} p_i(x) f(w_i(x)).$$

A set  $A_0$  such that  $F(A_0) = A_0$  is called invariant with respect to the IFS  $\{w_i : i \in I\}$ . If, in addition, for every nonempty compact subset  $A$  of  $X$ , the sequence  $(F^n(A))$  converges in the Hausdorff distance to  $A_0$ , the set  $A_0$  is called an attractor (or fractal) corresponding to the IFS  $\{w_i : i \in I\}$ .

Assume that  $I$  is finite and for every  $i \in I$ , the function  $w_i$  is Lipschitzian with the Lipschitz constant and the function  $p_i$  is constant. The following facts are well known [21, 25].

**Fact 9.1.1.** If  $L_i < 1$  for  $i \in I$ , then the IFS is  $\{w_i : i \in I\}$  asymptotically stable (on sets), the operator  $P$  given by (9.1) is *asymptotically stable* (on measures), and

$$A_0 = \text{supp } \sim_*$$

where  $A_0$  is the attractor (or fractal) corresponding to the iterated function system  $\{w_i : i \in I\}$  and  $\sim_*$  is the invariant measure with respect to  $P$ .

**Fact 9.1.2.** If

$$\sum_{i \in I} p_i L_i < 1,$$

then an IFS with probabilities  $\{(w_i, p_i) : i \in I\}$ , is *asymptotically stable*.

## 9.2. Iterated Function System with Probabilities of the Generalized Cantor Sets (IFSPGCS)

Let  $X = [0, 1]$ . Let  $(X, \dots)$  be a complete separable metric space. If  $w_k : X \rightarrow X$  is defined by

$$w_k(x) = \frac{x}{2m-1} + \frac{2(k-1)}{2m-1}, p_k = \frac{1}{m},$$

where  $p_k(x)$  are probabilities such that  $\sum_{k=1}^m p_k(x) = 1$  for every  $x \in X$ , which control the

evolution distribution of  $w_k(x)$  with contracting factor or Lipschitz constant  $L_k = \frac{1}{2m-1}$  for  $2 \leq m < \infty$  and  $1 \leq k \leq m$ . Then the family  $\{(w_k, p_k) : k = 1, 2, \dots, m\}$  is called *iterated function system with probabilities of the generalized Cantor sets*.

Now since

$$\begin{aligned} \sum_{k=1}^m p_k L_k &= p_1 L_1 + p_2 L_2 + \dots + p_m L_m \\ &= \frac{1}{m} \cdot \frac{1}{2m-1} + \frac{1}{m} \cdot \frac{1}{2m-1} + \dots + \frac{1}{m} \cdot \frac{1}{2m-1} \\ &= \frac{1}{2m-1} < 1 \quad \text{for } 2 \leq m < \infty, \end{aligned}$$

then the iterated function system with probabilities of the generalized Cantor sets  $\{(w_k, p_k) : k = 1, 2, \dots, m\}$  are asymptotically stable.

For iterated function system with probabilities of the generalized Cantor sets  $(w, p)_m = \{(w_k, p_k) : k = 1, 2, \dots, m\}$ , we define the transition operator  $P_w : M \rightarrow M$  by the formula

$$P_w \sim(A) = \sum_{k=1}^m \int_{w_k^{-1}(A)} p_k d\sim \quad \text{for } A \in \mathbf{B}(X) \text{ and } \sim \in M. \quad (9.2)$$

**Theorem 9.2.1.** If  $P_w$  satisfies the following two conditions

- (i) Positive linearity:  $P_w(\}_1 \sim_1 + \}_2 \sim_2) = \}_1 P_w \sim_1 + \}_2 P_w \sim_2$  for  $\}_1, \}_2 \geq 0; \sim_1, \sim_2 \in M$
- (ii) Preservation of the norm:  $P_w \sim(A) = \sim(A)$  for  $\sim \in M$ , then  $P_w$  is a Markov operator for IFSPGCS  $(w, p)_m$ .

**Proof:** Let  $X = [0,1]$ . Let  $(X, \dots)$  be a complete separable metric space. The iterated function systems  $w_k : X \rightarrow X$  is defined by  $w_k(x) = \frac{x}{2m-1} + \frac{2(k-1)}{2m-1}$ ,  $p_k = \frac{1}{m}$ , for

$2 \leq m < \infty$  and  $1 \leq k \leq m$ . Let  $A = [0, \frac{1}{2m-1}] \cup [\frac{2}{2m-1}, \frac{3}{2m-1}] \cup \dots \cup [\frac{2(m-1)}{2m-1}, 1] \subset X$ .

(i) By (9.2) we have

$$\begin{aligned} P_w(\}_1 \sim_1 + \}_2 \sim_2)(A) &= \sum_{k=1}^m \int_{w_k^{-1}(A)} p_k (\}_1 d\sim_1 + \}_2 d\sim_2) \\ &= \sum_{k=1}^m \int_0^1 p_k (\}_1 d\sim_1 + \}_2 d\sim_2) = \sum_{k=1}^m \int_0^1 p_k \}_1 d\sim_1 + \sum_{k=1}^m \int_0^1 p_k \}_2 d\sim_2 = \}_1 + \}_2 \end{aligned}$$

$$\begin{aligned} \text{and } \}_1 P_w \sim_1 + \}_2 P_w \sim_2 &= \}_1 \sum_{k=1}^m \int_{w_k^{-1}(A)} p_k d\sim_1 + \}_2 \sum_{k=1}^m \int_{w_k^{-1}(A)} p_k d\sim_2 \\ &= \}_1 \sum_{k=1}^m \int_0^1 p_k d\sim_1 + \}_2 \sum_{k=1}^m \int_0^1 p_k d\sim_2 = \}_1 + \}_2 \end{aligned}$$

That is  $P_w(\}_1 \sim_1 + \}_2 \sim_2) = \}_1 P_w \sim_1 + \}_2 P_w \sim_2$  for  $\}_1, \}_2 \geq 0; \sim_1, \sim_2 \in M$ .

(ii) By (9.2) we have

$$P_w \sim(A) = \sum_{k=1}^m \int_{w_k^{-1}(A)} p_k d\sim = \sum_{k=1}^m \int_0^1 p_k d\sim = 1$$

$$\text{and } \sim(A) = \sim[0, \frac{1}{2m-1}] + \sim[\frac{2}{2m-1}, \frac{3}{2m-1}] + \dots + \sim[\frac{2(m-1)}{2m-1}, 1]$$

$$= \int_0^{\frac{1}{2m-1}} \frac{2m-1}{m} d\sim + \int_{\frac{2}{2m-1}}^{\frac{3}{2m-1}} \frac{2m-1}{m} d\sim + \dots + \int_{\frac{2(m-1)}{2m-1}}^1 \frac{2m-1}{m} d\sim = 1$$

[Using function of section 8.3.3 of Chapter 8]

That is,  $P_w \sim(A) = \sim(A)$  for  $\sim \in M$ .

Thus  $P_w$  is a Markov operator for IFSPGCS  $(w, p)_m$ . □

By the second condition of theorem 9.2.2 we can easily show that  $P_w \sim = \sim$  for  $\sim \in M$ . That is,  $P_w$  has a stationary or invariant measure  $\sim$ .

Thus we say that  $\sim \in M$  is a invariant measure for  $(w, p)_m$ .

Following Lasota and Yorke [46] we have a sequence of transformations

$$w_k : X \rightarrow X, \quad k = 1, 2, \dots, m.$$

and a probabilities vector  $\{p_1(x), p_2(x), \dots, p_m(x)\}$ ,  $p_k(x) \geq 0$ ,  $\sum_{k=1}^m p_k(x) = 1$  for  $x \in X$ ,  $k = 1, 2, \dots, m$ . If an initial point  $x_0$  is chosen, then we randomly select from the set  $\{1, 2, 3, \dots, m\}$  an integer such a way that probability of choosing  $k$  is  $p_k(x_0)$ ,  $k = 1, 2, \dots, m$ . When a number  $k_0$  is drawn we define  $x_1 = w_{k_0}(x_0)$ . Having  $x_1$  we select  $k_1$  according to the distribution  $p_k(x_1)$ ,  $k = 1, 2, \dots, m$  and we define  $x_2 = w_{k_1}(x_1)$  and so on. Denoting by  $\sim_n, n = 0, 1, \dots$  the distribution of  $x_n$ . i.e.,  $\sim_n(A) = \text{prob}(x_n \in A)$  for every non-negative integer  $n$ . We define  $P_w$  as transition operator such that  $\sim_{n+1} = P_w \sim_n$ , where  $\sim_n$  is the sequence of measures.

The above procedure can be easily formalized. Let  $\sim_0 = u_x$  be the Dirac measure supported at a point  $x \in X$ . According to the definition of the dual vector  $U$  we have

$$Uf(x) = \langle Uf, u_x \rangle = \langle f, P_w u_x \rangle = \langle f, \sim_1 \rangle$$

This means that  $Uf(x)$  is mathematical expectation of  $f(x_1)$  if  $x_0 = x$  is fixed.

On the other hand, according to our description, the expectation of  $f(x_1)$  is equal to

$$\sum_{k=1}^m p_k(x) f(w_k(x)).$$

Since  $x$  was arbitrary this gives

$$Uf(x) = \sum_{k=1}^m p_k(x) f(w_k(x)). \tag{9.3}$$

We admits this formula as the precise formal definition of our process and we define  $P_w$  as the Markov operator corresponding to  $U$  given by (9.3).

Therefore,  $P_w$  is the unique operator satisfying

$$\langle f, P_w \sim \rangle = \langle Uf, \sim \rangle = \sum_{k=1}^m \int_X p_k (f \circ w_k) d\sim \tag{9.4}$$

and it must be of the form

$$P_w \sim(A) = \sum_{k=1}^m \int_{w_k^{-1}(A)} p_k d\sim \tag{9.5}$$

For such  $P_w$ , equation (9.4) holds for every bounded Borel measurable  $f$  and  $\sim \in M$ . Equation (9.5) is the desired formal definition of Markov operator  $P_w$ .



Since the transformations  $w_k : X \rightarrow X$ , and the functions  $p_k : X \rightarrow \mathbf{R}$  for  $k = 1, 2, \dots, m$  are continuous,  $P_w$  given by (9.5) is a Feller operator.

Now we will study asymptotic behavior of  $P_w$  under some additional assumptions concerning  $p_k$  and  $w_k$ . We will say that the iterated function system with probabilities of the generalized Cantor sets  $(w, p)_m = \{(w_k, p_k) : k = 1, 2, \dots, m\}$  is non-expansive, has an invariant density or is asymptotically stable if the Markov operator (9.5) has the corresponding property.

We say that iterated function system with probabilities of the generalized Cantor sets  $(w, p)_m$  is asymptotically stable if  $P_w$  is asymptotically stable. Now we will formulate assumptions that ensure the non-expansiveness and asymptotic stability of iterated function system with probabilities of the generalized Cantor sets  $(w, p)_m = \{(w_k, p_k) : k = 1, 2, \dots, m\}$ .

### 9.3. Non-expansiveness of IFS with probabilities of the Generalized Cantor Sets

**Lemma 9.3.1.** The iterated function system with probabilities of the generalized Cantor sets  $(w, p)_m$  is uniform continuous. That is,  $w_k(x) = \frac{x}{2m-1} + \frac{2(k-1)}{2m-1}$  is uniform continuous for  $x, y \in X$ ,  $(2 \leq m < \infty)$  and  $1 \leq k \leq m$ .

**Proof.** Choose  $v > 0$ . Let  $u = (2m-1)v$ . Choose  $x_0, x \in X$ . Assume that  $|x - x_0| < u$ . Then

$$|w_k(x) - w_k(x_0)| = \left| \frac{x}{2m-1} - \frac{x_0}{2m-1} \right| = \frac{1}{2m-1} |x - x_0| < \frac{1}{2m-1} u = v$$

i.e.,  $|w_k(x) - w_k(x_0)| < v$ .

Thus IFS with probabilities of the generalized Cantor sets  $(w, p)_m$  is uniform continuous.

**Lemma 9.3.2.** The IFSPGCS  $(w, p)_m$  satisfies the Dini function if there is a function  $\check{S} : [0, \infty] \rightarrow [0, \infty]$  is a modulus of continuity for  $w_k$ . That is,  $|w_k(x) - w_k(y)| \leq \check{S}(|x - y|)$  for  $x, y \in X$ .

**Proof.** Assume that  $\check{S} : [0, \infty] \rightarrow [0, \infty]$  is defined by  $\check{S}(t) = kt$ , where  $k$  is a Lipschitz constant.

Now  $|w_k(x) - w_k(y)| = \left| \frac{x}{2m-1} + \frac{2(k-1)}{2m-1} - \frac{y}{2m-1} - \frac{2(k-1)}{2m-1} \right|$   
 $= \frac{1}{2m-1} |x - y| = L_k |x - y| = \check{S}(|x - y|)$ , where  $L_k = \frac{1}{2m-1}$  is a Lipschitz constant for  $(2 \leq m < \infty)$  and  $1 \leq k \leq m$ .

That is,  $|w_k(x) - w_k(y)| \leq \check{S}(|x - y|)$  for  $x, y \in X$ .

Thus  $S$  is a Dini function of the IFSPGCS  $(w, p)_m$ . □

**Lemma 9.3.3.** If the IFSPGCS  $(w, p)_m$  satisfies the inequality

$\sum_{k=1}^m p_k(x) \dots (w_k(x), w_k(y)) \leq r(\dots(x, y))$  for  $x, y \in X$ , where  $r < 1$  is a non-negative constant, then  $(w, p)_m$  is contraction transformation with contracting factor or Lipschitz constant  $L_k = \frac{1}{2m-1}$  for  $(2 \leq m < \infty)$  and  $1 \leq k \leq m$ .

**Proof.** The IFSPGCS  $(w, p)_m$  is  $w_k(x) = \frac{x}{2m-1} + \frac{2(k-1)}{2m-1}$ ,  $p_k = \frac{1}{m}$ , for  $x, y \in X$ , where

$p_k(x)$  are probabilities such that  $\sum_{k=1}^m p_k(x) = 1$  for every  $x \in X$ .

Now

$$\begin{aligned} \sum_{k=1}^m p_k(x) \dots (w_k(x), w_k(y)) &= \sum_{k=1}^m p_k(x) \|w_k(x) - w_k(y)\| \\ &= \sum_{k=1}^m p_k(x) \left\| \left( \frac{x}{2m-1} + \frac{2(k-1)}{2m-1} \right) - \left( \frac{y}{2m-1} + \frac{2(k-1)}{2m-1} \right) \right\| \\ &= \sum_{k=1}^m p_k(x) \left\| \frac{x}{2m-1} - \frac{y}{2m-1} \right\| = \sum_{k=1}^m p_k(x) \frac{1}{2m-1} \|x - y\| = L_k \cdot \dots(x, y) \end{aligned}$$

That is,  $\sum_{k=1}^m p_k(x) \dots (w_k(x), w_k(y)) \leq r(\dots(x, y))$  for  $x, y \in X$ , say  $r = L_k = \frac{1}{2m-1}$ .

Thus  $(w, p)_m$  is contraction transformation with contracting factor or Lipschitz constant  $L_k = \frac{1}{2m-1}$  for  $(2 \leq m < \infty)$  and  $1 \leq k \leq m$ . □

Since there exists a Dini function of the IFSPGCS  $(w, p)_m$ , there exists a continuous non-decreasing and concave function  $\check{\cdot} : [0, \infty] \rightarrow [0, \infty]$  such that  $\check{\cdot}(0) = 0, \check{\cdot}(\infty) = \infty$  and the Markov operator  $P_w$  corresponding to  $(w, p)_m$  is non-expansive with respect to the metric  $\check{\cdot}(\dots(x, y)) = \dots_{\check{\cdot}}(x, y)$  for  $x, y \in X$ , that is, we will calculate the value of  $\|P_w(\sim_1 - \sim_2)\|$  for operator (9.5).

$$\begin{aligned} \|P_w(\sim_1 - \sim_2)\| &= \|P_w \sim_1 - P_w \sim_2\| = \sup_{F_{\check{\cdot}}} | \langle f, P_w \sim_1 - P_w \sim_2 \rangle | = \sup_{F_{\check{\cdot}}} | \langle Uf, \sim_1 - \sim_2 \rangle | \\ &= \sup_{F_{\check{\cdot}}} | \langle \sum_{k=1}^m p_k(f \circ w_k), \sim_1 - \sim_2 \rangle | = \sup_{F_{\check{\cdot}}} | \langle \sum_{k=1}^m p_k f(w_k), \sim_1 - \sim_2 \rangle | \\ &= \sup_{F_{\check{\cdot}}} | \langle 1, \sim_1 - \sim_2 \rangle | = \sup_{F_{\check{\cdot}}} | \langle f, \sim_1 - \sim_2 \rangle | = \| \sim_1 - \sim_2 \| \end{aligned}$$

That is,  $\|P_w(\sim_1 - \sim_2)\| = \| \sim_1 - \sim_2 \|$

Thus  $P_w$  is non-expansive with respect to the metric  $\check{\cdot} \circ \dots$

Since the IFSPGCS  $(w, p)_m$  satisfies the Lemma 9.3.3 and the Markov operator  $P_w$  corresponding to  $(w, p)_m$  is non-expansive with respect to the metric  $\{ \circ \dots$ , the iterated function system of the generalized Cantor sets  $(w, p)_m$  is non-expansive with respect to the metric  $\{ \circ \dots$ .

**Theorem 9.3.4.** Let  $P_w$  be a non-expansive Markov operator. Assume that for every  $\nu > 0$  there is a Borel set  $A$  with  $\text{diam } A \leq \nu$ , a real number  $\tau > 0$  and an integer  $n$  such that

$$\liminf_{n \rightarrow \infty} P_w^n \sim(A) \geq \tau \text{ for } \sim \in M_1. \tag{9.6}$$

Then  $P_w$  is asymptotically stable.

**Proof:** Since a non-expansive Markov operator is a Feller operator,  $P_w$  is a Feller operator. Then  $P_w$  has an invariant distribution  $\sim_*$ . To complete the proof of asymptotic stability it remains to verify condition

$$\lim_{n \rightarrow \infty} \langle f, \sim_n \rangle = \langle f, \sim \rangle \text{ for all } f \in C(X).$$

When an invariant distribution exists the above condition is equivalent to a more symmetric relation

$$\lim_{n \rightarrow \infty} \| P_w^n(\sim_1 - \sim_2) \| = 0 \text{ for } \sim_1, \sim_2 \in M_1. \tag{9.7}$$

Let  $\sim_1, \sim_2 \in M_1$  and  $\nu > 0$ . Choose  $A \subset X$  and  $\tau, 0 < \tau < 1$ . Following Lasota and Yorke [39] we will define by an induction argument a sequences of integers  $(n_k)$  and four sequences of distributions  $(\sim_i^k), (\epsilon_i^k), k = 0, 1, 2, \dots, i = 1, 2$ . If  $k = 0$  we define  $n_0 = 0$  and  $\epsilon_i^0 = \sim_i^0 = \sim_i$ . If  $k \geq 1$  is fixed and  $n_{k-1}, \sim_i^{k-1}, \epsilon_i^{k-1}$  are given we choose according (9.6) a number  $n_k$  such that

$$P_w^{n_k} \sim_i^{k-1}(A) \geq \tau \text{ for } i = 1, 2.$$

and we define

$$\begin{aligned} \epsilon_i^k(B) &= \frac{P_w^{n_k} \sim_i^{k-1}(B \cap A)}{P_w^{n_k} \sim_i^{k-1}(A)} \\ \sim_i^k(B) &= \frac{1}{1-\tau} \{ P_w^{n_k} \sim_i^{k-1}(B) - \tau \epsilon_i^{k-1}(B) \}. \end{aligned} \tag{9.8}$$

Since  $P_w^{n_k} \sim_i^{k-1}(A) \geq \tau$ , we have

$$P_w^{n_k} \sim_i^{k-1}(B) = P_w^{n_k} \sim_i^{k-1}(B \cap A) = P_w^{n_k} \sim_i^{k-1}(A) \epsilon_i^k(B) \geq \tau \epsilon_i^k(B).$$

Observe that  $\epsilon_i^k(X \setminus A) = 0$  and consequently

$$\| \epsilon_1^k - \epsilon_2^k \| = \sup_{f \in F} \left| \int_X f d\epsilon_1^k - \int_X f d\epsilon_2^k \right| = \sup_{f \in F} \left| \int_A f d\epsilon_1^k - \int_A f d\epsilon_2^k \right| \leq \text{diam } A \leq \nu. \tag{9.9}$$

Using equation (9.8) it is easy to verify by an induction argument that

$$P_w^{n_1+\dots+n_k} \sim_i = \dagger P_w^{n_2+\dots+n_k} \epsilon_i^1 + \dagger (1-\dagger) P_w^{n_2+\dots+n_k} \epsilon_i^2 + \dots + \dagger (1-\dagger)^{k-1} \epsilon_i^k + (1-\dagger)^k \sim_i^k, k \geq 1.$$

Since  $P_w$  is non-expansive this implies

$$\| P_w^{n_1+\dots+n_k} (\sim_1 - \sim_2) \| \leq \dagger \| \epsilon_1^1 - \epsilon_2^1 \| + \dagger (1-\dagger) \| \epsilon_1^2 - \epsilon_2^2 \| + \dots + \dagger (1-\dagger)^{k-1} \| \epsilon_1^k - \epsilon_2^k \| + (1-\dagger)^k \| \sim_1^k - \sim_2^k \|.$$

From this, condition (9.9) and the obvious inequality  $\| \sim_1^k - \sim_2^k \| \leq 2$  it follows

$$\| P_w^{n_1+\dots+n_k} (\sim_1 - \sim_2) \| \leq v + 2(1-\dagger)^k$$

Again, using the non-expansiveness of  $P_w^n$  we obtain

$$\| P_w^n (\sim_1 - \sim_2) \| \leq v + 2(1-\dagger)^n \text{ for } n \geq n_1 + \dots + n_k.$$

Since  $v > 0$  is arbitrary and  $k$  does not depend on  $\sim_1, \sim_2$  we have

$$\| P_w^n \sim_1 - P_w^n \sim_2 \| \leq v \text{ for } n \geq n_0 \text{ and every two measures } \sim_1, \sim_2 \in M_1.$$

So, we are given

$$\| P_w^n \sim - P_w^m \sim \| \leq v \text{ for } n, m \geq n_0 \text{ and every } \sim \in M_1.$$

Really, if  $n > m$  we have

$$P_w^n \sim = P_w^m (P_w^{n-m} \sim)$$

and because  $m \geq n_0$

$$\| P_w^m (\sim - P_w^{n-m} \sim) \| \leq v.$$

Since  $M_1$  is a complete metric space, the sequence  $(P_w^n \sim : n \in \mathbf{N})$  converges to some  $\sim_* \in M_1$ . Obviously  $P_w \sim_* = \sim_*$  and

$$\lim_{n \rightarrow \infty} \| P_w^n \sim - \sim_* \| = \lim_{n \rightarrow \infty} \| P_w^n (\sim - \sim_*) \| = 0 \text{ for every } \sim \in M_1.$$

This completes the proof. □

#### 9.4. Asymptotic Stability of IFS with probabilities of the Generalized Cantor Sets

**Theorem 9.4.1.** Let  $(w, p)_m = \{(w_k, p_k) : k = 1, 2, \dots, m\}$  be iterated function system with probabilities of the generalized Cantor set. If  $(w, p)_m$  satisfies the following conditions

- (i) there is a Dini function of  $(w, p)_m$
- (ii)  $\inf_{x \in X} p_k(x) > 0$  for every  $k \in \{1, 2, \dots, m\}$
- (iii) the transformations  $w_k : X \rightarrow X$  are Lipschitzian for every  $k \in \{1, 2, \dots, m\}$  and there

exists a non-negative integer  $\} _w$  such that  $\sum_{k=1}^m p_k(x) L_k \leq \} _w < 1$  for  $x \in X$ ,

then the iterated function system with probabilities of the generalized Cantor sets  $(w, p)_m$  is asymptotically stable.

**Proof:** (i) By Lemma 9.3.1, we say that the IFSPGCS  $(w, p)_m$  has a Dini function.

(ii) Since  $p_k(x) = \frac{1}{m}$  for  $2 \leq m < \infty$  and  $1 \leq k \leq m$ , clearly  $\inf_{x \in X} p_k(x) > 0$  for every  $k \in \{1, 2, \dots, m\}$ .

(iii) Since  $w_k(x) = \frac{x}{2m-1} + \frac{2(k-1)}{2m-1}$ ,  $p_k = \frac{1}{m}$ , is a Lipschitzian with Lipschitz's constant

$L_k = \frac{1}{2m-1}$  for  $x, y \in X$ ,  $2 \leq m < \infty$  and  $1 \leq k \leq m$ , then

$$\begin{aligned} \sum_{k=1}^m p_k(x)L_k &= p_1(x)L_1 + p_2(x)L_2 + \dots + p_m(x)L_m \\ &= \frac{1}{m} \cdot \frac{1}{2m-1} + \frac{1}{m} \cdot \frac{1}{2m-1} + \dots + \frac{1}{m} \cdot \frac{1}{2m-1} = \frac{1}{2m-1} \end{aligned}$$

That is,  $\sum_{k=1}^m p_k(x)L_k = \frac{1}{2m-1}$  for  $2 \leq m < \infty$ .

and

$$\} _w = \sup_{x \in X} \sum_{k=1}^m p_k(x)L_k = \frac{1}{3} \text{ for } m = 2.$$

Thus  $\sum_{k=1}^m p_k(x)L_k \leq \} _w < 1$  for  $x \in X$ ,

Since the IFSPGCS  $(w, p)_m$  satisfies the above three conditions, the IFS with probabilities of the generalized Cantor sets  $(w, p)_m$  is asymptotically stable.  $\square$

We say that a Markov operator  $P_w : M_T M$  satisfies the Prokhorov condition if there exists a compact set and a number  $S$  such that

$$\liminf_{n \rightarrow \infty} P_w^n \sim(Y) \geq S \text{ for } \sim \in M_1. \tag{9.10}$$

This condition is clearly satisfied if  $X$  is a compact space or if  $P_w$  is an asymptotically stable operator.

**Proposition 9.4.2.** Let  $(w, p)_m = \{(w_k, p_k) : k = 1, 2, \dots, m\}$  be an iterated function system with probabilities of the generalized Cantor sets such that  $w_1$  is bounded and  $\inf p_1 > 0$ . Then  $(w, p)_m = \{(w_k, p_k) : k = 1, 2, \dots, m\}$  has a stationary distribution and satisfies the Prokhorov condition  $\liminf_{n \rightarrow \infty} P_w^n \sim(Y) \geq S$  for  $\sim \in M_1$ , where  $Y$  is a compact set and a number  $S$ .

**Proof.** We know  $P_w \sim(A) = \sum_{k=1}^m \int_{w_k^{-1}(A)} p_k d\sim$  corresponding to  $(w, p)_m$ .

Let  $Y = [0, \frac{1}{3}] \cup [\frac{2}{3}, 1] \supset w_1(X)$  be a compact set. For every  $\sim \in M_1$  we have

$$P_w \sim(Y) = \sum_{k=1}^m \int_{w_k^{-1}(Y)} p_k d\sim = 1$$

That is,  $P_w^n \sim(Y) = \sum_{k_1=1}^m \cdots \sum_{k_n=1}^m \int P_{k_n}(w_{k_{n-1}} \circ \dots \circ w_{k_1}(x)) \cdots P_{k_1}(x) d\sim = 1$

and

$$\sim(w_1^{-1}(Y)) \inf\{p_1\} = \sim([0,1]) \inf\{p_1\} = \frac{1}{2} = S \text{ (say).}$$

Thus  $\liminf_{n \rightarrow \infty} P_w^n \sim(Y) \geq S$  for  $\sim \in M_1$ . □

**Theorem 9.4.3.** Suppose iterated function system with probabilities of the generalized Cantor sets  $(w, p)_m = \{(w_k, p_k) : k = 1, 2, \dots, m\}$  are essentially non-expansive and satisfies the Prokhorov condition. Also suppose that  $w_1$  satisfies the inequality

$$\sum_{k=1}^m p_k(x) \dots (w_1(x), w_1(y)) \leq r \dots (x, y) \text{ for } x, y \in X, \tag{9.11}$$

where  $r < 1$  is a non-negative constant, and has an attracting fixed point  $x_*$ , then

$$\lim_{n \rightarrow \infty} \dots (w_1^n(x), x_*) = 0 \text{ for } x \in X$$

If in addition  $\inf\{p_1\} > 0$ , then  $(w, p)_m = \{(w_k, p_k) : k = 1, 2, \dots, m\}$  is asymptotically stable.

**Proof.** Following Lasota and Yorke [46] consider the dynamical system  $(w_1, \frac{1}{2})$  given by only one transformation  $w_1$  and the probability  $\frac{1}{2}$ . Condition (9.11) implies that  $(w_1, \frac{1}{2})$  is non-expansive. The Markov operator  $P_w$  corresponding to  $(w_1, \frac{1}{2})$  is given by formula

$$P_w \sim(A) = \sum_{k=1}^m \int P_k d\sim = \sim(w_1^{-1}(A)) \text{ for } A = [0, \frac{1}{3}] \cup [\frac{2}{3}, 1] \subset X,$$

and has the property that a point measure  $\sim = u_x$  is transformed into the point measure  $P_w \sim = u_{w_1(x)}$ . For every  $x_0 \in X$  the sequence  $x_n = w_1^n(x_0)$  converges to attracting fixed point  $x_*$  and consequently for every  $x_0 \in X$  the sequence of measures  $P_w^n u_{x_0} = u_{x_n}$  converges weakly to  $u_{x_*} = P_w u_{x_*}$ .

Since the family of Dirac measures is linearly dense in  $M_1$  (in the Fortet Mourier metric) and the operators  $\{P_w^n\}$  are uniformly continuous, we have

$$\lim_{n \rightarrow \infty} \|P_w^n \sim - u_{x_*}\| = 0 \text{ for } \sim \in M_1.$$

Thus the system  $(w_1, \frac{1}{2})$  is asymptotically stable. □

# CHAPTER Ten

## SCIENTIFIC APPROACH OF FRACTALS

### OVERVIEW

In this chapter, we have presented some applications of fractals (without proof) by renowned mathematicians. These will help to go through further research.

### 10.1. [53] Fractals in Nature and Applications

Fractals are not just complex shapes and pretty pictures generated by computers. Anything that appears random and irregular can be a fractal. Fractals permeate our lives, appearing in places as tiny as the membrane of a cell and as majestic as the solar system. Fractals are the unique, irregular patterns left behind by the unpredictable movements of the chaotic world at work. In theory, one can argue that everything existent on this world is a fractal.

- the leaves in trees,
- the veins in a hand,
- water swirling and twisting out of a tap,
- a puffy cumulus cloud,
- tiny oxygen molecule, or the DNA molecule,
- the stock market

Fractals have more and more applications in science as follows:

#### 10.1.1. Fractals in Nature

Take a tree, for example. Pick a particular branch and study it closely. Choose a bundle of leaves on that branch. All three of the objects described - the tree, the branch, and the leaves – are identical. To many, the word chaos suggests randomness, unpredictability and perhaps even messiness. Weather is a favorite example for many people. Forecasts are never totally accurate, and long-term forecasts, even for one week, can be totally wrong. This is due to minor disturbances in airflow, solar heating, etc. Each disturbance may be minor, but the change it creates will increase geometrically with time. Soon, the weather will be far different than what was expected. With fractal geometry we can visually model much of what we witness in nature, the most recognized being coastlines and mountains. Fractals are used to model soil erosion and to analyze seismic patterns as well.

#### 10.1.2. [53] Fractals in Astronomy

Fractals will maybe revolutionize the way that the universe is seen. Cosmologists usually assume that matter is spread uniformly across space. But observation shows that this is not true. Astronomers agree with that assumption on "small" scales, but most of them think that the universe is smooth at very large scales. However, a dissident group of scientist's claims that the structure of the universe is fractal at all scales.

### **10.1.3. Fractals in Computer Science**

The biggest use of fractals in everyday life is in computer science. Many image compression schemes use fractal algorithms to compress computer graphics to less than a quarter of their original size [57]. Actually, the most useful use of fractals in computer science is the fractal image compression. This kind of compression uses the fact that the real world is well described by fractal geometry. By this way, images are compressed much more than by usual ways (e.g.: JPEG or GIF file formats). Another advantage of fractal compression is that when the picture is enlarged, there is no pixelisation. The picture seems very often better when its size is increased [53].

### **10.1.4. [53] Fractals in Fluid Mechanics**

The study of turbulence in flows is very adapted to fractals. Turbulent flows are chaotic and very difficult to model correctly. A fractal representation of them helps engineers and physicists to better understand complex flows. Flames can also be simulated. Porous media have a very complex geometry and are well represented by fractal. This is actually used in petroleum science.

### **10.1.5. [53] Fractals in Surface Physics**

Fractals used to describe the roughness of surfaces. A rough surface characterized by a combination of two different fractals.

### **10.1.6. [54] Fractals in Physiology and Medicine**

The nonlinear fractals provide insights into the organization of complex structures such as the tracheobronchial tree and heart as well as into the dynamics of healthy physiological variability. Alterations in fractals scaling may underlie a number of pathophysiological disturbances, including sudden cardiac death syndromes. Also biosensor interactions can be studied by using fractals.

#### **10.1.6.1. [55] Fractals in Physiology**

Some of the most visually striking examples of fractal forms are found in physiology such as the respiratory, the circulatory, and the nervous systems are remarkable instances of fractal structure, branches subdividing and subdividing and subdividing again. Careful analysis of the lung reveal fractal scaling, and it has been noted that this fractal structure makes the lungs more fault-tolerant during growth.

#### **10.1.6.2. [56] Fractals in Biological Time Series**

The fractal concept can be applied not just to irregular geometric forms that lack a characteristic (single) scale of length, but also to certain complex processes generate irregular fluctuations across multiple time scales, analogous to scale-invariant objects that have a branching of wrinkly structure across multiple length scales. The irregularity seen on different scales is not readily distinguishable, suggesting statistically self-similarity.



### **10.1.7. [53] Fractals in Telecommunications**

A new application is fractal-shaped antenna that reduces greatly the size and the weight of the antennas. The benefits depend on the fractal applied, frequency of interest, and so on. In general, the fractal parts produce ‘fractal loading’ and make the antenna smaller for a given frequency of use. Practical shrinkage of 2-4 times are realizable for acceptable performance. Surprisingly high performance is attained.

## **10.2. Some Applications of Fractals by Renowned Mathematicians**

### **10.2.1. Fractals and Cancer [James W. Baish, and Rakesh K. Jain, 2000]**

Abstract: Recent studies have shown that fractal geometry, a vocabulary of irregular shapes, can be useful for describing the pathological architecture of tumors and, perhaps more surprisingly, for yielding insights into the mechanisms of tumor growth and angiogenesis that complement those obtained by modern molecular methods. This article outlines the basic methods of fractal geometry and discusses the value and limitations of applying this new tool to cancer research.

### **10.2.2. Microbial Growth Patterns described by Fractal Geometry [M Obert, P Pfeifer and M Sernetz, 1990]**

Abstract: Fractal geometry has made important contributions to understanding the growth of inorganic systems in such processes as aggregation, cluster formation, and dendritic growth. In biology, fractal geometry was previously applied to describe, for instance, the branching system in the lung airways and the backbone structure of proteins as well as their surface irregularity. This investigation applies the fractal concept to the growth patterns of two microbial species, *Streptomyces griseus* and *Ashbya gossypii*. It is a first example showing fractal aggregates in biological systems, with a cell as the smallest aggregating unit and the colony as an aggregate. We find that the global structure of sufficiently branched mycelia can be described by a fractal dimension,  $D$ , which increases during growth up to 1.5.  $D$  is therefore a new growth parameter. Two different box-counting methods (one applied to the whole mass of the mycelium and the other applied to the surface of the system) enable us to evaluate fractal dimensions for the aggregates in this analysis in the region of  $D = 1.3$  to 2. Comparison of both box-counting methods shows that the mycelial structure changes during growth from a mass fractal to a surface fractal.

### **10.2.3. Fractals in the Nucleus [James G McNally and Davide Mazza, 2009]**

Abstract: Fractals are “self-similar” meaning that they exhibit similar fine-scale features at many magnifications. Over 20 years ago it was argued that folded polymers, including chromatin, should be fractals. The rationale was that as a polymer condenses it is repeatedly subject to the same constraints. Specifically, polymer strands as well as partially folded clumps of the polymer are all impenetrable. Thus, through the self-similar process of crumpling, the resultant condensed polymer becomes a fractal. This ‘fractal globule’ structure, as it is called, has advantages because it provides an efficient means to

package a long polymer in a small volume without entanglements. This facilitates unraveling the polymer when necessary, for example to gain access to specific DNA segments for transcription, replication or repair.

#### **10.2.4. Fractal Geometry of Airway Remodeling in Human Asthma** [Stacey R. Boser, Hannah Park, Steven F. Perry, Margaret G. Ménache and Francis H. Y. Green, 2005]

*Rationale:* Airway wall remodeling is an important aspect of asthma. It has proven difficult to assess quantitatively as it involves changes in several components of the airway wall.

*Objective:* To develop a simple method for quantifying the overall severity of airway wall remodeling in asthmatic airways using fractal geometry.

*Methods:* Negative-pressure silicone rubber casts of lungs were made using autopsy material from three groups: fatal asthma, nonfatal asthma, and nonasthma control. All subjects were lifelong nonsmokers. A fractal dimension was calculated on two-dimensional digital images of each cast.

*Results:* Nonasthma control casts had smooth walls and dichotomous branching patterns with nontapering segments. Asthmatic casts showed many abnormalities, including airway truncation from mucous plugs, longitudinal ridges, and horizontal corrugations corresponding to elastic bundles and smooth muscle hypertrophy, respectively, and surface projections associated with ectatic mucous gland ducts. Fractal dimensions were calculated from digitized images using an information method. The average fractal dimensions of the airways of both the fatal asthma and nonfatal asthma groups were significantly lower than that of the nonasthma control group. The lower fractal dimension of asthmatic airways correlated with a decreased overall structural complexity and pathologic severity of disease.

#### **10.2.5. Image Compression: A study of the iterated transform method** [E.W. Jacobs, Y. Fisher and R. D. Boss, 1992]

*Abstract:* This paper presents result from an image compression scheme based on iterated transforms. Result are examined as a function of several encoding parameters including maximum allowed scale factor, number of domains, resolution of scale and offset values, minimum range size, and target fidelity. The performance of the algorithm, evaluated by means of fidelity versus the amount of compression, is computed with an adaptive discrete cosine transform image compression method over a wide range of compression.

#### **10.2.6. Image Coding Based on a Fractal Theory of Iterated Contractive Image Transformations** [Amaud E. Jacquin, 1992]

*Abstract:* The conception of digital image coding techniques is of great interest in various areas concerned with the storage of transformation of images. For the past few years, there has been a tendency to combine different classical coding techniques in order to obtain greater coding efficiency.

This paper presents an independent and novel approach to image coding, based on a fractal theory of iterated transformations. The main characteristic of this approach are that (i) it

relies on the assumption that image redundancy can be efficiently exploited through self-transformability on a block-wise basis, and (ii) it approximates an original image by a fractal image. We therefore, refer to our approach as fractal block coding.

The coding-decoding system is based on the construction, for an original image to encode, or a specific image transformation-a fractal code-which, when iterated on any initial image, produce a sequence of images which converges to a fractal approximation of the original. We show how to design such a system for the coding of monochrome digital image at rates in the range of 0.5-1.0 b/pixel. Our fractal coder has performance comparable to state-of-the-art vector quantizers, with which it shares some aspect. Extremely promising coding results are obtained.

### 10.2.7. Fractals Block Coding Method Based on Iterated Function Systems

Following H. W. Tin, S. W. Leu, H. Sasaki, S. H. Chang [58]. Mandelbrot based the idea of self-similarity and demonstration how “fractal” sets could be regarded as limits of iteration involving generators in [59]. In other words, a fractal object is an object which can be assembled by its subdivided parts similar to the whole exactly or statistically. This concept leads to the creation of a class of fractal image coding methods. The first fractals block coding pioneered by Jacquin [60] and Barnsley [61, 62]. The fractal block coding seeks to approximate the image based on the sub blocks of that image. The basic theory of Jacquin’s block coding method is described as follows:

Let  $I$  be a grayscale image. In fractal block coding, image  $I$  is partitioned into non-overlapping range blocks  $R_i, i=1,2,\dots,N$ , so that  $I=\cup R_i$  and domain blocks  $D_j \subseteq I, j=1,2,\dots,M$ , where the size of each domain block is larger than that of each range block. To encode an image, each range block will find a domain block most similar to itself from the domain pool, in which the finding is based on minimum mean-squared error criteria. The search is performed with an affine transformation  $w_i$ , such that  $w_i:D_j \rightarrow R_i$  where  $D_j$  is the best matched domain block. A common form of the transformation is shown as:

$$w_i \begin{pmatrix} x \\ y \end{pmatrix} = \begin{pmatrix} a_i & b_i \\ c_i & d_i \end{pmatrix} \begin{pmatrix} x \\ y \end{pmatrix} + \begin{pmatrix} e_i \\ f_i \end{pmatrix} \quad (1)$$

where  $a_i, b_i, c_i$  and  $d_i$  control rotation and scaling, while  $e_i$  and  $f_i$  control linear translation.

Put a constrain to the transformation  $w_i$  for contraction so that for any two points  $p_1$  and  $p_2$ , the distance  $d$  between two points should fulfill the following inequality:

$$d(w_i(p_1), w_i(p_2)) < \gamma d((p_1, p_2)) \quad (2)$$

where  $\gamma$  is a coefficient and  $\gamma < 1$ . To encode an image would start from performing the transformation on domain block for a range block based on equation (1) and (2) it derives the following

$$w_i(D_j) = \gamma D_j + c_0 \quad (3)$$

where  $c_0$  is a coefficient. Theoretically, the union of the affine transformations for all range blocks will form the affine transformation for the whole image as expressed in the following equation [62, 63].

$$\dagger = \bigcup_{i=1}^N w_i \quad (4)$$

The encoding method would seek for a transformation of domain block to the best approximation of a selected range block. To determine the and for exactly transformation on each domain block, it should find the minimum distance between range block and domain block.

$$\min \sum_{n,m} (R_i)_{n,m} - (\dagger (D_j))_{n,m} \quad (5)$$

where  $n$  and  $m$  are size of blocks, usually are set to 2 or 4. The encoding method uses the following distance equation to compare the range block with domain block for determining the best matching:

$$d(\dagger (D_j), R_i) = \sum (\dagger (D_j) - R_i)^2 \quad (6)$$

Image encoding is achieved by recording the  $\dagger$ , the minimal distance, and the respect  $D_j$ . Fractal codes recorded in the codebook can later be used in approximating the range. To decode the image, the coding method would perform the transformation iteratively on some initial image  $\Omega_{init}$  stored in the code book until the encoded image is restored.

The decoding process for  $k$  th iteration is described as follows:

$$\Omega_k = \dagger (\Omega) \mathbb{E} (\Omega)$$

where  $\dagger$  is the transformation and  $\mathbb{E}$  is the ensemble function to assemble the transformation.

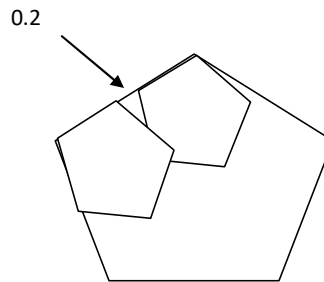
### 10.2.8. Iterated Function Systems Controlled by a Semi-Markov Chain (Orjan Stenplo, 1996)

Abstract: In this paper we consider a finite set of maps  $\{w_1, w_2, \dots, w_m\}, w_i : X \rightarrow X$ , where  $X$  is a complete metric space, together with a sequences  $\{I_n\}$  of random variables taking values in the finite set  $\{1, 2, \dots, m\}$ . This sequence controls the dynamic system  $Z_n = w_{i_{n-1}} \circ \dots \circ w_{i_0}$ . The case where  $\{I_n\}$  is a sequence of independent, identically distributed random variables (or a homogeneous Markov chain) is usually referred to as an iterated function system IFS (or a recurrent IFS). In the present paper, we consider the more general case when the controlling sequence is a semi-Markov chain. Under ‘‘average contractivity’’ conditions, we obtain some ergodic theorems. In applications, these class may broaden the class of images which can be created using iterated function systems.

**10.2.9. [64] Five Vertices and a Compression Factor of 2.5 (Pentaflake)**

Suppose we play the chaos game with the five vertices of a regular pentagon. Using a compression of 2.5, which is midway between 3 and 2.

Based on the location and the number of vertices, we should expect to see a figure that has 5 self-similar copies with compression factor of 2.5; 25 self-similar copies with compression factor of 6.25; etc. If the compression factor were 2, each of the smaller self-similar copies would overlap its neighbors. With a compression factor of 2.5, however, a gap will be left between corresponding sides of the copies. Since  $1/2.5 = 0.4$ , if we let the length of the side of the original pentagon be 1 unit, each of the 5 "largest" self-similar copies will extend for 0.4 units along one of the original sides; the gap between the copies will have length 0.2, as shown in the diagram. We note that the small pentagons have a small overlap. We may change the compression factor to 2.7 to eliminate these overlaps.



The result of playing this chaos game is pictured at right. Here we note that, because of the overlaps described before, there are also some small overlaps in this image.

Again, we may find it helpful to use Fractalina to see the resulting attractor. Though it is fairly easy to estimate coordinates for the vertices of a regular pentagon, finding those points exactly might prove to be an interesting challenge.

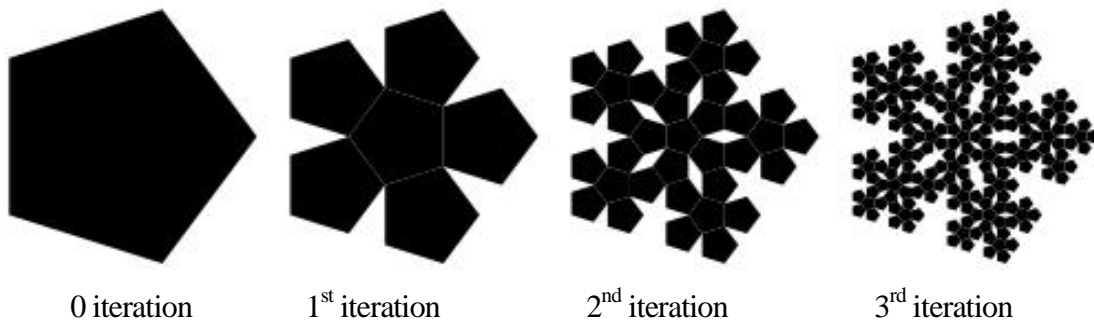


**Figure 10.1** Compression of Pentagon

# APPENDIX

## ALGORITHMS OF FRACTALS

### OVERVIEW

In this appendix, we have presented several programs of Mathematica and MatLab that will enable to display the images of the fractals found in this thesis paper.

#### 11.1. Programs of Two-Dimensional Fractals

11.1.1. The following Mathematica program produces the image of the Sierpinski triangles.

Mathematica Program:

```
f[1]={{0,0},{1,0},{0.5,0.8661}},6);
i=1;
g={};
While[i!=0,k=f[i][[1]];
  n=f[i][[2]];
  i--;
  If[n!=0,g=Join[g,k];
    {f[i+1],f[i+2],f[i+3]}={{#1,Mean[{#1,#2}],Mean[{#1,#3}]},n-
1}&@@@#&/@NestList[RotateLeft,k,2];
  i=i+3]]
Show@Graphics[{EdgeForm[Thin],Black,Polygon@g}]
```

11.1.2. The following Mathematica program produces the image of the Von Koch curve.

Mathematica Program:

```
(*carry out the forward and backward moves and the various
rotations by updating the global location'Lpos' and
direction
angle'Ltheta'.*)Lmove[z_String,Ldelta_]:=Switch[z,"+",Ltheta
+=Ldelta;,"-",Ltheta-
=Ldelta;,"F",Lpos+={Cos[Ltheta],Sin[Ltheta]},"B",Lpos-
={Cos[Ltheta],Sin[Ltheta]},_,Lpos+=0.];LSystem::usage="LSyst
em[axiom,{rules},n,Ldelta:90 Degree] creates the L-string
for the nth iteration of the list 'rules', starting with the
string 'axiom.';(*make the string:starting with'axiom',use
StringReplace the specified number of
times*)LSystem[axiom_,rules_List,n_Integer,Ldelta_:N[90
Degree]]:=Nest[StringReplace[#,rules]&,axiom,n];Off[General:
```

```

:spell1];(*initialize the position'Lpos' and the direction
angle'Ltheta';create the Line graphics primitive represented
by the L-system by mapping'Lmove' over the characters in the
L-string,deleting all the Nulls;then show the Graphics
object*)LShow[lstring_String,Ldelta_:N[90
Degree]]:=(Lpos={0.,0.};Ltheta=0.;Show[Graphics[Line[Prepend
[DeleteCases[Map[Lmove[#,Ldelta]&,Characters[lstring]],Null]
,{0,0}]]],AspectRatio→Automatic]);(*same as above,plus a
list of colors for each segment contained in'templist'--
unfortunately,'templist' isn't really'temp',but stays in
memory as a global variable;so sue
me*)LShowColor[lstring_String,Ldelta_:N[90
Degree]]:=(Lpos={0.,0.};Ltheta=0.;templist=Map[Line,Partitio
n[Prepend[DeleteCases[Map[Lmove[#,Ldelta]&,Characters[lstring
g]],Null],{0,0}],2,1]];ncol=N[Length[templist]];huelist=Tabl
e[Hue[k/ncol],{k,1.,ncol}];Show[Graphics[N[Flatten[Transpose
[{huelist,templist}]]]],AspectRatio→Automatic)];On[General::
spell1];LShowColor[(*Koch curve*)LSystem["F",{ "F"→"F+F--
F+F"},4],N[60 Degree]];

```

11.1.3. The following MatLab program produces the image of the Sierpinski carpet.

MatLab Program:

```

b0=logical([1 1 1;1 0 1;1 1 1]);
for n=1:5 %don't exceed 6 because of expanding array inside loop
    x=logical(zeros(3^n));
    b0=[b0 b0 b0;b0 x b0;b0 b0 b0];
end
imagesc(b0),colormap(gray(2));
imwrite(bn,'sierpinski1.png','png','bitdepth',1);

```

11.1.4. The following Mathematica program produces the image of the square fractal.

Method: First we find the points of attractor of IFS, then we use the Mathematica tools for the image of the square fractal.

```

vertices1={{0,0},{1,0},{1,1},{0,1},{0,0}};
p=Graphics[{Black,Polygon[vertices1]}];
Show[p,AspectRatio→Automatic]

```

```
vert1 = {0, 1, 2, 3, 4, 5, 6, 7, 8, 9, 10, 11, 12, 13, 14, 15, 16, 17, 18, 19, 20, 21, 22, 23, 24, 25, 26, 27, 28, 29, 30, 31, 32, 33, 34, 35, 36, 37, 38, 39, 40, 41, 42, 43, 44, 45, 46, 47, 48, 49, 50, 51, 52, 53, 54, 55, 56, 57, 58, 59, 60, 61, 62, 63, 64, 65, 66, 67, 68, 69, 70, 71, 72, 73, 74, 75, 76, 77, 78, 79, 80, 81, 82, 83, 84, 85, 86, 87, 88, 89, 90, 91, 92, 93, 94, 95, 96, 97, 98, 99};
vert2 = {0, 1, 2, 3, 4, 5, 6, 7, 8, 9, 10, 11, 12, 13, 14, 15, 16, 17, 18, 19, 20, 21, 22, 23, 24, 25, 26, 27, 28, 29, 30, 31, 32, 33, 34, 35, 36, 37, 38, 39, 40, 41, 42, 43, 44, 45, 46, 47, 48, 49, 50, 51, 52, 53, 54, 55, 56, 57, 58, 59, 60, 61, 62, 63, 64, 65, 66, 67, 68, 69, 70, 71, 72, 73, 74, 75, 76, 77, 78, 79, 80, 81, 82, 83, 84, 85, 86, 87, 88, 89, 90, 91, 92, 93, 94, 95, 96, 97, 98, 99};
vert4 = {0, 1, 2, 3, 4, 5, 6, 7, 8, 9, 10, 11, 12, 13, 14, 15, 16, 17, 18, 19, 20, 21, 22, 23, 24, 25, 26, 27, 28, 29, 30, 31, 32, 33, 34, 35, 36, 37, 38, 39, 40, 41, 42, 43, 44, 45, 46, 47, 48, 49, 50, 51, 52, 53, 54, 55, 56, 57, 58, 59, 60, 61, 62, 63, 64, 65, 66, 67, 68, 69, 70, 71, 72, 73, 74, 75, 76, 77, 78, 79, 80, 81, 82, 83, 84, 85, 86, 87, 88, 89, 90, 91, 92, 93, 94, 95, 96, 97, 98, 99};
vert5 = {0, 1, 2, 3, 4, 5, 6, 7, 8, 9, 10, 11, 12, 13, 14, 15, 16, 17, 18, 19, 20, 21, 22, 23, 24, 25, 26, 27, 28, 29, 30, 31, 32, 33, 34, 35, 36, 37, 38, 39, 40, 41, 42, 43, 44, 45, 46, 47, 48, 49, 50, 51, 52, 53, 54, 55, 56, 57, 58, 59, 60, 61, 62, 63, 64, 65, 66, 67, 68, 69, 70, 71, 72, 73, 74, 75, 76, 77, 78, 79, 80, 81, 82, 83, 84, 85, 86, 87, 88, 89, 90, 91, 92, 93, 94, 95, 96, 97, 98, 99};
p = Graphics[Polygon[vert1]];
q = Graphics[Polygon[vert2]];
s = Graphics[Polygon[vert4]];
t = Graphics[Polygon[vert5]];
Show[p, q, s, t, AspectRatio -> Automatic]
```



```

ver11 =
ver12 =
ver13 =
ver14 =
ver21 =
ver22 =
ver23 =
ver24 =
ver41 =
ver42 =
ver43 =
ver44 =
ver51 =
ver52 =
ver53 =
ver54 =

```

```

p1=Graphics[{Black,Polygon[ver11]};
p2=Graphics[{Black,Polygon[ver12]};
p3=Graphics[{Black,Polygon[ver13]};
p4=Graphics[{Black,Polygon[ver14]};
q1=Graphics[{Black,Polygon[ver21]};
q2=Graphics[{Black,Polygon[ver22]};
q3=Graphics[{Black,Polygon[ver23]};
q4=Graphics[{Black,Polygon[ver24]};

```

```

s1=Graphics[{Black,Polygon[ver41]};
s2=Graphics[{Black,Polygon[ver42]};
s3=Graphics[{Black,Polygon[ver43]};
s4=Graphics[{Black,Polygon[ver44]};
t1=Graphics[{Black,Polygon[ver51]};
t2=Graphics[{Black,Polygon[ver52]};
t3=Graphics[{Black,Polygon[ver53]};
t4=Graphics[{Black,Polygon[ver54]};
Show[p1,p2,p3,p4,q1,q2,q3,q4,s1,s2, s3,s4,t1,t2,t3,t4,AspectRatio→Automatic];

```

## 11.2. Programs of Three-Dimensional Fractals

11.2.1. The following Mathematica program produces the image of the Menger sponge.

Mathematica Program:

```

iters = 3. (* change iters to 2 if you're short on time or RAM;
           if anyone runs it with iters=4, I'd like to see
           the result. *);
side = 3. ^ iters ; cubmat (* cuboid-matrix, that is *) =
Table[
  If[i==side + 1. || j==side + 1. || k==side + 1.,
    (* Pad the table's edges with zeroes; if you want
    to see the complement of the sponge, transpose
    the 0. and 1. directly below. *)
    0., 1.],
  {i,1.,side + 1.},{j,1.,side+1.},{k,1.,side+1.}];
Do[ If[
  (Mod[Round[i/3.^n + 0.5],3]==2 &&
   (Mod[Round[j/3.^n + 0.5],3]==2 ||
    Mod[Round[k/3.^n + 0.5],3]==2)) ||
  (Mod[Round[j/3.^n + 0.5],3]==2 &&
   (Mod[Round[i/3.^n + 0.5],3]==2 ||
    Mod[Round[k/3.^n + 0.5],3]==2)) ||
  (Mod[Round[k/3.^n + 0.5],3]==2 &&
   (Mod[Round[i/3.^n + 0.5],3]==2 ||
    Mod[Round[j/3.^n + 0.5],3]==2)),
  (* then--taking advantage of eightfold symmetry--... *)
  (cubmat[[i,j,k]]=0.;
   cubmat[[side+1-i,j,k]]=0.;
   cubmat[[i, side+1-j,k]]=0.;
   cubmat[[i,j,side+1-k]]=0.;
   cubmat[[side+1-i, side+1-j,k]]=0.;

```

```

cubmat[[side+1-i,j,side+1-k]]=0.;
cubmat[[i, side+1-j, side+1-k]]=0.;
cubmat[[side+1-i,side+1-j,side+1-k]]=0.;;)
(* ...no cuboid goes there *)],
  {i,(side+1)/2},{j,(side+1)/2},{k,(side+1)/2},
  {n,0.,iters-1.}]
faces = { };
(* Instead of using the Cuboid graphics primitive,
we show only the polygons visible from
viewpoints in the default octant. *)
Do[
  If[ cubmat[[i,j,k]]==1. && cubmat[[i,j,k+1.]]==0.

      (* That is, if a face belongs at {i,j,k}
and there's nothing hiding it, add the
appropriate polygon to the list. *)],
    AppendTo[ faces,
(* cuboid tops... *)
  {{i,j,k+1.},{i,j+1.,k+1.},
  {i+1..j+1.,k+1.},{i+1.,j,k+1.}}] ],
  {i,1.,side},{j,1.,side},{k,1.,side} ]; (* Since the figure looks the same regardless of
which axis
is vertical, the polygon-corner list "faces" is computed
only for the tops of the cuboids, then rotated twice to get
lists of sides and fronts. *)
faces = Join[ faces (*tops*),
  (*sides *)Map[ RotateLeft[#,2]&,faces,{2}],
  (*fronts*)Map[
  RotateLeft[#,1]*{1,-1,1}+{0,side+2,0}&,
  faces,{2}]];
Show[Graphics3D[ {EdgeForm[], Map[ Polygon, faces ]}], Boxed->False]

```

### 11.3. Programs of Fractals in the Complex Plane

11.3.1. The following MatLab program produces the image of the Filled Julia set in the complex plane.

MatLab Program:

```

%%% Compute and draw the Julia set
clear;
clc;

%%% Parameters
c = 0.27+0.53i;      % complex number
niter=100;          % number of iterations
th=10;              % threshold to determine divergence
v=1000;             % resolution (<-> number of points to compute)

%%% Initialisation
r = max(abs(c),2);   % radius of the circle beyond which every point diverges
d = linspace(-r,r,v); % divide the x-axis
Z = ones(v,1)*d+i*(ones(v,1)*d)'; % create the matrix A containing complex
numbers
C = zeros(v,v); % Julia set point matrix

%%% Compute the julia set
for k = 1:niter
    Z = Z.*Z+ones(v,v).*c;
    C = C+(abs(Z)<=r);
end
%%% Figurefigure(1)
clf;
imagesc(C);
colormap(jet);
hold off;
axis equal;
axis off;

```

11.3.2. The following Mathematica program produces the image of the Mandelbrot set in a square region in the complex plane.

Mathematica Program:

```

Mandelbrot[c_]:=Module[{z=0,i=0},While[i<100&&Abs[z]<2,z=z^2
+c;i++];i];
DensityPlot[Mandelbrot[xc+Iyc],{xc,-2,1},{yc,-
1.5,1.5},PlotPoints->275,Mesh->False,Frame->False,ColorFunction->
(If[ #≠1,Hue[#],Hue[0,0,0]]&)]

```

11.3.3. The following MatLab program produces the image of the Mandelbrot set.

**MatLab Program:**

```

%% The Mandelbrot set
    x = linspace(-1.5,1.5,2000);
    y = linspace(-1.5,1.5,2000);
len_x = length(x);
len_y = length(y);
    iter = 100; %number of iterations
    xnew = 0;
    ynew = 0;
    a = 0;
    b = 0;
    xn = 0;
    yn = 0;
    rough = 0;
    c = zeros(len_y,len_x);
    zval = zeros(len_y,len_x);
h_msg = msgbox(' Please Wait ',' ');
for n=1:len_y
    c(n,:)=y(n)+i*x(:);
end
tic
for m=1:len_x*len_y
    a = imag(c(m));
    b = real(c(m));
    xn = 0;
    yn = 0;
    k = 0;
    while (k<=iter)&&((xn^2+yn^2)<4)
        xnew = xn^2 - yn^2 + a;
        ynew = 2*xn*yn + b;
        xn = xnew;
        yn = ynew;
        k = k+1;
    end
    zval(m) = k;
end
toc
close(h_msg);
%you can also try any one of these colormaps
%cmap = flipud(colormap(cool(iter)));
%cmap = flipud(colormap(copper(iter)));
%cmap = flipud(colormap(hot(iter)));
cmap = flipud(colormap(bone(iter)));
%cmap = flipud(colormap(summer(iter)));
%cmap = flipud(colormap(winter(iter)));
%cmap = flipud(colormap(spring(iter)));
%cmap = flipud(colormap(bone(iter)));
colormap(cmap);
image(zval)
axis tight off
%clear x y c
%imwrite(zval,cmap,'mandel123.png','png');

```

11.3.4. The following MatLab program produces the image of the complete Fern.

**MatLab Program:**

```

%%% Compute and draw the complete Fern
NumOfPts = 10000;
iterations = 50000;
pts = zeros(NumOfPts,2);
for j = 1:NumOfPts
    x = rand(1);
    y = rand(1);
    for i = 1:iterations
        p = rand(1);
        if p < .01
            xn = 0;
            yn = .16*y;
            x = xn;
            y = yn;
        elseif p < .08
            xn = .2*x-.26*y;
            yn = .23*x+.22*y+1.6;
            x = xn;
            y = yn;
        elseif p < .15
            xn = -.15*x+.28*y;
            yn = .26*x+.24*y+.44;
            x = xn;
            y = yn;
        else
            xn = .85*x+.04*y;
            yn = -.04*x+.85*y+1.6;
            x = xn;
            y = yn;
        end
    end%i
    pts(j,1) = x;
    pts(j,2) = y;
end%j
xs = pts(:,1);
ys = pts(:,2);
plot(xs,ys, '.', 'Color', 'g')
axis([min(xs)*1.5,max(xs)*1.5,min(ys)*1.05,max(ys)*1.05]);

```

11.4. The following MatLab program produces the image of the compression pentagon.

```

MatLab Program:
function recursion
global COLORMAP
golden = 1.618033988749894848204586; %golden ratio
n=4; %depth of recursion
COLORMAP=copper(4);
h=1;
pentaflake(n,0,0,36/180*pi,h);
axis([-3 3 -3 3])
axis equal off
function pentaflake(n,x,y,theta,len)
global COLORMAP
if n>0
golden = 1.618033988749894848204586;
d=len/golden;
h=len;
t=linspace(0+theta,2*pi+theta,5+1);
[offx,offy]=pol2cart(t+18/180*pi,d*(1+golden));%generate points
around middle pentagon
for k=1:5
patch(h*sin(t)+offx(k)+x,h*cos(t)+offy(k)+y,0*cos(t)+4-
n,'r',...
'facecolor','none','edgecolor',COLORMAP(n,:), 'linewidth',n);
pentaflake(n-1,x+offx(k),y+offy(k),theta,len/(golden+1));
end
patch(h*sin(t)+offx(k)+x,h*cos(t)+offy(k)+y,0*cos(t)+4-n,'r',...
'facecolor','none','edgecolor',COLORMAP(n,:), 'linewidth',n);
pentaflake(n-1,x,y,pi+theta,len/(golden+1));
end
return

```

## REFERENCES

- [1] P. S. Addison, *Fractals and Chaos: An Illustrated Course*, Institute of Physics, Bristol, 1997.
- [2] R. L. Devaney, *A First Course in Chaotic Dynamical Systems*, Boston University, Addison-Wesley, West Views Press, 1992.
- [3] M. J. Islam, M. S. Islam, *Generalized cantor sets and its fractal dimension*, *Bd. J. Sci. Ind. Res.*, 46(4) (2011), 499-506.
- [4] M. J. Islam, M. S. Islam, Lebesgue Measures of Generalized Cantor Sets, *Annals of Pure App. Math.*, 10(1) (2015), 75-87.
- [5] H. O. Peitger, H. Jungeus and D. Sourpe, *Chaos and Fracatls: New frontier of science*, Springer, New York, 1992.
- [6] M. J. Islam, M. S. Islam, Invariant Measures for Iterated Function Systems of Generalized Cantor Sets, *German J. Ad. Math. Sci.*, 1(2) (2016), 31-47.
- [7] A. Lasota, J. A. Yorke, Lower Bound Technique for Markov Operators and Iterated Function Systems, *Random and Comp. Dyn.*, 2(1) (1994), 41-77.
- [8] K. Falconer, *Fractal Geometry: Mathematical Foundation and Applications*, Wiley, New York, 1990.
- [9] D. L. Jaggard, Fractal Electrodynamics: Wave Interaction with Discretely Self-similar Structure, *Taylor and Francis Pub. Washington D.C.*, (1995), 231-281.
- [10] J. B. S. Yadav and S. Garg, *Programing Applications of Fractals*, P C quest 1990.
- [11] J. Feder, *Fractal*, Plenum Press, New York, 1988.
- [12] P. Gupta and J. P. S Raina, Miniaturization of Antenna Using Fractals, *Int. J. Com. Sci. Comm.*, 1(2) (2010), 437-440.
- [13] [http://en.wikipedia.org/wiki/Koch\\_snowflake](http://en.wikipedia.org/wiki/Koch_snowflake)
- [14] [http://www.uwosh.edu/faculty\\_staff/kuennene/Chaos/ChaosNotes7.pdf](http://www.uwosh.edu/faculty_staff/kuennene/Chaos/ChaosNotes7.pdf)
- [15] <http://fractalfoundation.org/OFC/OFC-10-3.html>
- [16] H. L. Royden, *Real Analysis*, Third Edition, Macmillan Publishing Company, U.S.A, 1988.
- [17] W. Rudin, *Real and Complex Analysis*, Third Edition, Tata McGraw-Hill, 1987.
- [18] J. H. Lifton, *Measure Theory and Lebesgue Integration*, 1999, available at <http://citeseerx.ist.psu.edu/viewdoc/download?doi=10.1.1.112.794&rep=rep1&type=pdf>
- [19] S. Lipschutz, *General Topology*, Int. Edition, Schaum's Outline Series, 1965.
- [20] *Borel Set*, available at [https://en.wikipedia.org/wiki/Borel\\_set](https://en.wikipedia.org/wiki/Borel_set)
- [21] M. F. Barnsley, *Fractals Everywhere*, Academic Press, Massachusetts, 1993.
- [22] J. E. Hutchison, Fractal and self-similarity, *Indiana Math. J.*, 30(1981), 713-743.
- [23] <http://wwwf.imperial.ac.uk/~jswlamb/M345PA46/M2AA1notes10Ch3.pdf>
- [24] J. Myjak and T. Szarek, Attractors of Iterated Function Systems and Markov Operators, *Abs. App. Analysis*, 8 (2003), 479-502.
- [25] A. Lasota and M. C. Mackey, *Chaos, Noise, Stochastic Aspects of Dynamics (Applied Mathematical Science) 2<sup>nd</sup> Edition*, Springer-Verlag, New York, 1994.
- [26] N. Loughlin, A. Wallis, *Fractal Geometry MT4513/5813*, 2006, available at <https://www.students.ncl.ac.uk/n.j.loughlin/fractal2.pdf>
- [27] K. T. Alligood, T. D. Sauer, J. A. Yorke, *Chaos, An Introduction to Dynamical Systems*, Springer, New York, 1997.



- [28] <http://ecademy.agnesscott.edu/~lriddle/ifs/ksnow/ksnow.htm>
- [29] B. Demir, Y. Ozdemir and M. Sultan, The Snowflake Curve as an Attractor of an Iterated Function System, *Commu. Korea Math. Soc.*, 28(1) (2003), 155-162.
- [30] <http://ecademy.agnesscott.edu/~lriddle/ifs/siertri/siertri.htm>
- [31] T. Szarek, *Invariant Measures for Non-expansive Markov Operators*, Warszawa: Polska Akademia Nauk, Instytut Matematyczny, 2003.
- [32] M. Isoifescu and R. Theodorescu, *Random Processes and Learning*, Springer, New York, 1969.
- [33] S. Karlin, Some random walks arising in learning models, *Pacific J. Math.*, 3 (1953), 725-756.
- [34] M. F. Norman, Some convergence theorems for stochastic learning models with distance diminishing operators, *J. Math. Psy.*, 5 (1968), 61-101.
- [35] G. Mihoc and O. Onicescu, Sur les chaines de variable statistiques, *Bull. Soc. Math. France*, 59 (1935), 174-192.
- [36] I. I. Gikman and A. V. Skorokhod, *Stochastic Differential Equations and their Applications*, Naukova Durnka, Kiev, Russia, 1982.
- [37] N. Ikeda and S. Watanabe, *Stochastic Differential Equations and Diffusion Processes*, North-Holland, Amsterdam, 1981.
- [38] M. F. Barnsley and S. Demko, Iterated Function System and the Global Construction of Fractals, *Proc. Roy. Soc. London*, A 399 (1985), 243-275.
- [39] J. H. Elton and M. Piccioni, Iterated Function Systems Arising From Recursive Estimation Problems, *Proba. Theo. Rel. Fields*, 91 (1992), 103-114.
- [40] K. J. Falconer, *Fractal Geometry: Mathematical Foundation and Applications*, Wiley, New York, 1990.
- [41] A. Lasota and J. A. Yorke, Semifractals on Polish Spaces, *Bull. Polish Acad. Sci. Math.*, 46 (1998), 179-196.
- [42] J. Ding, T. Y. Li, A. Zhou, Finite Approximation of Markov Operators, *J. Computa. App. Math.*, 147 (2002), 137-152.
- [43] R. Rudnicki, Markov Operators: Applications to Diffusion Process and Population Dynamics, *Applicationes Mathematicae*, 27(1) (2000), 67-79.
- [44] A. Lasota, M. C. Mackey, *Chaos, Fractals and Noise, Stochastic Aspects of Dynamics*, App. Math. Sci., Springer, New York, 1994.
- [45] T. Komorowski, J. Tyrcha, Asymptotic Properties of Some Markov Operators, *Bull. Polish Acad. Sci. Math.*, 37(1989), 221-228.
- [46] A. Lasota, J. A. Yorke, Lower Bound Technique for Markov Operators and Iterated Function Systems, *Random Com. Dyna.*, 2(1994), 41-47.
- [47] David C Seal, *An Introduction to Fractals and Hausdorff Measure*, available at [http://www.math.utah.edu/~dseal/fractals/Fractal\\_Thesis.pdf](http://www.math.utah.edu/~dseal/fractals/Fractal_Thesis.pdf)
- [48] P. Lertchoosakul, *Introduction of Hausdorff Measure and Dimension*, Dynamics Learning Seminar, Liverpool, 2012. Available at [pojlerchoosakul.webs.com/IntroductionToHausdorffDimension.pdf](http://pojlerchoosakul.webs.com/IntroductionToHausdorffDimension.pdf)
- [49] M. Soltanifar, On A Sequence of Cantor Fractals, *Rose Hulman Und. Math J.*, 7(1), 2006.
- [50] M. Hata, On the Structure of Self-similar Sets, *Japan J. Appl. Math.*, 2 (1985), 381-414.
- [51] T. Szarek, Invariant Measures for Iterated Function Systems, *Annales Polonici Mathematici*, LXXV.1 (2000), 87-98.

- [52] S. K. Liu, Z. T. Fu, S. D. Liu, K. Ren, Scaling equation for invariant measure, *Commun. Theo. Phys.*, 39(3) (2003), 295-296.
- [53] <http://kluge.in-chemnitz.de/documents/fractal/node2.html>
- [54] A. L. Goldberger, B. J. West, "Fractals in Physiology and Medicine" *The Yale J. Bio and Med.*, 60(1987), 421-435.
- [55] <http://classes.Yale.edu/fractals/panorama/Biology/Physiology/Physiology.html>
- [56] A. L. Goldberger et. al., "Fractal dynamics in physiology: Alterations with disease and ageing" *PANS* 99(2002), 2466-72.
- [57] <http://www.fractal.org/Bewustzijns-Besturings-Model/Fractals-Useful-Beauty.htm>
- [58] H. W. Tin, S. W. Leu, H. Sasaki, S. H. Chang, "A Novel Fractal Block Coding Method by Using New Shape-based Descriptor", *Appl. Math. Inf. Sci.* 8(2) (2014), 849-855.
- [59] B. B Mandelbrot, "*Fractal Geometry of Nature*", San Francisco, CA: Freeman, 1992.
- [60] A. E. Jacquin, "Image Coding Based on a Fractal Theory of Iterated Contractive Image Transformations", *IEEE Trans. Image Processing*, (1992), 18-30.
- [61] M. F. Barnsley, S. Demko, "Iterated function systems and global construction of fractal", *Pro. of the Royal Society of London*, (1985), 243-275.
- [62] M. F. Barnsley, L. P. Hurd, "*Fractal Image Compression*", AK Peters, Ltd. Wellesley, Massachusetts, 1993.
- [63] E. W. Jacobs, Y. Fisher, R. D. Boss, "Image compression: A study of the iterated transform method", *Signal Processing*, 29 (1992), 251-263.
- [64] Pentaflake, available at <http://mathworld.wolfram.com/Pentaflake.html>